

Springer Monographs in Mathematics

Andrei Bogatyrev

Extremal Polynomials and Riemann Surfaces



Springer

Springer Monographs in Mathematics

For further volumes:
<http://www.springer.com/series/3733>

Andrei Bogatyrev

Extremal Polynomials and Riemann Surfaces

Translated from Russian by Nikolai Kruzhilin



Springer

Andrei Bogatyrev
Institute of Numerical Mathematics
of the Russian Academy of Sciences
Moscow
Russia

Translator
Nikolai Kruzhilin
Steklov Mathematical Institute
Moscow
Russia

Russian original edition published as “Ekstremal’nye Mnogochleny i Rimanovy Poverkhnosti”,
MCCME, Moscow, 2005

ISSN 1439-7382
ISBN 978-3-642-25633-2 e-ISBN 978-3-642-25634-9
DOI 10.1007/978-3-642-25634-9
Springer Heidelberg Dordrecht London New York

Library of Congress Control Number: 2012936483

Mathematics Subject Classification (2010): 41A10, 41A50, 14Hxx, 30Fxx, 33E20, 33F05

© Springer-Verlag Berlin Heidelberg 2012

This work is subject to copyright. All rights are reserved, whether the whole or part of the material is concerned, specifically the rights of translation, reprinting, reuse of illustrations, recitation, broadcasting, reproduction on microfilm or in any other way, and storage in data banks. Duplication of this publication or parts thereof is permitted only under the provisions of the German Copyright Law of September 9, 1965, in its current version, and permission for use must always be obtained from Springer. Violations are liable to prosecution under the German Copyright Law.

The use of general descriptive names, registered names, trademarks, etc. in this publication does not imply, even in the absence of a specific statement, that such names are exempt from the relevant protective laws and regulations and therefore free for general use.

Printed on acid-free paper

Springer is part of Springer Science+Business Media (www.springer.com)

*To the blessed memory of Nikolai Sergeevich
Bakhvalov*

Contents

1	Least Deviation Problems	1
1.1	Examples of Optimization	1
1.1.1	Inverting a Symmetric Matrix	1
1.1.2	Explicit Runge–Kutta Methods	2
1.1.3	Electrotechnics	3
1.1.4	V. A. Markov’s Problem	4
1.1.5	Other Applications	5
1.2	Analyzing Optimization Problems	5
1.3	Chebyshev Subspaces	8
1.4	The Problem of Optimal Stability Polynomial	9
1.4.1	Properties of Optimal Stability Polynomials	10
1.5	Problems and Exercises	12
2	Chebyshev Representation of Polynomials	15
2.1	Real Hyperelliptic Curves	17
2.1.1	The Homology Space and the Lattice L_M	18
2.1.2	The Space of Differentials on the Curve	20
2.1.3	A Distinguished Form η_M on the Curve	20
2.2	Polynomials and Curves	21
2.2.1	The Stability of the Chebyshev Representation	24
2.3	Problems and Exercises	24
3	Representations for the Moduli Space	29
3.1	Four Definitions	29
3.1.1	The Teichmüller Space	30
3.1.2	The Deformation Space of a Kleinian Group	31
3.1.3	The Labyrinth Space	32
3.2	Auxiliary Results	33
3.2.1	The Fundamental Group of the Moduli Space	33
3.2.2	The Moduli Space: Orbits of the Group Mod	34
3.2.3	The Topology of the Deformation Space	35
3.2.4	The Subgroup Induced by the Ramified Covering $x(u)$	36

3.2.5	The Modular Group Action on the Group \mathfrak{G}	38
3.2.6	Equivalence of Labyrinths	40
3.2.7	A Quasiconformal Deformation	41
3.3	Equivalence of the Representations	44
3.3.1	An Isomorphism Between \mathcal{T}_g^k and \mathcal{G}_g^k	44
3.3.2	An Isomorphism Between \mathcal{T}_g^k and $\tilde{\mathcal{H}}_g^k$	46
3.3.3	An Isomorphism Between \mathcal{L}_g^k and \mathcal{G}_g^k	50
3.4	Problems and Exercises	51
4	Cell Decomposition of the Moduli Space	53
4.1	Curves and Trees	53
4.1.1	Foliations and global width Function	54
4.1.2	The Graph Γ of the Curve M	55
4.1.3	Characteristics of a Graph Γ	56
4.1.4	Properties of the Graph of a Curve	57
4.1.5	Recovery of the Curve M from Its Graph Γ	58
4.2	The Coordinate Space of a Graph	62
4.2.1	The Space of a Graph in the Moduli Space	64
4.3	A Classification of Extremal Polynomials	69
4.4	Problems and Exercises	71
5	Abel's Equations	73
5.1	The Period Map	74
5.1.1	The Homology Group Bundle and Translation of Cycles ...	74
5.1.2	The Bundle of Differentials and the Period Map	75
5.1.3	Properties of the Period Map	76
5.2	Abel's Equations on the Moduli Space	80
5.3	The Image of the Period Map	83
5.4	Problems and Exercises	87
6	Computations in Moduli Spaces	89
6.1	Function Theory in the Schottky Model	90
6.1.1	Linear Poincaré Theta-Series	90
6.1.2	The Convergence of Linear Poincaré Series	92
6.1.3	Arranging of Summation in Poincaré Series	95
6.1.4	Automorphic Functions and Their Derivatives	97
6.2	Variational Theory	99
6.2.1	The Analytic Dependence of Differentials on the Moduli ...	99
6.2.2	Variations of Abelian Integrals	101
6.2.3	Quadratic Poincaré Theta Series	103
6.2.4	Hejhal's Formulae	104
6.2.5	A Basis of Quadratic Poincaré Theta Series	107
6.3	Calculation of Polynomials	109
6.3.1	A Parametric Representation	109
6.3.2	Abel's Equations in the Space \mathcal{G}_g^k	110
6.3.3	The Scheme of the Algorithm	111
6.4	Problems and Exercises	112

7 The Problem of the Optimal Stability Polynomial	115
7.1 The Chebyshev Representation for Solutions	116
7.1.1 The Topological Type of the Associated Curve	116
7.1.2 The Moduli Space	117
7.1.3 The Subgroup Induced by the Covering	117
7.1.4 Cycles on a Riemann Surface	117
7.1.5 Abel's Equations	118
7.1.6 Equations on the Moduli Space	119
7.2 The Schottky Model	120
7.2.1 The Deformation Space	120
7.2.2 The Moduli Space and the Deformation Space	122
7.2.3 Constructive Function Theory	124
7.3 Equations on the Deformation Space	127
7.3.1 Abel's Equations	127
7.3.2 Constraints	128
7.3.3 The Jet of $T(u)$	128
7.3.4 The Projective Jet of $x(u)$	129
7.3.5 Variational Theory	129
7.3.6 Hejhal's Formulae	130
7.4 Numerical Experiments	132
7.5 Problems and Exercises	133
 Conclusion	 135
 References	 137
 Further Reading	 143
 Index	 147

Notations

$\mathbb{C}, \mathbb{R}, \mathbb{Q}, \mathbb{Z}, \mathbb{N}$	The sets of complex, real, rational, integer, and positive integer numbers, respectively.
$\hat{\mathbb{R}}$	The extended real line, a circle.
$\mathbb{CP}^1 = \hat{\mathbb{C}}$	The Riemann sphere.
$\mathbb{H} := \{x \in \mathbb{C}: \text{Im}(x) > 0\}$	The open upper half-plane.
$\#\{\dots\}$	The cardinal number of a set.
\square	The end of a proof.
$M(\mathbf{e})$	The real hyperelliptic curve with branch divisor \mathbf{e} .
$\mathbf{e} := \{e_s\}_{s=1}^{2g+2}$	An (unordered) system of $g - k + 1$ pairs of complex conjugate points and $2k$ real points.
∞_-, ∞_+	Two points on the curve M lying over the point at infinity.
J	The hyperelliptic involution of M .
\bar{J}	The anticonformal involution (reflection) on M .
C_s^+, C_s^-	Even and odd 1-cycles on M , respectively.
$H_1^-(M, \mathbb{Z})$	The lattice of odd integral 1-cycles on M (of rank $g + 1$).
L_M	The sublattice of $H_1^-(M, \mathbb{Z})$.
$\langle C^* C \rangle$	The value of a functional (cocycle) C^* at a cycle C .
η_M	The (real) abelian differential of the 3d kind assigned to M , with simple poles at infinity, residues ± 1 , and purely imaginary periods.
\mathfrak{A}_1^+	The group of affine orientation-preserving motions of the real line.
Br_m	The pure braid group on m strands.
\mathcal{H}_g^k	The moduli space of genus g curves with k real ovals.
$\mathcal{H}_g^k \cong \mathbb{R}^{2g}$	The universal covering space of the moduli space.
QC	The group of quasiconformal homeomorphisms of the upper half-plane \mathbb{H} fixing the points -1 , $+1$, and ∞ .

$\mathrm{QC}(\mathbf{e})$	The subgroup of homeomorphisms stabilizing the divisor \mathbf{e} .
$\mathrm{QC}^0(\mathbf{e})$	The identity component of $\mathrm{QC}(\mathbf{e})$.
\mathcal{T}_g^k	The Teichmüller space of the disc with $g - k + 1$ punctures and $2k + 1$ marked points on the boundary.
$\mathrm{Mod}(\mathbf{e})$	The modular group of the punctured half-plane $\mathbb{H} \setminus \mathbf{e}$.
\mathfrak{G}	The free product of $g + 1$ rank-two groups with generators G_s , $s = 0, 1, \dots, g$; also a realization of this abstract group by a Kleinian group.
$\mathrm{fix} G_s$	The fixed point set of the linear fractional map $G_s(u)$.
\mathfrak{S}	The Schottky group with generators $S_l := G_l G_0$, an index-two subgroup of \mathfrak{G} .
$\mathcal{D}(\mathfrak{G})$	The domain of discontinuity of the Kleinian group \mathfrak{G} .
$\Lambda(\mathfrak{G})$	The limit set of the group \mathfrak{G} .
\mathcal{G}_g^k	The deformation space of the special Kleinian group \mathfrak{G} .
$\mathfrak{g} = \{G_s\}_{s=0}^g$	An element of the deformation space: an ordered set of generators G_s of the group \mathfrak{G} .
$\{c_s, r_s\}_{s=1}^g$	A global system of coordinates in \mathcal{G}_g^k related to the parameters of linear second-order rotations G_s .
$\mathbf{R}(\mathfrak{g})$	A fundamental domain of the Kleinian group \mathfrak{G} generated by the system \mathfrak{g} of linear fractional transformations, which is bounded by the imaginary axis and circles C_1, C_2, \dots, C_g .
$\mu(x), \mu(x)\overline{dx}/dx$	A Beltrami coefficient and a Beltrami differential, respectively.
\mathcal{L}_g^k	A labyrinth space, a model for the universal covering space $\tilde{\mathcal{H}}_g^k$.
Λ	A labyrinth, a special system of $g + 1$ cuts connecting pairwise points in the branch divisor \mathbf{e} .
$H_1 \mathcal{H}_g^k$	The vector bundle of homology spaces over the moduli space.
$H_1^- \mathcal{H}_g^k$	The subbundle of odd 1-homology.
$\Omega^1 \mathcal{H}_g^k$	The vector bundle of real abelian differentials with simple poles at infinity.
$\Pi: \Omega^1 \tilde{\mathcal{H}}_g^k \rightarrow \mathbb{R}^{2g+1}$	The global period map.
$\Pi_-: \tilde{\mathcal{H}}_g^k \rightarrow \mathbb{R}^g$	The restriction of the global period map to the manifold of distinguished differentials η_M on curves M .
$W(x) := \left \mathrm{Re} \int_{(e_s, 0)}^{(x, w)} \eta_M \right $	A globally defined (Green's) function on the sphere.
Γ	The finite tree related to the foliation $(\eta_M)^2 > 0$.
$\Gamma $	A part of the graph Γ , the zero set of the function $W(x)$.

$\Gamma_{\bullet}^0 := \Gamma_{\bullet} \cap \mathbb{R}$
 $\text{Comb}\{\Gamma\}$

$\sigma(x)$

$\kappa(t)$

$\theta(t)$

$\mathbb{T}(C_*)$

\mathbf{i}

$\kappa(\mathbf{i})$

\mathbf{R}

$(u, u'; z, z')$

$E_s(u)$

E_{sl}

$\mathbf{M}(u) := \begin{vmatrix} -u & u^2 \\ -1 & u \end{vmatrix}$

$\text{diam}(\cdot)$

$\text{dist}(\cdot, \cdot)$

D_u^l

C_+, C_-, C_0, C_1

$E_+(u), E_-(u)$

$E_{++}, E_{+-}, E_{-+}, E_{--}$

$\Gamma_+^0 := \Gamma_{\bullet} \cap \mathbb{H}$, here $\bullet = |, -$ or empty.

A comb-like domain constructed from a weighted graph.

A cutoff function equal to 1 in a 2-dimensional neighbourhood of the point $x = 0$.

A ‘‘Courant tent’’, a function of the real variable t .

The Heavyside function of the real variable t .

A fibre of the period map Π_- over the point C_* in the space of functionals.

A $(g - k + 1)$ -subset of $\{1, 2, \dots, g\}$.

The braid on $g + 2$ strands corresponding to \mathbf{i} .

A fundamental domain of the Schottky group \mathfrak{S} in Chap. 6 bounded by $2g$ circles $-C_g, \dots, -C_2, -C_1, C_1, C_2, \dots, C_g$.

A Schottky function, the exponential of an abelian integral of the 3d kind with poles z and z' over a curve from u to u' .

The exponent of an abelian integral of the 1st kind taken from ∞ to u .

The Schottky constants, the exponentials of the period matrix of the curve.

The Hejhal matrix.

The Euclidean diameter of a set.

The Euclidean distance between points or sets.

The l th partial derivative with respect to u .

Four distinguished cycles on a curve $M \in \mathcal{H}_2^1$.

The Schottky functions in Chap. 7.

The Schottky constants in Chap. 7, the exponentials of entries of the period matrix of the curve.

Introduction

A couple of years before the Crimean War broke out, P.L. Chebyshev travelled to Great Britain to get to know the most advanced technologies of that time. On his return to Russia, he concentrated on a purely engineering problem of minimizing the friction in the joints of Watt's parallelogram which turns the back-and-forth motion of the steam engine into wheel rotation. Chebyshev's investigations led to the eventual replacement of the parallelogram linkage by the crankshaft, which is still in use today. As a by-product of the evolution of technology, the *Chebyshev polynomials* were discovered, *un miracle d'analyse*, in J. Bertrand's words, which since then have found their way into all the textbooks. These polynomials have turned out to solve the simplest problems of constrained minimization of the deviation

$$\|P_n\|_E := \max_{x \in E} |P_n(x)|, \quad (1)$$

where E is a compact subset of the real axis, over the space of real polynomials

$$\left\{ P_n(x) = \sum_{s=0}^n c_s x^s \right\} \cong \mathbb{R}^{n+1}. \quad (2)$$

Now, 150 years later, steam engines are no longer used, but an interest into least deviation problem is still here [33, 146]. Today it is connected, for example, with optimizing numerical algorithms [97, 114] and signal processing [14, 45]. We present several typical problems.

Problem A. *Let E be a system of several finite intervals on the real axis. Minimize the norm $\|P_n\|_E$ of a polynomial satisfying fixed linear constraints on its coefficients c_0, c_1, \dots, c_n .*

The least deviation polynomial with fixed leading coefficient is called the *Chebyshev polynomial* on E . The Zolotarëv problem [146, 160] corresponds to the case of one interval $E = [-1, 1]$ and several fixed leading coefficients of the polynomial. The V.A. Markov problem [101] corresponds to one interval E and one linear constraint.

Problem B. Find a polynomial $R_n(x)$ approximating the exponential function to order $p \leq n$ at $x = 0$, $R_n(x) = 1 + x + x^2/2! + \cdots + x^p/p! + o(x^p)$, such that the deviation $\|R_n\|_E$ does not exceed 1 on the largest possible interval $E = [-L, 0]$, $L > 0$.

The problem of *optimal stability polynomial* $R_n(x)$ was stated by several authors [65, 71, 105, 127, 142] in the late 1950s/early 1960s, in connection with designing explicit n -stage stable Runge–Kutta methods of accuracy order p .

Solving such extremal problems numerically for practically interesting degrees $n \approx 1,000$ is well known to be very complicated. The algorithms due to Remez [77, 98, 126], Lebedev [95], Peherstorfer–Schiefermayr [118], or convex programming methods [129, 146] require a large amount of computational resources for the following reasons: (1) the solution is sought by iterations in a high-dimensional space (of dimension of order n) and (2) the norm of a polynomial is a non-smooth function of its coefficients which is difficult to evaluate.

The classical approach, when a solution is expressed by an explicit formula, is free from these deficiencies [122]. One hundred and fifty years ago, when no computers were known, iterative methods of solution were considered unsatisfactory. The first least deviation problems were solved by producing analytic expressions for the polynomial and its argument, thus defining the polynomial parametrically:

$$T_n(u) := \cos(nu); \quad x(u) := \cos(u), \quad u \in \mathbb{C} \quad (3)$$

(Chebyshev [47]) and

$$Z_n(u) := \frac{1}{2} \left\{ \left[\frac{H(a+u)}{H(a-u)} \right]^n + \left[\frac{H(a-u)}{H(a+u)} \right]^n \right\}; \quad (4)$$

$$x(u) := \frac{\operatorname{sn}^2(u) + \operatorname{sn}^2(a)}{\operatorname{sn}^2(u) - \operatorname{sn}^2(a)}, \quad u \in \mathbb{C},$$

(Zolotarëv [160]). In the last formula, $H(\cdot)$ is the elliptic theta function with modulus $k \in (0, 1)$ in Jacobi's (outdated) notation [155], $\operatorname{sn}(\cdot)$ is the elliptic sine function with the same modulus, and $a := mK(k)/n$, $m = 1, 2, \dots, n-1$, is a phase shift, where $K(k)$ is the complete elliptic integral with the same modulus k . These parametric formulae can be treated as follows: the function $x(u)$ is automorphic with respect to the discontinuous action of some group \mathfrak{G} on the complex plane. The orbit manifold \mathbb{C}/\mathfrak{G} is the Riemann sphere (in the case (3)) or a torus (in the case (4)). The expressions for $T_n(u)$ and $Z_n(u)$ are well defined on the corresponding quotient spaces and are degree n polynomials of x . We see that classical solutions are related to algebraic curves of small genus $g = 0, 1$, and the complexity of their computation is independent of the degree n of the polynomial.

Developing the classical approach to problems of least deviation in the uniform norm, instead of the full space of polynomials (2), we shall seek the solution on certain low-dimensional submanifolds of this space. The *alternation principle* discovered by Chebyshev [33, 146] and subsequently explained by convex analysis

says that the following situation is typical. *Most critical points of the solution $T(x)$ are simple, correspond to the values $\pm\|T(x)\|_E$, and lie in E .* Polynomials of this kind are very special; they fill low-dimensional submanifolds of the space (2). Here is a geometric explanation for this. A solution to an extremal problem corresponds to a tangency between the (usually linear) submanifold of (2) corresponding to the constraints of the problem and the sphere formed by the polynomials of equal norm. A ball corresponding to the uniform norm is a convex curvilinear polytope: its boundary is not smooth and is partitioned into faces of various dimension. Low-dimensional faces are more protruding, so it is little surprising that planes touch these faces more often. (For example, the corners of an old suitcase are worn out the most; a pencil falling on the floor reaches it with its tip more often than flatwise, etc.) On the other hand, higher-dimensional faces of a ball are ruled and their contact with linear subspaces can occur along continua: then the corresponding minimum problem is not uniquely solvable. We shall show that for polynomials solving least deviation problems the above-described form is more common. This justifies the following definition.

Definition 1. A real polynomial $P(x)$ is called a (*normalized*) g -*extremal polynomial* if all of its critical points, apart from g points, are simple and the corresponding values of the polynomial are ± 1 .

Here the parameter g , the number of exceptional critical points, can be calculated by the formula

$$g = \sum_{x:P(x) \neq \pm 1} \text{ord } P'(x) + \sum_{x:P(x) = \pm 1} \left[\frac{1}{2} \text{ord } P'(x) \right], \quad (5)$$

where $\text{ord } P'(x)$ is the order of the zero of the derivative of P at the point $x \in \mathbb{C}$ and $[\cdot]$ is the integer part of a number.

The term “extremality” is used here for two reasons. On the one hand we distinguish the critical points which do not obey certain general rules. On the other, the polynomials with small value of g are more likely to solve various extremal problems involving the uniform norm. They are important for applications and, slightly abusing the language, we shall call them simply *extremal* polynomials. Polynomials with extremality parameters $g = 0$ and $g = 1$ were discovered 150 years ago and are known as Chebyshev and Zolotarëv polynomials, respectively. We give the graphs of several 2-extremal polynomials in Fig. 6.4.

Our aim in this book is to investigate g -extremal polynomials and to use them for an effective solution of optimization problems. The ideas behind our approach to problems of least deviation in the uniform norm and the technical realization of this approach are more complicated than the algorithms due to Remez, Lebedev, and other authors mentioned above. However it has an advantage: the complexity of computing a solution using explicit analytic formulae does not depend on the degree n of the polynomial, as we clearly see in the classical Chebyshev and Zolotarëv formulae. On the other hand, the bulk of calculations grows rapidly with

the parameter g , so the natural range of application for this method is the case when solutions have a high degree n , but only a few of constraints are imposed on their coefficients and the set E consists of a few components.

Polynomials, as well as rational and algebraic functions with few critical values, is a classical object of mathematical investigations, lying on the border between “continuous” and “discrete” mathematics.

One of the lines of these investigations goes back to Hurwitz [78]; it is related to classifying branched covers of the sphere, investigating the strata of the corresponding discriminant set, Lyashko–Loijenga maps, Belyi pairs, and Grothendieck’s *dessins d’enfants*. In recent years this approach has been extensively developed by the Moscow Mathematical School (see e.g. the comments and references to Problem 1970-15 in “Arnold’s Problems” [15] and also [87, 90, 91, 113, 158, 163]). For instance, in [136] polynomials with precisely two finite critical values (Shabat polynomials) and their applications to number theory are considered.

Another line of research dates back to Chebyshev [47] or, in fact, to Niels Abel [2]. It is related to the investigation of Pell’s equation¹ with polynomial coefficient, continued fraction expansions, and conditions for the reduction of abelian integrals, when these turn into integrals of lower genus and, in particular, can be reduced to elementary functions [19]. For a survey of this line of research we refer the reader to [139], [144] and also to [9, 13, 46, 86]. A characteristic feature of this second approach is effective calculations and links to applications. Bearing all this in mind, we take the second approach and wish to develop it to the level of effective numerical calculations [37, 40, 43].

Chebyshev’s programme. In [47] Chebyshev showed that solutions $P(x)$ of the minimax problems that he stated satisfy Pell’s equation

$$P^2(x) - D(x)Q^2(x) = 1 \quad (6)$$

with a square-free polynomial $D(x) := \prod_{s=1}^{2g+2} (x - e_s)$ determined by the data of the optimization problem. The first author to consider Pell’s equation with a polynomial coefficient $D(x)$ was Abel [2], who proposed two tests for its solvability: (1) the function $\sqrt{D(x)}$ expands in a periodic continued fraction; (2) for some choice of the coefficients c_s the primitive

$$\int \frac{x^g + \sum_{s=0}^{g-1} c_s x^s}{\sqrt{D(x)}} dx$$

can be expressed “in terms of logarithms” [46]. Chebyshev proposed to seek solutions to (6) as the cosines of hyperelliptic integrals. Here is his argument:

¹Pell’s equation is the Diophantine equation $P^2 - DQ^2 = 1$, where D is a fixed square-free integer coefficient and P and Q are unknown integers. It was considered by William Brounker (1657), Pierre Fermat, John Wallis. By confusion Euler related it to John Pell [58].

differentiating Pell's equation we easily see that the polynomial $P'(x)$ is a multiple of $Q(x)$, so that $P'(x) = n \left(x^g + \sum_{s=0}^{g-1} c_s x^s \right) Q(x)$, $n := \deg P$, with some coefficients c_s . Now substituting for $Q(x)$ its expression from (6) we obtain *Chebyshev's differential equation*

$$\frac{P'(x)}{\sqrt{P^2(x) - 1}} = n \frac{x^g + \sum_{s=0}^{g-1} c_s x^s}{\sqrt{D(x)}}, \quad n := \deg P.$$

Integrating it we readily obtain a solution to Pell's equation:

$$P(t) = \cos \left(in \int_{e_j}^t \frac{x^g + \sum_{s=0}^{g-1} c_s x^s}{\sqrt{D(x)}} dx \right);$$

in what follows we call this the Chebyshev representation for the solution. The function in the right hand side of this formula is a polynomial if and only if one of Abel's criteria holds.² In [47] Chebyshev criticized Abel's criteria as being not sufficiently effective, while here he asks *how, given a coefficient $D(x)$ of Pell's equation, can we understand whether (6) is solvable and, if the answer is "yes", how we can effectively find the solutions.*

For elliptic integrals this research programme was outlined by Chebyshev and was completely carried out by his student E. I. Zolotarëv in 1868–1877 [160–162].

The history of Zolotarëv's heritage is of interest. In 1872 he was attending lectures of Weierstrass in Berlin and communicated his achievements. This work revived Weierstrass's interest in the reductions of abelian integrals which eventually resulted in Weierstrass-Poincaré reduction theory [119]. In the 1930s Zolotarëv's works were still known in Germany and were applied by W. Cauer [44, 45] in electrical engineering. However, his contributions were later all but forgotten in the mathematical community, although some of them were repeatedly discovered anew. In the 1990s, thanks to enthusiastic efforts of several authors, the first among these being Todd [147] and Lebedev [96], Zolotarëv's "priority right" was restored. Surprisingly, Zolotarëv's name remained known to the community of electrical engineers all the time.

The next significant step in implementing Chebyshev's programme was made by N. I. Akhiezer, who used in these problems the language of geometric function theory. In 1928, for the solution of the Zolotarëv problem with three fixed coefficients, Akhiezer put forward an Ansatz involving Schottky functions of

²Alternatively, all the periods of the abelian integral in the last formula must be integer multiples of 2π , the period of \cos . This reflects the discrete aspect of the problem under consideration.

curves of genus $g = 2$. His work [9] was far ahead of his time, although his solution was incomplete: for instance, he could not tell whether the system of (Abel's) transcendental equations for the parameters of the substitution was solvable. Akhiezer's methods used the machinery of Green's functions in the plane cut in some special way, which shaded the connections with algebraic curves. Unfortunately, in his further papers [10, 12] on approximation theory Akhiezer limited himself to elliptic functions, which led to Zolotarëv polynomials and fractions.

Elliptic integrals were a subject of interest for researchers as long ago as the second half of the seventeenth century (John Wallis and the brothers Jacob and Johann Bernoulli). Elliptic integrals gave name to some of the simplest Riemann surfaces, elliptic curves. The theory of elliptic functions called by Klein the *heart and soul of mathematics of nineteenth century* [83], has been extensively developed for more than 250 years, and the literature devoted to it includes tens of thousands of publications. Numerical algorithms have been designed for an effective treatment of curves of genus $g = 1$ and now are implemented in modern computer software. This is one reason why the interest in elliptic functions has revived in recent decades. The interest has arisen in the theory of extremal and orthogonal polynomials [96, 112, 116], within the algebro-geometric approach to integrable systems and scattering by double-periodic potentials [59, 67, 68], and also in the complex geometric theory of one-dimensional integral equations [36, 39].

Riemann surfaces were introduced by Riemann in 1851 as ramified covers of the sphere. The basics of their theory were established by such German mathematicians as Jacobi, Weierstrass, Max Noether, Klein, Hurwitz, Fricke, Koebe, Weyl, and Teichmüller. The theory of Riemann surfaces has beautiful applications in mathematics (embeddings of minimal surfaces, optimization of numerical algorithms), theoretical and mathematical physics (conformal field theory, string theory, finite gap integration, matrix models), industry (electrical filters, encoding), and even medicine (parametrization of the brain surface). The large amount of knowledge about algebraic curves and their deformation spaces makes it possible to use these objects in calculations. Apparently, the first computer evaluation of special functions related to higher genus curves was also related to modelling non-linear waves in the mid-1980s [35]. Today effective computation of function-theoretic objects like abelian integrals, differentials, spinors, Riemann thetas, etc. on higher genus Riemann surfaces is a vibrant branch of numerical analysis with research groups all over the world (TU Berlin [22, 131], Imperial College (London) [50–52], University of Washington [53–55], Florida State University [30, 75, 76, 133, 134] to mention just a few).

Numerical analysis of Riemann surfaces and their moduli spaces is based on the use of Riemann theta functions [56, 61, 108] or Schottky functions [18, 27, 29, 132]. The second way is slightly easier because it allows us to avoid solving numerically the notorious Schottky problem of characterizing the period matrices of Riemann surfaces. In the context of optimization problems for polynomials this approach was put forward by Akhiezer [9] and developed further later on to yield numerical results [37, 41, 43]. It leans on a theorem [35] stating that *real*

algebraic curves can be uniformized by some special Schottky groups \mathfrak{S} , whose linear Poincaré theta series converge absolutely and uniformly on compact subsets of the domain of discontinuity of the group. This result fails for general Schottky groups: Poincaré even believed that linear series were never convergent (see the history of this issue and a survey of results in [7, 8, 110, 145]).

The reader's background. In this book we use methods from various areas of mathematics. The reader is assumed to be familiar with basic complex analysis [92], the theory of Riemann surfaces [60, 107, 123, 141], quasiconformal maps [3, 152] and geometry of discrete groups [32, 109]. Some background in Strebel foliations [143] and Teichmüller theory [4, 20] is also advisable (although not necessary).

The area of application. The following algorithms of numerical mathematics can be optimized with the use of our results here: (1) designing explicit stable difference schemes for ordinary differential equations [71]; (2) Chebyshev acceleration in the iterative solution of large systems of linear equations with a non-singular symmetric matrix. Our approaches can be used for optimizing electric schemes and electronic filters. Our method for calculating special functions connected with Riemann surfaces can be used for numerical simulation in conformal field theory and finite-gap integration.

Acknowledgements In working on this book in 1999–2004, the author was supported by a scholarship from ÖAD “Bewerber über aller Welt”, grants of the Science Support Foundation, a grant no. 01–01–06299 for the support of young scientists, of the Russian Foundation for Basic Research, and also by the RFBR grants no. 99–01–00141 and 02–01–00651. Various questions considered in the book were discussed at the following research seminars: the seminar at the Department of Complex Analysis of the Steklov Mathematical Institute of the Russian Academy of Sciences, under the supervision of academician A. A. Gonchar and Professor E. M. Chirka; the seminar at the Department of Optimal Control of the Faculty of Mechanics and Mathematics of the Moscow State University under the supervision of Professor V.M. Tikhomirov; the seminar at the Department of Dynamical Systems and Approximation Theory of the Faculty of Natural Sciences of the Johannes Kepler University of Linz (Austria) under the supervision of Professor F. Peherstorfer; the seminar at the Department of Differential Equations of the Steklov Mathematical Institute of the Russian Academy of Sciences, under the supervision of academicians D. V. Anosov and A. A. Bolibrukh and Professor Yu. S. Il'yashenko; the seminar on Riemann surfaces, Lie algebras, and mathematical physics at the Independent University of Moscow, under the supervision of Professors S. M. Natanzon, O. V. Shvartsman, and O. K. Sheinman; the seminar on graphs over surfaces and curves over number fields at the Faculty of Mechanics and Mathematics of the Moscow State University, under the supervision of Professor G. B. Shabat; the seminar on numerical mathematics and mathematical physics at the Institute for Numerical Mathematics, under the supervision of academician N. S. Bakhvalov and Professor V. I. Lebedev; the seminar at the Department of Function Theory and Functional Analysis of the Faculty of Mechanics and Mathematics of the Moscow State University, under the supervision of Professor A. I. Aptekarev. The author used material subsequently included in this book in his lecture course at the Johannes Kepler University in 2000.

A Summary

Chapter 1 is concerned with our definition of extremal polynomials. We present examples of optimization of numerical algorithms leading to minimax problems of Chebyshev type. Then extremal problems are investigated with the use of convex analysis. A solvability criterion for least deviation problems with several linear constraints is established, which generalizes the classical alternance principle. The shares of polynomials of different types among solutions of problems with fixed number of constraints are evaluated: the most typical solutions are polynomials which we call extremal, with small extremality parameter g . Properties of optimal stability polynomial are investigated.

Chapter 2. The representation for extremal polynomials discussed in this chapter goes back to Chebyshev and is a geometric interpretation of Pell's equation with a polynomial coefficient. With each polynomial $P(x)$ we associate a hyperelliptic curve

$$M = M(\mathbf{e}) = \left\{ (x, w) \in \mathbb{C}^2 : w^2 = \prod_{s=1}^{2g+2} (x - e_s) \right\}, \quad (7)$$

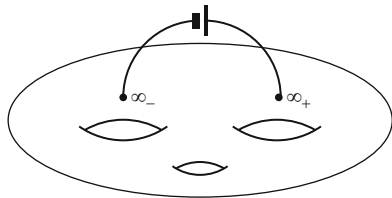
with branch divisor $\mathbf{e} := \{e_s\}_{s=1}^{2g+2}$ consisting of the zeros of odd multiplicity of $P^2(x) - 1$. The genus g of this curve is equal to the number of exceptional critical points of $P(x)$ counted with multiplicities by formula (5). In a natural way $P(x)$ induces a map $\tilde{P}(x, w)$ between covering spaces in the diagram

$$\begin{array}{ccc} (x, w) \in M(\mathbf{e}) & \xrightarrow{\tilde{P}} & \mathbb{CP}^1 \ni u \\ \downarrow \chi & & \downarrow \sigma \\ x \in \mathbb{CP}^1 & \xrightarrow{P} & \mathbb{CP}^1 \end{array} \quad (8)$$

where $\chi(x, w) := x$ is a two-sheeted covering ramified over the points in \mathbf{e} and $\sigma(u) := \frac{1}{2}(u + 1/u)$ is a two-sheeted covering ramified over ± 1 . The map $\tilde{P}(x, w)$ intertwines deck transformations of the covering spaces: $\tilde{P}(x, -w) = 1/\tilde{P}(x, w)$, so the divisor of $\tilde{P}(x, w)$ consists of two points: a pole of order $n := \deg P$ at infinity ∞_+ on one sheet and a zero of the same order at infinity ∞_- on the other sheet. The converse result also holds: any (normalized) meromorphic function \tilde{P} on $M(\mathbf{e})$ with divisor $n(\infty_- - \infty_+)$ satisfies the intertwining condition and induces a map $P(x)$ between the bases. This latter is a polynomial of degree n which a fortiori has the required number of simple critical points corresponding to the values ± 1 .

In the framework of this construction the problem of describing g -extremal polynomials of fixed degree n is equivalent to describing all the curves M of the form (7) possessing a meromorphic function with divisor $n(\infty_- - \infty_+)$. The problem

Fig. 1 An abelian integral of the 3rd kind on a Riemann surface is a complex potential of a flow with one source and one sink



of existence and representation for such a function is solved in terms of the curve M itself, with the help of Abel's criterion [69]. On each curve (7) there exists a unique abelian differential of the third kind

$$\eta_M = \left(x^g + \sum_{s=0}^{g-1} c_s x^s \right) \frac{dx}{w} \quad (9)$$

with purely imaginary periods. This normalization has a physical interpretation due to Helmholtz: suppose that the surface is made of conducting material and attach infinitely thin wires to the points ∞_{\pm} on the surface. Once the wires are connected to the battery, electric current arises along the surface, whose potential is the real part of the corresponding abelian integral $\int \eta_M$ (Fig. 1).

From the distinguished 1-form η_M on M we can recover the polynomial $P(x)$ of degree n up to a sign, by the explicit formula

$$P(x) = \pm \cos \left(ni \int_{(e,0)}^{(x,w)} \eta_M \right), \quad x \in \mathbb{C}, (x, w) \in M. \quad (10)$$

The result of the calculation of the right-hand side of (10) is independent of the choice of the path of integration, the branch point e , and the point $(x, w) \in M$ lying over x , the argument of the polynomial. This formula is a generalization of the classical representations (3), (4) for Chebyshev and Zolotarëv polynomials and Peherstorfer's representation for (non-classical) Chebyshev polynomials on several intervals [116]. It describes g -extremal polynomials using just a few parameters, the moduli of the curve M . However, these moduli are not arbitrary; they must satisfy several relations.

For a curve M associated with a polynomial of degree n the differential form η_M coincides with $n^{-1} d \log \tilde{P}(x, w)$, so a curve M is associated with a polynomial of degree n if and only if the periods of the distinguished 1-form η_M on the curve lie in the lattice $2\pi i n^{-1} \mathbb{Z}$. For a real curve M , on which we can define the reflection $\bar{J}(x, w) := (\bar{x}, \bar{w})$, half of these periods must be zero, and the other half must satisfy the system of Abel's equations

$$-i \int_{C_s^-} \eta_M = 2\pi \frac{m_s}{n}, \quad s = 0, 1, \dots, g, \quad (11)$$

where the m_s are integers and $\{C_s^-\}_{s=0}^g$ is a basis of the lattice of integral 1-cycles on M changing sign after the reflection \tilde{J} .

Chapter 3. It is convenient to assume that the curve M associated with a polynomial is a point in the moduli space of real hyperelliptic curves of genus g with marked point ∞_+ on an oriented real oval. This space consists of several components \mathcal{H}_g^k , $k = 0, \dots, g+1$, distinguished by the number of real points in the variable branch divisor \mathbf{e} . Each component of the moduli space is a smooth $2g$ -dimensional real manifold homeomorphic to the product of a cell and the *configuration space* of the (half)plane. The fundamental group of \mathcal{H}_g^k , which is isomorphic to the Artin *braid group* on $g-k+1$ strands, acts on the universal cover $\tilde{\mathcal{H}}_g^k$ of the moduli space by deck transformations. We consider four representations (models) for $\tilde{\mathcal{H}}_g^k \cong \mathbb{R}^{2g}$; one of these, an analytic uniformization of the moduli space \mathcal{H}_g^k , is used in what follows for the effective calculation of extremal polynomials.

Chapter 4. To visualize the description of all extremal polynomials we develop graph technique. A point M in the moduli space defines the *horizontal foliation* of the distinguished quadratic differential $(\eta_M)^2$ on the Riemann sphere. Strebel's theory [143] is concerned with such foliations. The foliation in question is orthogonal to level curves of the function $W(x) := \left| \operatorname{Re} \int_{(e,0)}^{(x,w)} \eta_M \right|$, which is globally defined on the Riemann sphere. As a result, the structure of the horizontal foliation $(\eta_M)^2 > 0$ is rather simple: its trajectories do not form cycles or mix. The union of certain pieces of critical trajectories of the foliation and the zero level set of the function $W(x)$ forms a graph Γ ; its edges are labelled by their lengths in the metric associated with the quadratic differential. All the restrictions on the topology and weights of the graph Γ are easy to write out, so an abstract weighted graph Γ satisfying these conditions can be realized as the graph associated with a unique curve M in the moduli space. Fixing the topology of the graphs Γ , but considering variable weights we decompose each component \mathcal{H}_g^k of the moduli space into finitely many cells $\mathcal{A}[\Gamma]$, in which the periods of the distinguished abelian differential η_M on the curve form a part of a natural system of coordinates. In particular, in each cell $\mathcal{A}[\Gamma]$ the curves M in the moduli space which are associated with polynomials of fixed degree can be described by the system of linear equations in this natural system of coordinates (11).

Chapter 5. In a fixed moduli space \mathcal{H}_g^k we investigate Abel's equations (11), which describe the points associated with polynomials of degree n . Integrals of the differential form η_M over independent odd 1-cycles $C^- := -\tilde{J}C^+$ on M define locally the *period map* on \mathcal{H}_g^k . Usually, the moduli space is not simply connected and the period map cannot be extended to a global map because going about a non-trivial cycle in the moduli space results in a change of basis in the lattice of odd 1-cycles on the curve. The resulting monodromy is described by the Burau representation ([28], 1932) of the braid group; it vanishes after passing to the universal cover $\tilde{\mathcal{H}}_g^k$. At points in the universal cover we have a distinguished basis of the odd homology space: it can be obtained by the parallel translation of a fixed basis at the marked point M_0 which corresponds to a natural flat Gauss–Manin

connection in the vector bundle of homology spaces. Then the left-hand sides of the equations in (11) define a global period map from the universal cover into the $(g + 1)$ -dimensional real Euclidean space. We shall explicitly find the image of the universal covering space $\tilde{\mathcal{H}}_g^k$ under this map: for $k = g + 1$ this is the interior of a g -simplex, for $k = g$ a union of k open simplexes, and for $k < g$ an infinite countable union of open g -simplexes numbered by braids. We also show that the period map is a submersion. In particular, the points in the moduli space associated with polynomials of degree n form smooth manifolds $\mathbb{T}(\cdot)$ of dimension g , which correspond to the lattice on the right-hand sides of Abel's (11). These manifolds are dense in the moduli space in the limit as $n \rightarrow \infty$.

Chapter 6 is concerned with effective calculations in the moduli space for two problems:

- (1) Solving Abel's equations (11).
- (2) Recovering extremal polynomials by formula (10) and recovering their derivatives of various orders to satisfy the constraints of the least deviation problem.

To this end we uniformize the curves M , points in the moduli space, by certain special Schottky groups. Summing Poincaré theta series we obtain abelian differentials on curves and, in particular, η_M . Abel's equations and our representation for extremal polynomials can be re-written in terms of global coordinate variables on the universal cover \mathcal{H}_g^k which are related to the parameters of the generators of the Schottky group.

Chapter 7. How can we solve any given least deviation problems using our approach? We propose to make use of a suitable Ansatz. *First* we must analyse the problem and find the discrete parameters of the Ansatz: the topological invariants g and k and the indices m_0, m_1, \dots, m_g corresponding to the low-dimensional face of a ball in the space of polynomials (2) that contains the solution. *Next* we must set and solve numerically a system of $2g$ transcendental equations for the point $M \in \mathcal{H}_g^k$ in the moduli space associated with the solution $P_n(x)$. Abel's equations describe a smooth submanifold of the moduli space which is (locally) parametrized by g coordinate functions, the continuous parameters of the Ansatz. These can be found with the help of the data of the extremal problem, the constraints on the coefficients of the polynomials and the end-points of the set E . The variational formulae in Chap. 6 allow us to arrange various versions of descent methods [31] to solve the problem of navigation in the moduli space.

We consider the above scheme to solve optimization problems in greater detail, taking for example the calculation of the optimal stability polynomial $R_n(x)$ approximating the exponent to order $p = 3$ at the origin and deviating from zero at most by 1 on the maximal possible interval on the real axis. Problem B for $p = 3$ and any degree n reduces to the solution of 4 equations in the 4-dimensional moduli space of algebraic curves \mathcal{H}_2^1 . Keeping in mind the reader who is only interested in numerical applications we have written this chapter to be understandable to those who have not read the other chapters of the book.

The **Conclusion** contains a list of open problems.

Chapter 1

Least Deviation Problems

We begin this chapter by listing areas of science and technology where we come across problems relating to optimization of the uniform norm. After that we investigate least deviation problems using methods of convex analysis. We deduce a generalized alternation principle which completely characterizes solutions of such problems. In giving the definition of an extremal polynomial in the introduction we were motivated by this principle. We shall see that most solutions are polynomials with small value of the parameter g calculated by formula (5) in the introduction. Finally, we investigate the problem of finding the optimal stability polynomial: we show that it is solved by an extremal polynomial with $g \leq p - 1$.

1.1 Examples of Optimization

1.1.1 *Inverting a Symmetric Matrix*

Consider a typical computational algorithm such that optimizing it we arrive at a least deviation problem. We solve a system of linear equations $Au = f$ with a non-singular symmetric matrix A . When we have a large matrix, which occurs, for instance, in discretizing equations of mathematical physics, such direct methods as Gaussian elimination are too labour-consuming and cannot be applied, and so iterative algorithms are used for finding solutions. Consider a simple two-step iterative method

$$u_{j+1} := u_j - \alpha_j (Au_j - f), \quad j = 0, 1, 2, \dots,$$

in which the parameters α_j are determined by the condition that after n steps of the procedure the error $\varepsilon_n := u_n - u$ must be minimal. The error at the n th step can be expressed linearly in terms of the initial error:

$$\varepsilon_n = P_n(A)\varepsilon_0, \quad P_n(t) := \prod_{j=0}^{n-1} (1 - \alpha_j t),$$

and its Euclidean norm is no greater than the norm of the initial error times the deviation of the polynomial on the spectrum of the matrix: $\max_{t \in \text{Sp}(A)} |P_n(t)|$.

Calculating the spectrum is an even more laborious procedure than solving a system of linear equations, but often (for instance, for some physical reasons) we know a compact subset E of the real axis containing the spectrum of the matrix. In that case, for the parameters of the iterative procedure we take the reciprocal values of the zeros of a polynomial solving the following minimum problem: *among the polynomials in the space (2) satisfying $P_n(0) = 1$ find a polynomial that has the smallest uniform norm on the compact subset E of the real axis.*

1.1.2 Explicit Runge–Kutta Methods

The Runge–Kutta method has been used for the numerical integration of systems of ordinary differential equations for more than a century. Explicit schemes for solution of the Cauchy problem

$$\begin{cases} dy/dt = f(y, t), \\ y(0) = y_0, \end{cases} \quad y(t) \in \mathbb{R}^m, \quad (1.1)$$

for ordinary differential equations have many advantages: they are simple to implement, can easily be parallelized, and take relatively little memory resources in comparison with implicit schemes. At the same time, for *stiff* problems (when a solution has a rapidly changing component) Courant's stability condition imposes too strong restrictions on the step h . For example, in the case of the simplest *Euler scheme* we consider a uniform time grid $t_j := jh$, $j = 0, 1, 2, \dots$, and take the solution $y(t_{j+1})$ to be approximately

$$y_{j+1} := y_j + hf(y_j, t_j).$$

The local stability condition for the Euler scheme has the form $h < 2/\lambda$, where λ is the spectral radius of the current Jacobian matrix of the map $f(y, t)$. If the system (1.1) of equations to be solved is obtained by discretizing an evolution equation of mathematical physics in the space variables, then λ can be very large: for instance, the finite-difference Laplace operator is unbounded in the limit. Using variable time steps we can significantly (by a factor of millions) increase the average magnitude of step while keeping the method stable [93]. Applying the multistage Runge–Kutta method, with step h consisting of n smaller steps, to the simplest equation $dy/dt = \lambda y$, $\lambda > 0$, we obtain a relation between the values of an approximate solution at

consecutive nodes: $y_{j+1} := R_n(\lambda h)y_j$, where $R_n(x)$ is a real polynomial of degree n , the *stability function* of the method. If a Runge–Kutta method has accuracy order p , then its stability function must approximate the exponential function with the same accuracy at the origin [71, 142]:

$$\begin{aligned} R_n(x) &= 1 + x + x^2/2 + \cdots + x^p/p! + x^{p+1}P_{n-p-1}(x), \\ \deg P_{n-p-1}(x) &= n - p - 1. \end{aligned} \quad (1.2)$$

Maximizing the *stability region* $\{x: |R_n(x)| \leq 1\}$ of the Runge–Kutta method on the real axis, for instance, when solving parabolic-type equations by the method of lines, results in Problem B in the introduction [94, 103]. Zeros of classical Chebyshev and Zolotarëv polynomials are used in the DUMKA software package [71], which has proved to be effective in many non-linear evolution problems of mathematical physics [157].

1.1.3 Electrotechnics

The alternating current resistance of a passive (that is, consisting of passive elements: capacitors, inductors (coils), and resistors) bipolar circuit is a rational function of the current frequency. The following optimization problem arises in the design of digital or analogue multiband electrical filters.

Let E be a closed set of disjoint (frequency) intervals on the real axis. In each interval the transition function $F(\omega)$ is equal to 0 (stopband) or 1 (passband). One must find $R(\omega)$, the best rational approximant of given degree n to the transition function in the uniform metric on E :

$$\|R - F\|_E := \max_{\omega \in E} |R(\omega) - F(\omega)| \longrightarrow \min.$$

When the set E contains just two intervals, the solution is known explicitly: it is a slight modification of a Zolotarëv fraction, the solution of Zolotarëv's third problem [162], which has a parametric representation in terms of elliptic functions:

$$R(u) = sn(K(\tau)|\tau); \quad x(u) = sn(K(n\tau)|n\tau), \quad u \in \mathbb{C}, \quad (1.3)$$

where $sn(\cdot|\cdot)$ is the elliptic sine function and $K(\cdot)$ is the complete elliptic integral with modulus τ . This function (its graph is given in Fig. 1.1) shares many common properties with Chebyshev polynomials; the latter occur as a certain limiting case of Zolotarëv fractions. W Cauer in 1930-ies used this function as a frequency response function for the synthesis of the so-called elliptic electrical filter with one stopband and one passband. These filters are widely used in contemporary electronic industry and display the sharpest transition between the passband and stopband.

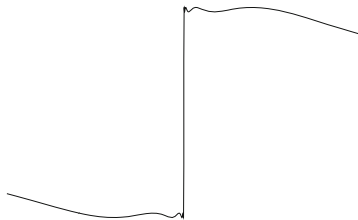


Fig. 1.1 The graph of the Zolotarëv fraction of degree $n = 8$

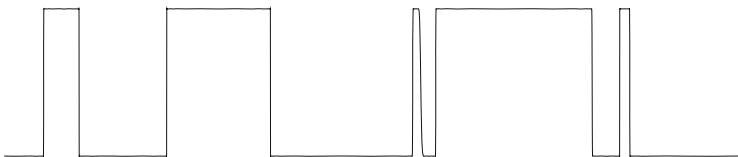


Fig. 1.2 The best rational approximant of degree $n = 88$ to a transition function

The solution of the above-stated problem with an arbitrary number of bands also has an analytic representation in terms of higher analogues of (1.3), see details in [26]. The best rational approximant of degree $n = 88$ to a certain transition function F is presented in Fig. 1.2 (computed by D.V.Yarmolich). For other optimization problems arising in electrical engineering see [14, 44, 45, 49, 154].

1.1.4 V.A. Markov's Problem

In 1892 V. A. Markov considered the following problem [102]:

Find a polynomial $P(x)$ of degree at most n and with uniform norm 1 on a finite interval E that delivers the maximum to a fixed linear form $\langle p^ | P \rangle$ of the coefficients of a polynomial.*

Special cases of this problem, when $\langle p^* | P \rangle$ is one of the coefficients of $P(x)$, the value of $P(x)$, or the value of some derivative of $P(x)$ at a fixed point, were considered by A. A. Markov [101]. In its simplest form, for $n = 2$ A. A. Markov's problem was posed by D.I. Mendelev in his treatise “Études des dissolutions aqueuses, fondée sur les changements de leurs poids spécifiques” (1887). The solution of the above problem reduces to Problem A of least deviation with one constraint $\langle p^* | P \rangle = 1$.

Lemma 1.1. *If $P(x)$ is a (not necessarily unique) solution of V.A. Markov's problem, then $\frac{P(x)}{\langle p^* | P \rangle}$ is a solution of Problem A with one constraint $\langle p^* | P \rangle = 1$. If $P(x)$ is a (not necessarily unique) solution of of problem A with a single constraint, then $P(x)/\|P\|_E$ is a solution of V.A. Markov's problem.*

1.1.5 Other Applications

The following problems provide further examples of problems of least deviation in the uniform metric:

1. Picking interpolation nodes for functions of prescribed smoothness defined on a compact subset of the real axis [31].
2. Examples of extremal polynomials are also provided by the Chebyshev splines of type $[n, 0; k_+, k_-]$, $n, k_{\pm} \geq 0$, that is, the polynomials of degree n with zeros of order k_{\pm} at $x = \pm 1$ which have an $(n + 1 - k_+ - k_-)$ -alternance on $[-1, 1]$.
3. Optimizing one-dimensional quadrature formulae of Gauss type [31, 97].

Definition 1.1. A function $F(x)$ is said to have an l -alternance on the compact set E if there are l different points of E where $F(x)$ takes the values $\pm \|F\|_E$ and the values in the neighbouring points have opposite signs.

1.2 Analyzing Optimization Problems

The most common solutions of least deviation problems are polynomials whose normalizations are extremal in the sense of the definition in the introduction. The reason for this is explained by convex analysis [129, 146]. We now look at Problem A in the introduction:

Let E be a finite system of closed real intervals. Minimize the norm $\|P_n\|_E$ of a polynomial, provided that fixed linear constraints are imposed on its coefficients c_0, c_1, \dots, c_n .

Assume that we look for the solution of Problem A on a fixed affine plane L_{n+1-r} of codimension r in the space of polynomials (2). Such an $(n + 1 - r)$ -plane can be described as the result of a translation of the annihilator of an r -dimensional subspace L_r^* of the dual space. With each non-trivial polynomial $T(x)$ in (2) we associate a convex polyhedral cone in the dual space, which we define below. By the extremal points of the polynomial $T(x)$ with respect to E we shall mean the set

$$\text{ext}_E(T) := \{x \in E : T(x) = \pm \|T\|_E\}.$$

We assign to each extremal point x a functional x^* on the space of polynomials: $\langle x^* | P \rangle := P(x) \cdot \text{sign } T(x)$. The *conical hull* of these functionals

$$\text{cone}\{x_1^*, x_2^*, \dots, x_m^*\} := \left\{ \sum_{s=1}^m \alpha_s x_s^* : \alpha_s \geq 0; \sum_{s=1}^m \alpha_s > 0 \right\}, \quad m = \#\text{ext}_E(T), \quad (1.4)$$

does not contain the origin because $\left\langle \sum_{s=1}^m \alpha_s x_s^* | T \right\rangle = \|T\|_E \sum_{s=1}^m \alpha_s > 0$; we associate it with the polynomial T . By the *dual cone* we shall mean the cone of polynomials

which are positive at each functional in (1.4) (note that only the non-negativity is required in the standard definition).

Theorem 1.1. *A polynomial $T(x) \in L_{n+1-r}$ delivers a minimum in the least deviation Problem A if and only if the subspace L_r^* intersects the cone (1.4) associated with the polynomial.*

Remark 1.1. The cone in this statement, which is generated by all extremal points of the polynomial T can be replaced, in view of Carathéodory's principle, by a cone generated by at most $n+2-r$ extremal points. Thus adjusted, Theorem 1.1 becomes an interpretation of I. Singer criterion of extremality in [138] and [146].

Proof. A polynomial $T \in L_{n+1-r}$ fails to be a solution of Problem A if and only if the norms of the polynomials decrease in some direction issued from T and lying in the plane L_{n+1-r} . Such a direction can be defined by a polynomial $P(x)$ annihilating all functionals in L_r^* and taking values of the same sign as T at the extremal points of T . The following two assertions are therefore equivalent:

- (i) $T(x)$ is a solution of Problem A and
- (ii) The annihilator of L_r^* is disjoint from the cone dual to (1.4).

We can dualize (ii).

1. *If the lineal L_r^* intersects the cone (1.4), then the annihilator of L_r^* is disjoint from the cone dual to (1.4).* For if their intersection is also non-empty, then there exist a functional p^* in the first intersection and a polynomial $P(x)$ in the second such that $0 = \langle p^* | P \rangle > 0$.
2. *If L_r^* is disjoint from the cone (1.4), then the annihilator of L_r^* intersects the cone dual to (1.4).* Indeed, assume that L_r^* is disjoint from the cone (1.4). Now using induction we shall increase L_r^* to a hyperplane disjoint from the cone. This hyperplane annihilates a polynomial which is positive on the half-space bounded by the hyperplane and containing the cone. This polynomial belongs to both the dual cone and $(L_r^*)^\perp$, and so these two sets intersect. It remains to describe the increasing procedure for L_r^* .

At each step, if $r < n$, then we consider a two-dimensional subspace L_2^* linearly independent of L_r^* . Its intersection with the convex cone $L_r^* + \text{cone}\{x_1^*, x_2^*, \dots, x_m^*\}$ is a convex two-dimensional sector with opening less than π for it does not contain the origin. Hence L_2^* contains a one-dimensional subspace L_1^* disjoint from $L_r^* + \text{cone}\{x_1^*, x_2^*, \dots, x_m^*\}$. Setting $L_{r+1}^* := L_1^* + L_r^*$ we complete the induction step. \square

For a fixed subset E of the real axis various Problems A of least deviation differ in the position of the plane L_{n+1-r} and therefore can be indexed by points in the real projective Grassmannian $\text{Gr}(n+2, n+2-r)$ of dimension $r(n+2-r)$. We see that more problems can be posed than there exist solutions, so that the question of the rate of the occurrence of each polynomial in (2) among the solutions of least deviation problems suggests itself. The affine planes L_{n+1-r} incident to a fixed point in the space (2) will be indexed by the directing lineals $L_r^* \in \text{Gr}(n+1, r)$.

In the following statement we characterize the set of Problems A solved by a fixed polynomial $T(x)$.

Lemma 1.2. *The lineals L_r^* in the Grassmannian $\text{Gr}(n+1, r)$ which intersect the fixed cone (1.4) form a closed subset of a Schubert cycle of codimension $\max(0, n+2-r-\#\text{ext}_E(T))$ which has a non-empty (relative) interior.*

Proof. The lineals L_r^* intersecting the cone (1.4) form a closed subset of the Grassmannian because adding the vertex to the cone we make it closed. The set in question lies in some Schubert cycle which we describe below.

Functionals generating the cone (1.4) associated with a polynomial $T(x)$ are linearly independent if their number $m := \#\text{ext}_E(T)$ does not exceed the dimension of the space (2). Assume that the linear span of (1.4) belongs to a filtration of the dual space:

$$0 \subset \mathbb{R}^1 \subset \mathbb{R}^2 \subset \dots \subset \mathbb{R}^{n+1}.$$

If a subspace L_r^* intersects the cone, then we obtain the first inequality in the following system (while the other inequalities hold by dimensional considerations):

$$\dim(L_r^* \cap \mathbb{R}^{\min(m, n+1)}) \geq 1; \quad \dim(L_r^* \cap \mathbb{R}^{n+s+1-r}) \geq s, \quad s = 1, 2, \dots, r,$$

which means that L_r^* lies in the Schubert cycle whose Young diagram is an $(n+1-r) \times r$ rectangle without the (horizontal) row of length $\max(n+2-r-m, 0)$ in the lower right corner. We shall now indicate a subdomain of this Schubert cycle the elements of which intersect the cone (1.4).

In the proof of Theorem 1.1 we established the existence of a support hyperplane of the cone (1.4) containing its origin, but disjoint from the cone proper. Consider now an arbitrary subspace L_l^* of dimension $l := \min(m, n+2-r)-1$ that lies in the intersection of this hyperplane and the linear span of the cone. For a fixed point p^* in the relative interior of the cone there exists a neighbourhood of the origin $\mathcal{O} \subset L_l^*$ such that $p^* + \mathcal{O}$ lies in the cone. We consider now the set of pairs (y^*, L_{r-1}^*) , where $y^* \in \mathcal{O}$ and L_{r-1}^* is a subspace of the support hyperplane such that $\dim(L_{r-1}^* \cap L_l^*) = 0$. Such subspaces L_{r-1}^* fill an open subset of the Grassmannian $\text{Gr}(n, r-1)$, which contains at any rate a Schubert cycle of the maximum dimension $(r-1) \cdot (n+1-r)$. Each pair (y^*, L_{r-1}^*) defines an r -subspace spanned by L_{r-1}^* and the vector $p^* + y^*$ and intersecting the cone. By construction, distinct pairs define distinct r -subspaces. We have thus defined an embedding in the set of r -subspaces intersecting the cone (1.4) of a domain in the space of dimension $(r-1) \cdot (n+1-r) + l = r(n+1-r) - \max(n+2-r-m, 0)$ equal to the dimension of the Schubert cycle in the previous paragraph. \square

DISCUSSION. We see that the greater is the number of extremal points of a polynomial on E , the higher is the dimension of the space of Problems A solved by this polynomial. Of course, our arguments do not mean that a slight perturbation of the conditions of an arbitrary problem brings the number of extremal points of the solution T (which also is not necessarily unique) close to the expected quantity $n+2-r$. Although each polynomial with $\#\text{ext}_E(T) < n+2-r$ is a solution of fewer

problems, the number of such polynomials is much greater. A crude dimension evaluation shows that these two effects roughly counterbalance each other: in (2) the polynomials with $\# \text{ext}_E(T) = m$ lie on submanifolds of codimension $m - 1$ and each is a solution of an $((r - 1) \cdot (n + 1 - r) + m - 1)$ -dimensional set of problems, which yields precisely the dimension of the Grassmannian $\text{Gr}(n + 2, n + 2 - r)$, the index set of least deviation problems.

1.3 Chebyshev Subspaces

Which least deviation problems automatically have extremal polynomials as solutions? Each extremal point of a polynomial T lying in the interior of E is critical, and the value $\pm \|T\|_E$ at this point has an even multiplicity. That is, we are interested in problems whose solutions have many extremal points, provided that the boundary of E consists of few points. For instance, the number of extremal points of a solution is at least $n + 2 - r$ if the polynomials satisfying the homogeneous constraints of the problem form a *Chebyshev* subspace.

Definition 1.2. Finite dimensional space of functions is said to be Chebyshev on E iff any function in this space has no more zeroes in E , than the dimension of the space minus one.

The main source of Chebyshev subspaces is provided by *divisor spaces* occurring in algebraic geometry. Let D be a divisor (a formal finite sum of points with integer multiplicities) in the Riemann sphere that is symmetric relative to the real axis and assume that $D + n \cdot \infty \geq 0$. By the space of this divisor we shall mean the subspace of polynomials in (2) such that the multiplicities of their zeros (and poles: a pole has a negative multiplicity) at an arbitrary point in the Riemann sphere are no smaller than the multiplicity of this point in the divisor:

$$\mathcal{L}(-D) := \{P \in \mathbb{R}[x]: (P) \geq D\}. \quad (1.5)$$

The codimension of $\mathcal{L}(-D)$ in the space of polynomials (2) is equal to the minimum of $\deg D + n$ and $n + 1$. If the support of the divisor D is disjoint from the set E , then the divisor space is Chebyshev on E . The constraints in the corresponding least deviation problem fix the values of the solution T at the finite points in D (and the values of its first derivatives if the multiplicity of the point is higher than 1), and also fix several leading coefficients of T if the point at infinity has multiplicity higher than $(-n)$ in the divisor.

Theorem 1.2 (S. N. Bernstein [33]).

1. If a lineal $(L_r^*)^\perp$ is Chebyshev on a set E , then the solution of the corresponding least deviation problem A has at least $n + 2 - r$ extremal points in E .

2. If the same lineal is Chebyshev on the convex hull of E , then the solution is unique and is characterized by the property of having an $(n + 2 - r)$ -alternance on E (the definition of alternance was given in Sect. 1.1.5.)

Proof. 1. If $T(x)$ is a solution of the least deviation problem, then by Theorem 1.1 for some extremal points x_s of this polynomial and positive weights α_s we obtain

$$\sum_{s=1}^m \alpha_s \cdot \text{sign } T(x_s) \cdot P(x_s) = 0 \quad \text{for each } P(x) \in (L_r^*)^\perp. \quad (1.6)$$

- Assume that the number m of extremal points in (1.6) is less than $n + 2 - r$. The dimension of $(L_r^*)^\perp$ is $n + 1 - r$, therefore there exists a polynomial $P(x) \in (L_r^*)^\perp$ vanishing at $n - r$ points: at x_1, x_2, \dots, x_{m-1} and at some $n + 1 - r - m$ points in $E \setminus \text{ext}_E(T)$. Since $(L_r^*)^\perp$ is a Chebyshev space, it follows that $P(x_m) \neq 0$, and therefore in (1.6) we have $\alpha_m = 0$, a contradiction.
2. Assume that the solution $T(x)$ has the same sign at two neighbouring extremal points, x_s and x_{s+1} . We consider a polynomial $P(x) \in (L_r^*)^\perp$ vanishing at the remaining $n - r$ extremal points (see the remark to Theorem 1.1). Then equality (1.6) takes the form $\alpha_s P(x_s) + \alpha_{s+1} P(x_{s+1}) = 0$. This means that $P(x)$ must also have a zero on the interval $[x_s, x_{s+1}]$, in contradiction with the Chebyshev property of the space $(L_r^*)^\perp$ on $\text{conv } E$. Thus, each solution T has an $(n + 2 - r)$ -alternance on E . Conversely, each polynomial $T(x) \in L_{n+1-r}$ having an $(n + 2 - r)$ -alternance on E is a unique solution. If there exists another polynomial whose deviation on E does not exceed that of $T(x)$, then their difference belongs to $(L_r^*)^\perp$ and has at least $n + 1 - r$ zeros on $\text{conv } E$, so that it is trivial. \square

1.4 The Problem of Optimal Stability Polynomial

Problem B of finding an optimal stability polynomial can be reduced to the least deviation problem A with *Chebyshev constraints* that we have just considered.

Theorem 1.3 ([40, 127]). *The problem of optimal stability polynomial is uniquely solvable. A polynomial*

$$R_n(x) = 1 + x + \frac{x^2}{2!} + \dots + \frac{x^p}{p!} + o(x^p) \quad (1.7)$$

and an interval $E = [-L, 0]$ on which $\|R_n\|_E$ has deviation 1 solve Problem B if and only if R_n has an $(n + 1 - p)$ -alternance on $E \setminus \{0\}$.

Proof. As l increases, the closed ball $\{\|P\|_{[-l, 0]} \leq 1\}$ in the space of polynomials (2) contracts (linearly, but anisotropically) and, in the limit as $l \rightarrow \infty$, contains only constant polynomials, which cannot satisfy the constraints (1.7) if $p > 1$.

Hence there exist (i) a largest interval $E := [-L, 0]$ and (ii) a polynomial $R_n(x)$ with deviation 1 on E satisfying the constraints.

1. We claim that at the same time $R_n(x)$ is a solution of Problem A with constraints (1.7) on the interval $E' := [-L, -\varepsilon]$; here ε is any positive quantity that is smaller than 1, $L/2$, and $1/\max |P''(x)|$, where the maximum is considered over the compact set $\{(P, x): x \in [-L/2, 0]; \|P\|_{[-L, -L/2]} \leq 1; \deg P \leq n\}$. Indeed, assume that there exists a polynomial $P(x)$ in the space (2) satisfying the $r = p + 1$ constraints (1.7) and with deviation less than 1 on E' . In view of the local increase of $P(x)$ in a neighbourhood of the origin and the smallness of ε , $\|P\|_E \leq 1$. Since the value of $P(x)$ at the end-point $x = -L$ is less than 1 in absolute value, E can be increased while keeping the norm of $P(x)$ the same, which contradicts the maximality of E .

The linear constraints in (1.7) mean that the $r = p + 1$ lower coefficients of the polynomial are fixed. A polynomial of degree at most n which satisfies the corresponding homogeneous constraints has a zero of order r at $x = 0$, so it has at most $n - r$ zeros on E' , and therefore the corresponding subspace is Chebyshev. By Bernstein's Theorem 1.2 the least deviation polynomial $R_n(x)$ is unique and has an $(n + 1 - p)$ -alternance on E' .

2. Conversely, let $R_n(x)$ be a polynomial of the form (1.7) with an $(n + p - 1)$ -alternance on the half-open interval $[-L, 0)$ and with deviation 1 in this interval. By Theorem 1.2, $R_n(x)$ solves the least deviation problem with constraints (1.7) on the set $E' = [-L, -\varepsilon]$, where $\varepsilon > 0$ is sufficiently small. The optimal stability polynomial has deviation 1 on E' and satisfies the same constraints. Since the least deviation problem has a unique solution, R_n is the optimal stability polynomial. \square

1.4.1 Properties of Optimal Stability Polynomials

The existence of an alternance enables us to find an estimate for the number of zeros of the optimal stability polynomial and its derivative in the stability region $E = [-L, 0]$. Their precise number is described by the following result.

Lemma 1.3. *The solution $R_n(x)$ of the optimization Problem B and its derivative $R'_n(x)$ have only simple zeros, which lie in E and $\mathbb{C} \setminus \mathbb{R}$ in the following amounts:*

The number of zeros of R_n	in E	in $\mathbb{C} \setminus \mathbb{R}$
p even	$n - p$	p
p odd	$n - p + 1$	$p - 1$

The number of zeros of dR_n/dx	in E	in $\mathbb{C} \setminus \mathbb{R}$
p even	$n - p + 1$	$p - 2$
p odd	$n - p$	$p - 1$

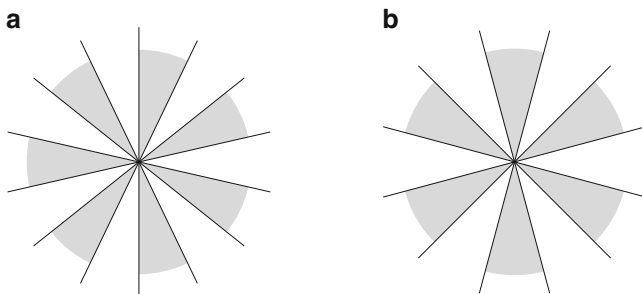


Fig. 1.3 Order stars in a neighbourhood of the origin for (a) even p and (b) odd p

Proof. Assume that a real polynomial approximates the exponential function at the origin with precise order p : $P_n(x) - \exp(x) \sim x^{p+1}$. Then it has at least $2[p/2]$ distinct complex zeros [1]. The proof of this statement is based on the analysis of the topology of the *order stars* [71].

We consider two open subsets of the complex plane: black and white, that are symmetric relative to the real axis. At points in the white subset the function $P_n(x)/\exp(x)$ is less than 1 in absolute value, in the black subset its absolute value is greater than 1. These two subsets, which are called the *order stars*, have the following easily verified properties [71]:

- (a) The black and the white sets have precisely one unbounded component each.
- (b) In the neighbourhood of the origin these subsets make up curvilinear sectors of angle $\pi/(p+1)$ and of alternating colours (see Fig. 1.3).
- (c) Each bounded component of the white set contains a zero of the polynomial (use the maximum principle for the harmonic function $\log |P(x) \exp(-x)|$).
- (d) The black set has no bounded components (they would contain poles of the polynomial) and is therefore connected.

Hence one concludes that an arbitrary component of the white set contains at most one sector: otherwise (d) fails. If a white component contains a sector lying strictly in the upper or the lower half-plane, then the entire component lies in this half-plane since the white subset is mirror-symmetric. In addition, such a component must be bounded: by (a) the unbounded component intersects both half-planes. We see from Fig. 1.3 that for even p there exist p white sectors disjoint from the real axis and for odd p there exist at least $p-1$ such sectors. Each of them lies in some bounded white component disjoint from the real axis and containing a zero of the polynomial $P_n(x)$ by (c). Correspondingly, our polynomial has at least $2[p/2]$ complex zeros and its derivative has at least $2[(p-1)/2]$ complex zeros.

One can say more about the position of the zeros of the optimal stability polynomial $R_n(x)$ and its derivative. Between two neighbouring points of the alternance there exists a zero of the polynomial, and each point of the alternance lying in the interior of E is a zero of its derivative. The interval between the origin and the extreme right point x_1 in the alternance contains either a zero of the polynomial

(when $R_n(x_1) = -1$) or a zero of its derivative (when $R_n(x_1) = 1$). For even p we have already found $(n - p) + p = n$ distinct zeros of R_n and for odd p we have found $(n - p) + (p - 1) = n - 1$ distinct zeros of R'_n . Hence $R_n(x_1) = (-1)^p$ and the distribution of zeros is as required in the lemma. \square

1.5 Problems and Exercises

1. Find the value of the parameter (5) for the Chebyshev spline of type $[n, 0; k_+, k_-]$ (see the definition in Sect. 1.1.5).

Answer. $g = \max(k_+ - 1, 0) + \max(k_- - 1, 0)$.

2. A *Shabat polynomial* is a polynomial with precisely two finite critical values; for definiteness let these be ± 1 . Find the extremality order g (defined by (5)) of a Shabat polynomial $P(x)$ from the topology of the associated graph $P^{-1}([-1, 1])$.
3. Prove Lemma 1.1.
4. Prove the first theorem of V. A. Markov [102]:

A polynomial $T(x)$ solves Problem A with one linear constraint $\langle p^ | T(x) \rangle = 1$ if and only if the space (2) contains no polynomial $P(x)$ which (1) satisfies the homogeneous linear constraint $\langle p^* | P \rangle = 0$ and (2) takes values of the same sign as T at all extremal points of T : $P(x)/T(x) > 0$, $x \in \text{ext}_E(T)$.*

5. Let $x_1 > x_2 > \dots > x_m$ be the extremal points of a polynomial $T(x)$ on a closed interval E . Consider the Lagrange interpolation polynomials with these nodes: $\Phi(x) := \prod_{s=1}^m (x - x_s)$; $\Phi_s(x) := \Phi(x)/(x - x_s)$. Prove the second theorem of V. A. Markov [102]:

A polynomial $T(x)$ solves Problem A with one linear constraint $\langle p^ | T(x) \rangle = 1$ if and only if (1) for $m < n + 1$ and $s = 0, 1, \dots, n - m$, $\langle p^* | x^s \Phi(x) \rangle = 0$, and (2) some quantities in the set $(-1)^s \langle p^* | \Phi_s \rangle T(x_s)$, $s = 1, \dots, m$, are distinct from zero, but no two of them have distinct signs.*

Hint. Assume that there exists a polynomial $P(x)$ mentioned in the first Markov theorem. Divide $P(x)$ by $\Phi(x)$ with a remainder and expand the remainder in the polynomials $\Phi_s(x)$. Now bearing in mind that the sign of $\Phi_s(x_s)$ is opposite to the sign of $(-1)^s$ we can derive a contradiction with conditions (1) and (2).

6. Prove a theorem due to Carathéodory: let X be a subset of \mathbb{R}^n ; then any point in its convex hull is a convex combination of at most $n + 1$ points in X .
7. Prove that the cone (1.4) associated with a polynomial $T(x)$ has dimension equal to $m := \#\text{ext}_E(T)$, provided that $m \leq n + 1$.

Hint. The values which functionals generating the cone take at the basis $1, x, x^2, x^3 \dots$ of the space of polynomials make up a Vandermonde matrix.

8. Give an example of a polynomial $T(x)$ of degree n and a set E such that the number $m := \#\text{ext}_E(T)$ of extremal points is larger than $n + 1$. Show that always $m \leq 2n$.
9. Let D be a divisor symmetric relative to the real axis such that $D + n \cdot \infty \geq 0$. Prove that, if its support is disjoint from compact subset E of the real axis, then $\mathcal{L}(-D)$ is a Chebyshev space on E , that is, the number of zeros (with multiplicities) on E of a polynomial $P(x) \in \mathcal{L}(-D)$ is at least one less than the dimension of the space.
10. Prove properties (a–d) of order stars, which have been used in the proof of Lemma 1.3.
11. Use Viète's formulae to prove that a real polynomial $P(x)$ approximating the exponential function at the origin $x = 0$ with order p (so that $P(x) - \exp(x) = o(x^p)$) has at least $[p/2]$ pairs of complex conjugate roots.
12. On the basis of Lemma 1.3 show that for odd p the optimal stability polynomial has a similar graph to the classical Chebyshev polynomial of degree $n - p + 1$. What is the qualitative graph of the optimal stability polynomials for even p ?

Chapter 2

Chebyshev Representation of Polynomials

Essentially, all the quantities in this (Abel-Pell) equation are unknown, even the degree of the polynomial. Nonetheless it is possible to solve it!

M. Sodin and P. Yuditskii [139]

Chebyshev and his students Zolotarëv, the brothers V. A. and A. A. Markov, Korkin, and Posse reduced extremal problems for polynomials to Pell's equation, a geometric interpretation of which is suggested in the following construction.

CONSTRUCTION ([37, 40]). With an arbitrary polynomial $P(x)$ we associate the two-sheeted Riemann surface

$$M = M(\mathbf{e}) = \left\{ (x, w) \in \mathbb{C}^2 : w^2 = \prod_{s=1}^{2g+2} (x - e_s) \right\}, \quad (2.1)$$

ramified over the points $\mathbf{e} := \{e_s\}_{s=1}^{2g+2}$ at which the polynomial takes the values ± 1 with odd multiplicity (that is, these are simple values in the general case).

DISCUSSION. Here is a purely topological motivation for the construction [37, 38]; the motivation related to Pell's equation may be found in [26]. Polynomials $P(x)$ such that the great majority of the inverse images of the points ± 1 are simple critical points can be constructed in accordance with the following pattern. Consider a cover of the Riemann sphere ramified to the second order over the points ± 1 ; the simplest example here is the Zhukovskii function $\sigma(u) := (u + 1/u)/2$. A composite map factoring through such a covering has a property close to the required one: any point in the inverse image of ± 1 is critical, with even ramification order. To take account of the points $\mathbf{e} \subset P^{-1}(\pm 1)$ at which the value $P(x)$ is taken with odd multiplicity, consider a covering surface ramified to the second order over \mathbf{e} : the simplest surface of this kind is $M(\mathbf{e})$ with the natural projection $\chi(x, w) := x$ onto the Riemann sphere:

$$\begin{array}{ccc}
 (x, w) \in M(\mathbf{e}) & \xrightarrow{\tilde{P}} & \mathbb{CP}^1 \ni u \\
 \chi \downarrow & & \downarrow \sigma \\
 x \in \mathbb{CP}^1 & \xrightarrow{P} & \mathbb{CP}^1
 \end{array} \tag{2.2}$$

Any map \tilde{P} between the covering spaces satisfying the equivariance condition $\tilde{P}(x, -w) = 1/\tilde{P}(x, w)$ with respect to the deck transformations of the two covering spaces induces a map P between the bases which has an odd ramification order at the points in $\mathbf{e} \subset P^{-1}(\pm 1)$ and an even order at the points in $P^{-1}(\pm 1) \setminus \mathbf{e}$. The converse result also holds: any map P between the base spaces of the diagram (2.2) which is ramified to an even order over ± 1 , except at the points in \mathbf{e} , can be lifted to an equivariant map of the covering spaces in the diagram (2.2). We see that finding extremal polynomials $P(x)$ is equivalent to finding equivariant functions $\tilde{P}(x, w)$ on suitable hyperelliptic Riemann surfaces. As regards the questions on the existence of such an equivariant function and its representation, they can be answered in terms of the Riemann surface M , which is described by $2g$ essential parameters. Thus we have considerably reduced the dimension of the problem (of course, provided that $2g \ll \deg P(x)$).

Lemma 2.1. *The genus of the curve associated with a polynomial $P(x)$ is equal to the extremality number g of P defined by formula (5).*

Proof. A polynomial P of degree n has $n - 1$ critical points in \mathbb{C} :

$$n - 1 = \sum_x \text{ord } P'(x) = g + \sum_{x: P(x)=\pm 1} \left[\frac{1}{2}(\text{ord } P'(x) + 1) \right].$$

Now we calculate $\deg \mathbf{e}$, the number of odd-order zeros of the polynomial $P^2(x) - 1$.

$$2n = \sum_{x: P(x)=\pm 1} (\text{ord } P'(x) + 1) = \deg \mathbf{e} + \sum_{x: P(x)=\pm 1} 2 \left[\frac{1}{2}(\text{ord } P'(x) + 1) \right],$$

which shows that $\deg \mathbf{e} = 2g + 2$, that is, the genus of the hyperelliptic curve $M(\mathbf{e})$ is g . We have used two identities for integers: $m = \lfloor \frac{m}{2} \rfloor + \lfloor \frac{m+1}{2} \rfloor$ and $2\lfloor \frac{m}{2} \rfloor = m$ (resp. $m - 1$) when m is even (resp. odd). \square

Example 2.1. Let E be a closed interval and assume that the r constraints in extremal Problem A define a Chebyshev subspace $(L_r^*)^\perp$. Then the normalized solution $P_n(x) := T_n(x)/\|T_n\|_E$ corresponds to a curve M of genus $g \leq r - 1$. Indeed, the full inverse image $P_n^{-1}(\pm 1)$ contains $2n$ points counted with multiplicities. At least $n - r$ points of even multiplicity from the inverse image lie in the interior of E . At the $2g + 2$ ramification points of M the value of P_n has odd multiplicity, and therefore $2n \geq 2(n - r) + 2g + 2$.

2.1 Real Hyperelliptic Curves

We recall several concepts of the geometry of real hyperelliptic curves [111]. A compact complex curve M_c of genus g is said to be *hyperelliptic* if it admits a *conformal involution* J with $2g + 2$ fixed points. If $g > 1$, then such an involution is unique (if it exists), while for $g = 0, 1$ there exist infinitely many involutions J . A curve M_c is said to be *real* if it admits an *anticonformal involution* \bar{J} (a *reflection*). Whatever the genus, there can exist several anticonformal involutions, and therefore one must consider a pair (M_c, \bar{J}) . We now discuss the connections between these transformations. If a curve M_c admits a hyperelliptic involution J and an anticonformal involution \bar{J} , then these involutions commute for $g > 1$ ($\bar{J}J\bar{J}$ is another hyperelliptic involution). This is in general not so for $g = 0, 1$, but we shall assume that $\bar{J}J = J\bar{J}$. The interchangeability of the involutions means that \bar{J} acts on $\mathbb{CP}^1 = M_c/J$. The anticonformal involution of the Riemann sphere interchanges the interior and the exterior of its *isometric circle*. The points on this circle are either fixed (for instance, when $\bar{J}x = 1/\bar{x}$) or are taken to the antipodal points (for instance, when $\bar{J}x = -1/\bar{x}$). Hence the real hyperelliptic curves fall into two classes: with orientable quotient $M_c/\langle J, \bar{J} \rangle$ (=a disc) and with non-orientable one (=the projective plane). Throughout, we consider only the first class of curves, but keep for them the general name of *real hyperelliptic curves*.

We lift the circle of \bar{J} -fixed points from the sphere to the curve M_c . On the curve we obtain *real ovals* that are fixed by the \bar{J} -action on M_c and *coreal ovals* that are fixed by $\bar{J}J$. Assume that $2k$ ramification points (fixed points of the involution J), $k = 0, 1, \dots, g + 1$, are fixed by the reflection \bar{J} . If $k > 0$, then there exist on M_c precisely k real and k coreal ovals, and the projections of ovals in these two classes alternate on the circle of \bar{J} -fixed points on the Riemann sphere. The case $k = 0$ drops out of the general picture: for even g there exists only one oval, either real or coreal, while for odd g there exist two ovals of the same name (Fig. 2.1).

Real hyperelliptic curves have a convenient algebraic model (2.1) in which all *branch points* e_s are distinct and form the *branch divisor* $\mathbf{e} := \{e_s\}_{s=1}^{2g+2}$ symmetric with respect to the real axis. In Fig. 2.2 we plot by bold lines the *system of cuts* Λ on $\mathbb{C} \setminus \mathbf{e}$ outside which the function $w(x)$ has a single-valued branch. The curve $M(\mathbf{e})$ can be thought of as two sheets of $\mathbb{C} \setminus \Lambda$ glued crosswise along the cuts. The compactification M_c of the curve (2.1) is obtained by adding a pair of points at infinity: ∞_+ on the upper and ∞_- on the lower sheet. In this model the hyperelliptic and the anticonformal involutions have the following form: $J(x, w) := (x, -w)$; $\bar{J}(x, w) := (\bar{x}, \bar{w})$. For such a choice of \bar{J} the punctures ∞_{\pm} lie on a real oval and

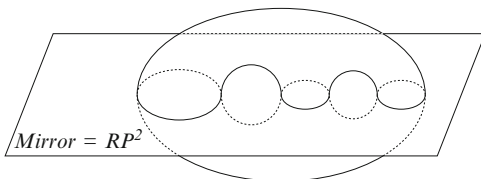


Fig. 2.1 A real genus two curve in \mathbb{C}^2 with three real ovals

the topological invariant k of the real curve M can be defined as the number of coreal ovals on it.

2.1.1 The Homology Space and the Lattice L_M

There are two punctures ∞_{\pm} on M , and therefore one must add to the usual $2g$ independent 1-cycles the cycle encircling an (arbitrary) puncture. In the $(2g + 1)$ -dimensional real *homology space* $H_1(M; \mathbb{R})$ we obtain a natural action of the anticonformal involution \bar{J} , which decomposes the space into the sum of the eigenspaces $H_1^{\pm}(M; \mathbb{R})$ corresponding to the eigenvalues ± 1 . The *even* 1-cycles C satisfy the equality $\bar{J}C = C$ and form the subspace $H_1^+(M; \mathbb{R})$. The *odd* 1-cycles C , defined by the condition $\bar{J}C = -C$, give rise to the subspace $H_1^-(M; \mathbb{R})$. We present an example of g even and $g + 1$ odd cycles on M in the case $k > 0$ in Fig. 2.2a,b, respectively (the dashed line means that the contour lies on the lower sheet). The sum $C_{\infty} := C_0^- + C_1^- + C_2^- + \dots + C_g^-$ is homologous to the cycle encircling a puncture of the curve at infinity and spans a distinguished 1-dimensional subspace $H_1^{\infty}(M)$ of $H_1^-(M)$. The first $k - 1$ even cycles $C_1^+, C_2^+, \dots, C_{k-1}^+$ and the first k odd cycles $C_0^-, C_1^-, \dots, C_{k-1}^-$ in the picture are canonically selected: they are the sums of several real ovals of the curve and the coreal oval, respectively. For

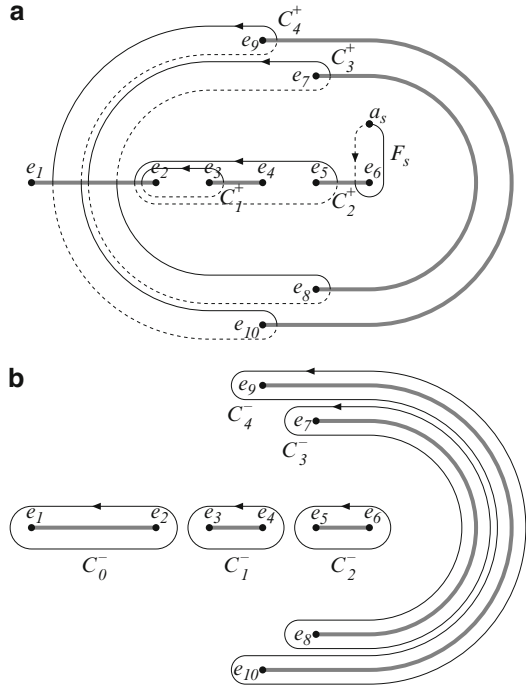


Fig. 2.2 The system of cuts Λ in the plane and a basis in the lattice (a) $H_1^+(M, \mathbb{Z})$ (b) $H_1^-(M, \mathbb{Z})$ for $g = 4, k = 3$

the remaining $g - k + 1$ cycles in either system there is no natural way to select them: we shall again come across this problem in what follows.

Lemma 2.2. *For $k > 0$ the cycles C_s^+ , $s = 1, \dots, g$, and C_s^- , $s = 0, 1, \dots, g$, plotted in Fig. 2.2 form bases of the corresponding subspaces $H_1^\pm(M, \mathbb{R})$ and of the lattices $H_1^\pm(M, \mathbb{Z}) := H_1^\pm(M, \mathbb{R}) \cap H_1(M, \mathbb{Z})$.*

Proof. Consider the relative homology space $H_1(M_c, \{\infty_\pm\}; \mathbb{Z})$ formed by 1-chains on the compact surface with boundaries at the punctures of M . We shall regard relative 1-cycles as functionals on $H_1(M; \mathbb{R})$, integer-valued on the lattice $H_1(M; \mathbb{Z})$. The corresponding pairing is described by the intersection form [63, 151].

It is easy to find relative 1-cycles \tilde{C}_j such that $\tilde{C}_j \circ C_s^- = \delta_{js}$, $j, s = 0, \dots, g$. Any relative cycle of this kind \tilde{C}_j starts from ∞_+ and goes to a ramification point along the upper sheet $\mathbb{C} \setminus \Lambda$ of the surface, after which it goes to ∞_- along the lower sheet. As there exists a biorthogonal basis of functionals, the cycles C_s^- , $s = 0, \dots, g$, are linearly independent in the Euclidean space $H_1^-(M, \mathbb{R})$. In a similar way, the C_s^+ , $s = 1, \dots, g$, are linearly independent in $H_1^+(M, \mathbb{R})$. Since $2g + 1 \leq \dim H_1^+(M) + \dim H_1^-(M) = \dim H_1(M) = 2g + 1$, these 1-cycles form bases in the even and odd homology subspaces on the punctured curve, respectively.

Each odd integral cycle C^- can be expanded with respect to the basis of the C_s^- . The coefficients of the expansions are integers $\tilde{C}_s \circ C^-$, and so this basis also is a basis of the lattice $H_1^-(M, \mathbb{Z})$. For even cycles the argument is similar. \square

The involution \bar{J} reverses orientation, and therefore $\bar{J}C \circ \bar{J}C' = -C \circ C'$ for any cycles C, C' in $H_1(M, \mathbb{R})$. If these cycles have the same parity, then their intersection index is zero. Looking at Fig. 2.2 we readily calculate all the remaining intersection indices.

Lemma 2.3. *Only the following entries of the intersection matrix of the homology basis introduced above are distinct from 0:*

$$\begin{aligned} C_s^+ \circ C_s^- &= 1, & s &= 1, \dots, k-1, \\ C_s^+ \circ C_s^- &= 2, & s &= k, \dots, g, \\ C_s^+ \circ C_0^- &= -C_s^+ \circ C_s^-, & s &= 1, \dots, g. \end{aligned} \tag{2.3}$$

For the investigation of the Chebyshev construction the sublattice L_M of the lattice of odd cycles that is generated by the elements $2C_0^-, 2C_1^-, \dots, 2C_{k-1}^-; C_k^-, C_{k+1}^-, \dots, C_g^-$ is of importance. For $k = 0$ the lattices L_M and $H_1^-(M, \mathbb{Z})$ coincide, while for $k > 0$ the lattice L_M has the following “coordinate-free” description.

Lemma 2.4. *If $k > 0$, then the following two lattices coincide with L_M :*

- (1) *the projection of the lattice $2H_1(M, \mathbb{Z})$ onto the subspace $H_1^-(M, \mathbb{R})$ along $H_1^+(M, \mathbb{R})$.*
- (2) *the cycles in $H_1^-(M, \mathbb{Z})$ which have even intersection indices with all components of the real ovals on M (the punctures at infinity partition one of the real ovals and it should be considered as a relative homology).*

Proof. The projection of the space $H_1(M, \mathbb{R})$ onto H_1^- along H_1^+ has the form $C \rightarrow \frac{1}{2}(C - \bar{J}C)$. The assertions of the lemma can be verified on the generators of the lattices. \square

2.1.2 The Space of Differentials on the Curve

The meromorphic 1-forms ξ on M whose only possible singularities are simple poles at infinity make up a complex linear space of dimension $g + 1$. This space contains a unique meromorphic differential with fixed residue at infinity and fixed g periods over the cycles in a basis of $H_1^+(M)$ (or in a basis of $H_1^-(M)/H_1^\infty(M)$): this follows from the Riemann bilinear relations [70] in view of what we know about the intersection matrix of a homology basis (see Problems 13 and 15 at the end of this chapter).

The anticonformal involution \bar{J} of the curve also acts on the space of differentials: $\xi \rightarrow \bar{J}\bar{\xi}$. Fixed points of this action are usually called [111] *real differentials*. In the algebraic model (2.1), real 1-forms with simple poles at infinity have the representation $\xi = P_g(x)w^{-1}dx$ with real polynomial $P_g(x)$ of degree g . Integration of real differentials over even cycles yields real quantities and integration over odd cycles yields purely imaginary quantities. The *period map* $\Pi(\xi)$ assigns to each real differential ξ an element of the real cohomology group $H^1(M, \mathbb{R})$ of the curve M :

$$\langle \Pi(\xi) | C^+ + C^- \rangle := \int_{C^+} \xi - i \int_{C^-} \xi, \quad C^\pm \in H_1^\pm(M, \mathbb{R}). \quad (2.4)$$

2.1.3 A Distinguished Form η_M on the Curve

There exists on M a unique 1-form η_M with purely imaginary periods, simple poles at infinity and residues ∓ 1 at ∞_\pm :

$$\eta_M = \left(x^g + \sum_{s=0}^{g-1} c_s x^s \right) \frac{dx}{w}. \quad (2.5)$$

The distinguished differential η_M also satisfies another normalization.

Lemma 2.5. *The differential (2.5) associated with the real curve M is real, and so it has zero periods over all the even cycles.*

Proof. We shall verify that η_M is a real differential: the meromorphic differential $\bar{J}\tilde{\eta}_M$ has residues ∓ 1 at the points ∞_{\pm} and purely imaginary periods. By the uniqueness of the differential so normalized we obtain $\bar{J}\tilde{\eta}_M = \eta_M$. Each real differential has real periods over even 1-cycles, but the distinguished differential η_M has purely imaginary periods, and so they are equal to zero. \square

2.2 Polynomials and Curves

The following result describes the range of the Chebyshev map taking polynomials to curves as well as the inverse map.

Theorem 2.1. *The construction described at the beginning of the chapter establishes a one-to-one correspondence between real polynomials $P_n(x)$ of degree n , considered up to the sign, and real hyperelliptic curves M for which the period map of the differential form η_M associated with the curve yields a $4\pi n^{-1}\mathbb{Z}$ -valued functional on the lattice L_M :*

$$-i \int_{C^-} \eta_M \in 4\pi n^{-1}\mathbb{Z}, \quad C^- \in L_M. \quad (2.6)$$

A polynomial can be recovered from the associated curve M by the formula

$$P_n(x) = P_n(e_s) \cos\left(ni \int_{(e_s, 0)}^{(x, w)} \eta_M\right), \quad (2.7)$$

where the result is independent of the integration path on M , of the choice between the two possible values of $w(x)$, and of the branch point e_s , $s = 1, \dots, 2g+2$, taken for the initial point of integration.

Proof. A. *The correspondence $P_n \rightarrow M$.* If a curve M of the form (2.1) corresponds to a polynomial $P_n(x)$ of degree n , then Pell's equation with polynomial coefficient $D(x) := \prod_{s=1}^{2g+2} (x - e_s) = w^2(x)$ is fulfilled:

$$P_n^2(x) - 1 = w^2(x) Q_{n-g-1}^2(x),$$

where $Q_{n-g-1}(x)$ is a real polynomial. We consider the meromorphic Akhiezer function $\tilde{P}(x, w) := P_n(x) + \sqrt{P_n^2(x) - 1} = P_n(x) + w Q_{n-g-1}(x)$ on the curve M_c . It intertwines the actions of the deck transformation groups of the coverings χ and σ in the diagram (2.2): $\tilde{P}(x, -w) = P_n(x) - w Q_{n-g-1}(x) = \frac{1}{\tilde{P}(x, w)}$.

This function has a pole of order n at ∞_+ , and therefore it has a zero of the same order at ∞_- , and its divisor contains only these two points.

We claim that the meromorphic differential

$$\eta := \frac{1}{n} \frac{d\tilde{P}}{\tilde{P}}$$

is equal to the distinguished differential η_M on the curve. Indeed, the only singularities of η are simple poles at infinity with residues ± 1 . All the periods of η are purely imaginary because for closed contours C on M we have

$$\int_C \eta = n^{-1} \log \tilde{P}(x, w) \Big|_C \in \frac{2\pi i}{n} \mathbb{Z}.$$

Let us calculate the period of the distinguished form η_M over the cycle C in the lattice L_M . When $k > 0$, it follows from Lemma 2.4 that $C = B - \bar{J}B$ for some integral cycle B . Hence

$$\int_C \eta_M = 2 \int_B \eta_M = \frac{2}{n} \log(\tilde{P}(x, w))|_B \in \frac{4\pi i}{n} \mathbb{Z}.$$

For $k = 0$ our argument is different: any basic odd cycle C is represented as $B - JB$ with a 1-chain $B = -\bar{J}B$, a symmetric arc with end-points at conjugate branch points e and \bar{e} . Now,

$$\int_C \eta_M = 2 \int_B \eta_M = \frac{2}{n} \log(\tilde{P}(x, w))|_B \in \frac{4\pi i}{n} \mathbb{Z}$$

since $\tilde{P}(e, 0) = P_n(e) = \pm 1 = P_n(\bar{e}) = \tilde{P}(\bar{e}, 0)$. We have shown that the inclusion (2.6) holds once the curve M stems from a real polynomial.

Inversion formula (2.7) follows from the equalities

$$\begin{aligned} P_n(x) &= \frac{(\tilde{P}(x, w) + \tilde{P}(x, -w))}{2} = \cos(i \log \tilde{P}(x, w)) \\ &= \cos \left(i \log \tilde{P}(e_s, 0) + ni \int_{(e_s, 0)}^{(x, w)} \eta_M \right) = P_n(e_s) \cos \left(ni \int_{(e_s, 0)}^{(x, w)} \eta_M \right). \end{aligned}$$

- B. *The correspondence $M \rightarrow P_n$.* If the curve M satisfies the assumptions of the theorem, then the functional $\Pi(\eta_M)$ is $\frac{2\pi}{n}\mathbb{Z}$ -valued at all the integral 1-cycles. For if $C \in H_1(M, \mathbb{Z})$, then $C - \bar{J}C \in L_M$ and $\langle \Pi(\eta_M) | C \rangle = \frac{1}{2} \langle \Pi(\eta_M) | C - \bar{J}C \rangle \in \frac{2\pi}{n} \mathbb{Z}$.

For $P_n(e_s) = \pm 1$ the right-hand side of (2.7) defines a meromorphic function on M_c , which is stable under the involution J and has poles of order n at the

points at infinity. Hence P_n is a polynomial of degree n in x , and it is real because

$$\begin{aligned} P_n(\bar{x}) &= P_n(e_s) \cos ni \left(\int_{(e_s,0)}^{(\bar{e}_s,0)} \eta_M + \int_{(\bar{e}_s,0)}^{(\bar{x},\bar{w})} \eta_M \right) \\ &\stackrel{(*)}{=} P_n(e_s) \cos ni \overline{\int_{(e_s,0)}^{(x,w)} \eta_M} = \overline{P_n(x)}. \end{aligned}$$

(In the transition $(*)$ we use the inclusion $\int_{(e_s,0)}^{(\bar{e}_s,0)} \eta_M \in \frac{2\pi i}{n} \mathbb{Z}$ and the fact that η_M is a real differential.) It is easy to verify that $P_n(x)$ takes values ± 1 with odd multiplicity at the branch points of the curve M and only at these points. \square

REMARKS. 1. The reader can find various versions of Theorem 2.1 in [37, 40, 128, 139], and [115].

2. Associated with complex (extremal) polynomials $P_n(x)$ are complex curves M , which are characterized by a simpler condition: $\int_C \eta_M \in \frac{2\pi i}{n} \mathbb{Z}$ for each integral cycle C on the curve. On a real curve M half these conditions hold automatically because the distinguished differential η_M is real and $\int_C \eta_M = 0$ for each even cycle C (see Lemma 2.5).
3. This theorem presents the following necessary and sufficient condition for the solvability of Pell's equation with complex polynomial coefficient $D(x)$: *all the periods of the differential $\eta_M / (2\pi i)$ (associated with the curve M defined by the coefficient $D(x)$) must be rational. When this condition is satisfied, all the solutions of Pell's equation are represented as follows:*

$$\begin{aligned} P_n(x) &= \pm \cos(ni \int_{(e,0)}^{(x,w)} \eta_M), \\ Q_{n-g-1}(x) &= \pm i w^{-1}(x) \sin(ni \int_{(e,0)}^{(x,w)} \eta_M), \end{aligned}$$

where the products of the degree n and all the above rational periods are integers (there are only $2g$ independent periods in the complex case and g periods in the real case). The method of the proof of the theorem goes back to Abel's famous paper [2].

4. A purely algebraic approach to the polynomial Pell equation, which is in fact based on the expansion of the function $\sqrt{D(x)}$ in a continued fraction, was presented in [99] and [140]. If the degree n of the solution is large, then this approach cannot be implemented in practice due to computational instability.
5. A generalization of Chebyshev's construction can be used for representing rational functions the majority of whose critical points are simple with the corresponding values belonging to a fixed four-point set [26]. The generalized construction, as well as the one under consideration here, is closely related to the Weierstrass-Poincaré reduction theory of abelian integrals [19, 82].

2.2.1 The Stability of the Chebyshev Representation

In calculations with finite accuracy we obtain curves M which only approximately satisfy Abel's equations (11). Can we use the Chebyshev representation (2.7) in this case? In the special case of Chebyshev polynomials for several intervals the stability of the representation was demonstrated in [37]. The method and result of that paper can be extended to the general case. We can also give a numerical proof: in calculations with an accuracy of 10^{-13} we can fulfil Abel's equations with an accuracy of 10^{-12} . Then in the case of degree $n = 50$, for a suitable choice of interpolation nodes, the function (2.7) coincides with its Lagrange interpolation polynomial to within 10^{-10} ; however, this accuracy drops as n increases.

For generic curves $M(\mathbf{e})$ the function (2.7) is single-valued only when considered on the universal cover of the curve. After the projection onto the x -plane it will be a multivalued analytic function with (locally second-order) branch points at points in the divisor \mathbf{e} . In a small neighbourhood of a fixed pair consisting of a divisor $\mathbf{e}^0 \ni 1$ and a point x^0 outside this divisor we can locally define the function

$$P_n(\mathbf{e}, x) := \cos \left(ni \int_{(1,0)}^{*(x,w)} \eta_M \right) \quad (2.8)$$

(the differential η_M depends on the divisor $\mathbf{e} \ni 1$). In Chap. 5 we show that the coefficients of the differential associated with the curve $M(\mathbf{e})$ depend analytically on the variable points of the branch divisor. Hence the function $P_n(\mathbf{e}, x)$ depends analytically on all of its arguments. If the point x^0 lies in \mathbf{e}^0 , then the function (2.8) in a neighbourhood of the pair (\mathbf{e}^0, x^0) is two-valued and ramified along the variety $\{x = e \in \mathbf{e}\}$. The differential of $P_n(\mathbf{e}, x)$ has a singularity of the type of $(x - e)^{-1/2}(dx - de)$ on this variety. However, if the curve $M(\mathbf{e}^0)$ satisfies Abel's equations, then the singularity vanishes, the function is smooth at (x^0, \mathbf{e}^0) , and the coefficients of the differential dP_n have order $O(n^2)$ at this point.

The arguments for the stability of the Chebyshev representation presented in the previous paragraph cannot be considered rigorous unless we have defined the space of branch divisors \mathbf{e} . This is the subject of the next chapter.

2.3 Problems and Exercises

1. Show that the set \mathbf{e} in formula (2.1) assigned to an arbitrary polynomial $P(x)$ contains an even number of points.
2. What is the smallest possible number of sheets of a cover ramified to the second order over each point in some prescribed subset of the Riemann sphere?

Answer. Two or four, depending on the parity of the number of branch points.

3. Prove that there can exist at most one hyperelliptic involution J of a compact curve M of genus $g > 1$.

Solution. Let J_1, J_2 be two involutions, each having $2g + 2$ fixed points. By the Riemann-Hurwitz formula the quotient M/J_1 is a sphere. The corresponding projection is realized by a second-degree function x in $\mathbb{C}(M)$, which can be taken to have its poles outside the fixed point set of J_2 . The function $x - xJ_2$ has at least $2g + 2$ zeros, but at most four poles, and therefore $x = xJ_2$. Hence $J_1 = J_2$.

4. List all the hyperelliptic involutions J of a sphere and a torus.
5. Give an example of a Riemann surface admitting several reflections (anticonformal involutions) \bar{J} .
6. What is the general form of a reflection \bar{J} of the Riemann sphere? Write the equation of the isometric circle of the reflection. Does it always exist? Does a reflection always have fixed points?
7. Show that the number of ramification points of a real hyperelliptic curve which are fixed by a reflection \bar{J} is even.
8. Produce an explicit basis in the lattice of even 1-cycles on the curve M for $k = 0$. See [26].
9. Show that the values of the integrals of a real differential over a cycle C and its reflection $\bar{J}C$ on the curve M are conjugate. Make a conclusion that the integral of the distinguished differential η_M over an even cycle vanishes.
10. Show that the hyperelliptic involution J acts on the 1-homology of a curve simply by changing the sign of each cycle.
11. Let M be a surface admitting a conformal involution with exactly l fixed points ($l = 2g + 2$ in the hyperelliptic case). The homology space $H_1(M, \mathbb{R}) \cong \mathbb{R}^{2g}$ splits naturally into the sum of the subspaces $H_1^\pm(M, \mathbb{R})$ formed by the even ($C = JC$) and odd ($C = -JC$) cycles. Find the dimensions of the subspaces of even/odd 1-cycles.
12. Consider an arbitrary basis C_1, C_2, \dots, C_{2g} of the lattice of integer cycles on a compact curve M of genus g . Prove the following Riemann bilinear relations for any smooth closed 1-forms η and ξ on M :

$$\int_M \eta \wedge \xi = - \sum_{j,s=1}^{2g} F_{sj} \int_{C_s} \eta \int_{C_j} \xi, \quad (2.9)$$

where the matrix (F_{sj}) is the inverse of the intersection matrix $(C_s \circ C_j)$.

Solution. Consider the closed 1-forms ζ_s which are the Poincaré duals of the C_s . Then $\int_{C_s} \zeta_j = C_j \circ C_s = \int_M \zeta_j \wedge \zeta_s$. We expand the form ξ in the basis of ζ_s with coefficients $a_s := - \sum_{j=1}^{2g} F_{sj} \int_{C_j} \xi$. Then

$$\int_M \eta \wedge \xi = \sum_{s=1}^{2g} a_s \int_{C_s} \eta = - \sum_{j,s=1}^{2g} F_{sj} \int_{C_s} \eta \int_{C_j} \xi.$$

13. Let η be a holomorphic form on a compact curve M of genus g . Show that its norm can be expressed as follows in terms of its periods:

$$0 \leq \|\eta\|^2 := i \int_M \eta \wedge \bar{\eta} = -i \sum_{j,s=1}^{2g} F_{sj} \int_{C_s} \eta \overline{\int_{C_j} \eta}, \quad (2.10)$$

where (F_{sj}) is the same matrix as in the previous problem.

14. Consider a (non-canonical) basis of $2g$ integral cycles on a compact curve of genus g . Which g of these cycles can be used for a normalization of a meromorphic differential with fixed principal parts at the singularities?

Solution. Adding a holomorphic differential to a meromorphic we do not affect the principal parts at singular points, but change periods. To normalize a meromorphic differential we prescribe its periods along g selected cycles C_1, C_2, \dots, C_g . Such a normalization is well-defined if and only if each holomorphic differential η with zero periods along the g selected cycles is trivial. We can see from (2.10) that for a well-defined normalization it is sufficient that $F_{sj} = 0$ for $s, j = g+1, \dots, 2g$. These equalities are equivalent to the condition that the intersection form is trivial on the cycles C_1, \dots, C_g . In other words C_1, C_2, \dots, C_g span a Lagrangian subspace of the homology space.

15. Let η be a holomorphic form on a real hyperelliptic curve. Show that the following conditions are equivalent:

- (a) $\eta = 0$.
- (b) η has zero periods over all even cycles.
- (c) η has zero periods over all odd cycles.
- (d) All the periods of η are real.
- (e) All the periods of η are purely imaginary.

16. Show that on a Riemann surface of genus g a meromorphic differential with fixed principal parts at the singularities can be normalized in one of the following ways:

- (a) Prescribing the periods over the g even cycles.
- (b) Prescribing the periods over the g odd cycles.
- (c) Prescribing the real parts of $2g$ periods.
- (d) Prescribing the imaginary parts of $2g$ periods.

17. Show that if Pell's equation with a polynomial coefficient is solvable, then it has a unique (up to a sign) solution $P_n(x)$ of the lowest positive degree n . All the other solutions can be obtained by superpositions with the classical Chebyshev polynomial: $P_{mn}(x) = \pm T_m(P_n(x))$.

18. Show that the set of solutions (P, Q) of a given Pell equation $P(x)^2 - DQ(x)^2 = 1$ admits the group structure with operation $(P_1, Q_1) * (P_2, Q_2) = (P_1 P_2 + DQ_1 Q_2, P_1 Q_2 + P_2 Q_1)$ and the identity element $(1, 0)$. Show that this group is isomorphic to \mathbb{Z} .

Hint. Use the Akhiezer function.

19. State and prove a complex version of Theorem 2.1 (see the remark after the theorem).
20. Investigate the stability of the Chebyshev representation.

Chapter 3

Representations for the Moduli Space

We have already seen that to investigate properties of the Chebyshev representation and, in particular, of Abel's equations we must consider the space of real hyperelliptic curves. For a fixed genus g this space consists of several components, which are distinguished by another topological invariant of a real curve, the number k of (co)real ovals on it. We shall denote these components by \mathcal{H}_g^k . Most of them are not simply connected, and so it will be more convenient to go over to their universal covers $\tilde{\mathcal{H}}_g^k$. Looking at the subject under consideration from different standpoints is always useful, and so we present four definitions of this space and prove their equivalence. The standard approach is to define $\tilde{\mathcal{H}}_g^k$ as the space of branch divisors \mathbf{e} of prescribed type, considered together with the history of their motion from a distinguished divisor \mathbf{e}^0 . Viewing a divisor as moving in a viscous medium and carrying particles of the medium with it, we arrive at the Teichmüller space \mathcal{T}_g^k of a punctured disc with several marked boundary points. This is a flexible tool, which establishes connections between different points of view on our subject. The deformation spaces \mathcal{G}_g^k of special Kleinian groups provide global systems of coordinates in the space under consideration and enable an effective construction of analytic objects. Using the labyrinth spaces \mathcal{L}_g^k , the most easily visualizable ones, in Chap. 5 we shall calculate the image of the period map on $\tilde{\mathcal{H}}_g^k$, which is defined by the left-hand sides of Abel's equations.

3.1 Four Definitions

We fix the topological invariants of a real curve (2.1): its genus $g = 0, 1, 2, \dots$ and the number $k = 1, 2, \dots, g + 1$ of coreal ovals on it. The case $k = 0$ is special in certain respects; it was considered in detail in [40, 41], and [42]; however, it is not interesting for optimization and we leave it out in this chapter. A *symmetric divisor \mathbf{e} of type (g, k)* is an unordered set of distinct points e_1, \dots, e_{2g+2} including $2k$ real points and $(g - k + 1)$ pairs of complex conjugate ones. The group \mathfrak{A}_1^+

of orientation-preserving affine motions of the real axis acts freely on such sets: $\mathbf{e} = \{e_s\}_{s=1}^{2g+2} \rightarrow A\mathbf{e} + B = \{Ae_s + B\}_{s=1}^{2g+2}$, $A > 0$, $B \in \mathbb{R}$. We shall call the orbits of this action the *moduli space* \mathcal{H}_g^k . Each orbit contains a unique *normalized divisor* in which the two extreme left real points are equal to -1 and $+1$.

Points in the moduli space correspond to conformal classes of real hyperelliptic curves (2.1) with fixed invariants g and k and a distinguished point ∞_+ on the oriented real oval. The space \mathcal{H}_g^k has the natural structure of a real $2g$ -manifold. In a neighbourhood of a marked normalized divisor \mathbf{e}^0 we set the local coordinates of a divisor $\mathbf{e} := \{-1, 1, e_1, \dots, e_{2g}\}$ to be equal to the values of the variables $\operatorname{Re} e_s$ and $\operatorname{Im} e_s$ for points e_s in the open upper half-plane \mathbb{H} , and the values of the $\operatorname{Re} e_s$ for real points e_s , $s = 1, 2, \dots, 2g$.

The space of classes of homotopy equivalent paths in \mathcal{H}_g^k going out of the marked point \mathbf{e}^0 in the moduli space is called the *universal covering space* $\tilde{\mathcal{H}}_g^k$. It has three representations, which we describe below.

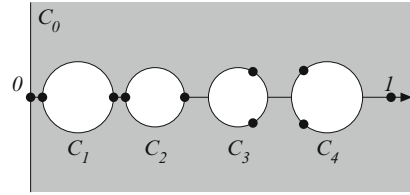
3.1.1 The Teichmüller Space

Consider the *quasiconformal* [3] homeomorphisms of the upper half-plane \mathbb{H} which fix the boundary points -1 , $+1$, and ∞ . They form a group \mathbf{QC} with respect to composition. Each $f \in \mathbf{QC}$ can be extended to a quasiconformal homeomorphism of \mathbb{C} by a reflection in the real axis. The motions f stabilizing a fixed normalized branch divisor \mathbf{e}^0 (but maybe rearranging points in it) make up a subgroup $\mathbf{QC}(\mathbf{e}^0)$. The motions f that can be joined to the identity map id by a homotopy of the punctured sphere $\mathbb{CP}^1 \setminus \mathbf{e}^0$ stabilizing infinity make up a normal subgroup $\mathbf{QC}^0(\mathbf{e}^0) \subset \mathbf{QC}(\mathbf{e}^0)$. It acts on \mathbf{QC} by right multiplication. The orbit space of this action $\mathcal{T}_g^k(\mathbf{e}^0) := \mathbf{QC}/\mathbf{QC}^0(\mathbf{e}^0)$ is called the *Teichmüller space*.¹ By definition the *Teichmüller distance* between classes $[f], [h] \in \mathcal{T}_g^k(\mathbf{e}^0)$ is the minimum of the logarithms of the dilatations of the quasiconformal maps $f_1 h_1^{-1}$ over all the representatives $f_1 \in [f]$ and $h_1 \in [h]$.

The *modular group* $\mathbf{Mod}(\mathbf{e}^0) := \mathbf{QC}(\mathbf{e}^0)/\mathbf{QC}^0(\mathbf{e}^0)$ acts on the Teichmüller space by right multiplication and the corresponding automorphisms are isometries. The choice of a distinguished divisor \mathbf{e}^0 is not essential for the definition of the Teichmüller space: a motion $h \in \mathbf{QC}$ gives rise to an isometry of $\mathcal{T}_g^k(\mathbf{e}^0)$ and $\mathcal{T}_g^k(h\mathbf{e}^0)$ by the formula $f \rightarrow f h^{-1}$. Obviously, $\mathbf{QC}(h\mathbf{e}^0) = h\mathbf{QC}(\mathbf{e}^0)h^{-1}$ and $\mathbf{QC}^0(h\mathbf{e}^0) = h\mathbf{QC}^0(\mathbf{e}^0)h^{-1}$, and therefore the modular groups $\mathbf{Mod}(\mathbf{e}^0)$ and $\mathbf{Mod}(h\mathbf{e}^0)$ are isomorphic and the above isometry $\mathcal{T}_g^k(\mathbf{e}^0) \rightarrow \mathcal{T}_g^k(h\mathbf{e}^0)$ is equivariant with respect to the actions of these modular groups on the two spaces.

¹This is a modification of the standard definition [66] of the Teichmüller space of a disc with $g - k + 1$ punctures and $2k + 1$ marked boundary points which is convenient for our aims.

Fig. 3.1 The circles C_1, C_2, \dots, C_g for $g = 4$, $k = 3$



Assigning to a motion $f \in \mathbf{QC}$ the branch divisor $\mathbf{e} := f(\mathbf{e}^0)$ we obtain a projection of the Teichmüller space onto the moduli space. The fibres of this projection are orbits of the modular group. We shall demonstrate that this projection coincides with the universal covering.

3.1.2 The Deformation Space of a Kleinian Group

By the *deformation space* \mathcal{G}_g^k we mean the set of ordered tuples $\mathbf{g} := \{G_s\}_{s=0}^g$ of second-order linear fractional rotations of the real sphere with real fixed points $c_s \pm r_s$ for $s < k$ or with complex conjugate fixed points $c_s \pm ir_s$ for $s \geq k$:

$$G_s u := G_s(u) := \begin{cases} -u, & s = 0, \\ c_s + r_s^2/(u - c_s), & s = 1, \dots, k-1, \\ c_s - r_s^2/(u - c_s), & s = k, \dots, g. \end{cases} \quad (3.1)$$

The real parameters c_s and $r_s > 0$ (*moduli*) are selected so that the following geometric condition holds: *there exist g disjoint subintervals of $(0, 1)$ numbered in increasing order such that the circles C_1, C_2, \dots, C_g with diameters on these intervals pass through the fixed points of the corresponding motions G_1, G_2, \dots, G_g (see Fig. 3.1).*

If this condition is fulfilled, then the y -axis $C_0 = i\mathbb{R}$ and the circles C_1, C_2, \dots, C_g bound the fundamental domain $\mathbf{R}(\mathbf{g})$ of the Kleinian group \mathfrak{G} generated by the rotations G_0, G_1, \dots, G_g . By Klein's combination theorem [89] the group \mathfrak{G} is the free product of $(g + 1)$ second-rank groups. The hyperbolic motions $\{S_l := G_l G_0\}_{l=1}^g$ generate a Schottky group \mathfrak{S} , $|\mathfrak{G} : \mathfrak{S}| = 2$. These two groups have a common domain of discontinuity \mathcal{D} and a common limit set, which lies on the real axis. The limit set has linear measure zero since the group \mathfrak{S} satisfies the following Schottky criterion [132]: *the fundamental domain \mathfrak{S} (the exterior of the $2g$ circles $-C_g, \dots, -C_1; C_1, \dots, C_g$) can be partitioned into triply connected domains (pants) by several additional circles.* This is crucial for our aims because the Poincaré theta series of \mathfrak{S} will converge absolutely and uniformly on compact subsets of \mathcal{D} , the domain of discontinuity of the group.

The orbit manifold of the group \mathfrak{G} is the Riemann sphere with natural reflection $\bar{J}u := \bar{u}$. The quotient manifold \mathcal{D}/\mathfrak{G} is a compact algebraic curve M_c of genus g , with the hyperelliptic involution $Ju := G_0u$ and anticonformal involution \bar{J} . The point $u = 1$ will play the role of the distinguished point ∞_+ on the real oval of M_c . We say that a holomorphic projection $x(u): \mathcal{D} \rightarrow \mathcal{D}/\mathfrak{G} \cong \mathbb{CP}^1$ is *normalized* if it takes the three points $u = 0, u = 1$, and $u = \infty$ to $x = 1, x = \infty$, and $x = -1$, respectively. Such a ramified covering $x(u)$ respects complex conjugation. Assigning to the Kleinian group the branch points of $x(u)$ (the projections onto \mathcal{D}/\mathfrak{G} of the fixed points of the rotations $\{G_s\}_{s=0}^g$) we define a map from the deformation space \mathcal{G}_g^k into the moduli space \mathcal{H}_g^k . In Sect. 3.3.2 we show that this is the universal covering, and the deck transformation group acts on the deformation space by preserving the Kleinian group \mathfrak{G} but changing its system of generators.

3.1.3 The Labyrinth Space

By a *labyrinth* attached to a divisor \mathbf{e} of type (g, k) we shall mean a system $\Lambda = (\Lambda_0, \Lambda_1, \dots, \Lambda_g)$ of disjoint simple smooth arcs connecting points in the divisor pairwise (see Fig. 3.2). The first k arcs in a labyrinth are canonically defined as the intervals on the real axis linking pairwise the real points in the divisor \mathbf{e} . As regards defining the other $(g - k + 1)$ arcs, there we have a certain freedom. These arcs connect complex conjugate points in \mathbf{e} , are invariant under the reflection in \mathbb{R} and circumvent the first group of arcs from the right. The intersections with the real axis define a natural ordering of the system of cuts. Two labyrinths Λ and Λ' attached to the same divisor \mathbf{e} are viewed as equivalent if they can be connected by a continuous deformation such that at each instant the deformed paths form a labyrinth attached to the same divisor \mathbf{e} . We call the set of labyrinths attached to normalized divisors in the moduli space \mathcal{H}_g^k and treated modulo this equivalence relation the *labyrinth space* \mathcal{L}_g^k .

The modular group also acts on the labyrinth space. A smooth representative $f \in \text{Mod}(\mathbf{e}^0)$ (which exists in each Teichmüller class [4, 66]) takes a labyrinth Λ attached to \mathbf{e}^0 to the labyrinth $f\Lambda$ (see Fig. 3.3). Orbits of this action are fibres of the natural projection $\mathcal{L}_g^k \rightarrow \mathcal{H}_g^k$ assigning to a labyrinth Λ its boundary points $\mathbf{e} := \partial\Lambda$.

DISCUSSION. The idea behind the introduction of labyrinths attached to a divisor \mathbf{e} is as follows: the punctured half-plane $\mathbb{H} \setminus \mathbf{e}$ cut along the arcs of a labyrinth is a

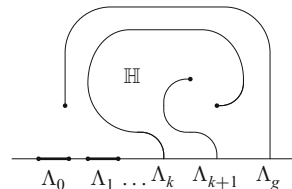
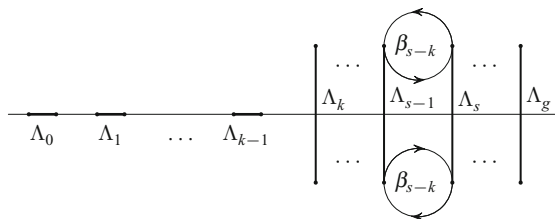


Fig. 3.2 The half-plane \mathbb{H} cut along a labyrinth Λ

Fig. 3.3 Dehn half-twists

$\beta_1, \dots, \beta_{g-k}$ as deck transformations of the labyrinth space \mathcal{L}_g^k



simply-connected set. On the one hand this construction fixes generators of the free group $\pi_1(\mathbb{H} \setminus \mathbf{e})$ (see Sect. 3.2.4) and on the other it allows us to follow the dynamics of the punctures. Whether the arcs in a labyrinth are smooth is not very important for us. For instance, we could assume in the spirit of [159] that the Λ_s are polygonal lines (with finitely many segments) and consider admissible deformations consisting of replacements of a pair of adjacent segments by a single link, provided that the (maybe degenerate) open triangle bounded by the three segments is disjoint from the labyrinth. This piecewise linear approach is more rigorous, but requires plenty of details, which eventually complicates grasping the relations between the spaces we have introduced. To avoid cumbersome details we shall not give rigorous definitions of a smooth arc and deformation of a smooth arc. Driven by the “uncertainty relation”² for the rigour and the transparency of presentation we embrace here the more intuitive approach of theoretical physicists.

3.2 Auxiliary Results

The proof of the equivalence of the four spaces \mathcal{H}_g^k , \mathcal{T}_g^k , \mathcal{G}_g^k , and \mathcal{L}_g^k introduced above is based on their properties to be established in this section.

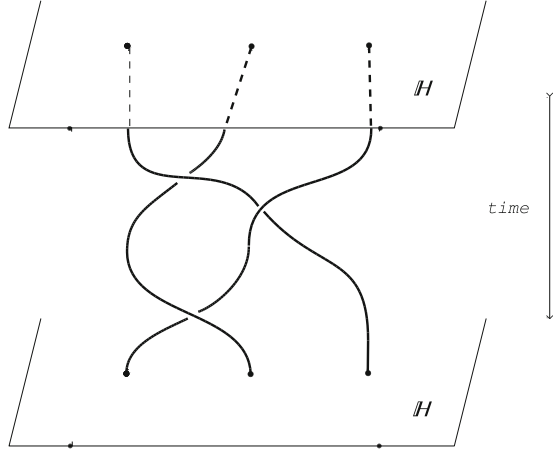
3.2.1 The Fundamental Group of the Moduli Space

Lemma 3.1. *The fundamental group of the moduli space \mathcal{H}_g^k , $k > 0$, is isomorphic to Br_{g-k+1} , the Artin braid group on $(g - k + 1)$ strands.*

Proof. A symmetric divisor is completely determined by its parts in the upper half-plane ($g - k + 1$ points) and on the real axis ($2k$ points). Hence the space of normalized divisors is the Cartesian product of the quotient of the space $\mathbb{H}^{g-k+1} \setminus \{\text{the diagonals}\}$ by rearrangements of the coordinate variables and a $(2k - 2)$ -cell. The fundamental group of this space is precisely the braid group Br_{g-k+1} [21] (Fig. 3.4). \square

²Niels Bohr used uncertainty principle in fields far from quantum mechanics. When asked what is the complementary quantity to “Truth”, he replied: “Clarity”.

Fig. 3.4 A loop in the moduli space \mathcal{H}_g^k is a braid on $g - k + 1$ strands over the upper half-plane



3.2.2 The Moduli Space: Orbits of the Group Mod

The following result is the first step in establishing connections between different spaces.

Lemma 3.2. *The spaces $\mathcal{T}_g^k(\mathbf{e}^0)/\text{Mod}(\mathbf{e}^0)$ and \mathcal{H}_g^k are homeomorphic.*

Proof. We assign to a map $f \in \text{QC}$ the symmetric normalized divisor $f\mathbf{e}^0$. This defines an injective map from the orbit set of the modular group action on the Teichmüller space into the moduli space. We shall show that this map is (A) continuous in the natural topology and (B) has a continuous inverse in the entire moduli space. This will prove that the two spaces are homeomorphic:

- (A) Recall that the topology of the moduli space \mathcal{H}_g^k is determined by local systems of coordinates, with variables equal to the independent real and imaginary parts of the points in the normalized divisor $\mathbf{e} := \{e_1, \dots, e_{2g}, -1, 1\}$ distinct from ± 1 . In the orbit space of the modular group $\mathcal{T}_g^k(\mathbf{e}^0)/\text{Mod}(\mathbf{e}^0) = \text{QC}/\text{QC}(\mathbf{e}^0)$ we introduce the Teichmüller metric:

$$\rho([f], [h]) := \inf_{[f], [h]} \log \frac{1 + \|\mu(x)\|_\infty}{1 - \|\mu(x)\|_\infty}, \quad (3.2)$$

where the infimum is taken over the representatives $f_1 \in [f]$ and $h_1 \in [h]$ of the classes; $\mu(x)$ is the Beltrami coefficient of the map $f_1 h_1^{-1}$; the norm $\|\mu(x)\|_\infty$ is the essential supremum of $\mu(x)$ in the plane. We can verify that the embedding $\mathcal{T}_g^k(\mathbf{e}^0)/\text{Mod}(\mathbf{e}^0) \rightarrow \mathcal{H}_g^k$ defined above is continuous in a neighbourhood of the class of the identity map $[\text{id}]$. There exists a formula for the “principal part” of a quasiconformal map $f(x)$ with a small Beltrami coefficient $\mu(x)$ and fixed points ± 1 and ∞ [3, 4, 66, 89]:

$$f(e) - e = (2\pi i)^{-1} \int_{\mathbb{C}} \mu(x) \frac{e^2 - 1}{x^2 - 1} \frac{dx \wedge d\bar{x}}{x - e} + O(\|\mu\|_{\infty}^2), \quad e \in \mathbb{C}, \quad (3.3)$$

where the remainder term has a uniform estimate on compact subsets of the plane. It is clear from (3.3) that classes $[f]$ close to $[\text{id}]$ in the Teichmüller metric only slightly deform the divisor \mathbf{e}^0 . Now the continuity in a neighbourhood of an arbitrary points $[h]$ can be obtained by replacing the distinguished divisor \mathbf{e}^0 : if a class $[f]$ is close to $[h]$ in the moduli space $\text{QC}/\text{QC}(\mathbf{e}^0)$, then the distance between the class $[fh^{-1}]$ and $[id]$ in the space $\text{QC}/\text{QC}(h\mathbf{e}^0)$ is the same. By the above, the divisor $fh^{-1}h\mathbf{e}^0 = f\mathbf{e}^0$ is a slight perturbation of $h\mathbf{e}^0$.

- (B) Let $\sigma(x)$ be an infinitely smooth cutoff function of the complex variable x with support small in comparison with the distance between the points in \mathbf{e}^0 , equal to 1 in a neighbourhood of $x = 0$, and conjugation-invariant: $\sigma(\bar{x}) = \sigma(x)$. In a small neighbourhood of the distinguished point \mathbf{e}^0 in the moduli space we define a map $\mathcal{H}_g^k \rightarrow \text{QC}$:

$$f(\mathbf{e}, x) := x + \sum_{s=1}^{2g} (e_s - e_s^0) \sigma(x - e_s^0), \quad \mathbf{e} \approx \mathbf{e}^0, x \in \mathbb{C}. \quad (3.4)$$

The map (3.4) is a local inversion of our embedding $\text{QC}/\text{QC}(\mathbf{e}^0) \rightarrow \mathcal{H}_g^k$ and it is continuous. Similar sections can be constructed in a neighbourhood of each point in the moduli space. Taking composite maps we define a continuous inverse $\mathcal{H}_g^k \rightarrow \mathcal{T}_g^k(\mathbf{e}^0)/\text{Mod}(\mathbf{e}^0)$ in a neighbourhood of an arbitrary prescribed point. \square

3.2.3 The Topology of the Deformation Space

The moduli c_s and $r_s > 0$, $s = 1, \dots, g$, form a global system of coordinates in the deformation space \mathcal{G}_g^k , $k > 0$, and allow us to identify the latter with a domain of \mathbb{R}^{2g} .

Lemma 3.3. *The space \mathcal{G}_g^k is the cell described by the system of inequalities*

$$r_s > 0, \quad s = 1, 2, \dots, g; \quad (3.5)$$

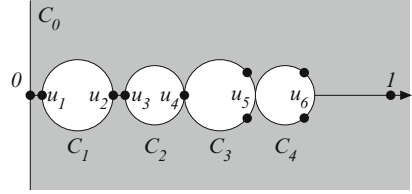
$$c_{s-1} + r_{s-1} < c_s - r_s, \quad s = 1, \dots, k-1, \quad (3.6)$$

where we set $c_0 + r_0 := 0$,

$$\begin{aligned} c_{k-1} + r_{k-1} &< G_k(c_{k-1} + r_{k-1}) < G_{k+1}G_k(c_{k-1} + r_{k-1}) \\ &< G_{k+2}G_{k+1}G_k(c_{k-1} + r_{k-1}) < \dots < G_g G_{g-1} \dots G_{k+1}G_k(c_{k-1} + r_{k-1}) < 1. \end{aligned} \quad (3.7)$$

Proof. The degree-two rotation G_s , $s = 1, \dots, k-1$, of the Riemann sphere has real fixed points and therefore the corresponding circle C_s is uniquely defined. On

Fig. 3.5 The limiting position of the circles for $g = 4$ and $k = 3$



the other hand one can move the real diameter of the remaining circles C_s for $s = k, \dots, g$. We shift all the “movable” diameters to the extreme left position (see Fig. 3.5). The system of inequalities (3.6), (3.7) describes the ordering in the interval $(0, 1)$ of the end-points of the resulting diameters. The arising arrangement of diameters can uniquely be recovered from their end-points, which range over the cell $\{0 < u_1 < u_2 < \dots < u_{g+k-1} < 1\}$ of dimension $g + k - 1$. The direction from the mid-point of the s th shifted diameter to the fixed point $c_s + ir_s$ of the rotation G_s for $s = k, \dots, g$, gives us a point in another cell, $(0, \pi)^{g-k+1}$. Thus we have constructed a map of the space \mathcal{G}_g^k onto a cell of dimension $2g$, which is continuous and one-to-one. \square

3.2.4 The Subgroup Induced by the Ramified Covering $x(u)$

Each labyrinth Λ attached to a divisor \mathbf{e} defines a representation χ_Λ of the fundamental group of the punctured sphere $\pi_1(\mathbb{CP}^1 \setminus \mathbf{e}, \infty)$ into an abstract group \mathfrak{G}^3 which is equal to the free product of $(g + 1)$ rank-two groups with generators G_0, G_1, \dots, G_g . To a loop ρ starting at infinity and intersecting transversally (in arbitrary direction) the cuts $\Lambda_{s_1}, \Lambda_{s_2}, \dots, \Lambda_{s_l}$ one after another, we assign an element of this group:

$$\chi_\Lambda[\rho] := G_{s_1} G_{s_2} \dots G_{s_l}.$$

With a point $\mathbf{g} := \{G_s\}_{s=0}^g$ in the deformation space we associate the labyrinth $\Lambda := (xC_0, xC_1, \dots, xC_g)$, the normalized projection of the boundary of the fundamental domain $\mathbf{R}(\mathbf{g})$. The kernel of the corresponding representation χ_Λ is the subgroup of $\pi_1(\mathbb{CP}^1 \setminus \mathbf{e}, \infty)$ induced⁴ by covering $x(u)$ ramified over $\mathbf{e} := \{x(\text{fix } G_s)\}_{s=0}^g$. The subgroup induced by a covering can be proved to be completely determined by the branch divisor \mathbf{e} .

Lemma 3.4. *The kernel of the representation $\chi_\Lambda: \pi_1(\mathbb{CP}^1 \setminus \mathbf{e}, \infty) \rightarrow \mathfrak{G}$ is independent of the labyrinth Λ attached to the divisor \mathbf{e}*

³For instance, realized by the Kleinian group in Sect. 3.1.2, so we use the same notation as there.

⁴Let $Pr: X \rightarrow Y$ be a covering map respecting the marked points of fundamental groups of spaces X, Y . The subgroup $Pr\pi_1(X, *) \subset \pi_1(Y, *)$ is known as the subgroup induced by the covering Pr ; it is isomorphic to $\pi_1(X, *)$ [67]

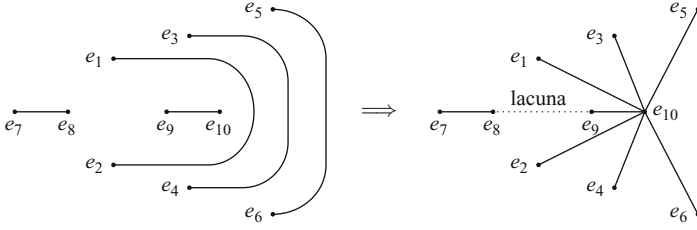


Fig. 3.6 Modifying the labyrinth Λ for $g = 4$ and $k = 2$

Proof. We shall show that $\ker \chi_\Lambda$ is equal to the normal subgroup of $\pi_1(\mathbb{CP}^1 \setminus \mathbf{e}, \infty)$ generated by all elements of the following two kinds: (a) a lasso making two rounds about the punctures and (b) a loop λ with mirror symmetry $[\lambda\bar{\lambda}] = 1$ that is disjoint from the cuts $\Lambda_0, \Lambda_1, \dots, \Lambda_{k-1}$. The above-described subgroup is independent of the choice of the labyrinth since the first k arcs in the labyrinth are canonically defined. We can readily verify that this subgroup lies in the kernel of χ_Λ . Now we demonstrate the reverse inclusion.

A cell decomposition of the Riemann sphere with $(2g + 2)$ vertices \mathbf{e} , $(2g + 1)$ oriented edges R , and one 2-cell gives us a system of free generators of the group $\pi_1(\mathbb{CP}^1 \setminus \mathbf{e})$: we associate with each edge R the class of the loop ρ intersecting only this edge from left to right. Such a cell decomposition can be constructed by deforming the labyrinth Λ . The intervals Λ_s , $s = 0, \dots, k - 1$, give us k edges R , and the *lacunae* between them give a further $(k - 1)$ edges. The lacking $2(g - k + 1)$ edges can be obtained by modifying the remaining arcs of the labyrinth Λ_s , $s = k, \dots, g$: we contract the intersection points $\mathbb{R} \cap \Lambda_s$ to the rightmost puncture on the real axis (see Fig. 3.6).

On generators related to the edges R the representation χ_Λ acts as follows:

$$\chi_\Lambda[\rho] = \begin{cases} G_s & \text{if } R \text{ is a (modified) cut } \Lambda_s, \\ 1 & \text{if } R \text{ is a lacuna.} \end{cases}$$

Since \mathfrak{G} is the free product of groups of rank 2, the kernel χ_Λ is the normal subgroup generated by all possible elements $[\lambda]$, $[\rho]^2$, $[\rho\bar{\rho}]$, where the $[\lambda]$ correspond to the $(k - 1)$ lacunae and the $[\rho]$ correspond to the other $(2g - k + 2)$ edges R . An immediate verification shows that all these elements generating $\ker \chi_\Lambda$ belong to the normal subgroup described above. \square

Naturally embedded in the fundamental group of the punctured sphere is the group of the punctured upper half-plane $\pi_1(\mathbb{H} \setminus \mathbf{e}, \infty)$. As in Lemma 3.4, the cuts in the labyrinth present a system of free generators coding the elements of this group: a loop ρ in the upper halfplane intersecting transversally the cuts $\Lambda_{s_1}, \Lambda_{s_2}, \dots, \Lambda_{s_l}$ one after another can be factored down to the generators λ_s , $s = k, \dots, g$, which intersect only the corresponding cuts Λ_s from left to right:

$$[\rho] = [\lambda_{s_1}]^{\varepsilon_1} [\lambda_{s_2}]^{\varepsilon_2} \dots [\lambda_{s_l}]^{\varepsilon_l}, \quad (3.8)$$

where $\varepsilon_j = \pm 1$ depending on the orientation of the local intersection of ρ with the cut Λ_{s_j} .

Lemma 3.5. *Let $\rho \subset \mathbb{H} \setminus \mathbf{e}$ be a loop without self-intersections and with initial point at ∞ . Then the irreducible factorization of $[\rho]$ in the generators (3.8) contains no equal letters following one another.*

Proof. This depends only on the homotopy class of the loop ρ , therefore we shall assume without loss of generality that ρ intersects the Λ_s transversally and at finitely many points. Making finitely many transformations of the type presented in Fig. 3.7 we replace ρ by a homotopic loop without self-intersections which has an irreducible factorization (3.8). If this representation contains two successive symbols $[\lambda_j]$, then we are in the situation of Fig. 3.8 up to orientation. A point going along ρ must return to infinity, but it cannot leave the shaded domain bounded by the loop itself and a piece of the cut Λ_j : otherwise the loop intersects itself or its factorization is reducible. \square

3.2.5 The Modular Group Action on the Group \mathfrak{G}

Motions $f \in \text{QC}(\mathbf{e})$ act in a natural way on the fundamental group of the punctured sphere $\mathbb{CP}^1 \setminus \mathbf{e}$, and the result of the action of f depends only on its homotopy class. The characterization of the normal subgroup $\ker \chi_\Lambda \subset \pi_1(\mathbb{CP}^1 \setminus \mathbf{e}, \infty)$ used in the proof of Lemma 3.4 demonstrates that it is stable with respect to this action. For instance, for a smooth representative f of the homotopy class we have $f \cdot \ker \chi_\Lambda =$

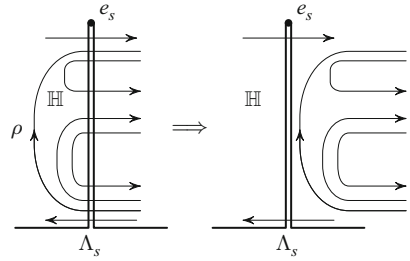


Fig. 3.7 A deformation of the loop ρ resulting in simplification of the factorization (3.8)

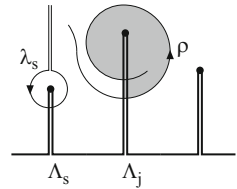


Fig. 3.8 An infinite spiral ρ and a generator λ_s

$\ker \chi_{f\Lambda} = \ker \chi_\Lambda$. We see that there is a well-defined action of the modular group $\text{Mod}(\mathbf{e}) := \text{QC}(\mathbf{e})/\text{QC}^0(\mathbf{e})$ on the quotient group $\pi_1(\mathbb{CP}^1 \setminus \mathbf{e}, \infty)/\ker \chi_\Lambda$. The latter can be identified with the abstract group \mathfrak{G} ,⁵ which is a free product of $g + 1$ groups of rank 2. The following result shows that the representation of $\text{Mod}(\mathbf{e})$ into the automorphism group of \mathfrak{G} is faithful.

Theorem 3.1. *The action of $f \in \text{QC}(\mathbf{e})$ on the group \mathfrak{G} is trivial if and only if $f \in \text{QC}^0(\mathbf{e})$.*

Proof. Assume that f acts trivially on the group \mathfrak{G} . We claim that the action of f on the fundamental group $\pi_1(\mathbb{CP}^1 \setminus \mathbf{e}, \infty)$ is also trivial. The fundamental group of the punctured sphere is generated by three classes of loops. These are loops in the punctured upper and lower half-planes and also loops in a sufficiently narrow punctured neighbourhood of the real axis. The action of f on the last class is trivial because it preserves the real axis. Its actions on loops in the first two classes agree in view of the mirror symmetry $f(\bar{x}) = \bar{f}(x)$. We shall therefore analyse the action of f on the fundamental group $\pi_1(\mathbb{H} \setminus \mathbf{e}, \infty)$.

Each generator $[\lambda_s]$ of the fundamental group of the punctured half-plane produced by a labyrinth contains a loop λ_s without self-intersections; its image $f\lambda_s$ is also a simple loop. By Lemma 3.5 the uncancellable factorization of the latter loop into generators

$$[f\lambda_s] = [\lambda_{s_1}]^{\varepsilon_1} [\lambda_{s_2}]^{\varepsilon_2} \dots [\lambda_{s_l}]^{\varepsilon_l}, \quad \varepsilon_* = \pm 1,$$

contains no letters with repeating lower index s_* . Trivial action of f on the group \mathfrak{G} takes us to the identity

$$\chi_\Lambda[f\lambda_s] := G_{s_1} G_{s_2} \dots G_{s_l} = G_s := \chi_\Lambda[\lambda_s]$$

in a free product of rank 2 groups. This can only occur in two cases, when $[f\lambda_s] = [\lambda_s]$ and when $[f\lambda_s] = [\lambda_s]^{-1}$. The second case is impossible because f respects the orientation.

Having established that the action of f on the fundamental group of the punctured Riemann sphere is trivial, we use a construction due to Ahlfors [3, 66]. Let $\mathbb{H} \rightarrow \mathbb{CP}^1 \setminus \mathbf{e}$ be the universal covering. Consider a lift $\tilde{f} : \mathbb{H} \rightarrow \mathbb{H}$ of f onto the covering spaces that fixes a preimage of the point $\infty \in \mathbb{CP}^1 \setminus \mathbf{e}$. This lift commutes with deck transformations of the universal covering because the action of f on the fundamental group of the base is trivial. Let $\tilde{f}_t(u)$ be the point partitioning the non-Euclidean interval $[\tilde{f}(u), u]$ in the Lobachevskii plane \mathbb{H} in the ratio $t : (1 - t)$, $t \in [0, 1]$. Considering the map of the base induced by $\tilde{f}_t(u)$ we obtain a homotopy of $\mathbb{CP}^1 \setminus \mathbf{e}$ stabilizing the point at infinity and connecting f with the identity map. \square

⁵The corresponding isomorphism is not canonical, but depends on the choice of the labyrinth, see Theorem 3.2.

3.2.6 Equivalence of Labyrinths

We start with the following preliminary observation.

Lemma 3.6. *If two labyrinths Λ and Λ' give rise to equal representations $\chi_\Lambda, \chi_{\Lambda'}: \pi_1(\mathbb{CP}^1 \setminus \mathbf{e}, \infty) \rightarrow \mathfrak{G}$, then also the systems of free generators (alphabets) $[\lambda_s]$ and $[\lambda'_s]$, $s = k, \dots, g$, of the fundamental group $\pi_1(\mathbb{H} \setminus \mathbf{e}, \infty)$ related to these labyrinths are the same.*

Proof. Consider a simple loop representing a class $[\lambda'_s]$. By Lemma 3.5 its irreducible factorization $[\lambda'_s] = [\lambda_{s_1}]^{\varepsilon_1} [\lambda_{s_2}]^{\varepsilon_2} \dots [\lambda_{s_l}]^{\varepsilon_l}$ with respect to the generators in the second system contains no repeating letters. Accordingly, the word $G_{s_1} G_{s_2} \dots G_{s_l}$ is irreducible. On the other hand $G_{s_1} G_{s_2} \dots G_{s_l} =: \chi_\Lambda([\lambda'_s]) = \chi_{\Lambda'}([\lambda'_s]) =: G_s$. In the group \mathfrak{G} such an equality is possible only if $[\lambda'_s] = [\lambda_s]^{\pm 1}$. The classes $[\lambda'_s]$ and $[\lambda_s]$ are conjugate in the fundamental group of the punctured sphere because the corresponding loops go counterclockwise about the same puncture. In a free group elements $[\lambda_s]$ and $[\lambda_s]^{-1}$ cannot be conjugate, and so $[\lambda'_s] = [\lambda_s]$. \square

Theorem 3.2. *Two labyrinths Λ and Λ' attached to a divisor \mathbf{e} are equivalent if and only if $\chi_\Lambda = \chi_{\Lambda'}$.*

Proof. A continuous deformation of the labyrinth Λ preserves the representation χ_Λ into the discrete group \mathfrak{G} , and therefore the same representation corresponds to equivalent labyrinths. Conversely, if $\chi_\Lambda = \chi_{\Lambda'}$, then we shall explicitly describe a deformation $\Lambda' \rightarrow \Lambda$. In view of the mirror symmetry, such a deformation is uniquely defined by the motion of the labyrinth in the upper half-plane. After an obvious deformation of Λ' we can assume that the labyrinths Λ and Λ' coincide on the real axis, and intersect transversally at finitely many points in the upper half-plane, as depicted in Fig. 3.9b.

Assume that $\Lambda_s \cap \Lambda'_i$ contains points x_1 and x_2 in the upper half-plane with opposite orientation of the intersections, and the segment of the arc Λ_s between them is disjoint from the labyrinth Λ' . The segments of Λ_s and Λ'_i cut by the points x_1 and x_2 bound a cell in \mathbb{H} disjoint from the labyrinth Λ' and, in particular, containing no punctures. This cell can be retracted—we depict the corresponding

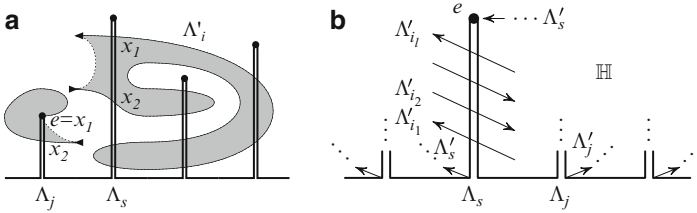


Fig. 3.9 (a) Deforming the labyrinth Λ' ; (b) factoring the loop $\rho := \partial(\mathbb{H} \setminus \Lambda_s)$ with respect to the generators

deformation in the background of Fig. 3.9a. We consider also the limiting case, when one of the points x_1 and x_2 is an end-point of Λ_s . Each of these deformations of Λ' reduces the number of its intersections with Λ . Hence in finitely many steps we arrive an equivalent labyrinth (still denoted by Λ') whose intersections with Λ do not have the form described above. We claim that now the intersection of the two labyrinths in the upper half-plane contains only points in \mathbf{e} . This actually means that the cuts Λ_s and Λ'_s , $s = k, \dots, g$, bound a cell in \mathbb{H} which is disjoint from both labyrinths. Retracting such cells we obtain a deformation $\Lambda' \rightarrow \Lambda$.

So assume now that $\Lambda_s \setminus \mathbf{e}$ intersects the arcs $\Lambda'_{i_1}, \Lambda'_{i_2}, \dots, \Lambda'_{i_l}$ in the upper half plane one after another, as in Fig. 3.9 b. We factor the loop ρ going along the boundary of $\mathbb{H} \setminus \Lambda_s$ with respect to the two systems of generators related to the labyrinths Λ and Λ' . Setting equal these expressions and bearing in mind that the corresponding alphabets coincide: $[\lambda'_i] = [\lambda_i]$, $i = k, \dots, g$, we obtain a commutation relation in the free group $\pi_1(\mathbb{H} \setminus \mathbf{e})$:

$$[\lambda_s] \cdot [\lambda_{i_1}]^{\varepsilon_1} [\lambda_{i_2}]^{\varepsilon_2} \dots [\lambda_{i_l}]^{\varepsilon_l} = [\lambda_{i_1}]^{\varepsilon_1} [\lambda_{i_2}]^{\varepsilon_2} \dots [\lambda_{i_l}]^{\varepsilon_l} \cdot [\lambda_s], \quad (3.9)$$

where $\varepsilon_j = \pm 1$ depending on the orientation of the intersection of Λ_s and Λ'_{i_j} . The word on the right-hand side of (3.9) is irreducible for otherwise we would be able to deform the labyrinth Λ' as in the previous paragraph. Hence this word consists of a single letter $[\lambda_s]$ and the labyrinth Λ' does not intersect the arc $\Lambda_s \cap \mathbb{H}$ at its interior points. \square

3.2.7 A Quasiconformal Deformation

The idea of a quasiconformal deformation of a group is due to Ahlfors and Bers [3, 4]; we merely adapt it to our aims. To start with, we mark an element $\mathbf{g}^0 := \{G_s^0\}_{s=0}^g$ of the deformation space \mathcal{G}_g^k which generates a Kleinian group \mathfrak{G}^0 and defines a projection $x^0(u): \mathcal{D}(\mathfrak{G}^0) \rightarrow \mathbb{CP}^1$ with the usual normalization $0, 1, \infty \rightarrow 1, \infty, -1$.

CONSTRUCTION. Let $f(x)$ be a quasiconformal automorphism of the Riemann sphere fixing the normalization set $x = -1, 1, \infty$ in the base of the ramified covering map $x_0(u)$. The latter map pulls back the Beltrami differential $\mu(x)\overline{dx}/dx := (f_{\bar{x}}\overline{dx})/(f_x dx)$ of $f(x)$ to the domain of discontinuity $\mathcal{D}(\mathfrak{G}^0)$ of the marked group. We extend the new differential $\tilde{\mu}(u)\overline{du}/du := \mu(x^0(u))(\overline{x_u^0 du})/(x_u^0 du)$ by zero to the limit set of the group \mathfrak{G}^0 , which has measure zero. Consider a quasiconformal homeomorphism $\tilde{f}(u)$ of the Riemann sphere satisfying the Beltrami equation

$$\frac{\partial}{\partial \bar{u}} \tilde{f}(u) = \tilde{\mu}(u) \cdot \frac{\partial}{\partial u} \tilde{f}(u) \quad (3.10)$$

and fixing three points in the plane: the two fixed points $u = 0, \infty$ of the generator G_0 and the pole $u = 1$ of the projection $x^0(u)$. The Beltrami differential $\tilde{\mu}(u)du/du$ is \mathfrak{G}^0 -invariant by construction, and therefore the uniqueness theorem for quasiconformal homeomorphisms states that $\tilde{f}(u)$ and $\tilde{f}(Gu)$ differ by a conformal motion of the Riemann sphere:

$$G^f \tilde{f} = \tilde{f} G, \quad G \in \mathfrak{G}^0, \quad G^f \in \text{PSL}_2(\mathbb{C}). \quad (3.11)$$

The group $\mathfrak{G}^f := \tilde{f} \mathfrak{G}^0 \tilde{f}^{-1}$ generated by such motions is isomorphic to \mathfrak{G}^0 , acts discontinuously on the domain $\mathcal{D}(\mathfrak{G}^f) := \tilde{f} \mathcal{D}(\mathfrak{G}^0)$, and is called the *quasiconformal deformation* of the group \mathfrak{G}^0 generated by the motion f . The set of generators \mathfrak{g}^0 of the marked group is taken to the generators $\mathfrak{g}^f := \{G_s^f\}_{s=0}^g := \{\tilde{f} G_s^0 \tilde{f}^{-1}\}_{s=0}^g$ of the deformed group.

The following lemma underlines the natural character of the construction of a quasiconformal deformation. It is an easy consequence of the uniqueness of the normalized quasiconformal map with a given Beltrami coefficient [3].

Lemma 3.7. 1. *If a quasiconformal map f deforms the group \mathfrak{G}^0 into \mathfrak{G}^f , then the holomorphic projection $x^f(u): \mathcal{D}(\mathfrak{G}^f) \rightarrow \mathbb{CP}^1$ with the standard normalization $u = 0, 1, \infty \mapsto x = 1, \infty, -1$ completes the commutative deformation diagram:*

$$\begin{array}{ccc} \mathcal{D}(\mathfrak{G}^0) & \xrightarrow{\tilde{f}} & \mathcal{D}(\mathfrak{G}^f) \\ \downarrow x^0 & & \downarrow x^f \\ \mathbb{CP}^1 & \xrightarrow{f} & \mathbb{CP}^1 \end{array} \quad (3.12)$$

2. *The deformation of the group \mathfrak{G}^0 by a composite map $f \circ h$ can be performed in two steps. First, h is used to deform the group \mathfrak{G}^0 into \mathfrak{G}^h : the left-hand square in the diagram*

$$\begin{array}{ccccc} \mathcal{D}(\mathfrak{G}^0) & \xrightarrow{\tilde{h}} & \mathcal{D}(\mathfrak{G}^h) & \xrightarrow{\tilde{f}} & \mathcal{D}(\mathfrak{G}^{fh}) \\ \downarrow x^0 & & \downarrow x^h & & \downarrow x^{fh} \\ \mathbb{CP}^1 & \xrightarrow{h} & \mathbb{CP}^1 & \xrightarrow{f} & \mathbb{CP}^1. \end{array} \quad (3.13)$$

Then \mathfrak{G}^h is taken for the marked group in the second deformation, with the use of f : the right hand square in (3.13). The homeomorphism $\tilde{f} \circ \tilde{h}$ is equal to $\tilde{f} \tilde{h}$ and the required deformation of the group \mathfrak{G}^0 is $\mathfrak{G}^{fh} = \tilde{f} \mathfrak{G}^h \tilde{f}^{-1}$.

Lemma 3.8. *For $f \in QC$ the quasiconformal deformation \mathfrak{g}^f of the marked element \mathfrak{g}^0 lies in the same space \mathcal{G}_g^k .*

Proof. The following objects are mirror-symmetric relative to the real axis: the Beltrami coefficient $\mu(x) = \overline{\mu(\bar{x})}$ of the function f , the regular covering map $x^0(u) = \overline{x^0(\bar{u})}$, and the normalization set $\{0, 1, \infty\}$. The uniqueness theorem for the normalized quasiconformal homeomorphism ensures that $f(u)$ commutes with

complex conjugation. Hence the new generators $G_s^f := \tilde{f} G_s^0 \tilde{f}^{-1}$, $s = 0, 1, \dots, g$, are real linear fractional transformations. The deformation of G_0 is always trivial because \tilde{f} stabilizes the fixed points of G_0 . We claim that the deformations G_s^f of the other rotations satisfy the geometric condition in Sect. 3.1.2. Indeed, the motion \tilde{f} fixes the end-points of the interval $(0, 1)$. Hence \tilde{f} takes the real diameters of the circles C_1, C_2, \dots, C_g to disjoint closed subintervals of $(0, 1)$, and we construct new circles $C_1^f, C_2^f, \dots, C_g^f$ with diameters on these subintervals. The generator G_s^f , $s = 1, \dots, g$, maps the circle C_s^f into itself, but reverses its orientation, and therefore G_s^f has two fixed points on C_s^f . They are real if $s < k$ and complex conjugate if $s \geq k$. Hence the new rotations G_s^f , $s = 0, \dots, g$, satisfy the above-mentioned geometric condition and define an element \mathbf{g}^f of the same deformation space \mathcal{G}_g^k . \square

In fact, the deformation of the marked group \mathfrak{G}^0 generated by a map $f \in \mathbf{QC}(\mathbf{e}^0)$, where \mathbf{e}^0 is the branch divisor of the corresponding normalized covering $x^0(u)$, can be explicitly described.

Lemma 3.9. *The quasiconformal deformation of the marked group \mathfrak{G}^0 generated by a map $f \in \mathbf{QC}(\mathbf{e}^0)$ coincides with the action on \mathfrak{G}^0 of the element $[f]$ of the modular group.*

Proof. Making punctures in the domain of discontinuity \mathcal{D} of the marked group at the fixed points of the elliptic transformations, we obtain a space $\overset{\circ}{\mathcal{D}}$ with a free action of the deck transformation group \mathfrak{G}^0 . Recall that any $f \in \mathbf{QC}(\mathbf{e}^0)$ stabilizes the group induced by the covering $x^0(u)$, and hence f can be lifted from the marked point $u = 1$ to an automorphism of the covering space $\overset{\circ}{\mathcal{D}}$:

$$\begin{array}{ccc} \overset{\circ}{\mathcal{D}} & \xrightarrow{\check{f}} & \overset{\circ}{\mathcal{D}} \\ \downarrow x^0 & & \downarrow x^0 \\ \mathbb{CP}^1 \setminus \mathbf{e}^0 & \xrightarrow{f} & \mathbb{CP}^1 \setminus \mathbf{e}^0 \end{array} \quad (3.14)$$

The resulting map \check{f} can be defined by continuity at the punctures in the domain of discontinuity and on the limit set of the distinguished group with the help of the equivariance condition $\check{f}G = (f \cdot G)\check{f}$, $G, (f \cdot G) \in \mathfrak{G}^0$. Recall that the action $G \rightarrow f \cdot G$ on the deck transformation group \mathfrak{G}^0 is induced by the action of f on the fundamental group of the punctured plane $\mathbb{CP}^1 \setminus \mathbf{e}^0$; see Sect. 3.2.5. The homeomorphism $\check{f}: \mathbb{CP}^1 \rightarrow \mathbb{CP}^1$ is quasiconformal, with Beltrami coefficient $\check{\mu}$. Hence \check{f} may differ from \tilde{f} in the deformation diagram (3.12) only by normalization. Calculating $\check{f}(u)$ at $u = 0, \infty$ we see that $\tilde{f} = \check{f}$ and obtain the following expressions for the deformed generators of the marked group:

$$G_s^f := \tilde{f} G_s^0 \tilde{f}^{-1} = \check{f} G_s^0 \check{f}^{-1} = f \cdot G_s^0. \quad \square \quad (3.15)$$

3.3 Equivalence of the Representations

The equivalence of the four definitions of the universal cover of the moduli space means the existence of (compatible) continuous bijections between the topological spaces $\tilde{\mathcal{H}}_g^k$, \mathcal{T}_g^k , \mathcal{G}_g^k , and \mathcal{L}_g^k introduced above. In the following three sections we establish several homeomorphisms in succession: between the Teichmüller space and the deformation space of a special Kleinian group, between the Teichmüller space and the universal cover of the moduli space, between the labyrinth space and the deformation space of the group. We now describe the other correspondences at an intuitive level.

$\mathcal{T}_g^k \leftrightarrow \mathcal{L}_g^k$. A smooth representative f of a Teichmüller class takes some marked labyrinth Λ^0 attached to the marked divisor \mathbf{e}^0 to a labyrinth $f\Lambda^0$ of the same type. Two labyrinths of the same type can always be transformed into one another by a suitable map f , which is unique up to isotopy of the punctured plane.

$\tilde{\mathcal{H}}_g^k \leftrightarrow \mathcal{L}_g^k$. The universal cover of the moduli space is the set of the branch divisors \mathbf{e} together with the history of their motion from the marked divisor \mathbf{e}^0 . One can recover this history by treating cuts in the labyrinth as the traces left by points in the divisor in their motion. Conversely, each path in the moduli space can be deformed so that the points in the divisor \mathbf{e} do not meet the traces of their motion in the complex plane. The picture in the plane thus obtained can be completed to a labyrinth.

3.3.1 An Isomorphism Between \mathcal{T}_g^k and \mathcal{G}_g^k

We fix an element $\mathbf{g}^0 := \{G_s^0\}_{s=0}^g$ of the deformation space \mathcal{G}_g^k which defines the normalized covering $x^0(u)$. The following result is typical [4, 66] for the theory of Teichmüller spaces

Theorem 3.3. *Quasiconformal deformations bring about a homeomorphism between \mathcal{G}_g^k and the Teichmüller space $\mathcal{T}_g^k(\mathbf{e}^0)$ with marked divisor $\mathbf{e}^0 := \{x^0(\text{fix } G_s^0)\}_{s=0}^g$ formed by the branch points of the covering $x^0(u)$.*

The proof of Theorem 3.3 splits naturally into two steps.

Lemma 3.10. *Two maps in QC deform a marked element \mathbf{g}^0 in the same fashion if and only if they define the same point in the Teichmüller space $\mathcal{T}_g^k(\mathbf{e}^0)$.*

Proof. 1. We start with a special case of the lemma, when one of the quasiconformal maps is the identity:

- (a) If $f \in \text{QC}^0(\mathbf{e}^0)$, then f does not deform the marked element \mathbf{g}^0 . Indeed, in this case the quasiconformal deformation of the group is equal to the action of the modular group by Lemma 3.9, and by Theorem 3.1 the latter action is trivial for $f \in \text{QC}^0(\mathbf{e}^0)$.
- (b) If f does not deform the marked element \mathbf{g}^0 , then $f \in \text{QC}^0(\mathbf{e}^0)$. Assume that the quasiconformal deformation generated by f is trivial; then $f \in \text{QC}(\mathbf{e}^0)$.

In this case we know that the deformation of the generators of the marked group is defined by (3.15). By Theorem 3.1 it follows from the equalities $f \cdot G_s^0 = G_s^0$, $s = 0, \dots, g$, that $f \in \mathbf{QC}^0(\mathbf{e}^0)$.

2. We reduce the general case of the lemma to the special case of part 1. Combining the deformation diagrams of the maps $f_1, f_2 \in \mathbf{QC}$ we obtain

$$\begin{array}{ccccc}
 \mathcal{D}(\mathfrak{G}^{f_1}) & \xleftarrow{\tilde{f}_1} & \mathcal{D}(\mathfrak{G}^0) & \xrightarrow{\tilde{f}_2} & \mathcal{D}(\mathfrak{G}^{f_2}) \\
 \downarrow x^{f_1} & & \downarrow x^0 & & \downarrow x^{f_2} \\
 \mathbb{CP}^1 & \xleftarrow{f_1} & \mathbb{CP}^1 & \xrightarrow{f_2} & \mathbb{CP}^1
 \end{array} \tag{3.16}$$

By part 2 of Lemma 3.7 on composite deformations, the deformations of the generators of the marked group \mathfrak{G}^0 are equal if and only if the map $f_2 f_1^{-1}$ does not deform the generators of \mathfrak{G}^{f_1} . We see from the special case considered above that this can occur if and only if $f_2 f_1^{-1} \in \mathbf{QC}^0(f_1 \mathbf{e}^0)$, which is equivalent to the general case of the lemma: $f_2 \in f_1 \cdot \mathbf{QC}^0(\mathbf{e}^0)$. \square

Lemma 3.11. *The image of the Teichmüller space \mathcal{T}_g^k contains the whole of \mathcal{G}_g^k .*

Proof. We shall explicitly construct a quasiconformal homeomorphism $\tilde{f}(u)$ of the Riemann sphere that:

- (a) Fixes the three points 0, 1, ∞ .
- (b) Takes the domain of discontinuity of the marked element $\mathfrak{g}^0 \in \mathcal{G}_g^k$ to the domain of discontinuity of a prescribed element $\mathfrak{g} := \{G_s\}_{s=0}^g$ of the same deformation space.
- (c) Respects complex conjugation and intertwines the actions of the Kleinian groups \mathfrak{G}^0 and \mathfrak{G} generated by the elements \mathfrak{g}^0 and \mathfrak{g} :

$$\tilde{f} G_s^0 = G_s \tilde{f}, \quad s = 0, \dots, g. \tag{3.17}$$

The equivariant map $\tilde{f}: \mathcal{D}(\mathfrak{G}^0) \rightarrow \mathcal{D}(\mathfrak{G})$ of the covering spaces induces a map $f \in \mathbf{QC}$ between the bases. By the uniqueness of a normalized quasiconformal map, f takes the marked element of the deformation space to the prescribed element.

We start by constructing the required map \tilde{f} in a neighbourhood of the marked element \mathfrak{g}^0 . It will map the fundamental domain $R(\mathfrak{g}^0)$ onto the fundamental domain of the variable element \mathfrak{g} with coordinates $\{c_s, r_s\}_{s=1}^g \approx \{c_s^0, r_s^0\}_{s=1}^g$ in the deformation space and will respect the boundary identifications. The equivariance property (3.17) will allow us to extend the map to the whole domain of discontinuity and by continuity, also to the limit set of the marked group. We shall assemble the required map from $2g$ simple “blocks” of the two types described below and corresponding to variations of individual moduli c_s and r_s .

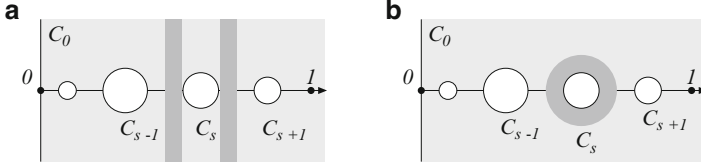


Fig. 3.10 Deforming the fundamental domain $R(g^0)$: (a) $\delta c_s \neq 0$; (b) $\delta r_s \neq 0$

CONSTRUCTION. 1. To any circle C_s , $s = 1, \dots, g$, we attach an edging consisting of vertical strips from $R(g^0) \setminus \{1\}$, as shown in Fig. 3.10a. Contracting one strip and expanding the other in the horizontal direction we can obtain a quasiconformal deformation \tilde{f} of the fundamental domain, which is the identity outside the two strips and coincides with the (conformal) horizontal translation between the strips. The translation magnitude is equal to the variation of the module c_s ; the other moduli do not change.

2. Each circle C_s , $s = 1, \dots, g$, is the inner boundary of a concentric annulus, lying in $R(g^0) \setminus \{1\}$ entirely as in Fig. 3.10b. (Non-uniformly) expanding/contracting this annulus along the radii while fixing its outer boundary component and setting \tilde{f} to be the identity outside the annulus we obtain the required deformation of the fundamental domain. The variation of r_s will be a function of the variation of the inner radius of the ring; the same holds for the variations of the c_s for $s \geq k$; the other moduli do not change.

We see that for two close points g^0 and g in the deformation space there exists a motion $f \in \text{QC}$ taking one to the other. If the distance between two points is large, then connecting them by a compact path we find a finite sequence of points $g^0, g^1, \dots, g^n := g$ such that g^s is a quasiconformal deformation of g^{s-1} generated by an explicitly described map $f_s \in \text{QC}$. By part 2 of Lemma 3.7, concerned with composite deformations, the quasiconformal map $f_n \dots f_2 f_1$ deforms the marked element g^0 into an arbitrary prescribed element g .

□

Proof (of Theorem 3.3). We showed in Lemmas 3.8 and 3.10 that the map $\mathcal{T}_g^k(\mathbf{e}^0) \rightarrow \mathcal{G}_g^k$ is well defined and injective, and Lemma 3.11 says that it is surjective. The continuity of the bijection $\mathcal{T}_g^k \leftrightarrow \mathcal{G}_g^k$ with respect to the Teichmüller metric on \mathcal{T}_g^k and the topology of \mathcal{G}_g^k follows from the construction of the direct and the inverse maps; see also formula (3.20) for infinitesimal quasiconformal transformations.

□

3.3.2 An Isomorphism Between \mathcal{T}_g^k and $\tilde{\mathcal{H}}_g^k$

The action of the modular group on a deformation space, which is described by Lemma 3.9, can readily be expressed in terms of the coordinates $\{c_s, r_s\}_{s=1}^g$. Dehn half-twists along contours encircling a pair of punctures in the half-plane (see

Fig. 3.3) generate the modular group [21] and act as follows on the generators of the Kleinian group \mathfrak{G} :

$$\beta_{s-k} \cdot (\dots, G_{s-1}, G_s, \dots)^t = (\dots, G_{s-1} G_s G_{s-1}, G_{s-1}, \dots)^t, \quad s = k+1, \dots, g; \quad (3.18)$$

the action of the twist β_{s-k} on the generators other than G_{s-1} and G_s is trivial. We can show (see Exercise 16) that this change of generators does not take us outside our deformation space. The transformation (3.18) is similar to the Artin representation of a braid group into the automorphism group of a free group. Now we shall see that this is not a mere coincidence: the modular group $\text{Mod}(\mathfrak{e}^0)$ is a braid group and formulae (3.18) describe deck transformations of the universal cover of the moduli space.

Theorem 3.4. 1. The spaces $\mathcal{T}_g^k(\mathfrak{e}^0)$ and $\tilde{\mathcal{H}}_g^k$ are homeomorphic.
2. The groups $\text{Mod}(\mathfrak{e}^0)$ and Br_{g-k+1} are isomorphic [17, 21].

Proof. We showed in Lemma 3.2 that the moduli space \mathcal{H}_g^k is the quotient of $\mathcal{T}_g^k(\mathfrak{e}^0)$ by the action of the modular group. We claim that $\text{Mod}(\mathfrak{e}^0)$ acts (A) freely and (B) discontinuously on the Teichmüller space and therefore the projection $\mathcal{T}_g^k(\cdot) \rightarrow \mathcal{H}_g^k$ is a covering map. This is a universal covering because the space $\mathcal{T}_g^k \cong \mathcal{G}_g^k$ is a cell by Lemma 3.3. Accordingly, the deck transformation group $\text{Mod}(\mathfrak{e}^0)$ of this covering is isomorphic to the fundamental group of the moduli space, which is isomorphic to the braid group Br_{g-k+1} by Lemma 3.1.

- A. Let for a representative $h \in \text{QC}(\mathfrak{e}^0)$ of the modular group there exists a motion $f \in \text{QC}$ such that $fh \in f \cdot \text{QC}^0(\mathfrak{e}^0)$. Thus, h represents the identity element of the modular group.
- B. Transformations in the modular group are isometries of the Teichmüller space, and so the discontinuity of the action of $\text{Mod}(\mathfrak{e}^0)$ will follow from discreteness of its orbits. We recall from Sect. 3.1.1 that, by taking another marked divisor \mathfrak{e}^0 , each orbit of the modular group can be isometrically transformed into an orbit passing through the marked point $[id]$ in the Teichmüller space. Thus, let $h_n \in \text{QC}(\mathfrak{e}^0)$ be a sequence generating infinitesimally small deformations of the generators of the marked group: $G_s^{h_n} \rightarrow G_s^0, s = 0, \dots, g$.

The deformation of generators was calculated in Lemma 3.9. It is as follows: $G_s^{h_n} = h_n \cdot G_s^0$. The isotropy group of $u = 1$ in \mathfrak{G}^0 is trivial, so the convergence $G_s^{h_n} u \rightarrow G_s^0 u$ implies that $h_n \cdot G_s^0 = G_s^0$ starting from some index n . By Theorem 3.1 the trivial action of h_n on the group \mathfrak{G}^0 means that h_n represents the identity element of the modular group. \square

The identifications of the Teichmüller space with the universal cover of the moduli space and the deformation space of the special Kleinian group give us two coordinate charts in \mathcal{T}_g^k . First, we have the global coordinate variables $\{c_s, r_s\}_{s=1}^g$ in \mathcal{G}_g^k , which range over a cell. Second, we have systems of coordinates in \mathcal{H}_g^k related to the branch points. The following result establishes a connection between the two systems of coordinates.

Theorem 3.5. *The map $\tilde{\mathcal{H}}_g^k \rightarrow \mathcal{G}_g^k$ is real analytic in local coordinates. Its Jacobi matrix is non-singular and has entries effectively calculated with the use of quadratic Poincaré series.*

Proof. To express our map in terms of local variables we must deform the generators of the marked group using the local section (3.4) of the projection in Lemma 3.2. It is sufficient to look at the map in the neighbourhood of the marked divisor \mathbf{e}^0 and, if necessary, to replace the marked divisor and the marked group with the help of part 2 of Lemma 3.7, concerned with composite deformations. As local coordinate variables in a neighbourhood of the marked point in the moduli space \mathcal{H}_g^k we shall take the (independent) real and imaginary parts of the complex points e_1, e_2, \dots, e_{2g} that form together with ± 1 a simple branch divisor $\mathbf{e} \approx \mathbf{e}^0$. The fixed points of the generators of the distinguished group deformed by $f(\mathbf{e}, x)$ define a map $\{e_s\}_{s=1}^{2g} \rightarrow \{c_s, r_s\}_{s=1}^g$ in a small complex neighbourhood of $\{e_s^0\}_{s=1}^{2g}$:

$$\left. \begin{aligned} c_s(\mathbf{e}) \pm r_s(\mathbf{e}), & \quad 0 < s < k \\ c_s(\mathbf{e}) \pm i r_s(\mathbf{e}), & \quad k \leq s \leq g \end{aligned} \right\} := \text{fix } G_s^f = \tilde{f}(\mathbf{e}, \text{fix } G_s^0). \quad (3.19)$$

Corresponding to symmetric divisors \mathbf{e} in a $2g$ -dimensional complex neighbourhood are a real $2g$ -plane and the real moduli c_s and $r_s > 0$. Now we prove the following results.

- A. *The complex map $\{e_s\}_{s=1}^{2g} \rightarrow \{c_s, r_s\}_{s=1}^g$ is holomorphic.*
- B. *The linear part (Jacobi matrix) of this map can be calculated explicitly.*
- C. *The Jacobi matrix of the map is non-singular.*
- A. The Beltrami coefficient $\mu(\mathbf{e}, x)$ of the function (3.4) depends holomorphically in $L_\infty(\mathbb{C})$ on the components of \mathbf{e} . The dependence on \mathbf{e} of the coefficient $\tilde{\mu}(\mathbf{e}, u) := \mu(\mathbf{e}, x) \overline{x_u^0} / x_u^0$, which is defined in the domain of discontinuity $\mathcal{D}(\mathfrak{G}^0)$, is also holomorphic. By a well-known result [3] the map $\tilde{f}(\mathbf{e}, \cdot)$ depends analytically on the components of \mathbf{e} . In particular, all the functions $v(\mathbf{e}) := \tilde{f}(\mathbf{e}, v)$, $v \in \{\text{fix } G_s^0\}_{s=1}^g$, are holomorphic; the functions $c_s(\mathbf{e})$ and $r_s(\mathbf{e})$ are their linear combinations.
- B. The differentials of the functions $v(\mathbf{e})$ can be calculated by the following formula for an infinitesimal deformation [3, 66] (here and throughout $\overset{o}{=}$ means equality to within terms of order $O\left(\sum_{s=1}^{2g} |e_s - e_s^0|^2\right)$):

$$\begin{aligned} 2\pi i (v(\mathbf{e}) - v(\mathbf{e}^0)) &\overset{o}{=} \int_{\mathbb{C}} \tilde{\mu}(\mathbf{e}, u) \frac{v(v-1)}{u(u-1)} \frac{du \wedge \overline{du}}{u-v} = \\ &= \int_{R(\mathfrak{g}^0)} \tilde{\mu}(\mathbf{e}, u) \left[\sum_{G \in \mathfrak{G}^0} \frac{(dG(u)/du)^2}{Gu(Gu-1)} \frac{v(v-1)}{Gu-v} \right] du \wedge \overline{du} = \\ &= v(v-1) \int_{\mathbb{C}} \mu(\mathbf{e}, x) \Omega^v(x) dx \wedge \overline{dx}. \end{aligned} \quad (3.20)$$

In the last but one integral the quadratic Poincaré series defines a meromorphic quadratic differential $\Omega^v(x)(dx)^2$ on the Riemann sphere $x^0(\mathbf{R})$ which depends on the point $v \in \{\text{fix } G_s^0\}_{s=1}^g$ as a parameter. Its singularities are simple poles, which can be placed at points in the divisor \mathbf{e}^0 and at infinity. Such quadratic differentials (*of finite area* [66]) form a complex vector space of dimension $2g$ with basis

$$\Omega_s(x)(dx)^2 := (x^2 - 1)^{-1}(x - e_s^0)^{-1}(dx)^2, \quad s = 1, \dots, 2g. \quad (3.21)$$

We continue (3.20) as follows:

$$\begin{aligned} (v^2 - v) \int_{\mathbb{C}} \mu(\mathbf{e}, x) \Omega^v(x) dx \wedge \overline{dx} &\doteq \\ &\doteq (v^2 - v) \int_{\mathbb{C}} \Omega^v(x) \sum_{s=1}^{2g} (e_s - e_s^0) \sigma_{\bar{x}}(x - e_s^0) dx \wedge \overline{dx} = \\ &= -(v^2 - v) \sum_{s=1}^{2g} (e_s - e_s^0) \int_{\text{supp } \sigma_{\bar{x}}(x - e_s^0)} d(\Omega^v(x) \sigma(x - e_s^0) dx) = \\ &= 2\pi i (v^2 - v) \sum_{s=1}^{2g} \text{Res}_{x=e_s^0} \Omega^v(x) (e_s - e_s^0). \end{aligned}$$

In the last equality we have used that the function $\sigma_{\bar{x}}$ has support in an annulus, moreover, $\sigma = 1$ on the inner component of the boundary and $\sigma = 0$ on the outer component. One readily recovers the differentials of the functions $c_s(\mathbf{e})$ and $r_s(\mathbf{e})$ from these expressions.

- C. Assume that the differential of the map $\{e_s\}_{s=1}^{2g} \rightarrow \{c_s, r_s\}_{s=1}^g$ degenerates at \mathbf{e}^0 .

Then there exists a non-trivial tangent vector $\mathbf{E} := \sum_{j=1}^{2g} \varepsilon_j \partial / \partial e_j$ such that for $\mathbf{e} = \mathbf{e}^0$

$$\mathbf{E}c_s(\mathbf{e}) = \mathbf{E}r_s(\mathbf{e}) = 0, \quad s = 1, 2, \dots, g.$$

Now we differentiate the condition of the equivariance of $\tilde{f}(\mathbf{e}, \cdot)$,

$$G^f \tilde{f}(\mathbf{e}, u) = \tilde{f}(\mathbf{e}, Gu), \quad G \in \mathfrak{G}^0, G^f \in \mathfrak{G}^f,$$

in the direction of \mathbf{E} . Then we see that the derivative of the deformation $\tilde{f}(\mathbf{e}, u)$ in the direction of \mathbf{E} at the point \mathbf{e}^0 under consideration defines a \mathfrak{G}^0 -invariant reciprocal differential $\mathbf{E}\tilde{f}(\mathbf{e}^0, u)(du)^{-1}$. We claim that all the coefficients ϵ_s of the vector \mathbf{E} must be zero. For a proof we pull back the basis element (3.21) to the domain of discontinuity $\mathcal{D}(\mathfrak{G}^0)$: $\hat{\Omega}_s(u)(du)^2 := \Omega_s(x^0(u))(dx^0(u))^2$. The product of a quadratic and a reciprocal differential is a smooth \mathfrak{G}^0 -invariant differential $\hat{\Omega}_s(u) \cdot \mathbf{E}\tilde{f}(\mathbf{e}^0, u)du$ on $\mathcal{D}(\mathfrak{G}^0)$, and therefore

$$\begin{aligned}
0 &= \int_{\partial R(g^0)} \tilde{\Omega}_s(u) \cdot \mathbf{E} \tilde{f}(e^0, u) du = \\
&= \int_{R(g^0)} d(\tilde{\Omega}_s \cdot \mathbf{E} \tilde{f} du) = - \int_{R(g^0)} \tilde{\Omega}_s \cdot (\mathbf{E} \tilde{f})_{\bar{u}} du \wedge \overline{du}
\end{aligned}$$

(differentiation of \tilde{f} with respect to e_s commutes with differentiation with respect to the variable \bar{u})

$$\begin{aligned}
&= - \int_{R(g^0)} \tilde{\Omega}_s(u) \sum_{j=1}^{2g} \varepsilon_j \sigma_{\bar{x}}(x^0(u) - e_j^0) \frac{\overline{x_u^0}}{x_u^0} du \wedge \overline{du} \\
&= - \int_{\mathbb{C}} \Omega_s(x) \sum_{j=1}^{2g} \varepsilon_j \sigma_{\bar{x}}(x - e_j^0) dx \wedge \overline{dx} = \sum_{j=1}^{2g} \varepsilon_j \int_{\text{supp } \sigma_{\bar{x}}(x - e_j^0)} d(\Omega_s(x) \sigma(x - e_j^0) dx) \\
&= -2\pi i \sum_{j=1}^{2g} \varepsilon_j \text{Res}_{x=e_j^0} \Omega_s(x) = -2\pi i \varepsilon_s / ((e_s^0)^2 - 1).
\end{aligned}$$

Since the quantity e_s^0 is finite, it follows that $\varepsilon_s = 0$. □

3.3.3 An Isomorphism Between \mathcal{L}_g^k and \mathcal{G}_g^k

In finding the subgroup induced by the ramified covering $x(u)$ in Sect. 3.2.4, to an element of the deformation space we assigned a special labyrinth, namely, the projection of the boundary of the fundamental domain corresponding to this element. The inverse correspondence is the basis of the following result.

Theorem 3.6. *The spaces \mathcal{L}_g^k and \mathcal{G}_g^k are homeomorphic.*

Proof. We shall establish a 1–1 correspondence between these spaces.

- A. The map $\mathcal{G}_g^k \rightarrow \mathcal{L}_g^k$. Corresponding to each element of the deformation space \mathcal{G}_g^k is a system of circles C_0, C_1, \dots, C_g bounding the fundamental domain of the Kleinian group generated by this element. We claim that the normalized projection $x(u)$ takes the boundary of the fundamental domain to a labyrinth Λ . For instance, let us verify that for $s < k$ the arcs $x C_s$ are real intervals. In fact, if $|u - c_s| = r_s$, then $u = G_s \bar{u}$ and we have the chain of equalities

$$x(u) = x(G_s \bar{u}) = x(\bar{u}) = \overline{x(u)} \in \mathbb{R}.$$

Admissible perturbations of the circles C_s , $s = k, \dots, g$, do not change the equivalence class of the labyrinth.

- B. The map $\mathcal{L}_g^k \rightarrow \mathcal{G}_g^k$. Corresponding to each divisor \mathbf{e} of type (g, k) is an orbit of the modular group acting on \mathcal{G}_g^k . There is a single normalized covering $x(u): \mathring{\mathcal{D}} \rightarrow \mathbb{CP}^1 \setminus \mathbf{e}$ associated with all points in this orbit. By Lemma 3.4 the subgroup induced by this covering is equal to the kernel of any representation of the form χ_Λ from the fundamental group of $\mathbb{CP}^1 \setminus \mathbf{e}$ into the abstract group $\mathfrak{G} := \langle G_0, G_1, \dots, G_g | G_s^2 = 1 \rangle$. Fixing a labyrinth Λ one can realize elements of \mathfrak{G} as deck transformations of $x(u)$, which are real linear fractional maps. For example, $G_0(u) = -u$ (the unique rotation of order 2 with fixed points 0 and ∞). We shall show that the realization of the remaining generators G_1, G_2, \dots, G_g satisfies the geometric condition in Sect. 3.1.2.

By definition the representation χ_Λ is trivial on the fundamental group of the Riemann sphere cut along the labyrinth Λ . Hence we obtain a well-defined map $u(x)$ of $\mathbb{CP}^1 \setminus \Lambda$ inverting $x(u)$, normalized by the condition $u(\infty) = 1$, and inheriting the mirror symmetry property $\bar{u}(x) = u(\bar{x})$. This map blows up the cuts in the labyrinth to smoothly embedded circles symmetrically threaded on the real axis in the same order as the cuts $\Lambda_0, \Lambda_1, \dots, \Lambda_g$. Hence

$$0 = \mathbb{R} \cap (u\Lambda_0) < \mathbb{R} \cap (u\Lambda_1) < \dots < \mathbb{R} \cap (u\Lambda_g) < 1. \quad (3.22)$$

Each set $\mathbb{R} \cap (u\Lambda_i)$, $i = 1, \dots, g$, consists of two points which are interchanged by $G_i(u)$ if $i \geq k$ or fixed by it if $i < k$. The circle C_i with centre on \mathbb{R} passing through the points $\mathbb{R} \cap (u\Lambda_i)$ contains the fixed points of the rotation $G_i(u)$ and is disjoint from the other circles of this kind by (3.22). We see that the system of generators G_0, G_1, \dots, G_g defines an element of the deformation space \mathcal{G}_g^k .

The maps in parts A and B of the proof are mutually inverse. Indeed, by construction the labyrinth $\{A_s\}_{s=0}^g$ and the labyrinth $\{xC_s\}_{s=0}^g$ obtained by applying to it the composite map $\mathcal{L}_g^k \rightarrow \mathcal{G}_g^k \rightarrow \mathcal{L}_g^k$ have the same representation χ_Λ ; hence they lie in the same class of labyrinth spaces by Theorem 3.2. By Theorem 3.5 the bijection $\mathcal{L}_g^k \leftrightarrow \mathcal{G}_g^k$ constructed above is continuous since the local coordinates in the labyrinth space have been borrowed from the moduli space \mathcal{H}_g^k . \square

3.4 Problems and Exercises

1. Show that the full affine group \mathfrak{A}_1 of the real axis does not act freely on the space of symmetric divisors \mathbf{e} , while its subgroup \mathfrak{A}_1^+ acts freely.
2. For $k = 0, 1, \dots, g$, a coordinate chart in the moduli space \mathcal{H}_g^k can be introduced as follows. Fix a pair of complex conjugate points in the divisor; for example, $\mathbf{e} = \{-i, i, e_1, \dots, e_{2g}\}$. Then take the independent real and imaginary parts of the variable points e_1, e_2, \dots, e_{2g} for the local coordinates of the divisor \mathbf{e} . Find the transition functions to coordinate charts introduced earlier in the moduli space.

3. Prove that the normalized projection $x(u): \mathcal{D}(\mathfrak{G}) \rightarrow \mathbb{CP}^1$ in Sect. 3.1.2 commutes with complex conjugation.
4. Prove that the limit set of the Kleinian group \mathfrak{G} in Sect. 3.1.2 lies on the real axis; in particular, the plane measure of this set is zero.
5. Show that the points in the limit set of the Schottky group \mathfrak{S} are in bijective correspondence with uncancellable infinite words on the alphabet formed by the generators of the group (for example, $S_2 S_1^{-1} S_g^{-2} \dots$). Deduce from this that the limit set of the group is uncountable for $g > 1$.
6. Let \mathfrak{G} be an arbitrary Kleinian group (that is, a group acting discontinuously on the plane) and \mathfrak{S} be its finite-index subgroup. Show that \mathfrak{G} and \mathfrak{S} have the same limit sets; see [89].
7. List all the elliptic elements of the group \mathfrak{G} in Sect. 3.1.2.
Answer. $G^{-1}G_s G$, $s = 0, \dots, g$, $G \in \mathfrak{G}$.
8. Show that the fixed elements of the hyperelliptic involution J of the quotient space \mathcal{D}/\mathfrak{G} by the Schottky group correspond to the fixed points of generators of the Kleinian group \mathfrak{G} in the fundamental domain \mathcal{D} .
9. Prove Lemma 3.1 for $k = 0$.
10. Find the Beltrami coefficient of the composition of quasiconformal maps h and f .
Answer. $\mu_{hf}(x) = \frac{\mu_f(x) + \mu_h(f(x))\kappa}{1 + \mu_f(x)\mu_h(f(x))\kappa}$, where $\kappa := \bar{p}/p$ and $p := f_x(x)$.
11. Let $\mu(u)\overline{du}/du$ be a Beltrami differential on the Riemann sphere which is invariant under a linear fractional transformation $S(u)$ and let $f(u)$ be the solution of the corresponding Beltrami equation. Show that the homeomorphisms $f(u)$ and $f(S(u))$ have equal Beltrami coefficients.
12. Show that the expression (3.2) defines a metric in the Teichmüller space and in the orbit space of the modular group.
13. Prove formula (3.3) in the case of a small normalized quasiconformal deformation; see [3].
14. Let $[\rho]$ be a loop associated with the edge $[e_9, e_{10}]$ in Fig. 3.6. Show that $[\rho]^2$ lies in the normal subgroup described in the beginning of Lemma 3.4.
15. Show that for each t the map $\tilde{f}_t(u)$ in Theorem 3.1 commutes with deck transformations of the covering $\mathbb{H} \rightarrow \mathbb{CP}^1 \setminus \mathbf{e}$. What is the image of the map mirror symmetric to $f(x)$?
16. Derive formula (3.18). Using elementary geometric methods show that this transformation does not take us out of the deformation space.
17. Consider a group acting freely by isometries on a metric space X and having discrete orbits. Show that it acts discontinuously on X .
18. Show that the space of quadratic differentials admitting simple poles only at fixed $m + 3$ points on the Riemann sphere has dimension m .
Hint. The divisor of a meromorphic quadratic differential on the sphere has degree -4 .
19. Give a direct proof (making no recourse to other models of the universal cover) that the labyrinth space \mathcal{L}_g^k is homeomorphic to $\tilde{\mathcal{H}}_g^k$.

Chapter 4

Cell Decomposition of the Moduli Space

For an efficient use of the Chebyshev representation for extremal polynomials we must investigate how the periods of the abelian differential η_M behave as functions of a point M in the moduli space. In this chapter we develop a combinatorial geometric approach to the investigation of the period map. To curves M in the moduli space we shall assign in a one-to-one fashion trees Γ of a special form with edges labelled by positive numbers. This defines a partitioning of the space

$\mathcal{H} := \bigsqcup_{g=0}^{\infty} \bigsqcup_{k=0}^{g+1} \mathcal{H}_g^k$ into cells $\mathcal{A}[\Gamma]$ enumerated by trees, in which some of the global coordinate variables are periods of the 1-form associated with the curve. A similar cell decomposition of the moduli spaces of curves is used in conformal field theory (Kontsevich, Penner, Fock, Chekhov; see the references in the survey paper [48]). Our techniques allow a graphical representation and classification of extremal polynomials. We shall use it in what follows to describe the image of the global period map defined on the universal covering spaces of components of the total moduli space \mathcal{H} .

4.1 Curves and Trees

The abelian integral of the third kind $y(x) := \int^x \eta_M$ is a Schwarz–Christoffel integral, which maps the suitably cut upper half-plane \mathbb{H} onto a certain comb-like domain with geometric parameters allowing one to recover all the periods of η_M . For the first time this important observation was made by Akhiezer in the case of curves associated with Chebyshev polynomials on several intervals (see a discussion in [37]). To describe the system of cuts we can conveniently use Strebel’s theory of foliations associated with quadratic differentials [143]. Throughout Sect. 4.1 the curve M is fixed, and therefore we drop the corresponding subscript of the associated 1-form η_M .

4.1.1 Foliations and global width Function

With a quadratic differential on a Riemann surface we can associate two foliations: the vertical and the horizontal ones [143]. In our case the quadratic differential $\eta^2(x)$ is defined on the Riemann sphere. Leaves of the horizontal foliation $\eta^2(x) > 0$ are level curves of the locally defined function $\text{Im} \int^x \eta$. Leaves of the vertical foliation $\eta^2(x) < 0$ are level curves of the globally defined function $W(x) := \left| \text{Re} \int_{(e_s, 0)}^{(x, w)} \eta \right|$. In view of the normalization of the differential η , the function $W(x)$:

- (a) Is well defined on the entire x -plane.
- (b) Vanishes at the branch points $x = e_j$, $j = 1, \dots, 2g + 2$.
- (c) Has a logarithmic pole at infinity and
- (d) Is harmonic outside its zero set.

In other words, the *width function* $W(x)$ is the Green's function of the plane cut along a piecewise smooth set Γ_1 containing all the branch points, $\Gamma_1 := \{x \in \mathbb{C} : W(x) = 0\}$.

The horizontal foliation $\eta^2(x) > 0$ is orthogonal to level curves of $W(x)$ and therefore contains no cycles or limit cycles. In Strebel's terminology the global structure of trajectories in the foliation is as follows: the leaves starting at finite *critical points* (that is, at points in the divisor (η^2) of the quadratic differential) partition the complex plane into strips, which come from infinity, pass through the zero set of $W(x)$, and return to infinity. The local structure of the foliation $\eta^2(x) > 0$ in the neighbourhood of its critical points is depicted in Fig. 4.1.

Example 4.1. For the genus-zero curve $M := \{w^2 = x^2 - 1\}$ associated quadratic differential is $\eta^2 = (x^2 - 1)^{-1} (dx)^2$, and the global width function is $W(x) = |\text{Re} \log(x + \sqrt{x^2 - 1})|$. The vertical and horizontal foliations of this quadratic differential are formed by the confocal ellipses and hyperbolae with foci at ± 1 , respectively. The horizontal foliation has two critical trajectories, the rays $(-\infty, -1]$ and $[1, \infty)$; their complement is a Strebel strip.

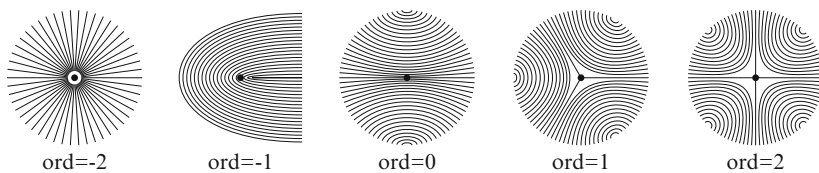


Fig. 4.1 The foliation $\eta^2 > 0$ in a neighbourhood of points with $\text{ord } \eta^2 = -2, -1, 0, 1, 2$

4.1.2 The Graph Γ of the Curve M

CONSTRUCTIONS ([42]). We associate with a curve $M \in \mathcal{H}$ a compact planar graph $\Gamma = \Gamma(M)$ consisting of two parts, Γ_+ and Γ_- . The component $\Gamma_+ := \{x \in \mathbb{C}: W(x) = 0\}$ is said to be *vertical*. By the *horizontal* component Γ_- we mean the all possible intervals of the horizontal foliation $\eta^2(x) > 0$ connecting finite critical points of the foliation with one another or with Γ_+ and oriented in the increasing direction of function $W(x)$. By *vertices* V of the graph Γ we mean all finite points of the divisor of η^2 and points in the intersection $\Gamma_+ \cap \Gamma_-$. Outside its vertices the graph is the union of finitely many intervals of vertical and horizontal trajectories of the quadratic differential η^2 , which we call its edges R . The measures $|\operatorname{Re} \eta|$ and $|\operatorname{Im} \eta|$ associated with η^2 enable us to define the *width* W and the *height* H of an arbitrary smooth curve in the plane, respectively. For instance, the width $W(R)$ of an edge $R \subset \Gamma$ is equal to the increase of the width function $W(x)$ along R , and the height $H(R)$ of each horizontal edge R is zero.

- REMARKS. 1. The vertical foliation of the quadratic differential η^2 is a Jenkins-Strebel foliation, as in the Kontsevich-Strebel (KS) construction [62, 84]. However, the topology of our foliation is entirely different: in the KS-case the critical trajectories of the foliation partition the surface into punctured discs, while in our case we have annuli (maybe with crumpled boundary). Furthermore, for our construction of a graph, by contrast with KS we use segments of *two* orthogonal foliations. In our case the quadratic differential η^2 usually has simple poles, not allowed in the KS-construction. Despite all these formal differences, the ideas behind these constructions are similar.
2. For the curve M generated by a polynomial $P_n(x)$ in the context of the Chebyshev correspondence in Chap.2 the vertical part of the graph $\Gamma_+ := P_n^{-1}([-1, 1])$ was earlier considered by many authors (see references in [37]). It proved to be useful in the investigation of least deviation polynomials on several intervals and was called the *support set of the polynomial*, the *n -regular set*, or the *maximal set of least deviation*. For the first time the full graph Γ associated with a generic polynomial was considered by Meiman [104] in 1960, where he also announced Lemma 4.3.

Thus, any real hyperelliptic curve gives rise to a planar graph Γ with edges of two types: oriented horizontal edges equipped with their widths W and non-oriented vertical edges equipped with their heights H . We give several typical graphs $\Gamma(M)$ in Figs. 4.2, 4.3b, 4.6, and 5.6, where the *vertical component* is plotted by double

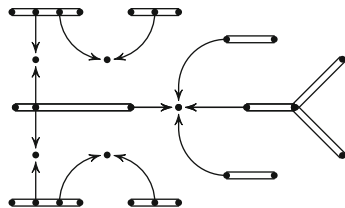


Fig. 4.2 The associated graph of some curve M for $g = 8$ and $k = 2$

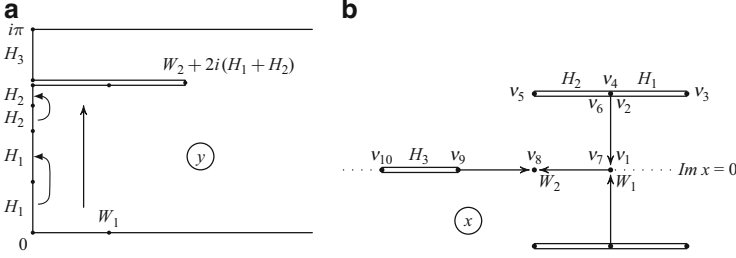


Fig. 4.3 (a) A comb-like domain with identifications of sides; (b) a weighted tree Γ

lines. In what follows we are interested in a graph only as a combinatorial object equipped with numbers. We say that two partially oriented graphs in the plane are equivalent if one of them can be transformed into the other by a motion of the half-plane \mathbb{H} extended to the whole plane by symmetry. We denote the equivalence class of a graph Γ by $[\Gamma]$ and the equivalence class of a graph with edges labelled by positive numbers by $\{\Gamma\}$.

4.1.3 Characteristics of a Graph Γ

Let us introduce several combinatorial characteristics of a graph whose meaning will be clear from what follows. We denote the subgraph of Γ lying in the upper half-plane or on the real axis by $\Gamma_\star^+ := \Gamma_\star \cap \mathbb{H}$ and $\Gamma_\star^0 := \Gamma_\star \cap \mathbb{R}$, respectively, where the subscript \star can be empty or equal to $|$ or $-$. The degree of a vertex V relative to the graph Γ_\star^\bullet will be denoted by $d_\star^\bullet = d_\star^\bullet(V)$. The horizontal edges are oriented, and therefore one can define also the quantities $d_{\text{in}}^\bullet(V)$ and $d_{\text{out}}^\bullet(V)$ equal to the numbers of incoming or outgoing edges of the graph Γ_\star^\bullet incident to the vertex V , respectively, where the superscript \bullet can be empty or equal to 0 or $+$.

DEFINITIONS. We set $\text{ord}(V) := d_|(V) + 2d_{\text{in}}(V) - 2$,

$$g(\Gamma) := \#\{V \in \Gamma : \text{ord}(V) \equiv 1 \pmod{2}\} / 2 - 1,$$

$$k(\Gamma) := \#\{V \in \Gamma^0 : \text{ord}(V) \equiv 1 \pmod{2}\} / 2,$$

$$\dim(\Gamma) := \#\{R \subset (\Gamma_+^+ \cup \Gamma_-^0)\} + \#\{V \in (\Gamma_-^+ \cup \Gamma_-^0) \setminus \Gamma_|\} - 1,$$

$$\text{codim}(\Gamma) := 2g(\Gamma) - \dim(\Gamma),$$

$$\text{codim}(V) := d_{\text{out}}^+(V) + \begin{cases} 2d_{\text{in}}(V) - 4, & V \in \Gamma_-^+ \setminus \Gamma_+^+, \\ d_{\text{in}}(V) - 2, & V \in \Gamma_-^0 \setminus \Gamma_+^0, \\ 2(d_|(V) \pmod{2}) + d_+^+(V) - 3, & V \in \Gamma_+^+, \\ d_|(V) \pmod{2} + d_+^+(V) - 1, & V \in \Gamma_+^0; \end{cases}$$

in the last definition $V \in \Gamma^0 \cup \Gamma^+$ and the residue mod 2 takes the values 0 or 1.

4.1.4 Properties of the Graph of a Curve

In the following result the combinatorial characteristics ord , g , and k are expressed in terms of the original curve M .

Lemma 4.1. *Let $\Gamma(M)$ be a graph corresponding to a curve $M \in \mathcal{H}_g^k$. Then:*

1. $\text{ord}(V)$ is the order of the quadratic differential η^2 at the vertex V .
2. $g(\Gamma)$ is the genus of M .
3. $k(\Gamma)$ is the number of coreal ovals on M .

Proof. 1. The quantity $2 + \text{ord}(V)$, which is either d_1 for $W(V) = 0$ or $2d_{\text{in}}$ for $W(V) > 0$, has the meaning of the number of trajectories in the vertical or respectively horizontal foliation of the quadratic differential η^2 that are incident to V . This integer is two greater than the order of η^2 at V [143].

2. Points at which the order of η^2 is odd are branch points of M .

3. $2k(M)$ is the number of real branch points of M . □

Weighted graphs $\{\Gamma\}$ associated with curves have several structural and quantitative constraints. Their complete list is given in the next lemma.

Lemma 4.2. A_1 . Γ is a finite tree symmetric about the real axis (together with all the structures on it).

A_2 . Horizontal edges starting at a vertex are separated by edges ending at it or by vertical edges. In particular, hanging vertices of the following form are forbidden: $\bullet \longrightarrow$

A_3 . If the order $\text{ord}(V)$ of a vertex V is zero, then $V \in \Gamma_+ \cap \Gamma_-$.

A_4 . The sum of the heights H of all vertical edges in a tree is π .

A_5 . If V belongs to Γ_+ , then $W(V) = 0$.

Proof. A_1 . We claim that Γ is a connected graph without cycles. Assume that it contains cycles; then its complement contains a bounded region. Integrating the square of the gradient of $W(x)$ over this region we obtain 0 because W is a harmonic function outside Γ vanishing on the vertical edges of the graph, while its normal derivative vanishes on the horizontal edges.

The graph is connected since the sum $\text{ord}(V)$ taken over all vertices is twice the number of edges minus twice the number of vertices, that is, it is equal to the number of components of Γ multiplied by -2 . By Lemma 4.1 this is also equal to the degree of the divisor of the quadratic differential η^2 on the sphere plus the order of its pole at infinity, which is -2 . The symmetry of the weighted graph can be seen from the fact that the quadratic differential is real: $\eta^2(\bar{x}) = \bar{\eta}^2(x)$.

A_2 . If $W(V) > 0$, then on horizontal trajectories of η^2 incident to V the function W increases and decreases alternately. Trajectories on which W decreases are exactly the incoming horizontal edges of Γ . On the other hand, if $W(V) = 0$, then the horizontal trajectories starting at V alternate with vertical trajectories, which coincide locally with vertical edges of Γ .

- A_3 . The graph has vertices at finite points in the divisor of the quadratic differential (at which $\text{ord}(V) \neq 0$ by Lemma 4.1) and at common points of the vertical and horizontal components of the graph Γ .
- A_4 . In the domain $\mathbb{C} \setminus \Gamma_+$ the differential $\eta(x)$ has a single-valued branch since each component of Γ_+ contains an *even* number of branch points of M . Deforming the boundary of the domain into a large circle we obtain

$$\pm 2\pi i = \int_{\partial(\mathbb{C} \setminus \Gamma_+)} \eta = i \int_{\partial(\mathbb{C} \setminus \Gamma_+)} \text{Im } \eta = \pm 2i \int_{\Gamma_+} |\text{Im } \eta| = \pm 2i \sum_{R \subset \Gamma_+} H(R).$$

- A_5 . This holds by definition. \square

The next lemma gives one a hint of how a hyperelliptic curve can be recovered from a weighted graph.

Lemma 4.3. *The abelian integral of the third kind $y(x) := \int^x \eta$ maps the upper half-plane cut along Γ homeomorphically onto a horizontal half-strip of height π with finitely many horizontal cuts starting at the vertical component of its boundary.*

Proof. The abelian integral has the following form: $y(x) = W(x) + iH(x)$, $x \in \mathbb{H} \setminus \Gamma$, where $W(x)$ is the global width function and $H(x)$ is the conjugate harmonic function with a single-valued branch in the simply connected domain $\mathbb{H} \setminus \Gamma$ normalized by the condition $H(x) = 0$ for $x > \Gamma^0$. We shall interpret the height function $H(x)$ in terms of the foliation $\eta^2 > 0$ restricted to the domain $\mathbb{H} \setminus \Gamma$.

Each leaf of the foliation starts and ends at the boundary of the domain, which consists of the following parts: $\infty, \mathbb{R} \setminus \Gamma, \Gamma_-, \Gamma_+$. Searching through all possible cases we can describe the behaviour of the leaves oriented in the increasing direction of $W(x)$ as follows: *finitely many leaves start at vertices of Γ_- , all other leaves start from Γ_+ ; all leaves go to infinity staying within the upper half-plane*. For instance, a leaf cannot start or end at $\mathbb{R} \setminus \Gamma$; otherwise its end-point is a critical point of the foliation (since the foliation is mirror-symmetric) and therefore lies in Γ .

The function H is constant on each leaf and is equal to $\lim \text{Arg}(x)$ as $x \rightarrow \infty$ along the leaf. Corresponding to each value of $H \in (0, \pi)$ there exists a unique leaf in the cut half-plane and the width function W allows one to distinguish points in this leaf. Hence the integral $y(x)$ maps $\mathbb{H} \setminus \Gamma$ one-to-one onto a comb-like domain described in the statement of the lemma (See Fig. 4.3.). \square

4.1.5 Recovery of the Curve M from Its Graph Γ

Let $\{\Gamma\}$ be a tree in the plane with edges of two types, non-oriented “vertical” and oriented “horizontal” ones. We call the positive numbers labelling the edges R their widths $W(R)$ if R is a horizontal edge or their heights $H(R)$ if R is a vertical edge. We set the height of horizontal edges and the width of vertical ones to be zero. On the vertices V of the tree we can (in fact, uniquely) introduce the width function $W(V)$

strictly increasing on (oriented) horizontal edges such that the width of each edge is equal to the increment of the width function between its end-points. If the tree satisfies conditions A_1 – A_5 , then we can associate with it a real hyperelliptic curve $M = M\{\Gamma\}$.

CONSTRUCTIONS ([42]). It follows from condition A_1 that $\mathbb{H} \setminus \Gamma$ is a simply-connected domain. A piece of its boundary inherits from $\{\Gamma\}$ the notions of vertices v , vertical and horizontal edges r , height function $H(r)$, and width function $W(v)$.

Going along the boundary of the cut half-plane from $-\infty$ to $+\infty$ defines a strict ordering of the vertices v and the edges r , so that we can define the height function at vertices in the boundary:

$$H(v) := \sum_{r > v} H(r).$$

Properties A_2 and A_5 ensure that the monotonicity patterns of the height and the width functions of vertices v under the motion in the positive direction along the boundary of $\mathbb{H} \setminus \Gamma$ are similar to the ones plotted in Fig. 4.4 (the horizontal pieces of the boundary adjacent to \mathbb{R} in the figure may absent, see e.g. graphs on Fig. 4.2 and Fig. 4.3b).

Indeed, the edges on the horizontal parts of the boundary of $\mathbb{H} \setminus \Gamma$ have zero height, and so the function $H(v)$ is locally constant there; on the vertical parts the height of edges is positive, and hence $H(v)$ decreases. The total decrease of the function $H(v)$ along the boundary of the upper half-plane cut along Γ is given by the heights of all edges in Γ^0 and twice the heights of all edges in Γ^+ . According to condition A_4 , its value is π . As to the width function, condition A_5 claims that $W(v) = 0$ on the vertical parts of the boundary of $\mathbb{H} \setminus \Gamma$, while from A_2 it follows that $W(v)$ has no local minima on the horizontal parts of the boundary of the cut half-plane.

Now in the y -plane we consider the comb-like domain

$$\text{Comb}\{\Gamma\} := \{y \in \mathbb{C}: 0 < \text{Re } y, 0 < \text{Im } y < \pi\}$$

$$\setminus \bigcup_{v \in \partial(\mathbb{H} \setminus \Gamma)} \left[iH(v), iH(v) + \max_{H(v')=H(v)} W(v') \right] \quad (4.1)$$

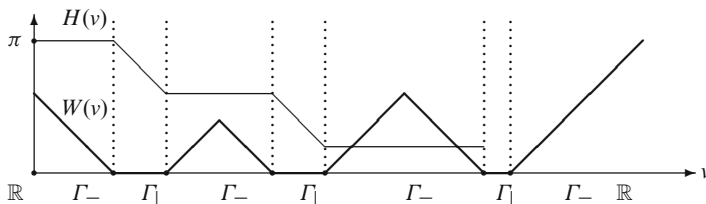


Fig. 4.4 The monotonicity patterns of the functions $H(v)$ and $W(v)$ on the boundary of the domain $\mathbb{H} \setminus \Gamma$

and map the vertices in the boundary of $\mathbb{H} \setminus \Gamma$ into the boundary of $\text{Comb}\{\Gamma\}$ by the formula

$$v \rightarrow y(v) := W(v) + iH(v) \pm i0, \quad (4.2)$$

where $'\pm'$ is the sign of the monotonicity of W at the vertex v . It is clear from the graph in Fig. 4.4 that the map between the boundaries is monotone relative to the ordering of the vertices, and therefore it associates uniquely edges r in the boundary of $\mathbb{H} \setminus \Gamma$ with edges $y(r)$ in the boundary of $\text{Comb}\{\Gamma\}$. Corresponding to each edge R of the graph Γ^+ there is a pair of edges r^-, r^+ in the boundary of the half-plane cut along Γ , its “sides”. The linear map of the interval $y(r^-)$ onto $y(r^+)$ which reverses the orientation of the boundary of the comb has the following form:

$$y \rightarrow \begin{cases} y + iH^+ - iH^-, & R \subset \Gamma_-^+, \\ -y + iH^+ + iH^-, & R \subset \Gamma_+^+, \end{cases} \quad (4.3)$$

where H^\pm is the mean value of the height $H = \text{Im } y$ on the interval $y(r^\pm)$. We shall treat the intervals $y(r^-)$ and $y(r^+)$ as identified in accordance with the rule (4.3).

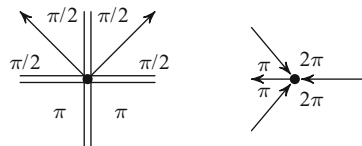
Taken with all the boundary identifications, the comb-like domain $\text{Comb}\{\Gamma\}$ is an abstract Riemann surface $\mathbb{H}\{\Gamma\}$ homeomorphic to a disc. A conformal map $x(y) : \mathbb{H}\{\Gamma\} \rightarrow \mathbb{H}$ with fixed infinity is defined up to motions in \mathfrak{A}_1^+ . It is clear from the gluing formula (4.3) that on the half-plane \mathbb{H} we obtain a well-defined meromorphic quadratic differential $(dy(x))^2$. It is real at the boundary and extends by symmetry into the lower half-plane. We take for $M\{\Gamma\}$ the two-sheeted surface (2.1) with branch points at the zeros and poles of odd multiplicity of the quadratic differential $(dy)^2(x)$, $x \in \mathbb{C}$.

Theorem 4.1. *The constructions in Sects. 4.1.2 and 4.1.5 establish a one-to-one correspondence between hyperelliptic curves $M \in \mathcal{H}$ and weighted graphs $\{\Gamma\}$ satisfying conditions A_1 – A_5 .*

Proof. A. Let $\{\Gamma\} \rightarrow M\{\Gamma\} \rightarrow \Gamma'(M)$ be the maps from Sects. 4.1.5 and 4.1.2 performed in succession. The construction of the first map associates with an abstract weighted graph $\{\Gamma\}$ its realization in the x -plane, the image of (a part of) the boundary of (4.1) and its reflection $\overline{\text{Comb}\{\Gamma\}}$. We denote this graph, its vertices, and various subgraphs by $x(\Gamma)$, $x(V)$, $x(\Gamma)$, $x(\Gamma_-)$, etc. We claim that the weighted graphs $x(\Gamma)$ and $\Gamma'(M)$ are equal.

An abstract weighted graph $\{\Gamma\}$ gives rise to a quadratic differential $(dy)^2(x)$ in the x -plane. The function $y(x) := \int_{x_0}^x dy$ defined in a neighbourhood of an arbitrary point x_0 is single-valued if the quadratic differential has an even order of zero (or pole) at x_0 . If this order is odd, $y(x)$ is double-valued. Accordingly, a small neighbourhood of x_0 is mapped onto either a multiply-sheeted disc glued from pieces of the comb-like domain (4.1) and its mirror reflection or onto a half of such a disc. Calculating the angles at the glued together vertices of combs corresponding to a vertex V of the graph Γ , we see that the disc consists of d_{i_n}

Fig. 4.5 Calculating the order of quadratic differential η^2 at the node V of the graph: $W(V) = 0$ (left) and $W(V) > 0$ (right)



sheets for $W(V) > 0$ or $d_1/2$ sheets for $W(V) = 0$ (see Fig. 4.5). Hence the order of the zero of the quadratic differential $(dy)^2(x)$ at $x_0 := x(V)$ is $\text{ord}(V)$.

Now we can realize the Riemann surface $M\{\Gamma\}$ as two sheets $\mathbb{C} \setminus x(\Gamma)$ glued crosswise along the edges $x(\Gamma)$. Indeed, all the branch points of the curve $M\{\Gamma\}$ are end-points of vertical edges of the graph $x(\Gamma)$ and each connected component of the subgraph $x(\Gamma)$ contains an even number of branch points (an edge has 2 end-points). The identifications (4.3) show that $dy(x)$ on the upper sheet and $-dy(x)$ on the lower one are glued into a single meromorphic differential on M with two simple poles at infinity. We shall show that this is the 1-form η_M associated with the curve by calculating its periods.

Assume that $\mathbb{R} \cup x(\Gamma)$ intersects transversally the projection of a closed contour $C \subset M$ onto the x -plane and partitions this projection into pieces C_1, C_2, C_3, \dots . We reverse the orientation of the pieces of C corresponding to the lower sheet of M . Then the integral of $dy(x)$ over C is equal to the sum of the increments of y along the images of the pieces C_1, C_2, C_3, \dots in the two symmetric combs $\text{Comb}\{\Gamma\}$ and $\text{Comb}\{\Gamma\}$. Each intersection point of the projection of the cycle C with $\mathbb{R} \cup x(\Gamma_-)$ yields a pair of points on the horizontal part of the boundary of the combs, which enter the above-mentioned alternating sum with opposite signs. Each intersection with $x(\Gamma)$ yields a pair of points in the vertical part of the boundary, which enter the sum with the same sign. The rules (4.3) of identification of the boundary edges of the combs now allow us to say that the integral of $\pm dy$ over an arbitrary closed cycle C in M is an integer linear combination of the quantities $iH(R)$, $R \subset \Gamma_1$. In particular, all the periods of the differential are purely imaginary. Condition A_4 enables us to calculate the residue of the 1-form at the point at infinity in the upper sheet, which is -1 .

The remaining verification that the weighted graphs $\Gamma'(M)$ and $x(\Gamma)$ are equal is a routine procedure. Property A_3 , which we have not used yet, guarantees that $x(\Gamma)$ has no vertices distinct from finite points in the divisor of the quadratic differential $(dy)^2$ or in the intersection of the vertical and horizontal components of $x(\Gamma)$.

- B. Conversely, let $M \rightarrow \Gamma(M) \rightarrow M'\{\Gamma\}$ be the maps in Sects. 4.1.2 and 4.1.5 performed successively. The conformal map $x(y)$ in the second construction was the inverse of the abelian integral $y(x)$ in Lemma 4.3 (it is in this way that one obtains the correspondences in (4.2) and (4.3)). Hence $M = M'$ up to an affine motion from \mathfrak{A}_1^+ . \square

4.2 The Coordinate Space of a Graph

We fix a topological class $[\Gamma]$ of graphs. The systems of weights on a graph meeting the conditions $A_1 - A_5$, satisfy the following constraints:

$$H(R) > 0; \quad \sum_{R \subset \Gamma_{\downarrow}^0} H(R) + 2 \sum_{R \subset \Gamma_{\downarrow}^+} H(R) = \pi, \quad (4.4)$$

where the edges R lie in $\Gamma_{\downarrow}^+ \cup \Gamma_{\downarrow}^0$;


$$W(V) > 0; \quad W(V') > W(V) \quad \text{when } V' > V, \quad (4.5)$$

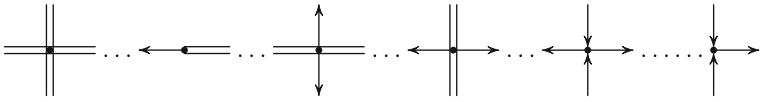
where the vertices V and V' belong to $(\Gamma_{\downarrow}^+ \cup \Gamma_{\downarrow}^0) \setminus \Gamma_{\downarrow}$ (recall that the vertices in the horizontal part Γ_{\downarrow} of the graph are partially ordered). This set of numbers parametrizes some manifold, depending on the topology of $[\Gamma]$, in the total moduli space \mathcal{H} , which is therefore partitioned into disjoint manifolds enumerated by admissible topological types $[\Gamma]$.

Definition 4.1. By the *coordinate space* $\mathcal{A}[\Gamma]$ of a graph Γ we shall mean the product of the open simplex (4.4) filled by the values of the variables $H(R)$ and the open cone (4.5) filled by the values of the variables $W(V)$.

Example 4.2. For the graph in Fig. 4.3b the coordinate space is an open 4-dimensional polyhedron in the space $\mathbb{R}^5 \ni (H_1, H_2, H_3, W_1, W_2)$ described by the constraints $2(H_1 + H_2) + H_3 = \pi$; $H_s > 0$, $s = 1, 2, 3$; $W_2 > W_1 > 0$.

Lemma 4.4. *The dimension $\dim(\Gamma)$ of a cell $\mathcal{A}[\Gamma]$ does not exceed $2g(\Gamma)$ and is equal to $2g(\Gamma)$ if and only if neighbourhoods of all vertices $V \in \Gamma$ have*

the form , and neighbourhoods of vertices $V \in \Gamma^0$ on the real axis can, in addition, have the following form (up to the central

symmetry): 
(the real axis is plotted by dots).

Proof. By considering separately all possible cases we can show that for $V \in \Gamma^0 \cup \Gamma^+$ we have $\text{codim}(V) \geq 0$, and only for vertices of the form described above $\text{codim}(V) = 0$. The latter combinatorial value was defined in Sect. 4.1.3. The calculation below demonstrates that the sum of the defects of the vertices V of the graph is equal to the codimension of the cell $\mathcal{A}[\Gamma]$ in the space $\mathcal{H}_g := \bigcup_{k=0}^{g+1} \mathcal{H}_g^k$:

$$\begin{aligned}
\sum_{V \in \Gamma^0 \cup \Gamma^+} \text{codim}(V) &= \sum_{V \in \Gamma^0 \cup \Gamma^+} d_{out}^+ + 2 \sum_{V \in \Gamma^\pm \setminus \Gamma_\downarrow} (d_{in} - 2) + \sum_{V \in \Gamma_-^0 \setminus \Gamma_\downarrow} (d_{in} - 2) \\
&+ \sum_{V \in \Gamma_\downarrow^+} (2(d_\downarrow \pmod{2}) + d_\downarrow^+ - 3) + \sum_{V \in \Gamma_\downarrow^0} (d_\downarrow \pmod{2} + d_\downarrow^+ - 1) \\
&= (2g(\Gamma) + 2) + \sum_{R \subset \Gamma^\pm} (1 + 2) + \sum_{R \subset \Gamma_-^0} 1 + \sum_{R \subset \Gamma_\downarrow^+} 2 - \sum_{V \in \Gamma^\pm \setminus \Gamma_\downarrow} 4 \\
&- \sum_{V \in \Gamma_-^0 \setminus \Gamma_\downarrow} 2 - \sum_{V \in \Gamma_\downarrow^+} 3 - \sum_{V \in \Gamma_\downarrow^0} 1 = (2g(\Gamma) + 2) + \left\{ \sum_{R \subset \Gamma^+} 3 - \sum_{V \in \Gamma^+} 3 \right\} \\
&+ \left\{ \sum_{R \subset \Gamma^0} 1 - \sum_{V \in \Gamma^0} 1 \right\} - \sum_{R \subset \Gamma_\downarrow^+} 1 - \sum_{R \subset \Gamma_\downarrow^0} 1 - \sum_{V \in \Gamma^\pm \setminus \Gamma_\downarrow} 1 \\
&- \sum_{V \in \Gamma_-^0 \setminus \Gamma_\downarrow} 1 = 2g(\Gamma) - \dim(\Gamma).
\end{aligned}$$

In the last equality we take into account the fact that the expression in the first curly brackets is equal to zero (each component of Γ^+ is a tree with one vertex removed) and the expression in the second curly brackets is equal to -1 (Γ^0 is a tree). \square

Example 4.3. Corresponding to the moduli space \mathcal{H}_3^2 there are 20 graphs $[\Gamma]$ with full dimension of the coordinate space $\dim(\Gamma) = 2g = 6$. We present them in Fig. 4.6 up to the symmetry relative to the vertical axis.

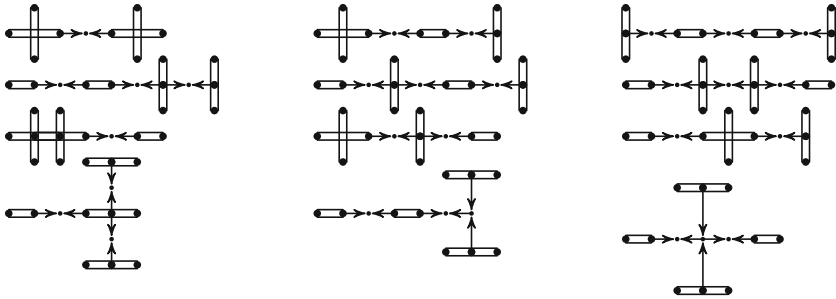
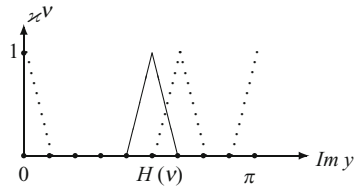


Fig. 4.6 Graphs encoding the full dimension cells in the space \mathcal{H}_3^2

Fig. 4.7 Courant's tent functions



4.2.1 The Space of a Graph in the Moduli Space

Theorem 4.2. *Each space $\mathcal{A}[\Gamma]$ is real-analytically embedded in the total moduli space \mathcal{H} .*

Proof. The proof proceeds in three steps:

1. Given the increments of the weights $\{W(V), H(R)\}_{V,R}$ of the graph $[\Gamma]$ we construct a one-to-one quasiconformal map $f(\cdot; y)$ of the corresponding comb-like domains, which respects the boundary identifications.
2. The map $f(\cdot; y)$ of comb-like domains induces in a natural way a quasiconformal motion $f(\cdot; x)$ of the upper half-plane, which transforms the branch divisor \mathbf{e} . We write out explicitly the linear part (Jacobi matrix) of this deformation.
3. We claim that the Jacobi matrix has the maximal rank $\dim[\Gamma]$.

We carry out the argument taking for example the graph presented in Fig. 4.3b. For other graphs $[\Gamma]$ our direct method will differ only in its second step, which depends on the combinatorial properties of the graph. In Chap. 5 we put forward another proof of the fact that the embedding of the coordinate space of the graph in the moduli space is analytic; it is based on the implicit function theorem.

Step 1. We fix a point in $\mathcal{A}[\Gamma]$ with coordinates $\{W^0(V), H^0(R)\}_{V,R}$. It corresponds to a normalized branch divisor $\mathbf{e}^0 \supset \{\pm 1\}$, a graph Γ_0 in the x -plane,¹ and the distinguished 1-form $\eta^0 = dy^0$ on the curve M_0 . For close points in $\mathcal{A}[\Gamma]$, which have coordinates $\{W(V), H(R)\}_{V,R}$, we define a map of comb-like domains $f(\{W, H\}; y): \text{Comb}\{\Gamma_0\} \rightarrow \text{Comb}\{\Gamma\}$. This map (i) expands/contracts the strips bounded by the horizontal lines drawn through the nodes $W^0(v) + iH^0(v) \pm i0$ at the boundary of the comb-like domain uniformly in the vertical direction; at the same time it (ii) shifts small neighbourhoods of these nodes in the horizontal direction.

CONSTRUCTIONS. The heights $H^0(v)$, where the v are nodes on the boundary of $\mathbb{H} \setminus \Gamma_0$, make up a grid on the interval $[0, \pi]$. Consider a Courant tent function $x^v(\cdot)$ of this grid, which is a piecewise linear interpolation of the function equal to 1 at $H^0(v)$ and to 0 at the other nodes of the grid, see Fig. 4.7. Now we define real functions of the y -variable ranging over the unperturbed comb, which depend on the nodes v as parameters:

¹This should not be confused with Γ^0 , the intersection of Γ with the real axis.

$$\sigma^v(y) := \sigma(y - W^0(v) - iH^0(v))$$

$$\times \begin{cases} 1 & \text{if } y^0(v) \text{ is an end-point of the cut,} \\ \theta(\operatorname{Im} y - H^0(v)) & \text{if } y^0(v) \text{ lies on the upper} \\ & \text{side of the cut,} \\ \theta(H^0(v) - \operatorname{Im} y) & \text{if } y^0(v) \text{ lies on the lower} \\ & \text{side of the cut,} \end{cases}$$

where $\sigma(y)$ is a cutoff function equal to 1 in a 2-dimensional neighbourhood of $y = 0$ and with support small in comparison with the distances between different nodes on the boundary of the unperturbed comb, $\theta(\cdot)$ is the Heavyside function equal to 1 for non-negative values of the independent variable and to 0 for negative values. Finally, we define a deformation of the comb-like domain, which depends on a point in the coordinate space $\mathcal{A}[\Gamma]$ as a parameter:

$$f(\{W, H\}; y) = y + i \sum_{H^0(v)} \delta H(v) \varkappa^v(\operatorname{Im} y) + \sum_v \delta W(v) \sigma^v(y), \quad (4.6)$$

where the first sum in (4.6) is taken over the different nodes $H^0(v)$ on $[0, \pi]$ and the second is taken over the nodes v on the boundary of the half-plane cut along Γ_0 . The perturbations $\delta W(v) + i\delta H(v)$ of the nodes on the boundary of the comb-like domain are results of the shifts $\delta W(V) := W(V) - W^0(V)$ and $\delta H(R) := H(R) - H^0(R)$ of the point in the coordinate space of the graph. The increments in (4.6) that do not vanish in the case of the graph in Fig. 4.3b are as follows:

$$\begin{aligned} \delta H(v_3) &= \delta H_1; & \delta W(v_1) &= \delta W(v_7) = \delta W_1; \\ \delta H(v_4) &= 2\delta H_1; & \delta W(v_8) &= \delta W_2; \\ \delta H(v_5) &= 2\delta H_1 + \delta H_2; & & \\ \delta H(v_6) &= \delta H(v_7) = \delta H(v_8) = & & \\ &= \delta H(v_9) = 2\delta H_1 + 2\delta H_2. & & \end{aligned} \quad (4.7)$$

Lemma 4.5. *For a small displacement $\{\delta H(R), \delta W(V)\}_{V,R}$ in the coordinate space of the graph $[\Gamma]$, the function $f(\{W, H\}; y)$ maps the comb-like domain $\operatorname{Comb}\{\Gamma_0\}$ quasiconformally onto $\operatorname{Comb}\{\Gamma\}$ and respects the boundary identifications.*

Proof. Note that for nodes on the vertical part of the boundary of the comb-like domain the increments $\delta W(v)$ vanish. Nodes, vertical, and horizontal edges of the boundary of $\operatorname{Comb}\{\Gamma_0\}$ are taken to similar elements of the boundary of the perturbed comb (4.1), which is constructed in accordance with the new

set of weights $\{H^0(R) + \delta H(R), W^0(V) + \delta W(V)\}_{R,V}$, where the increments $\delta W(V)$ are small. The old comb-like domain will be quasiconformally mapped onto the new one, with Beltrami coefficient $\mu(\{W, H\}, y) := f_{\bar{y}}/f_y(\{W, H\}; y)$ depending on the weights $\{W(V), H(R)\}_{V,R}$ as a real analytic function into $L_\infty(\text{Comb}\{\Gamma_0\})$. Now we verify that the deformation of the comb commutes with the gluing maps (4.3), separately for vertical and horizontal pieces of the boundary.

On vertical edges of the boundary of the comb-like domain the gluing map (4.3) and the deforming map (4.6) are linear functions of the imaginary part of the independent variable y . Hence it is sufficient to verify their interchangeability at the end-points of these edges. Let v_+ and v_- be boundary points corresponding to a vertex V of the graph Γ_0 and lying on opposite sides of the vertical edge. Then

$$iH^0(v_-) \xrightarrow{\text{gluing}^0} iH^0(v_+) \xrightarrow{f} iH^0(v_+) + i\delta H(v_+) = iH(v_+);$$

$$iH^0(v_-) \xrightarrow{f} iH^0(v_-) + i\delta H(v_-) = iH(v_-) \xrightarrow{\text{gluing}} iH(v_+).$$

The horizontal segment $[y(v_+^\alpha), y(v_+^\beta)]$ of the boundary of the comb-like domain is glued to the segment $[y(v_-^\alpha), y(v_-^\beta)]$ if v_+^α and v_+^β lie on the same side of the horizontal edge of the graph Γ and v_-^α and v_-^β lie on the other side of it. In that case $H(v_-^\alpha) = H(v_-^\beta)$, $H(v_+^\alpha) = H(v_+^\beta)$, $W(v_+^\alpha) = W(v_-^\alpha)$, and $W(v_+^\beta) = W(v_-^\beta)$, and the calculations below show that the gluing map commutes with the deformation. Let y be an arbitrary point in the horizontal segment $[y(v_+^\alpha), y(v_+^\beta)]$. Then:

$$\begin{aligned} y &\xrightarrow{\text{gluing}^0} y + iH^0(v_-^\alpha) - iH^0(v_+^\alpha) \\ &\xrightarrow{f} y + iH^0(v_-^\alpha) + i\delta H(v_-^\alpha) - iH^0(v_+^\alpha) + \sum_{\gamma=\alpha,\beta} \delta W(v_-^\gamma) \sigma(\text{Re } y - W^0(v_+^\gamma)); \\ y &\xrightarrow{f} y + i\delta H(v_+^\alpha) + \sum_{\gamma=\alpha,\beta} \delta W(v_+^\gamma) \sigma(\text{Re } y - W^0(v_+^\gamma)) \\ &\xrightarrow{\text{gluing}} y + iH(v_-^\alpha) - iH(v_+^\alpha) + i\delta H(v_+^\alpha) + \sum_{\gamma=\alpha,\beta} \delta W(v_-^\gamma) \sigma(\text{Re } y - W^0(v_+^\gamma)). \quad \square \end{aligned}$$

Step 2. We return to the proof of Theorem 4.2. The map of the upper half-plane

$$\tilde{f}(\{H, W\}; x) := x(y) \circ f(\{H, W\}; y) \circ y^0(x)$$

which is naturally induced by the deformation of comb-like domains is defined up to motions in \mathfrak{A}_1^+ . Hence we shall assume that the motion $\tilde{f}(\{H, W\}; \cdot)$ stabilizes the points $\{-1, 1, \infty\}$ and shall extend this map to the lower half-plane by symmetry. The Beltrami coefficient $\tilde{\mu}(x) := \mu(\{W, H\}, y^0(x)) \overline{y_x^0}/y_x^0$

of the quasiconformal deformation \tilde{f} depends on the weights $\{W, H\}$ in the real analytic fashion. The same can be said of the dependence of variable points in the image $\tilde{f}(\{H, W\}; \mathbf{e}^0)$ of the distinguished divisor $\mathbf{e}^0 := \{-1, 1, e_1^0, \dots, e_{2g}^0\}$ on a point in the coordinate space of the graph $[\Gamma]$. The linear part of the deformation of \mathbf{e}^0 is described by the formula

$$2\pi i \delta e_s := 2\pi i (\tilde{f}(\{H, W\}; e_s^0) - e_s^0) \stackrel{o}{=} ((e_s^0)^2 - 1) \int_{\mathbb{C}} \Omega_s(x) \tilde{\mu}(x) dx \wedge \overline{dx},$$

$$s = 1, \dots, 2g, \quad (4.8)$$

where $\stackrel{o}{=}$ denotes equality to within terms of order $O\left(\sum_V (\delta W(V))^2 + \sum_R (\delta H(R))^2\right)$; and $\Omega_s(x)(dx)^2$ is an element of the basis (3.21) of holomorphic quadratic differentials of finite area in $\mathbb{C} \setminus \mathbf{e}^0$. The linear part of the expression (4.8) with respect to δH and δW is

$$2\pi i \delta e_s \stackrel{o}{=} ((e_s^0)^2 - 1) \int_{\mathbb{C} \setminus \Gamma_0} \Omega_s(x) \frac{\overline{y_x^0}}{y_x^0} \frac{\partial}{\partial \bar{y}}$$

$$\times \left(i \sum_{H^0(v)} \delta H(v) \kappa^v(\text{Im } y) + \sum_v \delta W(v) \sigma^v(y) \right)_{y=y^0(x)} dx \wedge \overline{dx}. \quad (4.9)$$

Here the nodes v lie on the boundary of $\mathbb{C} \setminus \Gamma$, and the functions $\kappa^v(\cdot)$ and $\sigma^v(\cdot)$ with superscript v from the lower half-plane are obtained from the corresponding functions with superscript \bar{v} by mirror symmetry. Now we continue the transformation of the integral in (4.9):

$$2\pi i \delta e_s = -((e_s^0)^2 - 1) \int_{\mathbb{C} \setminus \Gamma_0} d \left[\frac{\Omega_s(x)}{y_x^0} \left(i \sum_{H^0(v)} \delta H(v) \kappa^v(\text{Im } y^0(x)) \right. \right.$$

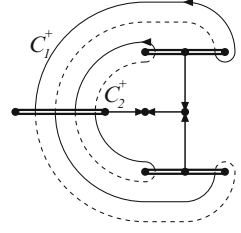
$$\left. \left. + \sum_v \delta W(v) \sigma^v(y^0(x)) \right) dx \right]$$

$$= -((e_s^0)^2 - 1) \int_{\partial(\mathbb{C} \setminus \Gamma_0)} \frac{\Omega_s(x)}{y_x^0} (\dots) dx. \quad (4.10)$$

In calculating the integral over the boundary of the complement to the graph Γ_0 we must bear in mind two things: (1) the function $y_x^0(x)$ changes its sign after crossing vertical edges of the graph Γ_0 and keeps sign after crossing its horizontal edges; (2) the sum of the boundary values of the term $\sum_{H^0(v)} \delta H(v) \kappa^v(\text{Im } y^0(x))$

is constant along vertical edges of the graph. For instance, in the case of the weighted graph in Fig. 4.3b the last integral is equal to

Fig. 4.8 The graph Γ and the basis of even 1-cycles



$$\begin{aligned}
 i \delta H(v_7) \left(\int_{v_6}^{v_9} \omega_s - \int_{\bar{v}_9}^{\bar{v}_6} \omega_s \right) + 2i \delta H(v_5) \left(\int_{v_5}^{v_6} \omega_s - \int_{\bar{v}_6}^{\bar{v}_5} \omega_s \right) \\
 + 2i \delta H(v_3) \left(\int_{v_2}^{v_3} \omega_s - \int_{\bar{v}_3}^{\bar{v}_2} \omega_s \right) + 2\pi i \sum_{v=v_7, v_8} \delta W(v) \text{Res } \omega_s(v),
 \end{aligned}$$

where $\omega_s := ((e_s^0)^2 - 1) \Omega_s(x)/y_x^0 dx$ is a holomorphic differential on the complex plane cut along the graph Γ_0 . The form ω_s changes sign after the hyperelliptic involution J of M_0 , and so, taking account of the expressions (4.7) for the increments $\delta H(v_s)$, the 1-chain along which we integrate ω_s can be replaced by an *even cycle* on the curve M_0 . The coefficients of the expansion of this cycle with respect to the basis of the lattice of even cycles (see Fig. 4.8) are just the increments of the heights H_1 and H_2 :

$$2\pi i \delta e_s \stackrel{o}{=} i \sum_{j=1,2} \delta H_j \int_{C_j^+} \omega_s + 2\pi i \sum_{j=1,2} \delta W_j \text{Res } \omega_s(x_j), \quad (4.11)$$

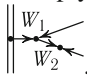
where x_j is the zero of the distinguished 1-form $\eta^0 = dy^0$ which has width function value W_j^0 .

Step 3. Assume that the differential of the map of the coordinate space of the graph $[\Gamma]$ in the moduli space \mathcal{H} does not have full rank at the distinguished point. This means that for some non-trivial displacement $\{\delta H_1, \delta H_2, \delta W_1, \delta W_2\}$ the right-hand side of (4.11) vanishes for all 1-forms ω on the curve M_0 such that $\omega \cdot \eta^0$ belongs to the space of holomorphic quadratic differentials with finite area on $\mathbb{C} \setminus e^0$. Taking ω equal to the holomorphic differential ζ_j with normalization $\int_{C_i^+} \zeta_j = \delta_{ij}$, $i = 1, 2$, we see that $\delta H_j = 0$. Taking ω equal to the meromorphic differential with simple poles over x_j that has the normalization $\int_{C_i^+} \omega = 0$, $i = 1, 2$, we see that the increment δW_j also vanishes. \square

DISCUSSION. The coordinate spaces $\mathcal{A}[\Gamma]$ form a cell decomposition of the moduli space \mathcal{H} . We indicate without proof the neighbourhood relations between the cells. At the boundary of a coordinate space some inequalities in (4.4) and (4.5) become non-strict. If the width of a horizontal edge vanishes, then the corresponding edge is contracted into a vertex of the graph. The same occurs in the case when the height of a vertical edge vanishes; however there can be a further transformation

of the graph to comply with condition A_2 : as $H \rightarrow 0$, a fragment



transformed into , if $W_1 < W_2$. In Strebel's terminology this corresponds to the contraction of a strip in the foliation $\eta_M^2 > 0$. The boundaries of the cells $\mathcal{A}[\Gamma]$ can reach the boundary of the moduli space \mathcal{H}_g^k if the corresponding transformation of the graph $[\Gamma]$ changes its genus. This reflects the fact that moduli spaces of lower genera lie on the boundary of moduli spaces of higher genera.

4.3 A Classification of Extremal Polynomials

One application of our graph techniques is a geometric representation and a classification of g -extremal polynomials by means of the graphs of the associated curves. The tradition of using graphs in the description of polynomials and other algebraic functions goes back to Hurwitz's well-known paper [108] (1891); see also [29] and [30].

In the plane of the values of the polynomial $P(x)$ we draw the interval $[-1, 1]$ red and connect each critical value of $P(x)$ with $[-1, 1]$ by an interval from the foliation of confocal hyperbolae with foci at ± 1 , which we draw black. We pull back this figure to the plane of the independent variable x of the polynomial and wipe off the hanging black edges one after another. The result is precisely the graph $\Gamma(M)$ for the curve M associated with the polynomial; its red part is “vertical” and its black part is “horizontal”. The graphs associated with polynomials satisfy (in addition to A_1 – A_5) an additional constraint on the heights of the vertical edges.

Theorem 4.3. *A weighted graph $\{\Gamma\}$ corresponds to a curve M associated with a polynomial of degree n if and only if for each vertex $V \in \Gamma^+ \cup \Gamma^0$ of odd order $\text{ord}(V)$ there exists a corresponding vertex v on the boundary of $\mathbb{H} \setminus \Gamma$, of height $H(v) \in \pi\mathbb{Z}/n$. If this condition is fulfilled, then it holds for each vertex v corresponding to the branch point V .*

Proof. With each branch point V in the statement of the theorem, apart from the right end-points of the projections of coreal ovals, we shall associate an odd 1-cycle on M . At the boundary of $\mathbb{H} \setminus \Gamma$ we pick an arbitrary node v corresponding to V and link it with the conjugate point \bar{v} by a simple arc C_v disjoint from the graph Γ and circumventing it from the right. Looking at the intersection form we can verify that the $(g + 1)$ cycles

$$C_v^- := \begin{cases} C_v, & V \in \mathbb{R}, \\ C_v - JC_v, & V \in \mathbb{H}, \end{cases} \quad (4.12)$$

form a basis in the lattice $H_1^-(M, \mathbb{Z})$. It follows from Lemma 2.4 that the sublattice L_M is formed by the odd 1-cycles such that in their decompositions an element C_v^- of the basis has even coefficients if the branch point $V(v)$ is real. The periods of the

distinguished form η_M over the cycles in our basis can be expressed in terms of the heights of the nodes v :

$$\langle \Pi(\eta_M) | C_v^- \rangle := \begin{cases} -2H(v), & V \in \mathbb{R}, \\ -4H(v), & V \in \mathbb{H}. \end{cases}$$

By Theorem 2.1 a curve M is assigned to a polynomial of degree n if and only if the period map of the differential η_M on the lattice L_M is $4\pi\mathbb{Z}/n$ -valued. In our terms this means that $4H(v) \in 4\pi\mathbb{Z}/n$ for all the nodes v generating the special basis (4.12).

The above argument does not involve the branch points V that are the right end-points of the projections of coreal ovals of the curve. Using for them the same scheme we can construct 1-cycles which are integer combinations of cycles in the special basis (4.12). Hence the remaining heights $H(v)$ lie in the lattice $\pi\mathbb{Z}/n$ since it contains the heights of the nodes v generating the special basis in question. \square

A characteristic feature of g -extremal polynomials used as substitutions in the solution of least deviation problems is as follows: their non-exceptional critical points lie on the real axis. Accordingly, the classifying graph $\{\Gamma\}$ of the normalized polynomial must be concentrated on \mathbb{R} in some sense, for instance,

$\sum_{R \subset \Gamma^+} H(R) \ll \pi$. We claim that the oscillatory behaviour of the polynomial on the real axis (a “qualitative” sketch of its graph) is determined by a neighbourhood of the subgraph Γ^0 . Assume that a polynomial $P_n(x)$ with positive leading coefficient corresponds to a graph Γ in the plane. In accordance with the Chebyshev representation (2.7), the value of the polynomial at a point v on the boundary of the upper half-plane cut along Γ is

$$P_n(v) = \cos ni(W(v) + iH(v)) = \cos nH(v) \cosh nW(v) + i \sin nH(v) \sinh nW(v). \quad (4.13)$$

If $v \in \mathbb{R}$, then the imaginary part of this value vanishes since $W(v) := 0$ on Γ^0 , $H(v) \in \pi\mathbb{Z}/n$ on Γ_-^0 , and we have $H(v) = 0$ for $v > \Gamma^0$ and $H(v) = \pi$ for $v < \Gamma^0$. By the same formula (2.7) the value in (4.13) has multiplicity

$$\text{mult } P_n(v) = (1 + \text{ord}(v)/2) \cdot \begin{cases} 1, & H(v) - iW(v) \notin \pi\mathbb{Z}/n, \\ 2, & H(v) - iW(v) \in \pi\mathbb{Z}/n. \end{cases}$$

In particular, each edge $(v^-, v^+) \subset \Gamma^0$ contains $|[-nH(v^-)/\pi] + [nH(v^+)/\pi] + 1|$ simple critical points of $P_n(x)$, whose values alternate between 1 and -1 . Thus we have found all the critical points of the polynomial on the real axis and the corresponding critical values, with their multiplicities. This is sufficient for sketching a “qualitative” graph of $P_n(x)$. Extremal polynomials can also be calculated using computer software (see Fig. 4.9 where the graph of Chebyshev polynomial on four segments is shown) we devote Chap. 6 to this topic.

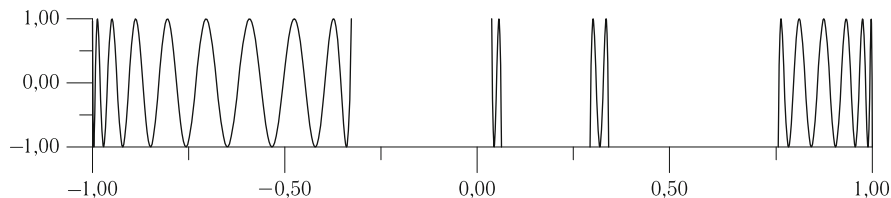


Fig. 4.9 Polynomial $P_{37}(x)$ with a graph $\frac{18}{37}\pi, \frac{3}{37}\pi, \frac{4}{37}\pi, \frac{12}{37}\pi$ (only the points with $|P_{37}(x)| \leq 1$ are shown)

4.4 Problems and Exercises

1. Sketch the vertical and horizontal foliations of the quadratic differential η_M^2 for a curve M with real branch points.

Hint. In this case the zeros of η_M lie on the projections of finite real ovals of M .

2. Let M be the curve associated with a polynomial $P_n(x)$. Show that the horizontal (vertical) foliation of the quadratic differential η_M^2 coincides with the foliation of confocal hyperbolae (ellipses) with foci at ± 1 pulled back to the x -plane by $P_n(x)$.

Hint. In this case the foliation $(\eta_M)^2 > 0$ coincides with the inverse images under the map $P_n + \sqrt{P_n^2 - 1}$ of the rays outcoming from the origin.

3. If $\phi(x)(dx)^2$ is a meromorphic quadratic differential on a compact Riemann surface M , then M can be partitioned into *annuli*, (possibly punctured) *discs*, *spiral domains*, and *strips* in a canonical way (see the definitions in [143] and [66]). Show that for the foliation associated with the distinguished quadratic differential η_M^2 on M this partitioning consists only of stripes starting at the point ∞_+ and ending at the point ∞_- of the Riemann surface.
4. Show that the number of leaves through a fixed point of the foliation associated with a quadratic differential $\phi(x)(dx)^2$ is two greater than the order of the zero of the coefficient of $\phi(x)$ at this point.
5. Derive from Axioms A_2 and A_5 that if at a vertex V the width function is zero, then this vertex lies on the vertical part of the graph Γ .

Solution. If V does not lie in Γ_1 , then $d_{\text{in}}(V) > 0$. Hence there exists a vertex at which the function takes a (strictly) smaller value than at V . In finitely many steps we descend to a vertex $V' \in \Gamma_1$ of the graph such that $W(V') < 0$.

6. Find all the stable graphs of curves (that is, graphs with $\text{codim}(\Gamma) = 0$) in the spaces \mathcal{H}_2^1 , \mathcal{H}_3^0 , and \mathcal{H}_3^1 .
7. Prove the theorem of the analytic embedding of the coordinate space of a graph in the moduli space in the case of a general graph Γ .
8. Find the classifying graph Γ for a classical Chebyshev polynomial, a Zolotarëv polynomial (4), and a Chebyshev polynomial for several intervals.

9. Show that the graph Γ of a curve M associated with a polynomial can be constructed following the instructions at the beginning of Sect. 4.3.
10. Find the graph Γ for the Chebyshev spline of type $(n, 0, k_-, k_+)$ (see the definition in Sect. 1.1.5).

Answer. This graph contains only the vertical component; it looks like a line interval with two brooms at the ends. Each broom is formed by $2k_{\pm} - 1$ bristles of length $\pi/(2n)$.

11. Create a combinatorial algorithm generating all the admissible weighted graphs $\{\Gamma\}$ (that is, ones satisfying conditions A_1 – A_5).
12. Show that for any admissible graph its dimension $\dim(\Gamma)$ is not less than its genus $g(\Gamma)$. Describe the graphs with $\dim(\Gamma) = g(\Gamma)$.

Chapter 5

Abel's Equations

In this chapter we study the structure of the set of curves M associated with real polynomials of degree n by means of the Chebyshev correspondence. In view of Theorem 2.1, for genus g curves of this type their branch points are constrained by the following relations:

$$-i \int_{C_s^-} \eta_M = 2\pi \frac{m_s}{n}, \quad m_s \in \begin{cases} \mathbb{Z}, & s = 0, 1, \dots, k-1, \\ 2\mathbb{Z}, & s = k, \dots, g, \end{cases} \quad (5.1)$$

where $\{C_s^-\}_{s=0}^g$ is the basis of the lattice of odd 1-cycles on M which we fixed earlier. Since η_M has zero periods over all even 1-cycles, the Riemann bilinear relations bring this system of equations to Abel's classical criterion for the existence of a meromorphic function on M with divisor $n \cdot (\infty_- - \infty_+)$.¹

Locally, the left-hand sides of Abel's (5.1) are single-valued analytic functions of the branch points of the curve; however, they are globally multivalued: interchanging two branch points in the upper half-plane we obtain another basis in the lattice of odd cycles. This ambiguity is described in terms of a braid group action on the universal cover of the moduli space of curves.

We shall investigate the period map Π_- defined by means of the natural extension of the left-hand side of Abel's equations to the moduli space. Only g relations in (5.1) are independent because the cycle $\sum_{s=0}^g C_s^-$ contracts to a pole of η_M with known residue. Correspondingly, the period map Π_- sends $\tilde{\mathcal{H}}_g^k \cong \mathbb{R}^{2g}$ into \mathbb{R}^g . We claim that the differential of Π_- has full rank everywhere, and so level surfaces of this map are smooth g -submanifolds of the universal cover of the moduli space. The polynomials of degree n correspond to fibres in $\tilde{\mathcal{H}}_g^k$ projecting onto a lattice of rank g defined by the right-hand sides of Abel's equations. The inverse image of the lattice is dense in the moduli space in the limit as $n \rightarrow \infty$. Using the techniques

¹The Akhiezer function $\tilde{P} := P + \sqrt{P^2 - 1}$ in the diagram (2.2).

which we develop here we shall give another proof of Theorem 4.2 on the analytic embedding of the coordinate space of a graph in the moduli space, stated earlier. The machinery of the previous chapter enables us to find the image of the period map. For $k = g + 1$ the image $\Pi_-(\mathcal{H}_g^k)$ is the interior of a g -simplex, for $k = g$ it is the union of k open g -simplexes, and for $k < g$ we obtain infinitely many open g -simplexes indexed by braids in Br_{g-k+1} and by $(g-k+1)$ -subsets of a g -element set.

5.1 The Period Map

For the investigation of the periods of abelian differentials on variable curves M we must consider two “superstructures” on the moduli space, namely, two vector bundles: the *bundle of homology groups* $H_1\mathcal{H}_g^k$ and the *bundle of real meromorphic differentials* $\Omega^1\mathcal{H}_g^k$ on the base \mathcal{H}_g^k .

5.1.1 The Homology Group Bundle and Translation of Cycles

The fibre over a point $M \in \mathcal{H}_g^k$ of the real vector bundle $H_1\mathcal{H}_g^k$ is the $(2g+1)$ -dimensional homology space $\tilde{H}_1(M, \mathbb{R})$ of the curve M . This bundle splits in the natural way into the sum of subbundles $H_1^+\mathcal{H}_g^k$ and $H_1^-\mathcal{H}_g^k$ the fibres of which are the eigenspaces of the operator \tilde{J} of anticonformal involution in homology which correspond to the eigenvalues ± 1 . A local trivialization of the homology bundle is described as follows.

Consider a point $M(\mathbf{e})$ in the base of the bundle which ranges over a sufficiently small neighbourhood of the marked point $M_0 = M(\mathbf{e}^0)$. Let $f(\mathbf{e}, x)$ be a planar diffeomorphism commuting with complex conjugation, taking the marked divisor \mathbf{e}^0 to the prescribed divisor \mathbf{e} , and equal to the identity outside a small neighbourhood of the points in the marked divisor. One example of such a map is the local section (3.4) of the projection $\mathbf{QC} \rightarrow \mathcal{H}_g^k$. This transformation of the plane lifts to a map of two-sheeted covering spaces $M(\mathbf{e}^0) \rightarrow M(\mathbf{e})$ and induces an isomorphism between their homology. This isomorphism $H_1(M(\mathbf{e}^0)) \simeq H_1(M(\mathbf{e}))$ respects the splitting into the even and odd 1-cycles and the integral homology. We can use this natural identification of the 1-homology at close points in the moduli space for a local trivialization of the homology group bundle because it is independent of the choice of the diffeomorphism $f(\mathbf{e}, x)$: all the maps satisfying the above conditions are homotopic in the punctured plane $\mathbb{C} \setminus \mathbf{e}^0$.

We can also consider the homology group bundle over the universal cover $\tilde{\mathcal{H}}_g^k$ of the moduli space. Associated with the labyrinth model \mathcal{L}_g^k of the universal covering space is a basis of global sections of the subbundle $H_1^-\tilde{\mathcal{H}}_g^k$. Indeed, if $k \leq g$ there

is no distinguished basis in the space of odd 1-cycles on the curve $M(\mathbf{e})$, while a labyrinth Λ attached to a branch divisor suggests such a basis.

Definition 5.1. Going counterclockwise along the sides of the cuts $\Lambda_0, \Lambda_1, \dots, \Lambda_g$ on the upper sheet of the surface $M(\mathbf{e})$ as in Fig. 2.2b produces a *distinguished basis* $C_0^-, C_1^-, \dots, C_g^-$ in the space $H_1^-(M, \mathbb{R})$.

The transition functions of the homology group bundle are locally constant, and therefore it possesses a natural flat (Gauss–Manin [150]) connection, which enables us to translate homology to nearby fibres. The action of this connection on integer 1-cycles can be described as follows. On the two-sheeted model of the curve M we draw a closed contour representing a cycle and avoiding the ramification points. Leaving this contour fixed and perturbing the branch points we translate the cycle to close curves M . We denote the result of the translation of an element C of the homology group bundle along a path τ in the base \mathcal{H}_g^k by $C \cdot \tau$. This right action of paths is well defined on cycles in the fibre over the initial point of the path and the result $C \cdot \tau$ lies in the fiber over the endpoint of the path. It is associative: $C \cdot (\tau_1 \tau_2) = (C \cdot \tau_1) \cdot \tau_2$, and depends only on the homotopy class of the path. The parallel translation of cycles defined by the Gauss–Manin connection is compatible with the splitting of the homology group bundle into the subbundles $H_1^\pm \mathcal{H}_g^k$ mentioned above and preserves all the integer homology lattices considered earlier. The distinguished basis associated with a labyrinth defines sections of the homology group bundle which are horizontal with respect to the above connection.

Example 5.1. The Dehn half-twist β_{s-k} in Fig. 3.3, $s = k + 1, \dots, g$, corresponds to an elementary braid in the group Br_{g-k+1} and to a loop in the moduli space. The translation of the distinguished basis of a labyrinth along this loop changes only two of its elements: $(\dots, C_{s-1}^-, C_s^-, \dots)^t \rightarrow (\dots, -C_s^-, 2C_s^- + C_{s-1}^-, \dots)^t$. In deformation the cycle C_{s-1}^- goes to the lower sheet of the Riemann surface and dragging it back to the upper sheet results in a change of sign. We see that the monodromy of the Gauss–Manin connection is non-trivial if so is the topology of the moduli space.

The flat connection defines an *action of the braid group* Br_{g-k+1} on the real cohomology space of the marked curve by duality. Namely, we define the action of $\beta \in \pi_1(\mathcal{H}_g^k, M_0) \cong \text{Br}_{g-k+1}$ on a functional $C_* \in (H_1(M_0, \mathbb{R}))^*$ by the formula $\langle \beta \cdot C_* | C \rangle := \langle C_* | C \cdot \beta \rangle$, $C \in H_1(M_0, \mathbb{R})$. We see from the above example that the coordinate description of the braid group action on functionals in $(H_1^-(M_0))^*$ coincides with the Burau representation [21, 28].

5.1.2 The Bundle of Differentials and the Period Map

The real meromorphic differentials ξ on a curve M which have at worst simple poles at the distinguished points ∞_\pm form a real $(g + 1)$ -dimensional vector space.

The union of such spaces parametrized by points M in the base \mathcal{H}_g^k is the vector bundle of *differentials* $\Omega^1 \mathcal{H}_g^k$. The bundle of differentials is trivial: in the algebraic model (2.1) with *normalized* branch divisor \mathbf{e} (the two extreme left real branch points are equal to ± 1) each differential $\xi \in \Omega^1 \mathcal{H}_g^k$ has a unique representation of the form

$$\xi = P_g(x) \frac{dx}{w} := \left(\sum_{s=0}^g b_s x^s \right) \frac{dx}{w}. \quad (5.2)$$

We see that an element of $\Omega^1 \mathcal{H}_g^k$ is completely determined by a point in the base and a real polynomial $P_g(x)$ of degree at most g . As local coordinate variables in the bundle of differentials we shall take the coefficients b_s of the polynomials $P_g(x)$ and the independent real and imaginary parts of the variable points e_s in the normalized divisor \mathbf{e} .

The period map (2.4) enables us to couple local sections of the homology group bundle and local sections of the bundle of differentials over the same base. In the standard fashion [69] we obtain a bundle of differentials $\Omega^1 \tilde{\mathcal{H}}_g^k$ over the universal cover of the moduli space. The Gauss–Manin connection enables us to identify fibres of the homology group bundle $H_1 \tilde{\mathcal{H}}_g^k$ over the universal covering space with its fibre over the marked point $\tilde{M}_0 \in \tilde{\mathcal{H}}_g^k$. The bracket in (2.4) defines now the *global period map* $\Pi: \Omega^1 \tilde{\mathcal{H}}_g^k \rightarrow H^1(M_0, \mathbb{R})$. The superposition of Π and the restriction of a functional to the subspace $H_1^\bullet(M_0, \mathbb{R}) \subset H_1(M_0, \mathbb{R})$, $\bullet = +, -, \infty$ defines a *partial period map* $\Pi_\bullet: \Omega^1 \tilde{\mathcal{H}}_g^k \rightarrow (H_1^\bullet(M_0, \mathbb{R}))^*$. We investigate the fibres of the period map in the next section.

5.1.3 Properties of the Period Map

The simplest period map Π_∞ defines the residue of the differential at infinity. Its typical fibre

$$\mathbf{N} := \{ \xi \in \Omega^1 \tilde{\mathcal{H}}_g^k : \langle \Pi(\xi) | C_\infty \rangle = 2\pi \}$$

is a smooth $3g$ -cell formed by the differentials with residues ± 1 at the distinguished points ∞_\mp in the curve $\tilde{M} \in \tilde{\mathcal{H}}_g^k$.

Lemma 5.1. *The cell \mathbf{N} is partitioned into smooth submanifolds (strata) consisting of differentials of the following form with zeros of fixed orders:*

$$\xi = \prod_{s=1}^{2g+2} (x - e_s)^{\varepsilon_s} \prod_{j=1}^l (x - a_j)^{\alpha_j} \frac{dx}{w}, \quad (5.3)$$

where the zeros a_j are pairwise distinct and do not coincide with the branch points e_s ;

$$\varepsilon_s \geq 0, \quad \alpha_j \geq 1, \quad \sum_{s=1}^{2g+2} \varepsilon_s + \sum_{j=1}^l \alpha_j = g,$$

Proof. We shall show that the $(2g + l)$ -dimensional stratum (5.3), parametrized by the values of the zeros e_s and a_j lying in the closed upper half-plane, is smooth. The independent variables $\operatorname{Re} e_s$ and $\operatorname{Im} e_s$ define a local system of coordinates in the base of the bundle of differentials. We complement it to a local system of coordinates on \mathbf{N} by considering the values of the polynomial $P_g(x)$ in (5.2) at g distinct fixed points x_1, \dots, x_g on the real axis. The linear change of variables $\{b_j\}_{j=0}^{g-1} \rightarrow \{P_g(x_s)\}_{s=1}^g$ has a determinant distinct from zero (a Vandermonde determinant). It remains to show that the mapping from the positions of zeroes $\{a_j\}_{j=1}^l$ to the space of monic degree g polynomials arising in the right-hand side of (5.3) has full rank. In other words, the matrix $\|\frac{\partial P_g(x_s)}{\partial a_j}\|_{sj} = \|- \alpha_j \frac{P_g(x_s)}{x_s - a_j}\|_{sj}$ is of full rank. If it were not so, there would exist a polynomial of degree at most $g - 1$ with zeros x_1, \dots, x_g . \square

We see that we can introduce the following local coordinate variables on the $(2g + l)$ -dimensional stratum (5.3): $\operatorname{Re} e_s$ and $\operatorname{Re} a_j$ for real points e_s, a_j , and $\operatorname{Re} e_s, \operatorname{Re} a_j, \operatorname{Im} e_s, \operatorname{Im} a_j$ for e_s and a_j in the upper half-plane, $s = 1, \dots, 2g$, $j = 1, \dots, l \leq g$. Also the manifold of forms η_M participating in Abel's equations will be stratified: it is the intersection of \mathbf{N} and the set $\Pi_+^{-1}(0)$ of differentials with purely imaginary periods. Throughout this section we treat the period map Π and the corresponding partial maps Π_+ and Π_- as defined on the $3g$ -cell \mathbf{N} . We have the following result.

- Theorem 5.1.** 1. The fibres of the maps $\Pi_+ : \mathbf{N} \rightarrow (H_1^+(M_0, \mathbb{R}))^*$ and $\Pi_- : \mathbf{N} \rightarrow (H_1^-(M_0, \mathbb{R}))^*$ are smoothly embedded $2g$ -cells with non-singular projections onto the base of the vector bundle $\Omega^1 \tilde{\mathcal{H}}_g^k$.
2. The fibres of Π_+ (of Π_-) are transversal to the strata (5.3) in the space \mathbf{N} and the fibres of Π_- (of Π_+ , respectively).
3. The “rational” fibres of Π (that is, fibres such that $\Pi(\xi) \in 2\pi H^1(M_0, \mathbb{Q})$) are dense in \mathbf{N} .

All these assertions are local; they can be proved by introducing appropriate local systems of coordinates in \mathbf{N} some of the coordinate variables in which are periods of the variable differential ξ .

CONSTRUCTIONS. A. We fix integral 1-cycles $C_1^+, C_2^+, \dots, C_g^+$ and C_1^-, \dots, C_g^- , C_∞ forming bases in the homology subspaces $H_1^+(M_0)$ and $H_1^-(M_0)$ of the marked curve, respectively, where the odd cycle C_∞ encircles clockwise the puncture at ∞_+ . Pairing these cycles with 1-forms by formula (2.4) gives us $2g + 1$ globally defined real analytic functions $\gamma_1^+(\xi), \gamma_2^+(\xi), \dots, \gamma_g^+(\xi)$ and $\gamma_1^-(\xi), \dots, \gamma_g^-(\xi), \gamma_\infty(\xi) = -2\pi \operatorname{Res} \xi|_{\infty_+}$ on the bundle $\Omega^1 \tilde{\mathcal{H}}_g^k$. The space \mathbf{N} of differentials with residues ± 1 is described by the equation $\gamma_\infty(\xi) = 2\pi$, and the fibres of the restrictions of the partial period maps Π_\bullet to \mathbf{N} are defined by the additional equations $\gamma_s^\bullet(\xi) = \operatorname{const}_s^\bullet, s = 1, \dots, g, \bullet = +, -$.

- B. We consider the further g real analytic functions on \mathbf{N} , $\psi_s(\xi) := \int_{(-1,0)}^{(x_s, w(x_s))} \xi$, where x_1, \dots, x_g are different fixed points in $(-\infty, -1)$ and integration proceeds along a real oval on the curve. Here and throughout, we assume that the variable branch divisor is normalized.
- C. On each $(2g+l)$ -dimensional stratum (5.3) we also define locally l real analytic functions $\phi_s(\xi)$, $s = 1, \dots, l$. On the curve M we consider a path F_s connecting two zeros $(a_s, \pm w(a_s))$ of the differential ξ which project onto the same point in the x -plane. In a small neighbourhood on the stratum this path can be assumed to depend continuously on ξ : the end-points of F_s “float” together with the zeros of the differential (see Fig. 2.2a). The choice of F_s is homotopically non-unique, but two possible paths differ by a cycle on M : if the zero a_s lies in the projection of a real oval on M , then $F_s - \bar{J}F_s \in H_1^-(M, \mathbb{Z})$; if a_s lies in the projection of a coreal oval, then $F_s + \bar{J}F_s \in H_1^+(M, \mathbb{Z})$; for a pair of complex conjugate zeros $a_s, a_{\bar{s}}$ we have $\bar{J}F_s - F_{\bar{s}} \in H_1(M, \mathbb{Z})$.

Fixing the paths F_s we can locally introduce on the stratum l the complex-valued functions $f_s(\xi) := \int_{F_s} \xi$, whose real and imaginary parts give us the missing coordinate variables. Namely, for each zero a_s on a real oval on M we set $\phi_s := \operatorname{Re} f_s$; for a_s in a coreal oval on M we set $\phi_s := \operatorname{Im} f_s$; finally, for a pair of complex conjugate zeros $a_s, a_{\bar{s}}$ we set $\phi_s := \operatorname{Re} f_s$ and $\phi_{\bar{s}} := \operatorname{Im} f_{\bar{s}}$.

Lemma 5.2. 1. The $2g+l$ functions γ_s^\pm , $s = 1, \dots, g$; ϕ_j , $j = 1, \dots, l$, form a local real analytic coordinate system² on the stratum (5.3).
 2. The $3g$ functions γ_s^\pm , $s = 1, \dots, g$; ψ_j , $j = 1, \dots, g$, form a local real analytic coordinate system on the manifold \mathbf{N} .

Proof. 1. The positions of the variable branch points e_1, \dots, e_{2g} of the curve M and the zeros a_1, \dots, a_l of the differential ξ are complex-valued functions of the local coordinates on the stratum. The differentials of the new coordinate variables have the following expressions:

$$d\gamma_s^+ = -\left(\sum_{j=1}^{2g} \left[\left(\varepsilon_j - \frac{1}{2}\right) \int_{C_s^+} \frac{\xi}{x - e_j}\right] de_j + \sum_{j=1}^l \left[\alpha_j \int_{C_s^+} \frac{\xi}{x - a_j}\right] da_j\right),$$

$s = 1, \dots, g,$

$$d\gamma_s^- = i\left(\sum_{j=1}^{2g} \left[\left(\varepsilon_j - \frac{1}{2}\right) \int_{C_s^-} \frac{\xi}{x - e_j}\right] de_j + \sum_{j=1}^l \left[\alpha_j \int_{C_s^-} \frac{\xi}{x - a_j}\right] da_j\right),$$

$s = 1, \dots, g,$

²This is a variant of Hubbard-Masur coordinates introduced in [81]

$$d\phi_s = - \begin{bmatrix} \text{Re} \\ \text{or} \\ \text{Im} \end{bmatrix} \left(\sum_{j=1}^{2g} \left[\left(\varepsilon_j - \frac{1}{2} \right) \int_{F_s} \frac{\xi}{x - e_j} \right] de_j + \sum_{j=1}^l \left[\alpha_j \int_{F_s} \frac{\xi}{x - a_j} \right] da_j \right),$$

$$s = 1, \dots, l.$$

If they are linearly dependent, then there exists on M a non-trivial *real* differential

$$\omega = \left(\sum_{j=1}^{2g} \frac{E_j}{x - e_j} + \sum_{j=1}^l \frac{A_j}{x - a_j} \right) \xi$$

with constants E_j and A_j such that all integrals over the cycles C_s^\pm vanish, as well as the real (and/or imaginary, in accordance with the definition of ϕ_s) parts of the integrals over the paths F_s . The real symmetry $\overline{\int_{F_s} \omega} = \int_{\bar{J}F_s} \omega$ and the above relations between $\bar{J}F_s$ and F_s yield the equalities $\int_{F_s} \omega = 0, s = 1, \dots, l$.

The poles of ω can be located only at ramification points of the curve M , and the residues at these points vanish because ω is *odd*, that is, changes sign after the hyperelliptic involution. Since all the cyclic and polar periods of ω are equal to zero, the abelian integral $y(x, w) := \int_{(1,0)}^{(x,w)} \omega$ is a single-valued function on M . The function $y(x, w)$ is also odd with respect to the involution of the curve, and therefore the equalities $\int_{F_s} \omega = 0$ mentioned above show that y vanishes at the points in M lying over the zeros $a_s, s = 1, \dots, l$. The even function $y(x, w)w$ has a unique singularity, a pole at infinity, and so it is a polynomial in x . The degree of the polynomial yw is at most $g + 1$, and it has $g + 2$ zeros with multiplicities taken into account: the zeros e_s of multiplicity ε_s for $s = 1, \dots, 2g$ and of multiplicity $1 + \varepsilon_s$ for $e_s = \pm 1$, and the zeros a_j of multiplicities $\alpha_j, j = 1, \dots, l$. Hence $\omega = 0$ and the differentials of the real analytic functions $\gamma_s^\pm, s = 1, \dots, g; \phi_j, j = 1, \dots, l$, are linearly independent on the stratum (5.3) of the space of differentials.

2. The proof of the second assertion of the lemma follows the same pattern: we write out the differentials of the functions γ_s^\pm and ψ_j expressed in terms of the local coordinate variables on \mathbf{N} . If they are linearly dependent, then there exists an abelian differential of the second kind ω with zero periods. The function $w \int_{(1,0)}^{(x,w)} \omega$ will be a polynomial in x . This polynomial has degree at most $g + 1$, but it has $g + 2$ zeros at the points $\pm 1, x_1, \dots, x_g$.

□

Proof (of Theorem 5.1). Fibres of the map Π_+ (resp. Π_-) are level sets of the functions $\gamma_1^+, \dots, \gamma_g^+$ (of $\gamma_1^-, \dots, \gamma_g^-$ resp.). In Lemma 5.2 we showed that the differentials of the $2g$ functions $\gamma_s^\pm(\xi)$ are linearly independent in the cotangent space of \mathbf{N} and, moreover, on each stratum (5.3) in \mathbf{N} . This yields almost all the required results: (1) fibres of Π_+ (of Π_-) are smooth $2g$ -submanifolds of \mathbf{N} ; (2) these fibres intersect the strata (5.3) in smooth $(g + l)$ -submanifolds and they

intersect fibres of Π_- (of Π_+), respectively, in smooth g -submanifolds; (3) the fibres of Π at which $\gamma_s^\pm/2\pi$ are rational constants are dense in the space \mathbf{N} .

Now we unravel the situation of the projections of fibres of the partial period maps onto the base. On a fixed curve M there exists a unique real differential ξ with residue -1 at ∞_+ and with prescribed real periods $\gamma_1^+, \dots, \gamma_g^+$ (or with prescribed imaginary periods $i\gamma_1^-, \dots, i\gamma_g^-$). This produces a bijection of fibres of Π_\pm onto the base $\tilde{\mathcal{H}}_g^k$, which we know to be a cell. The non-degeneracy (= the maximum possible rank) of the restriction of the projection $\mathbf{N} \rightarrow \tilde{\mathcal{H}}_g^k$ to a fibre of Π_\pm follows from the infinitesimal version of these arguments. Indeed, a vertical tangent vector to \mathbf{N} at the point ξ is naturally identified with a holomorphic real differential ω on the curve M carrying ξ . If this vector is tangent to the fibre of the period map, then all the integrals of ω over the cycles C_s^+ , $s = 1, \dots, g$ (over the cycles C_s^- , respectively), vanish. Hence ω and therefore also the vertical tangent vector to the fibre of Π_\pm are trivial. \square

5.2 Abel's Equations on the Moduli Space

For the study of Abel's equations we identify the submanifold of $\Omega^1 \tilde{\mathcal{H}}_g^k$ consisting of the distinguished differentials η_M and the base of this vector bundle. We know from part 1 of Theorem 5.1 that the manifold $\mathbf{N} \cap \Pi_+^{-1}(0)$ projects onto $\tilde{\mathcal{H}}_g^k$ without singularities. Now the partial period map Π_- is defined directly on the universal covering space of the moduli space. The braid group Br_{g-k+1} acts on both spaces: the universal covering space $\tilde{\mathcal{H}}_g^k$ of the moduli space and the cohomology space $H^1(M_0)$ of the marked curve: see the last paragraph in Sect. 5.1.1.

Lemma 5.3. *The period map $\Pi_-: \tilde{\mathcal{H}}_g^k \rightarrow (H_1^-(M_0, \mathbb{R}))^*$ is equivariant with respect to the action of Br_{g-k+1} .*

Proof. Points in the universal covering space $\tilde{\mathcal{H}}_g^k$ are homotopy classes of paths $\tau \subset \mathcal{H}_g^k$ starting at the marked point M_0 . The braid group $\text{Br}_{g-k+1} \cong \pi_1(\mathcal{H}_g^k, M_0) \ni [\beta]$ acts on them by deck transformations $[\tau] \rightarrow [\beta\tau]$. The assertion of this lemma follows from the chain of equalities

$$\langle \Pi_-([\beta] \cdot [\tau]) | C \rangle := -i \int_{C \cdot (\beta\tau)} \eta_M = -i \int_{(C \cdot \beta) \cdot \tau} \eta_M =: \langle [\beta] \cdot \Pi_-([\tau]) | C \rangle.$$

\square

We shall refer to the inverse image $\Pi_-^{-1}(C^*)$ of a functional $C^* \in (H_1^-(M_0, \mathbb{R}))^*$ in the universal covering space $\tilde{\mathcal{H}}_g^k$ as the manifold $\mathbb{T}(C_*)$. For instance, Abel's equations (5.1) define locally such a manifold for the functional C_* defined on the basis of the lattice of odd 1-cycles in M_0 by the equalities $\langle C_* | C_s^- \rangle = 2\pi m_s/n$, $s = 0, 1, \dots, g$. Now we collect the properties of these

manifolds that we already know from Theorems 2.1 and 5.1 and Lemmas 5.2 and 5.3.

Theorem 5.2 ([40]). 1. Any \mathbb{T} is a smooth g -dimensional submanifold of $\tilde{\mathcal{H}}_g^k$.
 2. Two \mathbb{T} -manifolds are either disjoint or coincide.
 3. $\mathbb{T}(\beta \cdot C_*) = \beta \cdot \mathbb{T}(C_*)$, $C_* \in \Pi_-(\tilde{\mathcal{H}}_g^k)$, $\beta \in \text{Br}_{g-k+1}$.
 4. The functions ψ_s , $s = 1, \dots, g$, produce a local coordinate system on \mathbb{T} .
 5. The points in the universal cover $\tilde{\mathcal{H}}_g^k$ associated with polynomials of degree n fill \mathbb{T} -manifolds corresponding to the functionals in the dual lattice $4\pi n^{-1}(L_{M_0})^*$.
 6. The “rational” manifolds $\mathbb{T}(C_*)$, $C_* \in 2\pi(H_1^-(M_0, \mathbb{Q}))^*$, corresponding to various polynomials, are dense in $\tilde{\mathcal{H}}_g^k$.

Remark 5.1. We proved the density of the image of the Chebyshev correspondence in the moduli space of curves with real branch points in [37]. Peherstorfer [117] and Totik [148] proved this result by other methods.

DISCUSSION. The analysis of the period map and its fibres \mathbb{T} is important for understanding the nature of g -extremal polynomials. We can suggest the following questions for investigation.

1. Find the image of the universal covering space $\tilde{\mathcal{H}}_g^k$ under the partial period map Π_- .
2. Is the projection of a \mathbb{T} -manifold onto the moduli space injective? In other words, does the action of the braid group on the subset $\Pi_-(\tilde{\mathcal{H}}_g^k)$ of the space of functionals $(H_1^-(M_0, \mathbb{R}))^*$ have fixed points?
3. Investigate the map of a “rational” manifold \mathbb{T} into an appropriate space of polynomials induced by the Chebyshev correspondence.
4. Describe the topology of a \mathbb{T} -manifold. As shown by this author [37], for $k = g + 1$ it is always a cell. The cell decomposition in Chap. 4 induces a cell decomposition of \mathbb{T} -manifolds, which enables us to analyse their topology. The intersection of a fibre of the period map with the inverse image of a cell $\mathcal{A}[\Gamma]$ in the universal covering space also is a cell: we fix certain linear combinations of the variables $H(R)$ in the coordinate space of the graph. However, to describe the topology of \mathbb{T} -manifolds knowing the neighbourhood relations between cells in a decomposition requires hard work and good geometric imagination even for small g . Our calculations for $g \leq 3$ show that $\mathbb{T}(C^*)$ is a cell whatever the functional C^* in the image of Π_- might be, but in case $g = 3$, $k = 1$. In the latter case the fiber may have several components, all of them are cells. Probably, the following result holds.

Conjecture 5.1. Each component of a \mathbb{T} -manifold is a cell [24].

We answer the first two questions in the next section. Here, as an application of the special local system of coordinates ϕ_j , ψ_j featuring in Lemma 5.2, we consider the third problem. We shall also present another proof of Theorem 4.2 in Chap. 4 on the embedding of the coordinate space of a graph in the moduli space.

Theorem 5.3. *Formula (2.7) for the recovery of a polynomial from the image of the Chebyshev correspondence defines a smooth embedding of the projection of the manifold $\mathbb{T}(C^*)$, $C^* \in 4\pi n^{-1}(L_{M_0})^* \cap \Pi_-(\mathcal{H}_g^k)$, onto the moduli space in the space of polynomials of degree n .*

Proof. As usual, we assume that the branch divisor \mathbf{e} is normalized so that the two extreme left real points in it are ± 1 . The map $\mathbb{T}(C^*)$ onto the space of polynomials is described by the formula

$$P_n(x) = \cos\left(ni \int_{(1,0)}^{(x,w)} \eta_M\right), \quad x \in \mathbb{C}, (x, w) \in M(\mathbf{e}),$$

which shows that at $+1$ and -1 the polynomial P_n takes the values $+1$ and $\pm 1 = \cos \frac{n}{2} \langle C^* | C_0^- \rangle$, respectively. Thus the image of the fibre \mathbb{T} lies in a codimension-two plane in the $(n+1)$ -dimensional Euclidean space of polynomials (2). We can take the quantities $P_n(x_s)$, $s = 1, \dots, n-1$, for global coordinates in this plane, where the x_s are distinct real points lying to the left of -1 . In the local system of coordinates $\{\psi_j\}$ on \mathbb{T} its map into the space of polynomials looks as follows:

$$P_n(x_s) = \begin{cases} \pm \cosh n\psi_s, & s = 1, \dots, g, \\ \text{a real analytic function} \\ \text{of } (\psi_1, \dots, \psi_g), & s = g+1, \dots, n-1. \end{cases}$$

By a suitable choice of the first g test points x_s we can (locally) achieve that the coordinates ψ_s are distinct from zero. Furthermore, the differentials of the first g coordinate variables of the space of polynomials, viewed as functions of ψ_s , are linearly independent. If the projection onto the moduli space does not glue together two different points in $\mathbb{T}(C^*)$ (see Question 2 on p. 81), then these produce different polynomials P_n by Theorem 2.1. \square

Proof (of Theorem 4.2). Theorem 5.1 allows us to identify \mathcal{H}_g^k and the manifold of distinguished forms $\eta_M \in \Omega^1 \mathcal{H}_g^k$ on curves M in the moduli space. This moduli space is partitioned into smooth strata (5.3) of dimension $g+l$, $l = 0, \dots, g$, and by Lemma 5.2 the functions $\gamma_1^-, \dots, \gamma_g^-; \phi_1, \dots, \phi_l$ can be taken for local coordinate variables on these strata.

From the topological structure of the tree $[\Gamma]$ we can find the multiplicities of all zeros of η_M and can decide if they coincide with the ramification points of the curve $M\{\Gamma\}$. Hence the image of the coordinate space of the graph $[\Gamma]$ lies in a stratum of the moduli space. In this image $\mathcal{A}[\Gamma]$ the above-mentioned coordinate variables on the stratum are integer linear combinations of the heights $H(R)$ and the widths $W(V)$. However, an injective linear map is an embedding, and in Theorem 4.1 we proved the injectivity. \square

5.3 The Image of the Period Map

Recall that the partial period map Π_- takes the universal cover $\tilde{\mathcal{H}}_g^k$ of the moduli space to the space of functionals on $H_1^-(M_0, \mathbb{R}) \cong \mathbb{R}^{g+1}$ by the formula $\langle \Pi_-(\tilde{M}) | C \rangle := -i \int_C \eta_M$, $C \in H_1^-(M_0, \mathbb{R})$. Here integration of the differential on M over cycles in the distinguished (and so distinct from M in general) curve M_0 proceeds with the use of the Gauss–Manin connection. We describe explicitly the image of this map in Theorem 5.4. For the statement of this theorem we require several definitions.

We fix topological invariants g and k , $0 \leq g$, $1 \leq k \leq g+1$. The points $h := (h_0, h_1, \dots, h_{g+1})$ in the Euclidean space \mathbb{R}^{g+2} such that

$$0 = h_0 < h_1 < h_2 < \dots < h_g < h_{g+1} = \pi, \quad (5.4)$$

fill an open g -simplex Δ_g . We define as follows the Burau action of the braid group Br_{g+2} in the ambient space of the simplex on the generators:

$$\left[\begin{array}{c} \bullet \text{---} \bullet \\ \bullet \text{---} \bullet \\ \bullet \text{---} \bullet \\ \bullet \text{---} \bullet \end{array} \begin{array}{c} s-1 \\ s \end{array} \right] \cdot (\dots, h_{s-1}, h_s, \dots)^t := (\dots, h_s, 2h_s - h_{s-1}, \dots)^t, \quad s = 1, 2, \dots, g+1; \quad (5.5)$$

a crossing on the $(s-1)$ th and s th strands affects only the variables h_{s-1} and h_s .

With each $(g-k+1)$ -subset i of the index set $1, 2, \dots, g$ we associate a braid $\kappa(i) \in \text{Br}_{g+2}$ (see Fig. 5.1). We move the strands of the trivial braid which have indices in i behind the plane containing the figure, and fixing their right-hand end-points shift them upwards without crossings. At the same time we shift the other strands downwards without crossings in the plane of the figure. The braid $\kappa(i)$ acts as follows on a point $h \in \mathbb{R}^{g+2}$: the variables h_s , $s \in i$, take the first $(g-k+1)$ positions in the order of their indices s . The other variables h_j , $j \notin i$, undergo successive reflections at all the points h_s , $s \in i$, with larger indices $s > j$ and after these transformations take the last $(k+1)$ positions in the order of their indices j .

Example 5.2. For $i = \{2, 3, 5, 7, 8\}$ and $g = 8$, $k = 4$, the braid $\kappa(i)$ is as on the right-hand side of the picture in Fig. 5.1. Its action takes a vector $(h_0, h_1, \dots, h_9)^t$ to

$$(h_2, h_3, h_5, h_7, h_8, 2h_8 - 2h_7 + 2h_5 - 2h_3 + 2h_2 - h_0, \\ 2h_8 - 2h_7 + 2h_5 - 2h_3 + 2h_2 - h_1, 2h_8 - 2h_7 + 2h_5 - h_4, 2h_8 - 2h_7 + h_6, h_9)^t.$$

We treat braids β on $g-k+1$ strands as elements of Br_{g+2} by adding to them horizontal strands below; see the left-hand side of the picture in Fig. 5.1.

On the universal cover $\tilde{\mathcal{H}}_g^k$ we mark the point represented by a labyrinth Λ^0 , as depicted in Fig. 3.3. The marked point lies over the point $M_0 := M(\mathbf{e}^0)$ in the moduli space, $\mathbf{e}^0 := \partial \Lambda^0$. The distinguished basis $C_0^-, C_1^-, \dots, C_g^-$ produced by the labyrinth Λ^0 as in Sect. 5.1.1 provides us with the system of coordinates

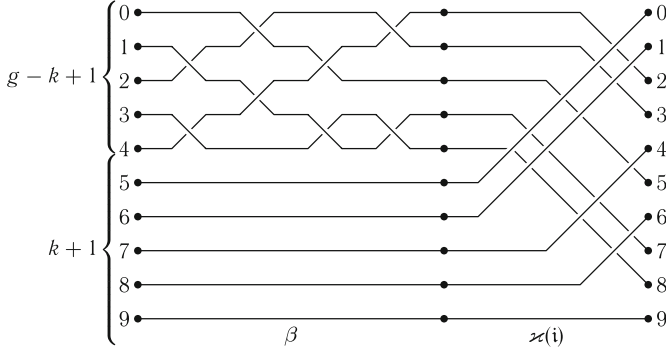


Fig. 5.1 The braids $\beta \in \text{Br}_{g-k+1}$ and $\kappa(i) \in \text{Br}_{g+2}$ for $g = 8, k = 4$, and $i = \{2, 3, 5, 7, 8\}$

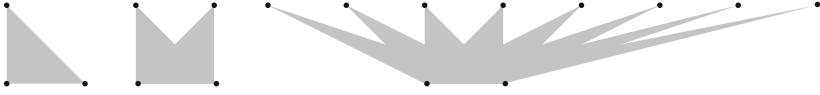


Fig. 5.2 The image of the period map $\Pi_-(\tilde{\mathcal{H}}_2^k)$ for $k = 3, 2, 1$ (from left to right)

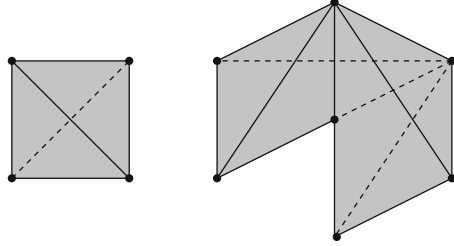


Fig. 5.3 The image of the period map $\Pi_-(\tilde{\mathcal{H}}_3^k)$ for $k = 4, 3$ (from left to right)

$\gamma_s := \langle \cdot | C_s^- \rangle$ in the space of functionals over the odd 1-cycles $(H_1^-(M_0, \mathbb{R}))^* \cong \mathbb{R}^{g+1}$. The hyperplane $\{\gamma_0 + \gamma_1 + \dots + \gamma_g = 2\pi\}$ in this space contains the image of $\tilde{\mathcal{H}}_g^k$ under the period map Π_- .

Theorem 5.4. *The set $\Pi_-(\tilde{\mathcal{H}}_g^k)$, $k > 0$, is the image under the following linear map $\gamma(h) : \mathbb{R}^{g+2} \rightarrow \mathbb{R}^{g+1}$ of the union of the open simplexes $\beta \cdot \kappa(i) \cdot \Delta_g$ in \mathbb{R}^{g+2} taken over all $\binom{k-1}{g}$ -subsets i and all braids β in Br_{g-k+1} :*

$$\gamma_s := \begin{cases} 2(h_{g-s+1} - h_{g-s}), & s = 0, \dots, k-1, \\ 4(-1)^{g+s} h_{s-k}, & s = k, \dots, g. \end{cases} \quad (5.6)$$

Example. We depict 2- and 3-dimensional images $\Pi_-(\tilde{\mathcal{H}}_g^k)$ of the universal covers of moduli spaces with simple geometry in Figs. 5.2 and 5.3.

Proof. By Lemma 5.3 the period map commutes with the action of the braid group $\beta \in \text{Br}_{g-k+1}$, therefore finding the image of Π_- in the space of functionals falls into the following two steps in a natural way.

1. Describe the action of the braid group Br_{g-k+1} on functionals in $(H_1^-(M_0))^*$.
2. Find the Π_- -image of a representative of each orbit of the covering transformation group in \mathcal{H}_g^k .

Step 1. The braid group $\text{Br}_{g-k+1} \cong \text{Mod}(\mathbf{e}^0)$ has $g - k$ generators $\beta_1, \dots, \beta_{g-k}$ represented by half-twists along curves encircling a pair of punctures of $\mathbb{H} \setminus \mathbf{e}^0$ (see Fig. 3.3) [21]. The half-twist β_s fixes all elements of the distinguished basis in odd homology apart from C_{s+k-1}^- and C_{s+k}^- , which are transformed by the Picard-Lefschetz formula [150]. The corresponding action of the generator on the space of functionals preserves all the coordinates but two: $\beta_s \cdot (\dots, \gamma_{s+k-1}, \gamma_{s+k}, \dots)^t = (\dots, -\gamma_{s+k}, 2\gamma_{s+k} + \gamma_{s+k-1}, \dots)^t$. In terms of the h -variables related to the coordinates γ by formulae (5.6) this corresponds to Burau multiplication (5.5) of braids by vectors.

Step 2. We lift each point $M(\mathbf{e})$ in the moduli space \mathcal{H}_g^k to the universal cover, by attaching a special labyrinth Λ to the branch divisor \mathbf{e} . On the boundary of the domain $\mathbb{H} \setminus \Gamma(M)$ we mark points v_0, v_1, \dots, v_{g+1} : two points on the real axis to the left and right of the interval Γ^0 ; one point in the projection of each finite real oval and one point at each vertex $V \in \mathbf{e} \cap \mathbb{H}$. We denote the index set of the $(g - k + 1)$ points in the last group by \mathbf{i} . We can use our freedom in the choice of the marked points so that the heights $h_s := H(v_s)$ satisfy conditions (5.4). Conversely, each point h in the simplex (5.4) and each admissible index subset \mathbf{i} can be obtained by looking at trees of the form indicated in Fig. 5.4. The first k intervals in the special labyrinth Λ are uniquely defined: they are the projections of coreal ovals. The remaining arcs in the labyrinth connect pairs of complex conjugate points v_s, \bar{v}_s , $s \in \mathbf{i}$, are disjoint from the tree $\Gamma(M)$ (apart from their end-points, of course), and meet the real axis to the right of the point v_0 (see Fig. 5.5, where $\mathbb{H} \setminus \Gamma$ is depicted as a horizontal half-strip). To calculate the period map at a point Λ in the universal cover of the moduli space one must integrate the form η_M over the elements of a basis of odd homology of this point that are translated from the marked point $\Lambda^0 \in \mathcal{L}_g^k \cong \tilde{H}_g^k$. We know that after

Fig. 5.4 A tree generating the subset $\mathbf{i} = \{2, 3, 5, 7, 8\}$

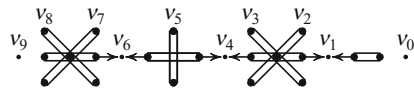
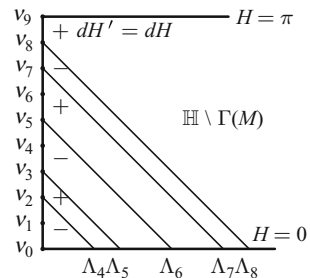


Fig. 5.5 A special labyrinth Λ in $\mathbb{H} \setminus \Gamma$



the translation of the distinguished basis from Λ^0 with the use of the natural flat connection we obtain the distinguished basis associated with the labyrinth Λ . The integrals over its elements can be expressed in terms of the heights h_s . Now we perform the corresponding calculations.

The differential η_M is holomorphic in the simply connected domain $\mathbb{H} \setminus \Lambda$, and therefore we can define there the global height function

$$H'(x) := \text{Im} \int_{x_0}^x \eta_M, \quad x_0 > \Gamma^0;$$

the branch of the differential is normalized by the condition $\text{Res } \eta_M|_{\infty} = -1$. The same equality defines a global height function $H(x)$ in $\mathbb{H} \setminus \Gamma(M)$. In components of $\mathbb{H} \setminus (\Gamma \cup \Lambda)$ the differentials $dH(x)$ and $dH'(x)$ are equal up to sign, which changes after crossing Λ or Γ . In the domain bounded by the arcs Λ_s and Λ_{s+1} of the labyrinth and the graph Γ we have $dH'(x) = (-1)^{g+s} dH(x)$.

The value of Π_- on the cycle C_s^- , $s = k, \dots, g$, is four times the increment of the height H' on the right-hand side of the cut Λ_s - from the real axis to the end-point v_* . The index of this end-point can be conveniently expressed in terms of the right action of the braid $\kappa(i)$ on the index set $s = 0, 1, \dots, g+1$ by permutations. For instance, $3 \cdot \kappa(i) = 7$ for the braid in Fig. 5.1. Finally, we obtain

$$\gamma_s = 4(-1)^{g+s} h_{(s-k) \cdot \kappa(i)}, \quad s = k, \dots, g.$$

The value of Π_- on the cycle C_s^- , $s = 0, \dots, k-1$, is equal to twice the increment of the height H' between the point v_* on the real oval adjoining Λ_s on the right and the point v_{**} on the real oval adjoining Λ_s on the left. Expressing the indices of the points v_* and v_{**} in terms of the braid $\kappa(i)$ we obtain

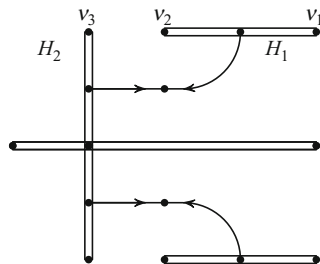
$$\gamma_s = 2H'(v_{(g-s+1) \cdot \kappa(i)}) - 2H'(v_{(g-s) \cdot \kappa(i)}), \quad s = 0, \dots, k-1.$$

The heights $H'(v_*)$ in the last formula can be expressed in terms of the known heights h_s . For $j = g-k+1, \dots, g+1$ we find the smallest index $m = m(j)$ between 0 and $g-k$ such that $j \cdot \kappa(i) < m \cdot \kappa(i)$. For instance, for the braid $\kappa(i)$ in Fig. 5.1 we have $m(6) = 0$ and $m(7) = 2$. If there exists no such index m , then $H'(v_{j \cdot \kappa(i)}) = h_{j \cdot \kappa(i)}$, otherwise

$$\begin{aligned} H'(v_{j \cdot \kappa(i)}) &= (H'(v_{j \cdot \kappa(i)}) - H'(v_{m \cdot \kappa(i)})) + (H'(v_{m \cdot \kappa(i)}) - H'(v_{(m+1) \cdot \kappa(i)})) + \dots \\ &\dots + (H'(v_{(g-k-1) \cdot \kappa(i)}) - H'(v_{(g-k) \cdot \kappa(i)})) + H'(v_{(g-k) \cdot \kappa(i)}) = \\ &= 2h_{(g-k) \cdot \kappa(i)} - 2h_{(g-k-1) \cdot \kappa(i)} + 2h_{(g-k-2) \cdot \kappa(i)} - \dots \pm 2h_{m \cdot \kappa(i)} \mp h_{j \cdot \kappa(i)}. \end{aligned}$$

Now the Burau representation allows us to write the results of our calculations in a concise form. \square

Fig. 5.6 The associated graph of a curve producing fixed points of the braid action on the image of Π_- in the case when $H_1 = H_2$



Remark 5.2. The last theorem answers exhaustively the first question in Sect. 5.2. Our techniques give an affirmative answer to the second question: there exist \mathbb{T} -manifolds which are invariant under non-trivial covering transformations of the universal covering space. In fact, let $h \in \kappa(i) \cdot \Delta_g$ be a point such that for some $s \in \{1, 2, \dots, g - k - 1\}$ its h_s -coordinate is the mean value of the neighbouring h_{s-1} - and h_{s+1} -coordinates. (For instance, the Π_- -image of the curve M in the space \mathcal{H}_3^1 with associated graph given in Fig. 5.6 has this property for $s = 1$.) In this case we can verify that $\beta_s^{-1} \beta_{s+1} \beta_s \cdot h = h$. Apparently, the topology of the projection of a manifold \mathbb{T} onto the moduli space \mathcal{H}_g^k can be different from the topology of the manifold itself.

5.4 Problems and Exercises

1. Using the cell decomposition of the moduli space prove that fibres of the period map from the space \mathcal{H}_2^1 are cells.
2. Let x_s , $s = 1, 2, \dots$, be different real points lying to the left of -1 . Consider the corresponding real functions $\psi_s := \int_{-1}^{x_s} \eta_M$ on a fibre \mathbb{T} of the period map. Prove that locally ψ_{g+1} is a real analytic function of $\psi_1, \psi_2, \dots, \psi_g$.
3. (Bogatyrev, [37]) On a hyperelliptic Riemann surface M of genus g with real branch points $\pm 1, a_s, b_s$, $s = 1, \dots, g$, consider the form $\xi = w^{-1} \prod_{s=1}^g (x - c_s) dx$ with real zeros c_s . Let $\{a_s, b_s, c_s\}_{s=1}^g \rightarrow \{\lambda_j, \mu_j, v_j\}_{j=1}^g$ be the map defined by the equalities

$$\lambda_j := \int_{a_j}^{c_j} \xi, \quad \mu_j := i \int_{b_{j-1}}^{a_j} \xi, \quad v_j := - \int_{c_j}^{b_j} \xi, \quad j = 1, \dots, g, \quad (5.7)$$

where $b_0 := -1$ and the integral is taken over the upper side of cuts made along the real axis. Show that (5.7) is a real analytic diffeomorphism of the $3g$ -simplex described by the inequalities

$$-1 < a_1 < c_1 < b_1 < a_2 < c_2 < b_2 < \dots < a_g < c_g < b_g < 1$$

onto the product of the g -simplex defined by the inequalities:

$$0 < \mu_s, \quad \sum_{s=1}^g \mu_s < \pi, \quad s = 1, \dots, g,$$

and the $2g$ -orthant

$$0 < \lambda_j, \quad 0 < v_j, \quad j = 1, \dots, g.$$

4. Setting $\xi = \eta_M$ in (5.3) we obtain a stratification of the moduli space \mathcal{H}_g^k . Express the coordinate variables $\gamma_1^-, \dots, \gamma_g^-; \phi_1, \dots, \phi_l$ on a stratum in terms of the coordinate variables $\{H(R), W(V)\}_{R,V}$ in $\mathcal{A}[\Gamma]$ for the graphs in Figs. 4.2a and 5.6.
5. (Birman, [21]) Show that formula (5.5) actually defines a representation of the braid group, that is, it respects the following relations between elementary braids: $\beta_i \beta_j \beta_i = \beta_j \beta_i \beta_j$, $|i - j| = 1$, and $\beta_i \beta_j = \beta_j \beta_i$, $|i - j| > 1$.
6. Show that the map (5.6) sends all the simplexes $\beta \cdot \kappa(i) \cdot \Delta_g$ in the statement of Theorem 5.4 into the hyperplane $\{\gamma_0 + \gamma_1 + \dots + \gamma_g = 2\pi\}$.
7. Find the periods of the distinguished form η_M on the curve associated with the Chebyshev spline of type $(n, 0, k_-, k_+)$ (see the definition in Sect. 1.1.5).
8. Prove Picard-Lefschetz formula [163]: Twisting a surface along its simple closed loop B sends each 1-cycle C on the surface to $C + (C \circ B)B$.
9. Show that the fibers of the period map Π_- may have several components when $g > k + 1$.

Chapter 6

Computations in Moduli Spaces

First of all, for an effective calculation of extremal polynomials we require the solution of Abel's (6.1) defined on the universal cover of the moduli space. These equations have been thoroughly investigated in Chap. 5; here we present only the details required for computations.

On each curve $M(\mathbf{e})$ of the moduli space there exists a unique differential of the third kind η_M with purely imaginary periods and simple poles at infinity such that $\text{Res } \eta_M|_{\infty_{\pm}} = \mp 1$. This differential is real: $\bar{J}\eta_M = \overline{\eta_M}$, therefore the integrals of η_M over the even cycles $C^+ := \bar{J}C^+$ on M vanish. The integrals of η_M over the odd cycles $C^- := -\bar{J}C^-$ define the period map locally on \mathcal{H}_g^k . As usual, the moduli space is multiply connected and the period map cannot be extended to a global map since going about a non-trivial cycle in \mathcal{H}_g^k results in a change of the basis of the odd homology lattice. This problem can be eliminated by a transition to the universal cover of the moduli space. Each labyrinth Λ lying over a point $M(\mathbf{e})$ in the moduli space defines a distinguished basis in the lattice $H_1^-(M, \mathbb{Z})$. Namely, the cycle C_s^- corresponds to counterclockwise motion along the sides of the cut Λ_s on the upper leaf of the Riemann surface $M(\mathbf{e})$. The left-hand sides of the equalities

$$-i \int_{C_s^-} \eta_M = 2\pi \frac{m_s}{n}, \quad s = 0, 1, \dots, g, \quad m_s \in \begin{cases} \mathbb{Z}, & s = 0, 1, \dots, k-1, \\ 2\mathbb{Z}, & s = k, \dots, g, \end{cases} \quad (6.1)$$

define the *period map* $\Pi_-: \tilde{\mathcal{H}}_g^k \rightarrow \mathbb{R}^{g+1}$, whose values lie in a hyperplane: the integral of η_M over the cycle $C_0^- + C_1^- + \dots + C_g^-$ is always $2\pi i$. We showed earlier that the period map is a submersion in \mathbb{R}^g , and found the image of Π_- .

The points M of the moduli space associated with real polynomials of degree n fill real analytic submanifolds of dimension g that are the inverse image, under the period map, of the lattice defined by the right-hand side of (6.1). These equations are equivalent to the existence on M of a real meromorphic function with divisor $n \cdot (\infty_- - \infty_+)$:

$$\tilde{P}_n(x, w) := \exp\left(n \int_{(e,0)}^{(x,w)} \eta_M\right). \quad (6.2)$$

Its composite with the Zhukovskii map is a g -extremal polynomial:

$$P_n(x) = (\tilde{P}_n(x, w) + 1/\tilde{P}_n(x, w))/2. \quad (6.3)$$

Now we set up a plan for developing our theory to the level of effective (numerical) computations. We shall use the representation of the universal cover of the moduli space as the deformation space \mathcal{G}_g^k of certain Kleinian groups. Thus we uniformize the curves M by the Schottky groups \mathfrak{S} corresponding to elements of the space \mathcal{G}_g^k . As is known [29, 35, 38], if Schottky's criterion holds, then linear Poincaré theta-series of such a group converge absolutely and uniformly on compact subsets of the domain of discontinuity \mathcal{D} . Summing these series we obtain abelian differentials on curves and, in particular, η_M . After identifying the labyrinth space \mathcal{L}_g^k and the deformation space \mathcal{G}_g^k of special Kleinian groups, the cycles $C_1^-, C_2^-, \dots, C_g^-$ related to the labyrinth are taken to the circles C_1, C_2, \dots, C_g bounding the fundamental domain of the group. The poles ∞_+ and ∞_- of the differential η_M are taken to the points $+1$ and -1 , respectively.

Abel's equations (6.1) and the Chebyshev representation (6.2), (6.3) can be written also in terms of the global coordinate variables $(c_s, r_s)_{s=1}^g$ in the deformation space \mathcal{G}_g^k . Thereupon we come across the problem of *navigation* in the moduli space.

From an arbitrary point in the deformation space one must descend to the smooth submanifold described by Abel's equations and moving along it, find the curve M corresponding to the polynomial $P_n(x)$ with prescribed constraints.

The variational formulae of Sect. 6.2.2 enable one to obtain a local solution of the navigation problem.

6.1 Function Theory in the Schottky Model

Throughout this section \mathbb{R} denotes the standard fundamental domain of the Schottky group \mathfrak{S} , the exterior of $2g$ circles $\pm C_1, \pm C_2, \dots, \pm C_g$. A point $\{c_s, r_s\}_{s=1}^g$ in the deformation space is assumed to be fixed.

6.1.1 Linear Poincaré Theta-Series

We obtain an abelian differential of the 3rd kind $\eta_{zz'}$ with poles at points z and z' in the standard fundamental domain \mathbb{R} of the Schottky group \mathfrak{S} by averaging the rational differential on the sphere over the group [29]:

$$\eta_{zz'}(u) := \sum_{S \in \mathfrak{S}} \left\{ \frac{1}{Su - z} - \frac{1}{Su - z'} \right\} dS(u) = \sum_{S \in \mathfrak{S}} \left\{ \frac{1}{u - Sz} - \frac{1}{u - Sz'} \right\} du. \quad (6.4)$$

The two sums are termwise equal in view of the infinitesimal form of the cross ratio identity

$$\frac{d/du S(u)(z - z')}{(Su - z)(Su - z')} = \frac{S^{-1}z - S^{-1}z'}{(u - S^{-1}z)(u - S^{-1}z')}, \quad S \in \text{PSL}_2(\mathbb{C}). \quad (6.5)$$

Differentiating (6.4) with respect to the position of the pole z we obtain abelian differentials of the second kind:

$$\omega_{mz}(u) := D_z^m \eta_{zz'}(u) = m! \sum_{S \in \mathfrak{S}} (Su - z)^{-m-1} dS(u), \quad m = 1, 2, \dots \quad (6.6)$$

We obtain a holomorphic differential (that is, a differential of the first kind) by placing the poles z and z' in the same orbit of the group \mathfrak{S} and isolating in (6.4) a telescopic sum:

$$\begin{aligned} \zeta_j(u) &:= \eta_{S_j z z} = \sum_{S \in \mathfrak{S}} \{ (u - SS_j z)^{-1} - (u - Sz)^{-1} \} du = \\ &= \sum_{S \in \mathfrak{S} \setminus \langle S_j \rangle} \sum_{m=-\infty}^{\infty} \{ (u - SS_j^{m+1} z)^{-1} - (u - SS_j^m z)^{-1} \} du = \\ &= \sum_{S \in \mathfrak{S} \setminus \langle S_j \rangle} \{ (u - S\alpha_j)^{-1} - (u - S\beta_j)^{-1} \} du = \\ &= \sum_{S \in \langle S_j \rangle \setminus \mathfrak{S}} \{ (Su - \alpha_j)^{-1} - (Su - \beta_j)^{-1} \} dS(u), \quad j = 1, \dots, g; \end{aligned} \quad (6.7)$$

summation proceeds over representatives of cosets by the subgroup $\langle S_j \rangle \subset \mathfrak{S}$ generated by the element S_j ; α_j and β_j are the attracting and the repelling fixed points of S_j , respectively. The terms of the sum (6.7) are independent of the choice of representatives of cosets in view of the cross ratio identity (6.5).

Integrating the series (6.4), (6.6), and (6.7) termwise over the circles $\{C_s\}_{s=1}^g$ oriented counterclockwise, we find the normalization of the differentials under consideration:

$$\int_{C_s} \eta_{zz'} = 0; \quad \int_{C_s} \omega_{mz} = 0; \quad \int_{C_s} \zeta_j = 2\pi i \delta_{sj}; \quad z, z' \in \mathbb{R}, \quad s, j = 1, \dots, g. \quad (6.8)$$

6.1.2 The Convergence of Linear Poincaré Series

There is a curious story behind the convergence of Poincaré thetas. H. Poincaré himself believed that the theta series he introduced always diverged in the linear case and therefore he used quadratic series (and ones of higher weight). Later Burnside gave examples of convergent linear Poincaré theta series, and his argument for their convergence followed that of Poincaré in the case of quadratic series. Having proved the convergence for several particular cases, Burnside conjectured that linear theta series always converge for Schottky groups. Myrberg gave a conterexample [110] of absolutely divergent linear series. Akaza [6–9] showed that absolute convergence is related to the Hausdorff dimension of the limit set of the group. Finally, Mityushev [106] showed that linear theta series for an arbitrary Schottky group converge conditionally, that is, after a certain rearrangement of terms.

In this section we present an estimate for the remainder in a series $\sum_S |S'(u)|$ of Eisenstein type over the Schottky group \mathfrak{S} which is uniform on compact subsets of the domain of discontinuity \mathcal{D} . It shows that the series (6.4), (6.6), and (6.7) in the previous section are convergent and yield estimates for their remainders. Computational practice shows that linear Poincaré series converge slowly if the distances between neighbouring circles which bound the fundamental domain of the group are small in comparison with the radii of the circles. Let us introduce a quantity \mathbf{q} characterizing the convergence rates of series for a fixed group \mathfrak{S} .

Definition 6.1. Let $z_s^- < z_s^+$, $s = 1, \dots, g$, be the points of intersection of the circle C_s and the real axis. Then we set $\mathbf{q} := \max_{s=1, \dots, g} q_s > 1$, where

$$\begin{aligned} q_1 &:= \frac{z_2^- - z_1^-}{z_2^- - z_1^+} : \frac{2z_1^-}{z_1^+ + z_1^-}; \\ q_s &:= \frac{z_{s+1}^- - z_s^-}{z_{s+1}^- - z_s^+} : \frac{z_{s-1}^+ - z_s^-}{z_{s-1}^+ - z_s^+}, \quad s = 2, \dots, g-1; \\ q_g &:= \frac{z_g^+ + z_g^-}{2z_g^+} : \frac{z_{g-1}^+ - z_g^-}{z_{g-1}^+ - z_g^+}. \end{aligned} \tag{6.9}$$

Remark 6.1. This definition has a deficiency: \mathbf{q} does not characterize the Schottky group as such, but rather the fundamental domain \mathbf{R} , which is defined with a certain degree of freedom because the circles C_s , $s = k, \dots, g$, passing through the complex conjugate fixed points of the generators G_s are not uniquely defined.

Definition 6.2. We introduce a norm on the Schottky group \mathfrak{S} in the usual way, by setting $|S| :=$ the length of the irreducible factorization of the element S with respect to the generators $S_j := G_j G_0$, $j = 1, \dots, g$. For example, $|S_1 S_2 S_1^{-1}| = 3$. It is convenient to visualize the Schottky group in the form of its *Caley graph*, an infinite tree often used in illustrations of a nuclear chain reaction (see, for example,

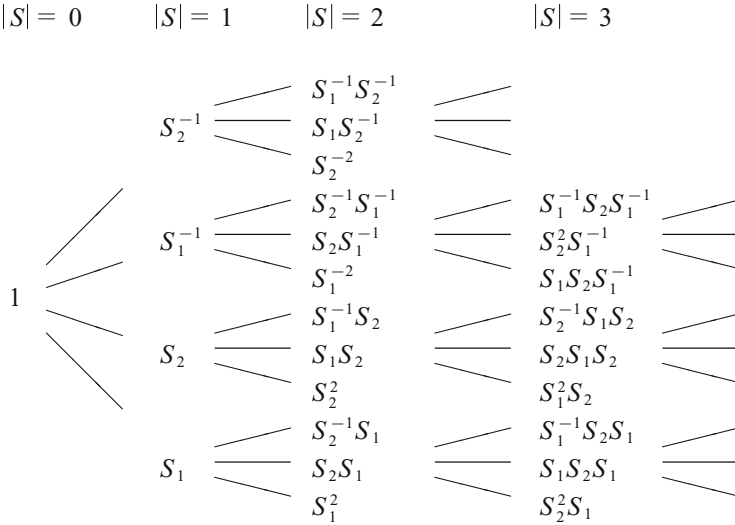


Fig. 6.1 The Caley graph of a Schottky group of genus $g = 2$ (only part of branches on the third level is depicted)

Fig. 6.1). We put elements of the group at vertices of the graph and connect an element $S \in \mathfrak{S}$ by edges with the elements $S_j^{\pm 1}S$, $j = 1, \dots, g$. Such a tree is broken into levels containing the elements of the group which have the same norm. We can introduce a partial order relation on the group by setting $S \geq S_*$ if S belongs to the subtree of the Caley graph “growing”¹ from the vertex S_* . The formal definition is as follows: $S \geq S_* \Leftrightarrow |S| = |S_*| + |SS_*^{-1}|$; for example, $S_1^{-1}S_2S_3S_1^{-1} \geq S_3S_1^{-1}$.

Lemma 6.1 ([23, 37]). *The remainder term of an Eisenstein-type series has the following asymptotic estimate, which is uniform on compact subsets \mathbf{K} of $\mathcal{D}(\mathfrak{S})$:*

$$\sum_{|S| > l} |S'(u)| \leq [\text{dist}^{-2}(\mathbf{K}, \Lambda(\mathfrak{S})) + o(1)] \left(\frac{\sqrt{q} - 1}{\sqrt{q} + 1} \right)^l \frac{\sqrt{q} + 1}{2}, \quad (6.10)$$

where $u \in \mathbf{K}$, $\Lambda(\mathfrak{S}) := \mathbb{CP}_1 \setminus \mathcal{D}(\mathfrak{S})$ is the limit set of the Schottky group and $o(1) \rightarrow 0$ as $l \rightarrow \infty$.

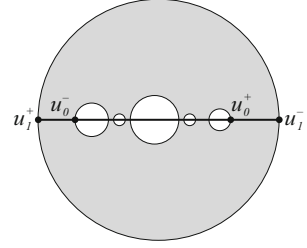
We preface the proof with several identities, which involve arbitrary linear fractional transformations $G \in \text{PSL}_2(\mathbb{C})$ and can be verified directly or with the use of the infinitesimal version of the cross-ratio identity (6.5).

The identities:

$$(E1) \quad (Gz - Gu)^2 = (z - u)^2 G'(z) G'(u),$$

¹The tree grows in the increasing direction of the norms of its vertices.

Fig. 6.2 The outer boundary of SR as the absolute of the Lobachevskii plane



$$(E2) \quad \frac{G'(z)}{G'(u)} = \left(\frac{u - G^{-1}\infty}{z - G^{-1}\infty} \right)^2,$$

$$(E3) \quad \frac{Gz - Gu}{G^{-1}z - G^{-1}u} = \frac{z - G\infty}{z - G^{-1}\infty} \frac{u - G\infty}{u - G^{-1}\infty}.$$

Proof (of Lemma 6.1). First we show that if $S \neq 1$, then the diameter of the outer circle at the boundary of the shifted fundamental domain SR is greater than the sum of the diameters of all the $(2g - 1)$ inner circles at least by a factor of $\frac{\sqrt{q}+1}{\sqrt{q}-1}$. Let $[u_0^-, u_0^+]$ be the smallest closed interval on the real axis containing the diameters of all the inner circles in SR , and let $[u_1^+, u_1^-]$ be the real diameter of the outer circle (see Fig. 6.2). An interval of fixed *non-Euclidean* length in the Poincaré disc attains the maximal *Euclidean* length in the case when it is concentric with the absolute. Applying this argument to the interval $[u_0^-, u_0^+]$ and the outer circle of SR , which we take for the absolute, we obtain

$$\frac{u_0^+ - u_0^-}{u_1^- - u_1^+} \leq \frac{\sqrt{q} - 1}{\sqrt{q} + 1}, \quad q := \frac{u_1^- - u_0^-}{u_1^- - u_0^+} : \frac{u_1^+ - u_0^-}{u_1^+ - u_0^+},$$

where q is one of the cross-ratios listed in (6.9).

The compact set K contains no points of the form $u = S^{-1}\infty$ for elements S of sufficiently large norm, and therefore the corresponding terms of the Eisenstein-type series are bounded on K :

$$\begin{aligned} \sum_{|S|>l} |S'(u)| &\stackrel{(E2)}{=} \sum_{|S|>l} |S'(-1)S'(1)|^{1/2} \frac{|1 - S^{-1}\infty||1 + S^{-1}\infty|}{|u - S^{-1}\infty|^2} \leq \\ &\leq [\text{dist}^{-2}(u, \Lambda(\mathfrak{S})) + o(1)] \sum_{|S|>l} |S'(-1)S'(1)|^{1/2}, \end{aligned}$$

where $o(1) \rightarrow 0$ as $l \rightarrow \infty$. Denoting the diameter of the outer circle of SR by $\text{diam}(SR)$ we obtain the required estimate for the remainder:

$$\begin{aligned}
\sum_{|S|>l} |S'(-1)S'(1)|^{1/2} &\stackrel{(E1)}{=} \sum_{|S|>l} \frac{1}{2} |S(-1) - S(1)| \leq \sum_{|S|>l} \frac{1}{2} \text{diam}(SR) = \\
&= \sum_{j=l+1}^{\infty} \sum_{|S|=j} \frac{1}{2} \text{diam}(SR) \leq \sum_{|S|=l+1} \frac{1}{2} \text{diam}(SR) \sum_{j=0}^{\infty} \left(\frac{\sqrt{q}-1}{\sqrt{q}+1} \right)^j \leq \\
&\leq \frac{\sqrt{q}+1}{4} \left[\frac{\sqrt{q}-1}{\sqrt{q}+1} \right]^l \left(\sum_{|S|=1} \text{diam}(SR) \right) \leq \frac{\sqrt{q}+1}{2} \left[\frac{\sqrt{q}-1}{\sqrt{q}+1} \right]^l. \quad \square
\end{aligned}$$

6.1.3 Arranging of Summation in Poincaré Series

Taking the 1-form $\eta_{zz'}$ as an example of computations, we briefly comment on calculating sums over a Schottky group. This 1-form can be represented by two different series over a Schottky group, the sums on the right- and left-hand sides of formula (6.4). To calculate a term of the right-hand series at, for instance, a vertex $S_j S$ of the Caley graph, we go one level down the tree and take the values of $S(z)$ and $S(z')$ stored at the vertex S . We store the quantities $S_j S(z)$ and $S_j S(z')$ at the vertex $S_j S$ under consideration and later use them to find the term of the series corresponding to this vertex. This scheme is particularly efficient when we need to calculate the values of the same series $\eta_{zz'}$ for several values of the variable u . On the other hand, if we need to calculate the values of several series $\eta_{zz'}$ at some point u , then we must store at the vertices of the tree the quantities $S(u)$ and $S'(u)$, and must use in computations the left-hand series in (6.4). In either case, to sum the terms of a series located at the same level of the Caley graph we require only data from the previous level.

Of course, the actual calculations are carried out over a finite subtree of the Caley graph of a group. If we take it to be a tree of finite height l , then from Lemma 6.1 above we derive an a priori estimate for the summation error. Practice shows that there is no sense in spending resources on the summation of small terms of the series until we take into account the larger ones. Hence it is more economical to take another subtree, which is determined in the process of calculations. Namely, if a term at a node S is less than some prescribed accuracy ε , then we need not carry out further computations for the subtree starting from this vertex. In Lemma 6.3 we provide estimates showing that the sum of the series over this infinite subtree has the same order as the term at its root S . With calculations organized in this way one knows the error only after the end of the process (a posteriori error estimate).

We require the following technical result.

Lemma 6.2. *The following two-sided bounds hold for some constants N_1 and N_2 depending on the parameters of the standard fundamental domain \mathbb{R} of the group \mathfrak{S} :*

(1)

$$N_1^{-1} \leq \frac{\text{diam}(S\mathbf{R})}{\text{diam}(S^{-1}\mathbf{R})} \leq N_1, \quad (6.11)$$

where S is an arbitrary non-identity element of \mathfrak{S} ;

(2)

$$N_2^{-1} \leq |S'(S_*u)| \frac{\text{diam}(S_*\mathbf{R})}{\text{diam}(SS_*\mathbf{R})} \leq N_2, \quad (6.12)$$

where S and S_* , $SS_* \geq S_* \neq 1$, are elements of \mathfrak{S} ; $u \in \mathbf{R}$.

Proof. 1. The real diameter of the outer circle of the shifted fundamental domain $S\mathbf{R}$ has end-points Sz and Su , where z and u lie on the boundary of \mathbf{R} . Hence

$$\begin{aligned} \frac{\text{diam}(S\mathbf{R})}{\text{diam}(S^{-1}\mathbf{R})} &\leq \left| \frac{Sz - Su}{S^{-1}z - S^{-1}u} \right| \stackrel{(E3)}{=} \left| \frac{z - S\infty}{z - S^{-1}\infty} \right| \left| \frac{u - S\infty}{u - S^{-1}\infty} \right| \leq \\ &\leq \left(\frac{2}{\text{dist}(\mathbf{R}, \Lambda(\mathfrak{S}))} + o(1) \right)^2 \leq N_1, \quad o(1) \rightarrow 0 \text{ as } |S| \rightarrow \infty. \end{aligned}$$

To obtain the lower bound we take real z and u on the boundary of the fundamental domain \mathbf{R} such that $\text{dist}(S^{-1}z, S^{-1}u) = \text{diam}(S^{-1}\mathbf{R})$.

2. For suitable real points z and w on the boundary of the fundamental domain \mathbf{R} we have the chain of inequalities

$$\begin{aligned} |S'(S_*(u))| \frac{\text{diam}(S_*\mathbf{R})}{\text{diam}(SS_*\mathbf{R})} &\leq |S'(S_*(u))| \left| \frac{S_*z - S_*w}{SS_*z - SS_*w} \right| \stackrel{(E1),(E2)}{=} \\ &= \frac{|S_*z - S^{-1}\infty| |S_*w - S^{-1}\infty|}{|S_*u - S^{-1}\infty|^2} \leq \left(1 + \frac{\text{diam}(S_*\mathbf{R})}{\text{dist}(S_*\mathbf{R}, S^{-1}\mathbf{R})} \right)^2 \leq N_2. \end{aligned}$$

Indeed, the inequality $SS_* \geq S_*$ is equivalent to the fact that the irreducible factorizations of S_* and S^{-1} start with distinct letters. Hence the domains $S_*\mathbf{R}$ and $S^{-1}\mathbf{R}$ lie in different “holes” of the fundamental domain \mathbf{R} . The distance between them cannot be small, however the diameter of $S_*\mathbf{R}$ tends to 0 when $|S_*| \rightarrow \infty$. The lower bound is obtained in a similar way. \square

The following result justifies the algorithm for finding the sum of a Poincaré series over a subtree of the Caley graph that is only determined in the process of computations.

Lemma 6.3. *If S_* is a fixed non-identity element of \mathfrak{S} , then*

- (1) $\sum_{S \geq S_*} |S'(u)| \leq N_3 |S'_*(u)|$, $u \in \mathbf{R}$,
- (2) $\sum_{S \geq S_*} |S(z) - S(u)| \leq N_3 |S_*(z) - S_*(u)|$, $z, u \in \mathbf{R}$,

where $N_3 = N_1^2 N_2 (\sqrt{q} + 1)/2$.

Proof. 1. We use identity (E1) and the bounds in Lemma 6.2:

$$\begin{aligned}
 \sum_{S:SS_* \geq S_*} \left| \frac{d}{du} SS_* u \right| &= |S'_*(u)| \sum_{S:SS_* \geq S_*} |S'(S_* u)| \leq \\
 &\leq |S'_*(u)| N_2 \sum_{S:SS_* \geq S_*} \frac{\text{diam}(SS_* \mathbf{R})}{\text{diam}(S_* \mathbf{R})} \leq |S'_*(u)| N_1 N_2 \sum_{S:SS_* \geq S_*} \frac{\text{diam}(S_*^{-1} S^{-1} \mathbf{R})}{\text{diam}(S_* \mathbf{R})}.
 \end{aligned} \tag{6.13}$$

The domains $S_*^{-1} S^{-1} \mathbf{R}$ with $SS_* \geq S_*$ are nested in the holes of one another, so we can repeatedly use the inequality in Lemma 6.1 for the ratio of the sum of the diameters of the inner circles and the diameter of the outer boundary of the domain. Now we continue (6.13). The right-hand side does not exceed

$$|S'_*(u)| N_1 N_2 \frac{\text{diam}(S_*^{-1} \mathbf{R})}{\text{diam}(S_* \mathbf{R})} \sum_{j=0}^{\infty} \left(\frac{\sqrt{\mathbf{q}} - 1}{\sqrt{\mathbf{q}} + 1} \right)^j \leq |S'_*(u)| N_1^2 N_2 (\sqrt{\mathbf{q}} + 1)/2.$$

2. In fact, the second estimate follows from the one above:

$$\begin{aligned}
 \sum_{S:SS_* \geq S_*} |SS_* z - SS_* u| &\stackrel{(E1)}{=} |S_* z - S_* u| \sum_{S:SS_* \geq S_*} |S'(S_* z) S'(S_* u)|^{1/2} \leq \\
 &\leq |S_* z - S_* u| N_2 \sum_{S:SS_* \geq S_*} \frac{\text{diam}(SS_* \mathbf{R})}{\text{diam}(S_* \mathbf{R})} \leq \dots \leq N_3 |S_* z - S_* u|. \quad \square
 \end{aligned}$$

6.1.4 Automorphic Functions and Their Derivatives

Schottky functions [29, 132] are the exponentials of the integrals of the series (6.4) and (6.7) and can be evaluated effectively:

$$(u, u'; z, z') := \exp \int_{u'}^u \eta_{zz'} = \prod_{S \in \mathfrak{S}} \frac{u - Sz}{u - Sz'} : \frac{u' - Sz}{u' - Sz'}, \tag{6.14}$$

$$E_j(u) := \exp \int_{\infty}^u \zeta_j = \prod_{S \in \mathfrak{S} \setminus \{S_j\}} \frac{u - S\alpha_j}{u - S\beta_j}, \quad j = 1, \dots, g. \tag{6.15}$$

They are transformed by well-known formulae under the action of the group \mathfrak{S} :

$$(S_j u, u'; z, z') = (u, u'; z, z') E_j(z) / E_j(z'), \quad (6.16)$$

$$E_s(S_j u) = E_s(u) E_{sj}. \quad (6.17)$$

Here E_{lj} , the exponential of the period of the holomorphic differential, has the representation

$$E_{lj} = E_{jl} = \prod_{S \in \langle S_l \rangle | \langle S_j \rangle} \frac{S\alpha_j - \alpha_l}{S\alpha_j - \beta_l} : \frac{S\beta_j - \alpha_l}{S\beta_j - \beta_l}, \quad l, j = 1, \dots, g, \quad (6.18)$$

where we take the product over two-sided cosets in the group \mathfrak{S} and for $j = l$ the coefficient $0/\infty$ corresponding to $S = 1$ is replaced by the dilation coefficient $\lambda_l := S'_l(\alpha_l)$.

A non-trivial meromorphic function on the orbit manifold of the group \mathfrak{S} can be expressed in terms of the Schottky function.

Lemma 6.4. *Let $F(u)$ be an automorphic function with divisor $\sum_{j=1}^{\deg F} (z_j - z'_j)$ in the fundamental domain of the group \mathfrak{S} . Then the following representation holds:*

$$F(u) = \text{const} \cdot \prod_{j=1}^{\deg F} (u, *; z_j, z'_j) \prod_{s=1}^g E_s^{m_s}(u), \quad (6.19)$$

where $m_s \in \mathbb{Z}$ is the increment of $(2\pi i)^{-1} \log F(u)$ over the cycle C_s . The derivatives of the automorphic function $F(u)$ with respect to the independent variable are calculated recursively by the formula

$$D_u^{m+1} F(u) = \sum_{l=0}^m \binom{l}{m} \cdot (D_u^{m-l} F(u)) \cdot D_u^l \left(\sum_{j=1}^{\deg F} \frac{\eta_{z_j z'_j}}{du} + \sum_{s=1}^g m_s \frac{\zeta_s}{du} \right). \quad (6.20)$$

The derivatives of coefficient of the forms $\eta_{zz'}$ and ζ_s are represented by absolutely convergent series:

$$D_u^l \left[\frac{\eta_{zz'}}{du}(u) \right] = l! \sum_{S \in \mathfrak{S}} \{ (S z' - u)^{-l-1} - (S z - u)^{-l-1} \}, \quad (6.21)$$

$$D_u^l \left[\frac{\zeta_j}{du}(u) \right] = l! \sum_{S \in \mathfrak{S} | \langle S_j \rangle} \{ (S \beta_j - u)^{-l-1} - (S \alpha_j - u)^{-l-1} \}. \quad (6.22)$$

Remark 6.2. The constraints imposed by Abel's theorem on the divisor of F are precisely the conditions for the automorphy of the right-hand side of (6.19).

Proof. We expand the meromorphic form dF/F in a sum of third-kind differentials and holomorphic differentials: $dF/F = \sum_{j=1}^{\deg F} \eta_{z_j z'_j} + \sum_{s=1}^g m_s \zeta_s$. Integrating to u and exponentiating we arrive at (6.19). Differentiating repeatedly the composite function $F(u) = \exp\left(\int_*^u dF/F\right)$ by the binomial formula we obtain (6.20). Effective expressions for the derivatives of the differentials in the formula can be derived from Riemann's bilinear relations:

$$\frac{\eta_{zz'}}{du}(u) = D_u \int_{z'}^z \eta_{uw} = \int_{z'}^z \omega_{1u}; \quad \frac{\zeta_j}{du}(u) = \int_w^{S_j w} \omega_{1u} \quad \text{for all } w \in \mathcal{D}.$$

Differentiating the required number of times with respect to the parameter under the integral sign and integrating termwise we obtain the series (6.21) and (6.22) absolutely convergent in \mathcal{D} . \square

6.2 Variational Theory

In connection with the solution of Abel's equations on the deformation space \mathcal{G}_g^k we are interested in the “reaction” of the Schottky functions (6.14) and (6.15) and the multipliers (6.18) on perturbations of the group \mathfrak{S} . Recall that the deformation space of the group can be realized as a domain in the Euclidean space with coordinates $\{c_s, r_s\}_{s=1}^g$ satisfying inequalities (3.5), (3.6), and (3.7).

6.2.1 The Analytic Dependence of Differentials on the Moduli

A well-known thesis [4, 34, 73] states that normalized abelian differentials on a Riemann surface depend in holomorphic fashion on its “natural” moduli (for example, the position of the branch points or the entries of the period matrix). In our case this means that the coefficients of the forms under consideration depend analytically on the variables $(c_s, r_s; u)$, $s = 1, \dots, g$, in the $(2g + 2)$ -dimensional region $\mathcal{D}\mathcal{G}_g^k$ formed by the values of the moduli $(c, r) \in \mathcal{G}_g^k$ and the uniformizing variable u , which itself ranges over the domain of discontinuity \mathcal{D} depending on the moduli $c := (c_1, \dots, c_g)$ and $r := (r_1, \dots, r_g)$. For example, this is a consequence of the absolute uniform convergence of the corresponding linear Poincaré theta series on compact subsets of $\mathcal{D}\mathcal{G}_g^k$. Below we present an approach which is valid for arbitrary Schottky groups, even when the linear theta series are divergent. It is based on an algebraic representation for differentials [16] and on the analytic dependence of algebraic moduli, points in the normalized branch divisor, on the transcendental moduli (c, r) .

Lemma 6.5. *The coefficients ζ_j/du , $\eta_{zz'}/du$ and ω_{mz}/du of the differential forms are analytic in the domain \mathcal{DG}_g^k , apart from the manifolds corresponding to the poles of the meromorphic differentials.*

Proof. This is a local result, and so we verify it in a neighbourhood of a marked point in the deformation space. Let $f(\mathbf{e}, x) \in \mathbf{QC}$ be a quasiconformal deformation (3.4) of the Riemann sphere depending on a normalized divisor $\mathbf{e} = \{-1, 1, e_1, \dots, e_{2g}\} \approx \mathbf{e}^0$ as a parameter. We know from Theorem 3.5 in Chap. 3 that a small complex $2g$ -dimensional neighborhood of the marked point \mathbf{e}^0 (the symmetry $\mathbf{e} = \bar{\mathbf{e}}$ no longer holds) is biholomorphically mapped to the complex neighborhood of the marked point in (c, r) -space. In the notation of Theorem 3.5, the projection $x(c, r; u) := x^{f(\mathbf{e}, \cdot)}(u) = f(\mathbf{e}, x^0(\tilde{f}^{-1}(\mathbf{e}, u)))$ of the domain of discontinuity of the deformed group onto the Riemann sphere is holomorphic with respect to the variables in the source domain. Also the function $w(c, r; u)$, connected with $x(c, r; u)$ by the algebraic equation

$$w^2 = (x^2 - 1) \prod_{s=1}^{2g} (x - e_s), \quad (6.23)$$

depends holomorphically on its variables.

In the algebraic model (6.23), a holomorphic 1-form on the curve has a representation

$$\zeta = w^{-1} \sum_{j=0}^{g-1} b_j x^j dx. \quad (6.24)$$

The normalized holomorphic 1-forms ζ_s are distinguished by the conditions $-i \int_{C_j} \zeta_s = 2\pi \delta_{sj}$, $j, s = 1, \dots, g$. The left-hand sides of the normalization conditions depend linearly on the b_j , and so all the dependence of the coefficients on the variable branch points is accumulated in the matrix $\left\| \int_{C_s} w^{-1} x^j dx \right\|_{sj}$ of size $g \times g$. This is a non-singular matrix (otherwise the curve (6.23) carries a non-trivial holomorphic form with zero periods over all the cycles C_s , which is impossible by Riemann's relations). We see that the b_j in the expression for a normalized differential are holomorphic functions of the branch points. Now it is clear from the representation (6.24) that the function ζ_s/du depends analytically on $(c, r; u)$ in the set where $w \neq 0$ and $x \neq \infty$. However, its singularities on this exceptional set are only apparent; to see this we can use Weierstrass' preparation theorem [69, 135] or write out a representation for ζ_s in terms of an appropriate local parameter on the curve.

For a third-kind differential, in the framework of the same model (6.23) we have a representation

$$\eta_{zz'}(c, r; u) = \left(\frac{w(c, r; u) + w(c, r; z)}{x(c, r; u) - x(c, r; z)} - \frac{w(c, r; u) + w(c, r; z')}{x(c, r; u) - x(c, r; z')} \right) \frac{dx}{2w} + \zeta. \quad (6.25)$$

For fixed points z and z' the periods of the meromorphic differential on the right-hand side of this expression depend holomorphically on the moduli (c, r) . Hence the coefficients of the holomorphic differential ζ compensating for these periods are also analytic functions of the moduli. We see from the algebraic model (6.25) of the differential that the coefficient $\eta_{zz'}/du$ depends analytically on $(c, r; u)$ on the set $w \neq 0$; $x \neq \infty$; $x(c, r, z) \neq x(c, r, u) \neq x(c, r, z')$. The singularities on this exceptional set are only apparent, provided that u does not lie in one orbit of the group \mathfrak{S} with the poles z and z' .

Note that the expression (6.25) for the differential also depends holomorphically on the position of the pole z . Differentiating repeatedly the coefficient of the 1-form $\eta_{zz'}$ with respect to z we obtain the required result also for the abelian differential ω_{mz} of the second kind. \square

6.2.2 Variations of Abelian Integrals

The abelian integrals, with prescribed limits, and their periods are functions of a point in the deformation space \mathcal{G}_g^k . For example, the expressions

$$\int_v^{v'} \eta_{zz'}; \int_v^{v'} \omega_{mz}; \int_{S_{jv}}^v \omega_{mz}; \int_v^{v'} \zeta_s; \int_{S_{jv}}^v \zeta_s; \quad s, j = 1, 2, \dots, g, \quad (6.26)$$

with fixed points $z, z'; v, v'$ in the fundamental domain of a Schottky group \mathfrak{S} depend on the moduli $\{c_s, r_s\}_{s=1}^g$. A small perturbation $\{\delta c_s, \delta r_s\}_{s=1}^g$ of the moduli results in small perturbations of the matrices $\hat{S}_j \in \mathrm{GL}_2(\mathbb{R})$ corresponding to the generators of the group \mathfrak{S} :

$$\hat{S}_j := \begin{vmatrix} c_j & c_j^2 \mp r_j^2 \\ 1 & c_j \end{vmatrix}, \quad \delta \hat{S}_j := \begin{vmatrix} 1 & 2c_j \\ 0 & 1 \end{vmatrix} \delta c_j \mp \begin{vmatrix} 0 & 2r_j \\ 0 & 0 \end{vmatrix} \delta r_j + o, \quad j = 1, \dots, g, \quad (6.27)$$

the sign \mp is equal to “−” for $j = 1, 2, \dots, k-1$ and “+” for $j = k, \dots, g$; $o := o\left(\sum_{s=1}^g |\delta c_s| + |\delta r_s|\right)$.

Theorem 6.1. *The variations of the functions (6.26) are described by the formulae*

$$\delta \int_v^{v'} \eta = (2\pi i)^{-1} \sum_{l=1}^g \int_{C_l} \eta(u) \eta_{vv'}(u) \cdot \mathrm{tr}[\mathbf{M}(u) \cdot \delta \hat{S}_l \cdot \hat{S}_l^{-1}] / du + o, \quad (6.28)$$

$$\delta \int_{S_{jv}}^v \eta = (2\pi i)^{-1} \sum_{l=1}^g \int_{C_l} \eta(u) \zeta_j(u) \cdot \mathrm{tr}[\mathbf{M}(u) \cdot \delta \hat{S}_l \cdot \hat{S}_l^{-1}] / du + o. \quad (6.29)$$

All the objects on the right-hand sides of these equalities relate to the unperturbed group; the circles C_l are counterclockwise oriented; $\eta(u)$ is one of the differentials $\eta_{zz'}$, ζ_s , and ω_{mz} with normalization (6.8); $\mathbf{M}(u) := (u, 1)^t(-1, u) \in \mathfrak{sl}_2(\mathbb{C})$ is the Hejhal matrix; $o := o\left(\sum_{s=1}^g |\delta c_s| + |\delta r_s|\right)$.

REMARKS. 1. Formula (6.28) resembles Hadamard's formula for the variation of the Green's function. Similar formulae were used by Schiffer and Spencer [130], Rauch [124, 125], Ahlfors [5].

2. Expressions on the right-hand sides of the variational formulae are similar to periods of the Eichler integral of the quadratic differentials $\eta_{zz'}\eta_{vv'}$, $\zeta_j\eta_{zz'}$ and $\zeta_j\zeta_l$. Connections between variation of the monodromy of projective structures (such as the Schottky uniformization under consideration) and the Eichler cohomology were discovered in [57, 74, 80].

3. The variational formulae (6.28) and (6.29) agree with numerical experiment.

Proof. We label all the objects related to the unperturbed group with the superscript 0. The fundamental domain \mathbb{R}^0 lies in the domain of discontinuity of the slightly perturbed group \mathfrak{S} . Hence the difference $\delta y(u)$ of the abelian integrals $y(u) := \int^u \eta$ and $y^0(u) := \int^u \eta^0$, which have the same singular points and are similarly normalized, is single-valued and holomorphic in \mathbb{R}^0 . We have the chain of equalities

$$\begin{aligned} (2\pi i)\delta \int_v^{v'} \eta &= 2\pi i(\delta y(v') - \delta y(v)) = \\ &= - \int_{\partial \mathbb{R}^0} \delta y(u) \eta_{vv'}^0(u) = - \int_{\partial \mathbb{R}^0} y(u) \eta_{vv'}^0(u). \end{aligned} \quad (6.30)$$

Indeed, by a change of variable we can transform the integral of $y^0(u) \eta_{vv'}^0(u)$ over the circle $-C_l^0$ into an integral over the circle C_l^0 and then use the equalities $y^0(S_l^0 u) - y^0(u) = \text{const}$ and $\int_{C_l^0} \eta_{vv'}^0 = 0$. We continue (6.30) as follows:

$$(2\pi i)\delta \int_v^{v'} \eta = \sum_{l=1}^g \int_{C_l^0} (y(u) - y((S_l^0)^{-1}u)) \eta_{vv'}^0 = \sum_{l=1}^g \int_{C_l^0} (y(u) - y(S_l(S_l^0)^{-1}u)) \eta_{vv'}^0; \quad (6.31)$$

here we use the same arguments as before: the difference between $y(S_l u)$ and $y(u)$ is a constant. Keeping only the linear parts of the expansion of $S_l(S_l^0)^{-1}u$ in powers of the variations of the moduli we get that

$$\begin{aligned} (2\pi i)\delta \int_v^{v'} \eta &= \sum_{l=1}^g \int_{C_l^0} \text{tr}[\mathbf{M}(u) \cdot \delta \hat{S}_l \cdot (\hat{S}_l^0)^{-1}] \eta_{vv'}^0(u) \eta(u) / du + o = \\ &= \sum_{l=1}^g \int_{C_l^0} \text{tr}[\mathbf{M}(u) \cdot \delta \hat{S}_l \cdot (\hat{S}_l^0)^{-1}] \eta_{vv'}^0(u) \eta^0(u) / du + o. \end{aligned}$$

In the last equality we have used the estimate $|\eta(u) - \eta^0(u)| = o(1)du$, which is uniform on the circle C_l^0 and follows from Lemma 6.5 on the analytic dependence of differentials on moduli.

The remaining variational formula (6.29) is obtained by passing to the limit in (6.31). For the variation of a period of the abelian differential we have

$$\delta \int_{S_{jv}}^v \eta := \int_{S_{jv}}^v \eta - \int_{S_{jv}^0}^v \eta^0 = \int_{S_{jv}^0}^v (\eta - \eta^0) + \int_{S_{jv}}^{S_{jv}^0} \eta. \quad (6.32)$$

In fact, we found the first integral on the right-hand side of (6.32) at the previous step of the proof: continuing both sides of (6.31) inside the circle C_j^0 analytically in v' and passing to the limit as $v' \rightarrow S_j^0(v)$ we obtain

$$2\pi i \int_{S_{jv}^0}^v (\eta - \eta^0) = \sum_{l=1}^g \int_{C_l^0} (y(u) - y(S_l(S_l^0)^{-1}u)) \zeta_j^0 - 2\pi i (y(S_{jv}^0) - y(S_{jv})).$$

Hence

$$2\pi i \delta \int_{S_{jv}}^v \eta = \sum_{l=1}^g \int_{C_l^0} (y(u) - y(S_l(S_l^0)^{-1}u)) \zeta_j^0(u),$$

and so expanding $S_l(S_l^0)^{-1}u$ in powers of the variations of the moduli we arrive at the expression (6.29) for the variation of a period of the differential. \square

The direct computation of the variations by formulae (6.28)–(6.29) is expensive because quadrature formulae require the calculation of series at many points. However, there exists a way round allowing us to arrive at the result after calculating the series only at $2g - 1$ points. Here we are based on Hejhal's paper [72], in which the map

$$\Xi(u)(du)^2 \mapsto \int_{C_m} \Xi(u) \mathbf{M}(u) du, \quad m = 1, \dots, g, \quad (6.33)$$

from the space of (meromorphic) quadratic differentials into $\mathfrak{sl}_2(\mathbb{C})$, which occurs in our variational formulae, was explicitly calculated for (relative) quadratic Poincaré theta series.

6.2.3 Quadratic Poincaré Theta Series

Let T be a non-trivial element of the group \mathfrak{S} with fixed points α (the attractor) and β (the repeller) and the dilation coefficient $\lambda := T'(\alpha)$, $|\lambda| < 1$. Consider the following quadratic differentials on the Riemann sphere, which are regular at infinity:

$$\begin{aligned}
R_T(u)(du)^2 &:= [(u-\alpha)(u-\beta)]^{-2}(du)^2; \\
R_T^{zz'}(u)(du)^2 &:= [(u-z)(u-z')(u-\alpha)(u-\beta)]^{-1}(du)^2, \quad z, z' \in \mathbf{R}; \\
R_T^{2z}(u)(du)^2 &:= (u-z)^{-2}(u-\alpha)^{-1}(u-\beta)^{-1}(du)^2, \quad z \in \mathbf{R}; \\
R_T^{3z}(u)(du)^2 &:= (u-z)^{-3}(u-\alpha)^{-1}(du)^2; \\
R_T^{pz}(u)(du)^2 &:= (u-z)^{-p}(du)^2, \quad p = 4, 5, \dots
\end{aligned} \tag{6.34}$$

Apart from the first differential $R_T(du)^2$, on the limit set of the group \mathfrak{S} these differentials have simple poles at worst. We average them over the group:

$$\Theta_2[R](u)(du)^2 := \sum_{S \in \mathfrak{S}} R(Su)(dS(u))^2, \quad R = R_T^{zz'}, R_T^{2z}, R_T^{3z}, R_T^{4z}, \dots \tag{6.35}$$

Then we obtain \mathfrak{S} -invariant meromorphic differentials with poles (of various orders) at points in the orbit of z (and also in the orbit of z' in the case of $R = R_T^{zz'}$). That the quadratic Poincaré series (6.35) is convergent follows from the classical area estimates [85, 120, 123] and—in our case—also from Lemma 6.1 on an estimate for the remainder of a linear Eisenstein-type series. The remaining differential $R_T(du)^2$ is invariant under the action of T , and so the quadratic Poincaré series diverges. However, the relative Poincaré series

$$\Theta_2[R_T](u)(du)^2 := \sum_{S \in \langle T \rangle | \mathfrak{S}} R_T(Su)(dS(u))^2, \tag{6.36}$$

formed (up to a constant factor) of the squares of the terms of the convergent series (6.7), converges. This gives us a holomorphic quadratic differential on the orbit manifold of the Schottky group \mathfrak{S} . Starting from Hejhal's formulae from the next section, we shall construct an explicit basis of quadratic Poincaré series (6.36) in the space of holomorphic quadratic differentials on the curve M . Picking quadratic Poincaré series with suitable singularities we can always represent a meromorphic quadratic differential $\mathcal{E}(u)(du)^2$ on M as a finite sum of series of the form (6.35) and (6.36). Here we point out that, as follows from the Riemann-Roch formula [60, 69, 137], there are no constraints on the principal parts of singularities of quadratic differentials (by contrast with linear differentials).

6.2.4 Hejhal's Formulae

Here we calculate explicitly the Hejhal map (6.33) for the quadratic Poincaré theta series under consideration. We state the result in terms of elements of the Schottky group accompanying a fixed element $T \in \mathfrak{S}$.

Definition 6.3. For fixed $m = 1, \dots, g$ we define the elements $T_j(m)$ of the group \mathfrak{S} accompanying an element T . Suppose that T has the following irreducible factorization with respect to the generators, in which we indicate all the occurrences of S_m :

$$T = (S_{\bullet} \dots S_m^{\varepsilon_1} \dots S_m^{\varepsilon_2} \dots S_m^{\varepsilon_l} \dots S_{\ast})(S_{\Delta} \dots S_m^{\varepsilon_{l+1}} \dots S_m^{\varepsilon_s} \dots S_{\nabla}) \cdot \\ \cdot (S_{\ast}^{-1} \dots S_m^{-\varepsilon_l} \dots S_m^{-\varepsilon_2} \dots S_m^{-\varepsilon_1} \dots S_{\bullet}^{-1}), \quad (6.37)$$

$\varepsilon_j = \pm 1$; $S_{\Delta} S_{\nabla} \neq 1$. Then we set

$$T_j(m) := (S_{\bullet} \dots S_m^{\varepsilon_1} \dots S_m^{\varepsilon_2} \dots S_m^{\varepsilon_j}) \cdot \begin{cases} S_m^{-1}, & \varepsilon_j = 1, \\ 1, & \varepsilon_j = -1, \end{cases} \quad j = 1, \dots, s. \quad (6.38)$$

Example 6.1. Let $T = S_3 S_2^{-1} (S_1 S_2 S_3) S_2 S_3^{-1}$; then there are two elements accompanying T for $m = 2$: $T_1(2) = S_3 S_2^{-1}$ and $T_2(2) = S_3 S_2^{-1} S_1$. For $m = 3$ we have $T_1(3) = 1$ and $T_2(3) = S_3 S_2^{-1} S_1 S_2$.

Theorem 6.2. For quadratic Poincaré theta series (6.35) and (6.36) the Hejhal map (6.33) is the finite sum presented in Table 6.1 (\hat{T} is the matrix representation for the element T of \mathfrak{S}).

Proof. We demonstrate all the methods of calculations with the first two lines of the table. Note first the key Hejhal identity

$$\mathbf{M}(Su) = \hat{S} \mathbf{M}(u) \hat{S}^{-1} S'(u), \quad S \in \mathrm{PSL}_2(\mathbb{C}). \quad (6.39)$$

Table 6.1 Hejhal map for (relative) Poincaré quadratic theta series

$R(u)$	$\int_{C_m} \Theta_2[R](u) \mathbf{M}(u) du$
$R_T(u)$	$\frac{2\pi i}{(\alpha - \beta)^3} \sum_{j=l+1}^s \varepsilon_j \hat{T}_j^{-1}(m) \left\ \begin{smallmatrix} \alpha + \beta & -2\alpha\beta \\ 2 & -\alpha - \beta \end{smallmatrix} \right\ \hat{T}_j(m)$
$R_T^{zz'}(u)$	$\frac{2\pi i}{\alpha - \beta} \left[\sum_{j=1}^l \varepsilon_j \hat{T}_j^{-1}(m) \left\{ \frac{\mathbf{M}(\alpha)}{(\alpha - z)(\alpha - z')} - \frac{\mathbf{M}(\beta)}{(\beta - z)(\beta - z')} \right\} \hat{T}_j(m) + \right. \\ \left. + \sum_{j=l+1}^s \frac{\varepsilon_j}{1 - \lambda} \hat{T}_j^{-1}(m) \left\{ \frac{\mathbf{M}(\alpha)}{(\alpha - z)(\alpha - z')} + \frac{\lambda \mathbf{M}(\beta)}{(\beta - z)(\beta - z')} \right\} \hat{T}_j(m) \right]$
$R_T^{2z}(u)$	$\frac{2\pi i}{\alpha - \beta} \left[\sum_{j=1}^l \varepsilon_j \hat{T}_j^{-1}(m) \left\{ \frac{\mathbf{M}(\alpha)}{(\alpha - z)^2} - \frac{\mathbf{M}(\beta)}{(\beta - z)^2} \right\} \hat{T}_j(m) + \right. \\ \left. + \sum_{j=l+1}^s \frac{\varepsilon_j}{1 - \lambda} \hat{T}_j^{-1}(m) \left\{ \frac{\mathbf{M}(\alpha)}{(\alpha - z)^2} + \frac{\lambda \mathbf{M}(\beta)}{(\beta - z)^2} \right\} \hat{T}_j(m) \right]$
$R_T^{3z}(u)$	$\frac{2\pi i}{(\alpha - z)^3} \left[\sum_{j=1}^l \varepsilon_j \hat{T}_j^{-1}(m) \mathbf{M}(\alpha) \hat{T}_j(m) + \sum_{j=l+1}^s \frac{\varepsilon_j}{1 - \lambda} \hat{T}_j^{-1}(m) \mathbf{M}(\alpha) \hat{T}_j(m) \right]$
$R^{pz}(u)$	0 $p = 4, 5, \dots$

- A. With the help of this identity we transform the expression for the Hejhal map of the relative quadratic Poincaré series $\Theta_2[R_T]$:

$$\int_{C_m} \Theta_2[R_T](u) \mathbf{M}(u) du = \sum_{S \in \langle T \rangle | \mathfrak{S}} \hat{S}^{-1} \left\{ \int_{SC_m} R_T(u) \mathbf{M}(u) du \right\} \hat{S}.$$

To calculate the last integral it is sufficient to find all transformations S in the group for which the poles of the function $R_T(u)$ lie inside the circle SC_m and also to determine the orientation of this circle. It is clockwise (counterclockwise) oriented if the domain $S\mathbf{R}$ lies inside the circle (outside the circle, respectively). To find the required elements S of the group we use the Nielsen ordering, when points in the limit set of the group \mathfrak{S} are coded by irreducible infinite words on the alphabet $\{S_j^{\pm 1}, j = 1, \dots, g\}$. Finite initial pieces of such a word take the standard fundamental domain of the group to contracting neighbourhoods of the corresponding point in the limit set. For example,

$$\begin{aligned} \alpha &\sim (S_{\bullet} \dots S_m^{\varepsilon_1} \dots S_m^{\varepsilon_2} \dots S_m^{\varepsilon_l} \dots S_*) (S_{\Delta} \dots S_m^{\varepsilon_{l+1}} \dots S_m^{\varepsilon_s} \dots S_{\nabla}) \cdot \\ &\quad \cdot (S_{\Delta} \dots S_m^{\varepsilon_{l+1}} \dots S_m^{\varepsilon_s} \dots S_{\nabla}) (S_{\Delta} \dots S_m^{\varepsilon_{l+1}} \dots S_m^{\varepsilon_s} \dots S_{\nabla}) \dots; \\ \beta &\sim (S_{\bullet} \dots S_m^{\varepsilon_1} \dots S_m^{\varepsilon_2} \dots S_m^{\varepsilon_l} \dots S_*) (S_{\nabla}^{-1} \dots S_m^{-\varepsilon_s} \dots S_m^{-\varepsilon_{l+1}} \dots S_{\Delta}^{-1}) \cdot \\ &\quad \cdot (S_{\nabla}^{-1} \dots S_m^{-\varepsilon_s} \dots S_m^{-\varepsilon_{l+1}} \dots S_{\Delta}^{-1}) \dots \end{aligned}$$

The required transformations S can be expressed in terms of elements accompanying the fixed element T of the group; they are listed in Table 6.2. Estimates for the length of an irreducible factorization with respect to the generators show that the elements $T_1(m), \dots, T_l(m), T_{l+1}(m), \dots, T_s(m)$ accompanying T lie in different right cosets of the Schottky group \mathfrak{S} by the subgroup $\langle T \rangle$. If we find the residue

$$\begin{aligned} \text{Res}_{u=\alpha} R_T(u) \mathbf{M}(u) &= (\alpha - \beta)^{-2} \mathbf{M}'(\alpha) - 2(\alpha - \beta)^{-3} \mathbf{M}(\alpha) = \\ &= (\alpha - \beta)^{-3} \begin{vmatrix} \alpha + \beta & -2\alpha\beta \\ 2 & -\alpha - \beta \end{vmatrix} \end{aligned} \quad (6.40)$$

and a similar residue of $R_T(u) \mathbf{M}(u)$ at $u = \beta$, we obtain the right-hand expression in the first line of Table 6.1. Note that (6.40) is an $\text{Ad } \hat{T}$ -invariant matrix, as follows from the identity

$$\begin{vmatrix} \alpha + \beta & -2\alpha\beta \\ 2 & -\alpha - \beta \end{vmatrix} = \begin{pmatrix} \alpha \\ 1 \end{pmatrix} (1, -\beta) + \begin{pmatrix} \beta \\ 1 \end{pmatrix} (1, -\alpha),$$

so the result of calculations is independent of the choice of representatives of cosets by the subgroup $\langle T \rangle$ in Table 6.2.

Table 6.2 Group elements which give nonzero terms of Poincaré series $\Theta_2[R_T]$

The pole	$S \in \mathfrak{S}$ such that the pole lies inside SC_m		
$u = \alpha$	$T_1(m), \dots, T_l(m);$	$T^q T_{l+1}(m), T^q T_{l+2}(m), \dots, T^q T_s(m),$	$q \geq 0$
$u = \beta$	$T_1(m), \dots, T_l(m);$	$T^q T_s(m), T^q T_{s-1}(m), \dots, T^q T_{l+1}(m),$	$q < 0$

- B. Now we transform the expression for the image of the series $\Theta_2[R_T^{zz'}]$ under the map (6.33) using Hejhal's identity:

$$\int_{C_m} \Theta_2[R_T^{zz'}](u) \mathbf{M}(u) du = \sum_{S \in \mathfrak{S}} \hat{S}^{-1} \left\{ \int_{SC_m} R_T^{zz'}(u) \mathbf{M}(u) du \right\} \hat{S}.$$

Note that the points $z, z' \in \mathbb{R}$ lie outside all the circles SC_k , while α and β lie inside SC_k only for the elements S listed in Table 6.2. To find the sum of the residues $\hat{S}^{-1} \text{Res}_{u=\alpha, \beta} R_T^{zz'}(u) \mathbf{M}(u) \hat{S}$ over the elements in Table 6.2 we must know the values of the series

$$\sum_{q=0}^{\infty} \hat{T}^{-q} \mathbf{M}(\alpha) \hat{T}^q = \sum_{q=0}^{\infty} \lambda^q \mathbf{M}(\alpha) = \mathbf{M}(\alpha)/(1 - \lambda)$$

and

$$\sum_{q=1}^{\infty} \hat{T}^q \mathbf{M}(\beta) \hat{T}^{-q} = \sum_{q=1}^{\infty} \lambda^q \mathbf{M}(\beta) = \lambda \mathbf{M}(\beta)/(1 - \lambda).$$

Calculations yield the right-hand expression in the second line of Table 6.1. \square

6.2.5 A Basis of Quadratic Poincaré Theta Series

Now using Theorem 6.2 we calculate Hejhal map for several simplest (relative) quadratic Poincaré series and put them to the Table 6.3.

Corollary 6.1 (to Theorem 6.2). *For $T = S_1, S_2, \dots, S_g$; $S_1 S_2^{-1} S_1, S_1 S_3^{-1} S_1, \dots, S_1 S_g^{-1} S_1$ the quadratic differentials in (6.36) form a basis in the $(2g - 1)$ -dimensional complex space of even (= invariant under the hyperelliptic involution J) holomorphic quadratic differentials on M_c .*

Proof. We shall verify that the quadratic differentials in question are invariant under hyperelliptic involution on M_c (which acts as $u \rightarrow -u$ in our model). In fact, all the motions T in the statement satisfy the relation $T(-u) = -T^{-1}(u)$ since each generator $S_j := G_j G_0$ is a composite of two rotations of order 2. Hence (a) $\alpha(T) + \beta(T) = 0$ and (b) the involution J of the group acting by the formula $JS(u) := -S(-u)$ induces an involution on the right cosets $\langle T \rangle | \mathfrak{S}$ of the group. These two

Table 6.3 Several simple Hejhal maps

T	$\int_{C_m} \Theta_2[R_T](u) \mathbf{M}(u) du$
S_j	$\frac{i\pi}{2\alpha^2} \begin{pmatrix} 0 & \alpha \\ \alpha^{-1} & 0 \end{pmatrix} \delta_{jm}$
$S_j S_m^{-1} S_j$	$-\frac{i\pi}{2\alpha^2} \hat{S}_j \begin{pmatrix} 0 & \alpha \\ \alpha^{-1} & 0 \end{pmatrix} \hat{S}_j^{-1}$
$S_m S_j^{-1} S_m$	$\frac{i\pi}{2\alpha^2} \left\{ \begin{pmatrix} 0 & \alpha \\ \alpha^{-1} & 0 \end{pmatrix} + \hat{S}_m \begin{pmatrix} 0 & \alpha \\ \alpha^{-1} & 0 \end{pmatrix} \hat{S}_m^{-1} \right\}$

Table 6.4 The values of quadratic differentials $\Theta_2[R_T](du)^2$ at $2g - 1$ functionals λ_j and μ_s

T	$\langle \lambda_1 \cdot \rangle$	$\langle \lambda_2 \cdot \rangle$...	$\langle \lambda_g \cdot \rangle$	$\langle \mu_2 \cdot \rangle$	$\langle \mu_3 \cdot \rangle$...	$\langle \mu_g \cdot \rangle$
S_1	L_1	0	...	0				
S_2	0	L_2	...	0				
								0
\vdots	\vdots		\ddots	\vdots				
S_g	0	0	...	L_g				
$S_1 S_2^{-1} S_1$					M_2	0	...	0
$S_1 S_3^{-1} S_1$					0	M_3		0
			*					
\vdots					\vdots		\ddots	
$S_1 S_g^{-1} S_1$					0	0	...	M_g

observations allow us to conclude that $\Theta_2[R_T]$ is an even function of u for T under consideration.

To prove that the system of quadratic differentials in the statement is complete we consider the linear functionals $\langle \lambda_j | \mathcal{E} \rangle$ and $\langle \mu_j | \mathcal{E} \rangle$ on the space of quadratic differentials $\mathcal{E}(u)(du)^2$ which are defined as the entries (1, 2) and (1, 1) of the matrix $\int_{C_j} \mathcal{E}(u) \mathbf{M}(u) du$. Using Table 6.3 we can write down the matrix of the values of the $2g - 1$ functionals $\langle \lambda_1 | \cdot \rangle, \dots, \langle \lambda_g | \cdot \rangle; \langle \mu_2 | \cdot \rangle, \dots, \langle \mu_g | \cdot \rangle$ at the quadratic differentials $\Theta_2[R_T](du)^2$ (see Table 6.4), where $L_j := i\pi\alpha^{-1}(S_j)/2$ and $M_j := \pm i\pi\alpha^{-3}r_1^{-2}c_1(\alpha^2 - \alpha^2(S_1))/2, \alpha := \alpha(S_1 S_j^{-1} S_1)$. It follows from the equality $\alpha^2 = \alpha^2(S_1)$ that $\alpha(S_1)$ is a fixed point of the transformation S_j , which is impossible for $j \neq 1$. Thus the diagonal entries of the matrix are distinct from zero, the matrix is non-singular and the quadratic differentials in question do form a basis. \square

Now we show that we can use quadratic Poincaré series to calculate directional derivatives of the abelian integrals (6.26) in the moduli space. To find the derivatives of periods of the holomorphic differentials ζ_s in (6.29) we use the holomorphic quadratic differentials $\zeta_l \zeta_s$. They are invariant under the involution of M , and so if we know the coefficients of the expansion of $\zeta_l \zeta_s$ with respect to the explicit basis of quadratic Poincaré series, we can use Table 6.3 to calculate the Hejhal map with $\mathcal{E}(du)^2 = \zeta_l \zeta_s$. To find the coefficient of the expansion it is sufficient to have a

complete system of effectively calculated functionals on the space of even quadratic differentials,

Lemma 6.6. *Fix a local system of coordinates at $2g - 1$ points on the hyperelliptic curve M such that no two points among these are interchanged by hyperelliptic involution. Then the values of the coefficients of quadratic differentials at these points form a complete system of functionals over the $(2g - 1)$ -dimensional space of even holomorphic quadratic differentials.*

Proof. Note that the completeness of the so-introduced system of functionals is independent of local systems of coordinates at the fixed points $p_1, p_2, \dots, p_{2g-1} \in M$ because a change of variables results in multiplying the functionals by non-zero constants.

Consider a second-degree function $x \in \mathbb{C}(M)$ taking finite values at the points under consideration and also consider $w \in \mathbb{C}(M)$ related to x by an equation $w^2 = P_{2g+2}(x)$, where P_{2g+2} is a polynomial of degree $2g + 2$ with simple zeros. Without loss of generality we assume that w is distinct from zero at the points p_1, p_2, \dots, p_m on M_c and take x for a local variable at these points; at the remaining (ramification) points $p_{m+1}, p_{m+2}, \dots, p_{2g-1}$ we take w for a local variable. The values of the functionals in question at the basis $w^{-2}x^j(dx)^2$, $j = 0, \dots, 2g - 2$, of the space of even quadratic differentials [60] make up a matrix with (j, s) entry equal to

$$\begin{cases} w^{-2}(p_s)x^j(p_s), & s = 1, \dots, m, \\ 4(P'_{2g+2}(p_s))^{-2}x^j(p_s), & s = m + 1, \dots, 2g - 1. \end{cases}$$

Multiplication by a diagonal matrix on the right transforms it into the Vandermonde matrix $\|x^j(p_s)\|$. By hypothesis $x(p_l) \neq x(p_s)$ for $p_l \neq p_s$, and so our matrix is non-singular and the functionals in question form a basis of the dual space. \square

In the case of meromorphic quadratic differentials $\eta_{zz'}\eta_{ww'}$, $\zeta_j\eta_{ww'}$, $\omega_{mz}\eta_{ww'}$, $\omega_{mz}\zeta_j$ we can pick a sum of quadratic differentials of the form (6.35) with suitable singularities and can expand the remaining holomorphic part with respect to an explicit basis [72] of relative quadratic Poincaré theta series. However, we use in applications only even meromorphic quadratic differentials, so the above basis will be sufficient for our aims.

6.3 Calculation of Polynomials

6.3.1 A Parametric Representation

As an application of Lemma 6.4 under the assumption that Abel's equations are satisfied we find a parametric representation for g -extremal polynomials which can be effectively calculated.

The circles C_1, C_2, \dots, C_g make up half the canonical basis of 1-cycles on the compact curve $M_c := \mathcal{D}(\mathfrak{S})/\mathfrak{S}$. Hence [60] abelian differentials on the curve can be normalized by prescribing their periods along these circles. In particular, the distinguished form η_M on the curve M with periods prescribed by Abel's equations (6.1) has a representation

$$\eta^* := \eta_{-11} + \sum_{s=1}^g \frac{m_s}{n} \zeta_s. \quad (6.41)$$

Now we readily obtain an expression for the Akhiezer function $\tilde{P}_n(x, w)$ in terms of the uniformizing variable u :

$$\tilde{P}_n(x, w) := \tilde{T}(u) = (u, \infty; -1, 1)^n \prod_{j=1}^g E_j^{m_j}(u). \quad (6.42)$$

The polynomial $P_n(x)$ corresponding to the curve M can be obtained from this by taking the composite with the Zhukovskii map (6.3). In a similar way we find the independent variable $x(u)$ (in general, defined up to an affine transformation) normalized by the condition $u = (0, 1, \infty) \rightarrow x = (0, \infty, -1)$:

$$x(u) = -(u, \infty; 0, 1)(u, \infty; 0, -1) = -(u, \infty; 0, 1)(-u, \infty; 0, 1). \quad (6.43)$$

Using formula (6.20) one can calculate the jets of the functions $\tilde{T}(u)$ and $x(u)$, and therefore the derivatives $D_x^m P_n(x)$, $m = 0, 1, 2, \dots$, of a fixed parametrically defined g -extremal polynomial. In terms of the values of these derivatives at various points one can express the constraints of the optimization problem: for instance, the two leading coefficients of $P_n(x)$ are the values of $P_n x^{-n}$ and $(nP_n - xD_x P_n)x^{1-n}$ for $u = 1$.

6.3.2 Abel's Equations in the Space \mathcal{G}_g^k

Of course, a meromorphic function with divisor $n(\infty_- - \infty_+)$ does not exist on each curve M_c . Conditions for the automorphy of the Akhiezer function (6.42) in the previous sections are equivalent to Abel's equations (6.1).

Theorem 6.3. *Abel's equations (6.1) are equivalent to the real relations*

$$E_s^{2n}(1) = E_{1s}^{m_1} E_{2s}^{m_2} \dots E_{gs}^{m_g}, \quad s = 1, \dots, g. \quad (6.44)$$

Remark 6.3. Conditions similar to (6.44) first appeared in Akhiezer work [9].

Proof. We can formulate Abel's equations as follows: *the differential (6.41) normalized by condition (6.1) must have purely imaginary periods on the curve.* This

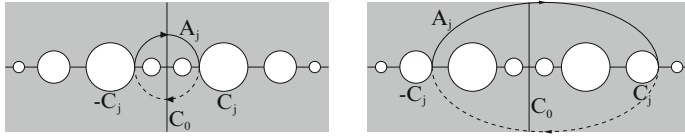


Fig. 6.3 Calculating $A_j - \bar{J} A_j$ for $j = 1, \dots, k-1$ (left) and for $j = k, \dots, g$ (right)

condition always holds on the cycles C_1, C_2, \dots, C_g in view of the normalization (6.8) of the holomorphic differentials. Let A_j , $j = 1, \dots, g$, be an arc in $\mathbb{R} \cap \mathbb{H}$ joining the real point $u \in -C_j$ and $S_j u \in C_j$. Using the intersection form we can verify that the $2g$ cycles C_1, \dots, C_g ; A_1, \dots, A_g form a basis of the lattice of 1-cycles on the compact curve $M_c := \mathcal{D}(\mathfrak{S})/\mathfrak{S}$. Now we want to know when the integrals of η^* over the new cycles A_j are also purely imaginary. We project A_j onto the space of odd cycles (see Fig. 6.3):

$$A_j - \bar{J} A_j = \begin{cases} 0, & j = 1, \dots, k-1, \\ \pm C_j, & j = k, \dots, g. \end{cases}$$

Since the differential η^* is real, taking account of the normalization conditions (6.8) we obtain the chain of equalities

$$\operatorname{Im} \int_{A_j} n \eta^* = \frac{1}{2} \int_{A_j - \bar{J} A_j} n \eta^* = \begin{cases} 0, & j = 1, \dots, k-1, \\ \pm \pi i m_j, & j = k, \dots, g. \end{cases}$$

Note that $\operatorname{Im} \int_{A_j} n \eta^* \in 2\pi i \mathbb{Z}$ since m_j is even when $j = k, \dots, g$. Hence the periods of η^* are purely imaginary if and only if $\exp\left(\int_{A_j} n \eta^*\right) = 1$. The transformation rules (6.16) and (6.17) for the Schottky functions transform these equalities for $j = 1, \dots, g$ into the statement of the theorem. \square

6.3.3 The Scheme of the Algorithm

Now we describe the scheme of the solution of least deviation problems in the framework of our approach:

1. Given the problem data, find the topological invariants g and k and the integer indices m_0, m_1, \dots, m_g corresponding to the solution $P_n(x)$. This is related to finding a low-dimensional face of the sphere $\{Q_n(x) : \|Q_n\|_E = \text{const}\}$ in the space of polynomials which contains the solution $P_n(x)$. The integers m_0, m_1, \dots, m_g can be guessed: their range is known from Theorem 5.4. Sometimes we know the asymptotic values of m_s/n as $n \rightarrow \infty$, for instance, in the least deviation problem for a monic polynomial on several intervals of the real axis [156].

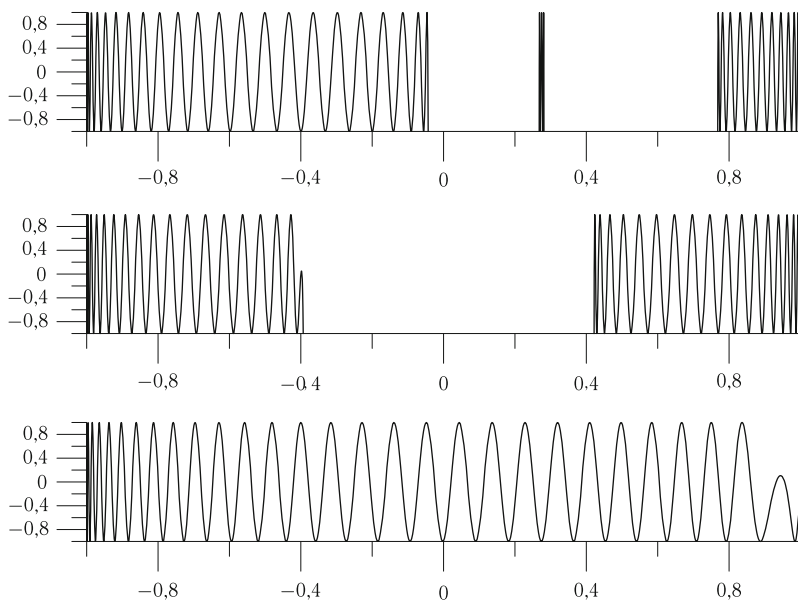


Fig. 6.4 The extremal polynomials $P_{73}(x)$ for $g = 2$ and $k = 3, 2, 1$

2. In the domain \mathcal{G}_g^k explicitly defined by inequalities (3.5), (3.6) and (3.7), make a descent onto the smooth g -dimensional submanifold \mathbb{T} described by Abel's equations (6.44) in Theorem 6.3. Locally, navigation in the moduli space is performed with the help of variational formulae (6.28) and (6.29) enabling one to implement Newton's or other descent methods [31]. For instance, in [37] a descent is performed along the gradient of the smooth distance function from the manifold \mathbb{T} with respect to a certain metric.
3. Using formulae (6.20) for derivatives of automorphic functions and variational formulae for abelian integrals, find on \mathbb{T} a point M corresponding to a polynomial satisfying the constraints of the least deviation problem.
4. Recover the solution $P_n(x)$ from the associated curve M using the parametric formulae (6.3), (6.42), and (6.43).

In Fig. 6.4 we plot the graphs of 2-extremal polynomials of degree $n = 73$ calculated by means of a software implementing steps 2, 3, and 4 of this scheme.

6.4 Problems and Exercises

1. Show that the cross ratio of four points $\frac{u-x}{u-y} : \frac{v-x}{v-y}$ does not change after a linear fractional transformation (applied to all the points). From this deduce identity (6.5).

2. Show that $\eta_{zz'}(u) = \eta_{-z-z'}(-u)$.

Hint. Use the involution $(JS)u := -S(-u)$ on the group \mathfrak{S} .

3. Show that a line interval of fixed *Euclidean* length in the Poincaré disc has the minimal *non-Euclidean length* if it is concentric with the absolute.
4. Assume that the domain of discontinuity \mathcal{D} of a Kleinian group \mathfrak{S} contains the point at infinity. Show that the linear Eisenstein-type series $\sum_{G \in \mathfrak{S}} |G'(u)|$ is convergent or divergent simultaneously for all points u in \mathcal{D} apart from the orbit of $u = \infty$. Show that this series is convergent if and only if the sum of the squares of the radii of all the isometric circles of transformations in the group is finite.
5. (Tsujii, ([149]) Show that the series $\sum_{G \in \mathfrak{S}} |G'(u)|$ diverges for a finitely generated Fuchsian group \mathfrak{S} of finite volume. Generally speaking, convergence of series of Eisenstein type is related to the Hausdorff dimension of the limit set of the group [8].
6. Show that the limit set of each Schottky group in the deformation space \mathcal{G}_g^k has linear measure zero.
7. Write out the automorphy conditions for the right-hand side of (6.19). Show that these conditions are equivalent to the ones imposed by Abel's theorem on the divisor $\sum_{j=1}^{\deg F} (z_j - z'_j)$ of an automorphic function $F(u)$.
8. (Rauch, [124, 125]) Consider a canonical homology basis $A_1, \dots, A_g; C_1, \dots, C_g$ on a Riemann surface M and the holomorphic forms ζ on M normalized by the equalities $\int_{C_j} \zeta_s = \delta_{sj}$. A deformation of the complex structure on M is determined by the Beltrami differential $\mu \overline{dz}/dz$. Prove Rauch's variational formula for the period matrix: $\delta \int_{A_j} \zeta_s = \int_M \zeta_s \zeta_j \mu \overline{dz}/dz + o(\|\mu\|)$.
9. (Poincaré, [121] and Ford, [64]) Assume that the domain of discontinuity of a Kleinian group \mathfrak{S} contains the point at infinity. Show that the quadratic series of Eisenstein type $\sum_{G \in \mathfrak{S}} |G'(u)|^2$ is convergent.
10. (Kra, ([85]) Let $R(u)$ be a rational function with poles in the limit set of a Fuchsian group \mathfrak{S} . Investigate the convergence of the quadratic Poincaré series $\Theta_2[R](u) := \sum_{S \in \mathfrak{S}} R(Su)(S'(u))^2$.
11. Let $T(u)$ be a linear fractional transformation with fixed point α and dilation coefficient $\lambda := T'(\alpha)$. Show that $(\alpha, 1)^t$ is an eigenvector of the matrix $\hat{T} \in SL_2$ representing T which corresponds to the eigenvalue $\sqrt{\lambda}$.
12. Show that the holomorphic differentials ζ_j in (6.7) and the meromorphic differentials $\eta_{zz'}$ in (6.4) with poles at $z, z' \in \mathbb{R}$ are real differentials.
13. Show that to find the argument $x(u)$ of a polynomial, alongside (6.43) we can use the formula $x = x_1/(1 - x_1)$, $x_1(u) = (u, 1; 0, \infty)^2$.
14. Consider a parametric representation of a function: $T(u) = T_0 + T_1 u + T_2 u^2 + \dots$; $x(u) = x_1 u + x_2 u^2 + \dots$, $dx/du(0) \neq 0$. Express the jet of the function $T(x(u))$ in terms of the coefficients of the jets of $T(u)$ and $x(u)$.

15. Write out a complete system of equations in the deformation space for the curve M associated with the Chebyshev spline of type $(n, 0, k_-, k_+)$ (see the definition in Sect. 1.1.5).
16. Prove formulae (6.16) and (6.17) for transformations of Schottky functions.
17. Prove formula (6.18) in the case $l = j$.

Chapter 7

The Problem of the Optimal Stability Polynomial

Zolotarëv's solution, which is based on the use of elliptic functions, is too complicated for practical purposes.

A.A. Markov [100]

In designing explicit n -stage stable Runge–Kutta methods of order p we come across the following optimization problem for polynomials:

Find a real polynomial $R_n(x)$ of degree at most n approximating the exponential function with order $p \leq n$ at the origin (so that $R_n(x) = 1 + x + x^2/2! + \cdots + x^p/p! + o(x^p)$) such that the bounds $-1 \leq R_n(x) \leq 1$ hold on a possibly large interval $[-L, 0]$, $L > 0$.

The solution of this problem for $p = 1$ was found in 1959 by Franklin [65]; it can be expressed in terms of the classical Chebyshev polynomials: $R_n(x) = T_n(1 + x/n^2)$. The Zolotarëv polynomials, which can be expressed parametrically in terms of elliptic functions, provide a solution of the same problem for $p = 2$ (Lebedev and Medovikov [94, 96]). Many authors (Lebedev and Medovikov [95], Medovikov [103], Riha [127], Metzger, Lomax, van der Houwen, Abdulle [1], Verwer [153]) pointed out that no closed analytic form is known for the solution $R_n(x)$ if $p > 2$ and put forward various iterative methods for its numerical evaluation. The direct numerical optimization is extremely labour-consuming and in effect impossible for polynomials of large degree. The best iterative method known [95] required ca. 96 hours of calculation on a many-processor work-station for the solution of the problem for $p = 3$ and $n = 576$ (Lebedev and Medovikov).

The analytic approach [25, 43] to the same problem put forward below required about a second of calculations on a considerably less powerful processor. Our analysis of the optimization Problem B in Chap. 1 enables us to figure out the characteristic features of the solution. We know that the optimal stability polynomial has many alternance points, so its extremality parameter g is not large.

7.1 The Chebyshev Representation for Solutions

On finding the curve M corresponding to the solution of the optimization problem we can recover the solution itself by the explicit formula (10). The complexity of the calculations by this formula in no way depends on the degree n of the solution, provided that one can effectively calculate the hyperelliptic integral.

7.1.1 The Topological Type of the Associated Curve

The branch points of the curve M associated with a polynomial $P_n(x)$ are odd-order zeros of the polynomial $P_n^2(x) - 1$. The total number $2g + 2$ of the branch points and their number $2k$ on the real axis are topological invariants of the real curve. They determine the genus g of the curve M and the number k of coreal ovals on it.

Theorem 7.1. *The real curve M associated with the optimal stability polynomial R_n contains precisely one real oval and has genus $g \leq p - 1$.*

Proof. We list again all the real zeros of the optimal stability polynomial $R_n(x)$ and its derivative, which we found in Lemma 1.3. There are $n - p$ zeros of this polynomials lying between consecutive alternance points on $[-L, 0)$. Furthermore, between the rightmost alternance point on this interval and $x = 0$ there must be a zero of the polynomial if p is odd or a zero of its derivative if p is even. The other real zeros of the derivative $R'_n(x)$ are the $n - p$ alternance points in the interior of $E := [-L, 0]$. In particular, the left end-point of E is an alternance point of the polynomial, but not a zero of its derivative.

The end-points of the interval E are simple zeros of the polynomial $R_n^2(x) - 1$; the $n - p$ points of the alternance lying in the interior of E are its double zeros. The inverse image $R_n^{-1}(\pm 1)$ contains no other points on the real axis since otherwise the polynomial $R_n R'_n$ would have zeros not described by Lemma 1.3. For example, the existence of a point $x \in R_n^{-1}(\pm 1)$ outside E means that the polynomial R_n or its derivative have a zero between x and E . The other cases can be considered in a similar way.

Hence there exist precisely $2p - 2$ inverse images (taking multiplicities into account) of the points ± 1 outside the real axis. If these inverse images are simple, then M has genus $p - 1$. If some of them are multiple, then g is smaller. \square

The natural conjecture that the genus of M is equal to $p - 1$ holds for $p < 4$.

Proposition 7.1. *For $p < 4$ the genus g is $p - 1$.*

Proof. If $p < 3$, then there exists in the upper half-plane at most one point in $R_n^{-1}(\pm 1)$ with multiplicities taken into account. If $p = 3$, then each of the points -1 and $+1$ has $n - 2$ inverse images (with multiplicities) on the real axis. Hence the upper half-plane contains precisely one simple inverse image of each of these points. \square

We see that for $p = 1$ the solution of the optimization problem from the Introduction can be expressed in terms of the 0-extremal (Chebyshev) polynomial and for $p = 2$ in terms of the 1-extremal (Zolotarëv) polynomial. In the rest of this chapter we shall thoroughly study the case $p = 3$, which corresponds to the 2-extremal polynomial.

7.1.2 The Moduli Space

For $p = 3$ the branch divisor of the curve M associated with the optimal stability polynomial consists of two real points and two pairs of complex conjugate points. It is convenient to normalize the branch divisor \mathbf{e} so that the left real branch point is at -1 and the right at 0 . Such branch divisors form a moduli space \mathcal{H}_2^1 of real dimension 4 with fundamental group \mathbb{Z} . Normalized in the above-described way is the branch divisor \mathbf{e} of the curve M associated with the polynomial $P_n(x) := R_n(Lx)$, which we shall call the *reduced* optimal stability polynomial.

7.1.3 The Subgroup Induced by the Covering

In this chapter we use another uniformization of elements of the moduli space by Schottky groups. Accordingly, we shall get another subgroup of the fundamental group of the punctured sphere $\hat{\mathbb{C}} \setminus \mathbf{e}$. We must also modify the construction of a labyrinth.

We join the branch points pairwise by cuts: an interval $\Lambda_0 := [-1, 0]$, a simple smooth curve Λ_+ lying in \mathbb{H} and connecting the branch points in the upper half-plane, and the mirror symmetric curve $\Lambda_- := \overline{\Lambda_+}$. The system of cuts $\Lambda := (\Lambda_+, \Lambda_0, \Lambda_-)$ defines a representation χ_Λ from $\pi_1(\hat{\mathbb{C}} \setminus \mathbf{e}, \infty)$ into the abstract group $\mathfrak{G} := \langle G_+, G_0, G_- | G_+^2 = G_0^2 = G_-^2 = 1 \rangle$, the free product of three groups of order 2. We associate with a loop ρ intersecting transversally one after another the cuts $\Lambda_\star, \Lambda_\bullet, \dots, \Lambda_\circ$ (where the subscripts $\star, \bullet, \dots, \circ$ take the values $+, 0, -$) the element

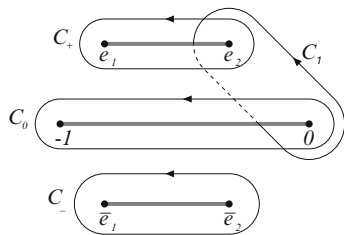
$$\chi_\Lambda[\rho] := G_\star G_\bullet \dots G_\circ$$

of this group. The representation into the discrete group \mathfrak{G} cannot change after a continuous deformation of the cuts. Two arbitrary cuts of the upper half-plane having the same end-points are isotopic, and therefore the representation χ_Λ and, in particular, its kernel, are independent of our choice of Λ_+ .

7.1.4 Cycles on a Riemann Surface

On each curve M in the moduli space \mathcal{H}_2^1 we distinguish four integral cycles. The contour C_0 goes counterclockwise along the two sides of the interval $[-1, 0]$. The

Fig. 7.1 The distinguished cycles on a curve M , an element of the moduli space \mathcal{H}_2^1



cycle C_+ encircles the pair of branch points in the upper half-plane (see Fig. 7.1, where we indicate by the bold lines the cuts Λ_+ , Λ_0 , Λ_- connecting pairwise the branch points).

The third cycle C_- is obtained from C_+ by a reflection and a change of orientation (throughout this chapter we use \pm to distinguish between the upper and lower half-planes, rather than between even and odd cycles). The fourth cycle C_1 goes along the sides of the cut connecting a branch point in the upper half-plane and the origin. By contrast with the first three, this cycle is not uniquely defined. The fundamental group of the moduli space acts naturally in the homology space of the curve (see Chap. 5 for greater detail); as a result, an integer number of cycles C_+ can be added to C_1 .

7.1.5 Abel's Equations

If the curve M is associated with a polynomial $P_n(x)$, then the distinguished differential has the following representation:

$$\eta_M = n^{-1} d \log \tilde{P}_n(x, w), \quad (7.1)$$

where $\tilde{P}_n(x, w) := P_n(x) + \sqrt{P_n^2(x) - 1}$ is the (Akhiezer) meromorphic function on M . In fact, in view of the equality $\tilde{P}_n(x, w)\tilde{P}_n(x, -w) = 1$, which can readily be verified, the divisor of the Akhiezer function consists of the points ∞_- and ∞_+ covering infinity, with multiplicities n and $-n$. The differential on the right-hand side of (7.1) has only simple poles at infinity with residues ± 1 and purely imaginary periods: the integral over each integral cycle can be expressed in terms of the increment of the argument of the Akhiezer function on this cycle and therefore belongs to the lattice $2\pi i\mathbb{Z}/n$. In particular,

$$\int_{C_1} \eta_M \in 2\pi i\mathbb{Z}/n. \quad (7.2)$$

If the curve M is generated by the reduced optimal stability polynomial, then the integrals over the contours C_0 and C_+ can be calculated exactly. The polynomial

$R_n(Lx) := P_n(x) = \frac{1}{2}(\tilde{P}_n(x, w) + 1/\tilde{P}_n(x, w))$ performs on $[-1, 0]$ precisely $n - 2$ oscillations between $+1$ and -1 . As (x, w) moves along the contour C_0 on the Riemann surface, the point $\tilde{P}_n(x, w)$ obtained from $P_n(x)$ by the inverse Zhukovskii map makes precisely $n - 2$ *counterclockwise* circuits round the unit circle. Hence $\int_{C_0} \eta_M = 2\pi i(n - 2)/n$. The cycle $C_0 + C_+ + C_-$ contracts to the pole ∞_+ of the differential η_M , the residue at which is -1 . The integrals over C_+ and $C_- = -\bar{J}C_+$ are equal because the differential is real, and therefore

$$\int_{C_+} \eta_M = 2\pi i n^{-1}. \quad (7.3)$$

We shall see below that (7.2) and (7.3) ensure that each integral of η_M over an integral cycle lies in $2\pi i\mathbb{Z}/n$. Hence $\tilde{P}_n(x, w) := \exp n \int_{(0,0)}^{(x,w)} \eta_M$ is a single-valued function on the Riemann surface M . The polynomial P_n generating the curve M can be obtained from the Akhiezer function \tilde{P}_n by means of the Zhukovskii map and can be calculated up to the sign by the explicit formula

$$P_n(x) = \cos\left(ni \int_{(0,0)}^{(x,w)} \eta_M\right), \quad x \in \mathbb{C}, (x, w) \in M. \quad (7.4)$$

7.1.6 Equations on the Moduli Space

In the neighbourhood of the origin the reduced optimal stability polynomial approximates the function $\exp(Lx)$ with third order:

$$P_n(x) = 1 + Lx + (Lx)^2/2 + (Lx)^3/6 + O(x^4). \quad (7.5)$$

Eliminating the unknown quantity $L = P'_n(0)$ we obtain

$$P''_n(0) = (P'_n(0))^2, \quad P'''_n(0) = (P'_n(0))^3. \quad (7.6)$$

Theorem 7.2. *In the four-dimensional moduli space \mathcal{H}_2^1 the system of four equations (7.2), (7.3), (7.6) has a unique solution M . The function (7.4) at this point M is the reduced optimal stability polynomial.*

Proof. We have already carried out the proof in one direction: the curve associated with the reduced optimal stability polynomial satisfies Abel's equations as well as the two constraints (7.6). We now claim that a curve satisfying these four equations gives rise to a solution of the optimization Problem B.

The four cycles: C_1 , C_+ and their reflections $\bar{J}C_1$, $\bar{J}C_+$ form a (non-canonical) basis in the lattice of integer 1-homology of the compact curve M ; their intersection indices make up an integer matrix with determinant ± 1 . The integral of η_M over each integral cycle on M lies in $2\pi i\mathbb{Z}/n$ (in view of Abel's equations (7.2), (7.3)

and since the differential is real). Hence formula (7.4) determines a single-valued meromorphic function on M . This function has singularities at the same points as the differential (that is, at infinity) and is invariant under the involution J , which changes the sign of the associated differential. Hence this function is a polynomial in x . Since η_M is real, it follows easily that so also is the polynomial $P_n(x)$. For x ranging from 0 to -1 the argument of the cosine function in (7.4) remains real and varies continuously from 0 to $-(n-2)\pi$ since $\int_{C_0} \eta_M = 2\pi i(n-2)/n$ by Abel's second equation (7.3). Accordingly, the deviation of $P_n(x)$ on $[-1, 0]$ is 1 and the polynomial itself possesses an $(n-2)$ -alternance on the interval $[-1, 0]$. We set $L := P'_n(0) > 0$; then by the constraints (7.6) the 4-jet of the polynomial $P_n(x)$ has the form (7.5). By the criterion of Theorem 1.3, $P_n(x/L)$ is the optimal stability polynomial. Since the latter must be unique, our system of four equations is uniquely solvable in the moduli space \mathcal{H}_2^1 . \square

7.2 The Schottky Model

For an effective treatment of Riemann surfaces we shall uniformize the curves M by means of Schottky groups; then the moduli space will be represented as the deformation space of some Kleinian group. The quantities participating in our system of 4 equations and defined on the moduli space can be calculated effectively in terms of linear Poincaré series, certain sums over the group. A uniformization for which these series converge in the entire moduli space is described in Chap. 6. We describe below another uniformization, for which Poincaré series converge better in a neighbourhood of a solution, particularly for large n . Unfortunately, using this approach one can only ensure that the series converges in a (fairly large) piece of the moduli space.

7.2.1 The Deformation Space

A linear fractional transformation of order 2 with complex fixed points $c \pm r$ has the following form:

$$G_+(u) := G_+u := c + r^2/(u - c). \quad (7.7)$$

Definition 7.1. By the *deformation space* \mathcal{G} we shall mean the set of transformations (7.7) taking the interior of some simple smooth closed curve C_+ lying entirely in the open first quadrant onto the exterior of this curve (see Fig. 7.2).

One can parametrize the deformation space by the complex coefficients c and r^2 of the transformation G_+ or by unordered pairs q, q' of fixed points of it, which must lie in the first quadrant. We now describe explicitly the range of the moduli in the space \mathbb{C}^2 .

Fig. 7.2 The fundamental domain of the group \mathfrak{G} related to a point in the deformation space \mathcal{G}

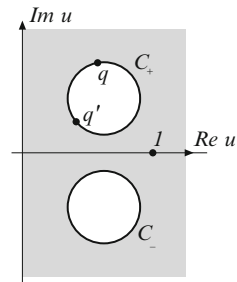
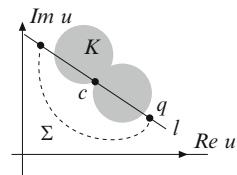


Fig. 7.3 The choice of the contour C_+



Theorem 7.3. *The space \mathcal{G} is defined by the following system of inequalities:*

$$|r| > 0; \quad \operatorname{Re} c > |\operatorname{Re} r|; \quad \operatorname{Im} c > |\operatorname{Im} r|; \quad \operatorname{Im}(c^2 - r^2) > |r|^2. \quad (7.8)$$

Proof. A. Let c and r^2 be the moduli defining a point in \mathcal{G} . The lower half-plane $-\mathbb{H}$ and the left half-plane $i\mathbb{H}$ lie outside C_+ . Their $G_+(u)$ -images lie inside C_+ , that is, in the interior of the first quadrant of the u -plane. The image of the lower half-plane is the disc with centre at $c - r^2/(c - \bar{c})$ and of radius $|r|^2/|c - \bar{c}|$; the left half-plane is mapped onto the disc with centre at $c - r^2/(c + \bar{c})$ and with radius $|r|^2/|c + \bar{c}|$. A disc lies in the first quadrant if and only if both real and imaginary parts of its centre are larger than its radius. Hence, bearing in mind that $c = G_+(\infty)$ lies in the first quadrant, we easily obtain inequalities (7.8).

B. We shall demonstrate how the contour C_+ required in the definition can be selected in the case when the moduli c and r^2 satisfy inequalities (7.8). Then the union of discs $K := G_+(-\mathbb{H}) \cup G_+(i\mathbb{H})$ lies in the interior of the first quadrant and contains no fixed points of the transformation $G_+(u)$. The line l passing through the points $c \pm r$ intersects the closure of K in a segment since the point $c = G_+(\infty)$ lies at the boundary of both discs. We can connect the fixed points $c \pm r$ of $G_+(u)$ by a smooth simple curve Σ lying in the first quadrant, to one side of l , and disjoint from the closure of K (see Fig. 7.3). We take the union of Σ and $G_+(\Sigma)$ for the contour C_+ ; then we obtain a smooth closed curve without self-intersections that lies entirely in the first quadrant; the action of G_+ interchanges its interior and exterior. Indeed, the map G_+ interchanges the half-planes to the left and to the right of l , while the doubly connected domain that is the complement of K with respect to the first quadrant is invariant.

□

Remark 7.1. It is not always possible to take a circle for C_+ . If this is possible, then we say that the corresponding point in the deformation space is *classical*: the reasons will soon be clear. We now show how large is the classical part of the space \mathcal{G} .

There exist precisely two circles passing through a fixed point q in the first quadrant and tangent to its sides. The interior of the convex hull of these circles (see Fig. 7.4), minus q itself, is the locus of points q' such that q and q' are fixed points of a classical element G_+ of the deformation space. Corresponding to the deformation space in this figure are points $q' \neq q$ in the first quadrant lying inside the circle with centre at $x + 2y + i(y + 2x)$ and of radius $2x + 2y$, where we set $q = x + iy$. The two circles determined above by q are tangent to this circle from inside. Fixing one fixed point q we define a two-dimensional section of the deformation space. The share of the classical part in this section depends only on the argument of q ranging in $(0, \pi/2)$. This dependence is shown in Fig. 7.5.

7.2.2 The Moduli Space and the Deformation Space

A point G_+ in the deformation space generates a group \mathfrak{G} on three generators: G_+u ; $G_0u := -u$; $G_-u := \overline{G_+u}$. By Klein's combination theorem [89] this group acts discontinuously in some subdomain $\mathcal{D} = \mathcal{D}(\mathfrak{G})$ of the sphere and all the relations in the group are consequences of three: $G_+^2 = G_0^2 = G_-^2 = 1$. The fundamental domain of this group is triply connected; it is bounded by the imaginary axis, the curve C_+ and its reflection $C_- := \overline{C_+}$. The Schottky group \mathfrak{S} of genus 2 with generators $S_{\pm} := G_{\pm}G_0$ is a subgroup of \mathfrak{G} of index 2. This Schottky group is *classical*, that is, has a fundamental domain bounded by circles if the generating point (c, r^2) in the deformation space is classical in the sense mentioned above.

The quotient manifold by the Schottky group admits a hyperbolic involution $J := G_0$ (with 6 fixed points $0, \infty, c \pm r, \bar{c} \pm \bar{r}$) and the reflection $\bar{J}u := \bar{u}$,

Fig. 7.4 A two-dimensional section of the classical part of the deformation space

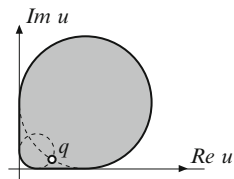
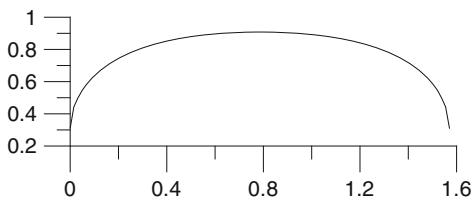


Fig. 7.5 The share of the classical part in a 2-dimensional section of the deformation space



so that it is a real hyperelliptic curve of genus 2. Selecting the natural orientation on the real line and distinguishing a point $u = 1$ on it (which will play the role of the distinguished point ∞_+) we obtain an element of the moduli space \mathcal{H}_2^1 . Now we describe explicitly the map from the deformation space \mathcal{G} into \mathcal{H}_2^1 .

The quotient \mathcal{D}/\mathfrak{G} is the Riemann sphere. We normalize the natural projection $x(u)$ of the discontinuity set \mathcal{D} of the group onto $\hat{\mathbb{C}}$ so that it takes the points $0, 1, \infty$ to $0, \infty, -1$, respectively. Such a projection is unique and respects complex conjugation: $x(\bar{u}) = \overline{x(u)}$. Projecting the 6 fixed points of the hyperelliptic involution J we obtain the normalized branch divisor \mathbf{e} , the element of the moduli space \mathcal{H}_2^1 associated with the element G_+ of the deformation space \mathcal{G} .

It follows from Koebe's classical theorem on cross cuts ("Rückkehrsnitte") that following this prescription we can recover all the points in the moduli space. However, the use of the quasiconformal machinery simplifies the argument.

Theorem 7.4. *The spaces \mathcal{G} and \mathcal{H}_2^1 are homeomorphic.*

Proof. A. *The map $\mathcal{G} \rightarrow \mathcal{H}_2^1$ is injective.* The projection $x(u)$ is an unramified cover of the Riemann sphere punctured at the points in the branch divisor.

The corresponding covering space is $\check{\mathcal{D}}$, the domain of discontinuity, which is punctured at the fixed points of all the elliptic elements of \mathfrak{G} .

Let G_+^0 and $G_+^1 \in \mathcal{G}$ be elements producing the same branch divisor $\mathbf{e} \in \mathcal{H}_2^1$. We shall mark by superscripts 0 and 1 the corresponding groups, projections, etc. The subgroup of $\pi_1(\mathbb{CP}^1 \setminus \mathbf{e}, \infty)$ induced by the covering $x^0(u)$ is the kernel of the representation χ_Λ in Sect. 1 defined by the cut $\Lambda_+ := x^0(C_+^0)$ in the upper half-plane. The subgroup induced by the other covering $x^1(u)$ is defined by the cut $x^1(C_+^1)$, which is isotopic to the former. We already observed in Sect. 7.1.3 that these groups coincide, therefore one can define a one-to-one map between the covering spaces $\check{f} = (x^1)^{-1}x^0: \check{\mathcal{D}}^0 \rightarrow \check{\mathcal{D}}^1$, normalized by the equality $\check{f}(1) = 1$. This map is equivariant with respect to the deck transformation groups: $\check{f}G_\pm^0 = G_\pm^1\check{f}$, $\check{f}G_0 = G_0\check{f}$. Using the continuity and equivariance we can define the map \check{f} at the punctures of \mathcal{D}^0 . The domain of discontinuity of the Schottky group is in the class O_{AD} (that is, each analytic function with finite Dirichlet integral in this domain is constant) and a univalent function in the domain of discontinuity is linear fractional [79]. The points 0 and ∞ are fixed by \check{f} alongside 1: either projection $x(u) = x^0(u)$ and $x^1(u)$ takes the paths $[0, 1]$ and $[1, \infty]$ to the intervals $[0, \infty]$ and $[\infty, -1]$, respectively. Hence \check{f} is the identity map. By the equivariance condition $G_+^0 = G_+^1$.

B. *The map $\mathcal{G} \rightarrow \mathcal{H}_2^1$ is onto.* Consider an arbitrary element G_+ of the deformation space mapped to a divisor \mathbf{e} in the moduli space. Let f be a plane diffeomorphism commuting with complex conjugation and taking \mathbf{e} to a given divisor \mathbf{e}' . We shall also additionally assume that f is conformal in a neighbourhood of the points in \mathbf{e} . We can pull back the Beltrami differential $\mu(x)\overline{dx}/dx := (f_{\bar{x}}dx)/(f_x dx)$ to the domain of discontinuity \mathcal{D} of \mathfrak{G} by means of the ramified covering $x(u)$. The new Beltrami differential $\tilde{\mu}(u)du/du$, $\tilde{\mu}(u) :=$

$\mu(x(u)) \frac{dx/du}{dx/du}$ is \mathfrak{G} -invariant. The limit set of the group has planar measure zero, therefore the coefficient $\tilde{\mu}(u)$ defines an element of $L_\infty(\mathbb{C})$ that is smooth on the discontinuity set \mathcal{D} of the group. There exists a unique quasiconformal homeomorphism $\tilde{f}(u)$ of the Riemann sphere satisfying Beltrami's equation $\tilde{f}_{\bar{u}} = \tilde{\mu} \tilde{f}_u$ and stabilizing the three points 0, 1, and ∞ . It follows from the \mathfrak{G} -invariance of the Beltrami differential that the homeomorphisms $\tilde{f}(u)$ and $\tilde{f}(Gu)$ differ by a conformal motion of the Riemann sphere:

$$G^f \tilde{f} = \tilde{f} G, \quad G \in \mathfrak{G}, \quad G^f \in \mathrm{PSL}_2(\mathbb{C}).$$

The element G_+^f , which is called a *quasiconformal deformation* of the element G_+ , has order 2 and takes the exterior of the smooth curve $\tilde{f}C_+$ to its interior. The curve $\tilde{f}C_+$ lies in the image of the first quadrant. We claim that *each quadrant is invariant under $\tilde{f}(u)$* , which means that G_+^f is an element of the deformation space \mathcal{G} .

The mirror symmetry of the Beltrami coefficient $\tilde{\mu}(\bar{u}) = \overline{\tilde{\mu}(u)}$ and the normalization set $\{0, 1, \infty\}$ shows that $\tilde{f}(u)$ commutes with complex conjugation. Hence $\tilde{f}\mathbb{R} = \mathbb{R}$. In view of the normalization, the deformation of G_0 is trivial, therefore for points $u \in i\mathbb{R}$ we have the chain of equalities $\tilde{f}(u) = \tilde{f}(-\bar{u}) = -\tilde{f}(\bar{u}) = -\tilde{f}(u)$. We see that the real and imaginary axes are invariant and, moreover, keep their orientations. Therefore all the quadrants are \tilde{f} -invariant.

It remains to show that the so-obtained element G_+^f of the deformation space is taken to the divisor $\mathbf{e}' \in \mathcal{H}_2^1$. Let $x^f(u): \mathcal{D}^f := \tilde{f}\mathcal{D} \rightarrow \hat{\mathbb{C}}$ be a projection normalized as before and corresponding to the element G_+^f . Using the uniqueness of the normalized quasiconformal map with fixed Beltrami coefficient we can show that $x^f \tilde{f} = f x$ (see Lemma 3.7.1). The branch divisor corresponding to G_+^f is formed by the points in $x^f \{\mathrm{fix} G_\pm^f, \mathrm{fix} G_0^f\} = x^f \tilde{f} \{\mathrm{fix} G_\pm, \mathrm{fix} G_0\} = f x \{\mathrm{fix} G_\pm, \mathrm{fix} G_0\} = f \mathbf{e} = \mathbf{e}'$.

□

Remark 7.2. The method of the proof of Theorem 3.5 enables one to prove that the local coordinate system (e_1, e_2) (the points in the normalized divisor \mathbf{e} in the upper half-plane) in the moduli space and the coordinate system (c, r^2) in the deformation space \mathcal{G} are related by a biholomorphism.

7.2.3 Constructive Function Theory

The Schottky groups \mathfrak{S} corresponding to the classical part of the deformation space satisfy the following Schottky criterion. *The fundamental domain \mathbf{R} bounded by the four circles C_+ , C_- , $-C_+$, $-C_-$ can be partitioned into triply connected domains (pants) bounded by circles.* As is known, the linear Poincaré series converge in this

case absolutely and uniformly on compact subsets of the domain of discontinuity of the group [132]. Now we can effectively construct various analytic objects invariant under the action of \mathfrak{S} .

Formulae (6.6) and (6.4) for abelian differentials of the second and third kinds remain the same. Both holomorphic forms on the curve $M = \mathcal{D}/\mathfrak{S}$ of genus 2 also have a familiar form:

$$\begin{aligned}\zeta_{\pm} &:= \eta_{S_{\pm}yy} = \sum_{S \in \mathfrak{S}|\langle S_{\pm} \rangle} \{(u - S\alpha_{\pm})^{-1} - (u - S\beta_{\pm})^{-1}\} du = \\ &= \sum_{S \in \langle S_{\pm} \rangle |\mathfrak{S}} \{(Su - \alpha_{\pm})^{-1} - (Su - \beta_{\pm})^{-1}\} dS(u),\end{aligned}\quad (7.9)$$

where α_{\pm} is the attracting fixed point and β_{\pm} the repelling fixed point of the linear fractional map S_{\pm} ; the sum is taken over representatives of the cosets by the subgroup $\langle S_{\pm} \rangle \subset \mathfrak{S}$ generated by the element S_{\pm} . The normalization of the differentials under consideration is as before:

$$\int_{C_{\pm}} \eta_{zz'} = 0; \quad \int_{C_{\pm}} \omega_{mz} = 0; \quad \int_{C_{\pm}} \zeta_{\pm} = 2\pi i; \quad \int_{C_{\pm}} \zeta_{\mp} = 0; \quad z, z' \in \mathbb{R}.\quad (7.10)$$

We define in the standard way the Schottky functions (6.14) and also the functions

$$E_{\pm}(u) := \exp \int_{\infty}^u \zeta_{\pm} = \prod_{S \in \mathfrak{S}|\langle S_{\pm} \rangle} \frac{u - S\alpha_{\pm}}{u - S\beta_{\pm}},\quad (7.11)$$

which are transformed in accordance with the well-known formulae

$$(S_{\pm}u, u'; z, z') = (u, u'; z, z') E_{\pm}(z) / E_{\pm}(z'),\quad (7.12)$$

$$E_{\circ}(S_{\bullet}u) = E_{\circ}(u) E_{\circ\bullet}, \quad \circ, \bullet \in \{+, -\}.\quad (7.13)$$

The constants occurring here have the familiar form

$$E_{\circ\bullet} = E_{\bullet\circ} = \prod_{S \in \langle S_{\bullet} \rangle |\mathfrak{S}|\langle S_{\circ} \rangle} \frac{S\alpha_{\circ} - \alpha_{\bullet}}{S\alpha_{\circ} - \beta_{\bullet}} : \frac{S\beta_{\circ} - \alpha_{\bullet}}{S\beta_{\circ} - \beta_{\bullet}},\quad (7.14)$$

where the product is taken over two-sided cosets of the group \mathfrak{S} and, when the subscripts \circ and \bullet coincide, the coefficient $0/\infty$ corresponding to $S = 1$ must be replaced by the dilatation coefficient $\lambda_{\circ} := S'_{\circ}(\alpha_{\circ})$.

One can reduce the resources required for the calculation of Poincaré series by making use of the two involutions J and \bar{J} on the group \mathfrak{S} . They are induced by the symmetries of M and commute: $JS(u) := -S(-u)$; $\bar{J}S(u) := \overline{S(\bar{u})}$, $S \in \mathfrak{S}$. The involution J is well defined on the cosets $\mathfrak{S}|\langle S_{+} \rangle$ and $\mathfrak{S}|\langle S_{-} \rangle$ of the group \mathfrak{S} ,

while \bar{J} takes the former cosets to the latter and conversely. We can group terms of Poincaré series mutually corresponding under either of the involutions. For instance, for $u \in \mathbb{R}$ we have

$$\eta_{-11}(u) = \frac{-2du}{u^2 - 1} + \sum_{1 \neq S \in \mathfrak{S}/\sim} 2 \operatorname{Re} \left[\frac{1}{u - S(-1)} - \frac{1}{u - S(1)} + \frac{1}{u + S(1)} - \frac{1}{u + S(-1)} \right] du,$$

where the elements $S \neq 1$ of \mathfrak{S} are divided into classes $S \sim JS \sim \bar{J}S \sim \bar{J}JS$. For real u we also have

$$\zeta_+(u) + \zeta_-(u) = 2 \sum_{S \in \mathfrak{S} \setminus \{S_+\}} \operatorname{Re} [(u - S(\alpha_+))^{-1} - (u - S(\beta_+))^{-1}] du.$$

In particular, it follows from these equalities that the meromorphic differential η_{-11} and the holomorphic differential $\zeta_+ + \zeta_-$ are real. Besides the reduction of computations, with the use of such transformations one can often stay within real arithmetic.

A non-trivial meromorphic function on the orbit variety of the group \mathfrak{S} can be expressed in terms of Schottky functions using an obvious analogue of Lemma 6.4.

Example 7.1. We calculate the projection $x(u)$ of the domain of discontinuity of the Kleinian group \mathfrak{G} onto the Riemann sphere which is normalized, as before, by the condition $(0, 1, \infty) \rightarrow (0, \infty, -1)$. The function $x(u)$ has a double zero at $u = 0$ and simple poles at $u = \pm 1$; in addition, the increment of the argument of $x(u)$ along the boundary circles C_{\pm} is 0. Hence $dx(u)/x(u) = \eta_{01}(u) + \eta_{0-1}(u) = \eta_{01}(u) + \eta_{01}(-u)$ and the projection has the following representation

$$x(u) = -(u, \infty; 0, 1)(-u, \infty; 0, 1). \quad (7.15)$$

Example 7.2. Assuming that Abel's equations are fulfilled we calculate the polynomial P_n at the corresponding point in the deformation space by formula (7.4). The distinguished differential η_M on the curve $M := \mathscr{D}/\mathfrak{S}$ is real, and therefore both integrals over the circles C_{\pm} are equal to $2\pi i/n$ by Abel's second equation (7.3). This differential has simple poles at the points ± 1 with residues ∓ 1 , and therefore it has the following form:

$$\eta^* = \eta_{-11} + \frac{1}{n}(\zeta_+ + \zeta_-). \quad (7.16)$$

The Akhiezer function on M has the following form as a function of the uniformizing variable u :

$$\tilde{P}_n(x, w) := \tilde{T}(u) = \exp\left(n \int_0^u \eta^*\right) = (u, 0; -1, 1)^n \frac{E_+(u)}{E_+(0)} \frac{E_-(u)}{E_-(0)}. \quad (7.17)$$

Finally, the 2-extremal polynomial $P_n(x)$ can be obtained from (7.17) by means of the Zhukovskii map.

7.3 Equations on the Deformation Space

Formulae (6.3) and (7.15), (7.17) in the previous section give us an effective parametric representation for the reduced optimal stability polynomial, provided that Abel's equations and the constraints are fulfilled at some point in the classical part of \mathcal{G} . We proceed to the derivation of these equations on the deformation space.

7.3.1 Abel's Equations

Lemma 7.1. *In the classical part of the deformation space \mathcal{G} the two real Abel (7.2) and (7.3) are equivalent to the single complex condition*

$$E_+^{2n}(1) = E_{++}E_{+-} \quad (7.18)$$

REMARKS. 1. Condition (7.18) is equivalent to Abel's equation on the whole of \mathcal{G} , provided that we define the quantities involved in this condition without the use of Poincaré series (which may diverge).

2. Condition (7.18) is equivalent to the automorphy of the function (7.17).

Proof. A. If Abel's second equation (7.3) holds, then in the Shottky model the distinguished differential η_M has the form (7.16). Equation (7.2) is equivalent to the condition $\exp\left(n \int_{C_1} \eta_M\right) = 1$. Using in succession Riemann's relation, the transformation rules for Schottky functions (7.13), and the oddness of the holomorphic differentials $\zeta_+(-u) = -\zeta_+(u)$ we obtain the sequence of equalities

$$\begin{aligned} 1 &= \exp\left(n \int_u^{S+u} \eta^*\right) = \exp\left(n \int_1^{-1} \eta_{S+uu} + \int_u^{S+u} (\zeta_+ + \zeta_-)\right) = \\ &= \left(\frac{E_+(-1)}{E_+(1)}\right)^n E_{++}E_{+-} = \frac{E_{++}E_{+-}}{(E_+(1))^{2n}}. \end{aligned}$$

B. Going backwards along the above chain of equalities, from condition (7.18) we obtain $\int_{C_1} \eta^* \in 2\pi i \mathbb{Z}/n$. The normalization (7.10) of the abelian differential yields $\int_{C_+} \eta^* = 2\pi i/n$. It remains to demonstrate that η^* is the associated

differential on the curve $M = \mathcal{D}/\mathfrak{S}$ with punctures in the orbits of $u = \pm 1$. The differential η^* is real, and so the integrals over the reflected cycles $\bar{J}C_1$ and $\bar{J}C_+$ on M are also purely imaginary. Considered on the orbit space of the group the differential η^* has simple poles at the distinguished points ± 1 with residues ∓ 1 and purely imaginary periods, therefore $\eta^* = \eta_M$. \square

7.3.2 Constraints

If Abel's equations are fulfilled, then the function (7.4) is a polynomial, which in the Schottky model can be defined parametrically by formulae (7.15), (7.17), (6.3). Now we find the first three derivatives of $P_n(x)$ at the origin; to this end we consider the jets of the functions $T(u) := P_n(x)$ and $x(u)$:

$$\begin{aligned} T(u) &:= \cosh\left(\int_0^u n\eta^*\right) =: 1 + T_2u^2 + T_4u^4 + T_6u^6 + \dots, \\ x(u) &= -\exp\left(-\int_0^u \eta_{10} + \eta_{-10}\right) =: x_2u^2 + x_4u^4 + x_6u^6 + \dots \end{aligned} \quad (7.19)$$

For the derivatives of $P_n(x)$ at the origin we have the formulae

$$\begin{aligned} P'_n(0) &= T_2/x_2; \\ P''_n(0) &= 2(T_4x_2 - T_2x_4)/x_2^3; \\ P'''_n(0) &= 6[2(T_2x_4 - T_4x_2)x_4 + (T_6x_2 - T_2x_6)x_2]/x_2^5. \end{aligned} \quad (7.20)$$

After substituting the expressions (7.20) the constraints (7.6) depend only on the projective jet $x_2 : x_4 : x_6$ of $x(u)$. This is as expected: the constraints were obtained by eliminating the scaling factor L , so they survive dilations of the independent variable x .

7.3.3 The Jet of $T(u)$

We calculate the coefficients y_l^* of the Taylor expansion $\eta^*/du = y_0^* + y_2^*u^2 + y_4^*u^4 + \dots$ with the use of the convergent series

$$\begin{aligned} y_l^* &= \frac{1}{l!} D_u^l \left[\frac{\eta^*}{du}(u) \right]_{u=0} = \sum_{S \in \mathfrak{S}} (S(1))^{-l-1} - (S(-1))^{-l-1} + \\ &\quad + \frac{2}{n} \sum_{S \in \mathfrak{S} \setminus \{S_+\}} \operatorname{Re}[(S(\beta_+))^{-l-1} - (S(\alpha_+))^{-l-1}], \quad l = 0, 2, 4, \dots \end{aligned}$$

The first three non-trivial coefficients in the expansion of $T(u) := \cosh\left(n \int_0^u \eta^*\right)$ in powers of u are as follows:

$$\begin{aligned} T_2 &= \frac{(ny_0^*)^2}{2}; \\ T_4 &= \frac{(ny_0^*)(ny_2^*)}{3} + \frac{(ny_0^*)^4}{24}; \\ T_6 &= \frac{(ny_0^*)(ny_4^*)}{5} + \frac{(ny_2^*)^2}{18} + \frac{(ny_0^*)^3(ny_2^*)}{18} + \frac{(ny_0^*)^6}{720}. \end{aligned} \quad (7.21)$$

7.3.4 The Projective Jet of $x(u)$

Comparing the coefficients of different powers of u in the equality $dx(u) = (\eta_{01}(u) + \eta_{01}(-u))x(u) =: 2(1/u + y_1u + y_3u^3 + \dots)x du$ we obtain

$$x_2 : x_4 : x_6 = 2 : 2y_1 : (y_1^2 + y_3).$$

The coefficient y_l of the Taylor expansion of $\eta_{01}(u)/du$ in a neighbourhood of the origin can be calculated by the formulae

$$y_l = \frac{1}{l!} D_u^l \left[\frac{\eta_{01}}{du}(u) - 1/u \right]_{u=0} = 1 + \sum_{1 \neq S \in \mathfrak{S}} (S(1))^{-l-1} - (S(0))^{-l-1}, \quad l = 1, 3, \dots$$

7.3.5 Variational Theory

For an effective solution of our system of four equations (7.18), (7.6) on the deformation space one must find the derivatives of the quantities involved in these equations with respect to the moduli. Abel's equations in the form (7.18) contain a period of the integral of the differential η^* . The constraints (7.6) in the Schottky model are certain relations between abelian integrals with fixed limits of integration. Indeed, using Riemann's relations one can transform the coefficients of the jets of the differentials η^* and η_{01} to the required form:

$$\begin{aligned} l!y_l^* &= D_u^l \left[\frac{\eta^*}{du}(u) \right]_{u=0} = D_u^{l+1} \int^u \eta^*(u)|_{u=0} = \\ &= \int_1^{-1} \omega_{(l+1)0} + \frac{1}{n} \left[\int_w^{S+w} \omega_{(l+1)0} + \int_w^{S-w} \omega_{(l+1)0} \right]. \end{aligned}$$

The position of the point w is not important here. The differential η_{01} has a singularity at $u = 0$, and therefore the coefficients of its jet are regularizations of divergent integrals:

$$l! y_l = D_u^l \left(\frac{\eta_{01}}{du}(u) - 1/u \right) \Big|_{u=0} = \lim_{u \rightarrow 0} \left[\int_1^0 \omega_{(l+1)u} + \frac{l!}{(-u)^{l+1}} \right].$$

Using an obvious modification of the variational formulae in Sect. 6.2.2, we obtain the derivatives of all the quantities participating in the equations on the deformation space \mathcal{G} :

$$\begin{aligned} \delta \int_{C_1} \eta^* &\approx -(2\pi i)^{-1} \sum_{\bullet=+,-} \int_{C_\bullet} \eta^*(u) \zeta_+(u) \operatorname{tr}[\mathbf{M}(u) \cdot \delta \hat{S}_\bullet \cdot \hat{S}_\bullet^{-1}] / du, \\ \delta y_l &\approx (2\pi i l!)^{-1} \sum_{\bullet=+,-} \int_{C_\bullet} \omega_{(l+1)0}(u) \eta_{10}(u) \operatorname{tr}[\mathbf{M}(u) \cdot \delta \hat{S}_\bullet \cdot \hat{S}_\bullet^{-1}] / du, \quad l = 1, 3, \\ \delta y_l^* &\approx -(2\pi i l!)^{-1} \sum_{\bullet=+,-} \int_{C_\bullet} \omega_{(l+1)0}(u) \eta^*(u) \operatorname{tr}[\mathbf{M}(u) \cdot \delta \hat{S}_\bullet \cdot \hat{S}_\bullet^{-1}] / du, \quad l = 0, 2, 4. \end{aligned}$$

7.3.6 Hejhal's Formulae

As we know, an efficient use of variational formulae is based on expanding the quadratic differentials such as $\eta^* \zeta_+$ and $\omega_{(l+1)0} \eta^*$ with respect to a basis consisting of Poincaré quadratic theta series, for which the Hejhal map

$$\mathcal{E}(u)(du)^2 \xrightarrow{[\pm]} \int_{C_\pm} \mathcal{E}(u) \mathbf{M}(u) du \in \mathfrak{sl}_2(\mathbb{C}) \quad (7.22)$$

is explicitly known. Consider the following real even quadratic differentials regular at infinity:

$$\begin{aligned} R_\pm(u)(du)^2 &:= [u^2 - \alpha_\pm^2]^{-2} (du)^2; \\ R_0(u)(du)^2 &:= [(u^2 - \alpha_+^2)(u^2 - \alpha_-^2)]^{-1} (du)^2; \\ R^{-11}(u)(du)^2 &:= [(u^2 - 1)(u^2 - \alpha_+^2)(u^2 - \alpha_-^2)]^{-1} (du)^2; \\ R^{2;0}(u)(du)^2 &:= [u^2(u^2 - \alpha_+^2)(u^2 - \alpha_-^2)]^{-1} (du)^2; \\ R^{m;0}(u)(du)^2 &:= u^{-m} (du)^2, \quad m = 4, 6. \end{aligned} \quad (7.23)$$

Averaging them over \mathfrak{S} we obtain three holomorphic quadratic differentials on the orbit manifold $M := \mathcal{D}/\mathfrak{S}$ and also even meromorphic differentials with simple poles at ± 1 or poles of orders 2, 4, and 6 at $u = 0$:

$$\Theta_2[R_{\pm}](u)(du)^2 := \sum_{S \in \langle S_{\pm} \rangle | \mathfrak{S}} R_{\pm}(Su)(dS(u))^2, \quad (7.24)$$

$$\Theta_2[R](u)(du)^2 := \sum_{S \in \mathfrak{S}} R(Su)(dS(u))^2, \quad R = R_0, R^{-11}, R^{2;0}, R^{4;0}, R^{6;0}. \quad (7.25)$$

The absolute convergence of these series on compact subsets of the domain of discontinuity of the group is a consequence of the convergence of (6.4) and (7.9). For instance, the relative quadratic Poincaré series (7.24) are formed by the squares of terms of the linear series (7.9). The Hejhal maps for these series can be calculated by termwise integration.

Theorem 7.5 (Hejhal's formulae). *The values of the map (7.22) at the quadratic theta series (7.24) and (7.25) are presented in Table 7.1. Here $\lambda_{\pm} := S'_{\pm}(\alpha_{\pm})$ is the dilation coefficient of the generator S_{\pm} of the Schottky group.*

Proof. The proof of Hejhal's formulae repeats word for word the calculations in the proof of a similar result in the previous chapter. \square

One consequence of Hejhal's formulae is as follows.

Lemma 7.2. *The quadratic Poincaré series $\Theta_2[R_+](du)^2$, $\Theta_2[R_-](du)^2$, and $\Theta_2[R_0](du)^2$ form a basis in the space of holomorphic quadratic differential on the curve M in the Schottky model.*

Proof. The space of holomorphic quadratic differentials of a curve of genus g has dimension $3g - 3$. We claim that on a curve of genus $g = 2$ the three differentials $\Theta_2[R_+](du)^2$, $\Theta_2[R_-](du)^2$, and $\Theta_2[R_0](du)^2$ are linearly independent. Consider three functionals over quadratic differentials: the quantities at the positions (1, 1) and (1, 2) for the Hejhal map $[+]$ in (7.22) and the quantity at the position (1, 2) for the map $[-]$. The values of these functionals at the differentials $\Omega_0(du)^2$, $\Omega_+(du)^2$, and $\Omega_-(du)^2$ form an upper triangular matrix with non-singular diagonal: $-i\pi/(\alpha_+^2 - \alpha_-^2)$, $i\pi/(2\alpha_+)$, $i\pi/(2\alpha_-)$. Hence these differentials are linearly independent and form a basis in the space of quadratic differentials on the curve. \square

Table 7.1 Hejhal map for several quadratic Poincaré series

$R(u)$	$\int_{C_{\pm}} \Theta_2[R](u)M(u)du$
R_0	$\frac{i\pi}{\alpha_{\pm}(\alpha_{\pm}^2 - \alpha_{\mp}^2)(1 - \lambda_{\pm})} (M(\alpha_{\pm}) + \lambda_{\pm}M(-\alpha_{\pm}))$
R_{\pm}	$\frac{i\pi}{2\alpha_{\pm}^2} \begin{vmatrix} 0 & \alpha_{\pm} \\ \alpha_{\pm}^{-1} & 0 \end{vmatrix}$
R^{-11}	$\frac{i\pi}{\alpha_{\pm}(\alpha_{\pm}^2 - 1)(\alpha_{\pm}^2 - \alpha_{\mp}^2)(1 - \lambda_{\pm})} (M(\alpha_{\pm}) + \lambda_{\pm}M(-\alpha_{\pm}))$
$R^{2;0}$	$\frac{i\pi}{\alpha_{\pm}^3(\alpha_{\pm}^2 - \alpha_{\mp}^2)(1 - \lambda_{\pm})} (M(\alpha_{\pm}) + f\lambda_{\pm}M(-\alpha_{\pm}))$
$R_{\mp}; R^{4;0}; R^{6;0}$	0

How can we calculate the Hejhal map at a meromorphic quadratic differential such as $\eta^* \zeta_+$, $\omega_{(l+1)0} \eta^*$ or $\omega_{(l+1)0}(\eta_{10} + \eta_{-10})$? We subtract from it a quadratic Poincaré series with suitable singularities and expand the remaining holomorphic quadratic differential with respect to the basis in Lemma 7.2, for which the Hejhal map is described by explicit formulae.

7.4 Numerical Experiments

The system of four equations (7.18), (7.6) with substituted quantities (7.20) has at most one solution in the classical part of the deformation space \mathcal{G} for fixed degree n . The author developed software for finding this solution by Newton's method. The first approximation for a low degree n was found by the trial-and-error method. The solution with numerical accuracy of our system of four equations for fixed n can be used as an initial approximation in Newton's method for systems of degrees $n+1$, ..., $n+5$ and even $n+50$ if n is large. We solved the equations to within 10^{-13} for degrees up to $n=1001$; here all the solutions (c, r^2) occur in the classical part of the deformation space. We could see no tendency towards deceleration of the convergence of the Poincaré series with growth of n : $\text{Re } c, \text{Im } c \gg |r|$ (see Table 7.2).

We also calculated the length L of the stability interval. For $p=1$, when the solution can be expressed in terms of the Chebyshev polynomial, $L=2n^2$. We see from Table 7.2 that for $p=3$ the quantity L/n^2 stabilizes—this was also pointed out by other authors. We plot the graph of the reduced optimal stability polynomial of degree $n=31$ for $p=3$ in Fig. 7.6.

Table 7.2 Solutions of four equations (7.18), (7.6) on the deformation space. Length of stability interval.

n	c	r^2	L/n^2
27	$0.058294188 + i0.072379887$	$3.92447195D - 005 + i1.12862487D - 005$	0.498393
107	$0.014619780 + i0.018280095$	$2.48122506D - 006 + i7.45913680D - 007$	0.500954
157	$0.009961570 + i0.012458796$	$1.15218232D - 006 + i3.46919646D - 007$	0.501047
199	$0.007858553 + i0.009829401$	$7.17095951D - 007 + i2.16027548D - 007$	0.501078
251	$0.006230206 + i0.007793080$	$4.50726679D - 007 + i1.35825821D - 007$	0.501097
301	$0.005195168 + i0.006498569$	$3.13412277D - 007 + i9.44617098D - 008$	0.501106
401	$0.003899525 + i0.004877994$	$1.76582873D - 007 + i5.32302909D - 008$	0.501116
501	$0.003121143 + i0.003904348$	$1.13124444D - 007 + i3.41035348D - 008$	0.501120
576	$0.002714732 + i0.003395971$	$8.55824263D - 008 + i2.58013073D - 008$	0.501122
651	$0.002401967 + i0.003004732$	$6.69986418D - 008 + i2.01991310D - 008$	0.501124
751	$0.002082125 + i0.002604635$	$5.03438797D - 008 + i1.51782584D - 008$	0.501125
851	$0.001837454 + i0.002298568$	$3.92072592D - 008 + i1.18208166D - 008$	0.501126
951	$0.001644239 + i0.002056868$	$3.13952470D - 008 + i9.46561689D - 009$	0.501126
1001	$0.001562108 + i0.001954128$	$2.83371730D - 008 + i8.54364345D - 009$	0.501126

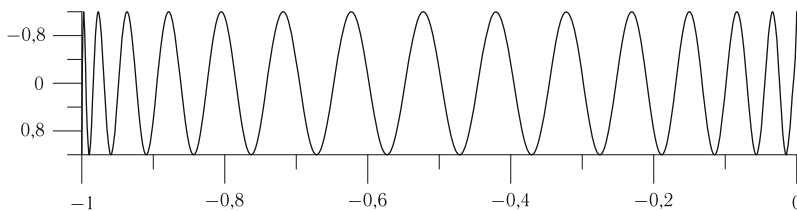


Fig. 7.6 The graph of the reduced optimal stability polynomial for $p = 3$, $n = 31$

7.5 Problems and Exercises

1. What points $q \neq q'$ in the first quadrant of the plane can be fixed points of a classical element of the deformation space \mathcal{G} ?

Answer. The following two inequalities are necessary and sufficient: $t^+(q) > t^-(q')$, $t^+(q') > t^-(q)$, where $t^\pm(x + iy) := x + y \pm \sqrt{2xy}$.

2. Give an example of a Schottky group whose fundamental domain cannot be bounded by circles.
3. (Ford, [64]) Prove Klein's combination theorem:

Theorem 7.6. Let $\mathfrak{G}_1, \dots, \mathfrak{G}_m$ be Kleinian groups with fundamental domains R_1, \dots, R_m such that for $s \neq j$ the exterior of R_s lies in R_j . Then $\mathfrak{G}_1, \dots, \mathfrak{G}_m$ generate a Kleinian group \mathfrak{G} which is the free product of its factors. The fundamental domain of \mathfrak{G} is the intersection $\bigcap_{s=1}^m R_s$.

4. (Hurwitz and Courant, [79], Tsuji, [149]) Show that the domain of discontinuity \mathcal{D} of an arbitrary Schottky group \mathfrak{G} lies in the class 0_{AD} , that is, any analytic function $f(u)$ with finite Dirichlet integral in this domain is constant.

Solution. Let R be a standard fundamental domain of the Schottky group, that is, the exterior of $2g$ contours in the plane. Let \mathcal{D}_n be the closure of the union of translated fundamental domains $\bigcup_{|S| \leq n} SR$. The required result follows from the estimates

$$\left| \int_{\mathcal{D}} df \wedge d\bar{f} \right| \leftarrow \left| \int_{\mathcal{D}_n} df \wedge d\bar{f} \right| = \left| \int_{\partial \mathcal{D}_n} f \wedge d\bar{f} \right| \leq \text{const} \left| \int_{\mathcal{D}_{n+1} \setminus \mathcal{D}_{n-1}} df \wedge d\bar{f} \right| \rightarrow 0.$$

Here we have used an inequality which is a consequence of the following lemma.

Lemma 7.3. Let B be a domain containing a contour C . Then the following estimate holds for each holomorphic function $f(u)$ in B :

$$\left| \int_C f \wedge d\bar{f} \right| \leq \text{const}(B, C) \left| \int_B df \wedge d\bar{f} \right|.$$

The constant in this inequality is invariant under conformal maps $S(u)$ of the domain: $\text{const}(S(B), S(C)) = \text{const}(B, C)$.

Proof. We have

$$\left| \int_C f(u) \wedge d\bar{f}(u) \right| = \left| \int_C (f(u) - f(u_0)) \wedge d\bar{f}(u) \right| \leq \max_{u \in C} |f'(u)|^2 |C|^2 / 2,$$

where $u_0 \in C$ and $|C|$ is the length of C . For a holomorphic function $F(u)$ in a disc of radius r ,

$$\int_{|u| < r} F'(u) du \wedge d\bar{u} = \int_{|u|=r} F(u) d\bar{u} = - \int_{|u|=r} F(u) \frac{r^2 du}{u^2} = -2\pi i r^2 F'(0).$$

Setting $F'(u) = (f')^2(u)$ we obtain $\max_{u \in C} |f'(u)|^2 \leq (2\pi r^2)^{-1} \left| \int_B df \wedge d\bar{f} \right|$, where r is the distance between the contour C and the boundary of B . □

5. (Hurwitz and Courant, [79]) Show that a function univalent in the domain of discontinuity of a Schottky group is linear fractional.
6. Show that the limit set of an arbitrary (finitely generated) Schottky group has planar measure zero.
7. Give estimates for the remainder term of a linear Poincaré series for a classical Schottky group corresponding to a point in the deformation space \mathcal{G} .
8. Show that the projective jet $x_2 : x_4 : x_6 : \dots$ of the function $x(u)$ in Sect. 7.3.4 is equal to $k_2 : k_4 : k_6 : \dots$, where

$$k_l := \frac{1}{l!} \left[\frac{\omega_{l0}}{du} \right]_{u=1} = \sum_{S \in \mathfrak{S}} (S(1))^{-l-1} S'(1), \quad l = 2, 4, 6, \dots$$

Hint. Show that the differential $dx(u)$ is proportional to $\omega_{11}(u) + \omega_{11}(-u)$.

9. Prove Hejhal's formula in Theorem 7.5.

Conclusion

Of course, this is not the last word in the investigation and application of the Chebyshev approach to optimization problems in polynomial spaces. For instance, there can be further development along the following lines:

1. Describe the stratification of the sphere $\{||P||_E = 1\}$ in the space (2) by smooth faces. To our knowledge, this is an unsolved problem even in the case when E is a single interval.
2. Determine integers g, k, m_0, \dots, m_g corresponding to the solution of an extremum problem from the data of this problem.
3. Investigate the topology of the fibres of the period map $\Pi_-: \tilde{\mathcal{H}}_g^k \rightarrow \mathbb{R}^g$. We conjectured above that each component of a fiber is a cell.
4. Linear Poincaré theta series are poorly convergent in a neighbourhood of (a part of) the boundary of our moduli space. The question of improving the convergence arises. A more general question was put by Klein in 1923: regularize absolutely divergent theta series.
5. Develop global methods for solving equations (for instance, Abel's equations) in moduli spaces of curves. Newton's method works very well in a small neighbourhood of a solution, but its global dynamics is completely unpredictable.
6. Use other uniformizations of curves M for calculations. Fuchsian uniformization cannot be used because then linear Poincaré theta series will be divergent [149]. Another Schottky uniformization, not equivalent to the one presented here (and based on an incomplete dissection) was used in [37]; in this case Abel's equations and the parametric representation for polynomials get another form.
7. Use Riemann theta functions in the computations of the theory. The advantage of this approach is a higher convergence rate of series, particularly for large genera g . But it also has two deficiencies: (1) the Schottky problem of describing the period matrices of (hyperelliptic) Riemann surfaces in the Siegel upper half-

- space [108] must be solved numerically; (2) the image of an algebraic curve in its Jacobian under the Abel–Jacobi map must be localized numerically.
8. Construct a compactification of the moduli space \mathcal{H}_g^k such that the cell decomposition of Chapter 4 becomes a cell complex.
 9. Prove or disprove that the value L/n^2 for optimal stability polynomials converges for each $p = 2, 3, \dots$. Give the value of this limit in terms of Riemann surfaces.

References

1. Abdulle, A.: On roots and error constants of optimal stability polynomials. *BIT* **42**, 177–182 (2000)
2. Abel, N.H.: Sur l'intégration la formule différentielle $\frac{\rho dx}{\sqrt{R}}$, R et ρ étant des fonctions entières. *J. Reine Angew. Math.* **1**, 105–144 (1826).
3. Ahlfors, L.V.: *Lectures on Quasiconformal Mappings*, Van Nostrand: Toronto, Ont. (1966)
4. Ahlfors, L., Bers, L.: *Spaces of Riemann Surfaces and Quasiconformal Mappings*, Moscow, Inostrannaya Literatura (1961). (A Russian translation of several papers: Bers, L.: Quasiconformal mappings and Teichmüller's theorem. In: *Analytic Functions*, pp. 89–119, Princeton Univ. Press, Princeton, N.J. (1960); Ahlfors, L.: The complex analytic structure of the space of closed Riemann surfaces. *Ibid.*, pp. 45–66; Bers, L.: Spaces of Riemann surfaces. In: *Proc. Internat. Congr. Math.* (Edinburgh, 1958), pp. 349–361; Bers, L.: Simultaneous uniformization. *Bull. Amer. Math. Soc.* **66**, 94–97 (1960); Bers, L.: Holomorphic differentials as functions of moduli. *Bull. Amer. Math. Soc.* **67**, 206–210 (1961); Ahlfors, L.: On quasiconformal mappings. *J. Anal. Math.* **3** 1–58; correction, 207–208 (1954))
5. Ahlfors, L.V.: The complex analytic structure of the space of closed Riemann surfaces. In: *Analytic Functions*, pp. 45–66, Princeton Univ. Press, Princeton, N.J. (1960)
6. Akaza, T., Inoue, K.: Limit sets of geometrically finite free kleinian groups. *Tohoku Math. J.* **36** 1–16 (1984)
7. Akaza, T.: Singular sets of some Kleinian groups. *Nagoya Math. J.* **29**, 145–162 (1967)
8. Akaza, T., Inoue, K.: On the limit set of a geometrically finite Kleinian group. *Sci. Rep. Kanazawa Univ.* **27**, 85–115 (1982)
9. Akhiezer, N.I.: Über einige Funktionen die in gegebenen Intervallen am wenigsten von Null abweichen. *Izv. Kazan Fiz.-Mat. Obshch.* textbf3, no. 3 (1928)
10. Akhiezer, N.I.: Über einige functionen welche in zwei gegebenen Intervellen am wenigsten von Null abweichen I–III. *Izv. Akad. Nauk SSSR* **9**, 1163–1202 (1932); **3**, 309–344 (1933); **4**, 499–536 (1933)
11. Akhiezer, N.I.: Orthogonal polynomials on several intervals. *Dokl. Akad. Nauk SSSR.* **134**:1, 9–12 (1960). (in Russian)
12. Akhiezer, N.I.: *Lectures in the Theory of Approximation*. Nauka, Moscow (1965), 2nd edn. English transl. of 1st edn.: Achieser, N.I.: *Theory of Approximation*. Dover Publ., New York (1992)
13. Akhiezer, N.I., Levin B.Ya.: Inequalities for derivatives similar to Bernoulli's inequality. *Dokl. Akad. Nauk SSSR* **117**:5, 735–738 (1957). (in Russian)
14. Antoniou, A.: *Digital Filters: Analysis, Design, and Applications*, McGraw-Hill (1979)
15. Arnold, V.I.: *Arnold's Problems*. Phasis, Moscow (2000). English transl.: Springer-Verlag, Berlin; PHASIS, Moscow (2004)

16. Arbarello, E., Cornalba, M., Griffiths, P.A., Harris, J.: *Geometry of Algebraic Curves I-II*. Springer, New York 1985.
17. Artin, E.: *Theorie der Zöpfe*. Abh. Math. Semin. Univ. Hamburg. **4**, 47-72 (1925)
18. Baker, H.F.: *Abel Theorem and Allied Theory*. Cambridge (1897)
19. Belokolos, E.D., Enolskii, V.Z.: Reduction of abelian unctons and completely integrable equations. *J. Math. Sci.* **106** 3395–3486 (2001); **108** 295–374 (2002)
20. Bers, L. Uniformization, moduli and Kleinian groups. *Bull. London Math. Soc.* **4**, 257-300 (1972)
21. Birman, J.S.: *Braids, Links, and Mapping Class Groups*. Princeton University Press, Princeton, NJ: (1974)
22. Bobenko, A.I., Klein, Ch. (Eds.): *Computational Approach to Riemann Surfaces*. Lecture Notes in Mathematics, Vol. 2013, Springer (2011)
23. Bogatyrev, A.B.: Chebyshev polynomials and navigation in moduli space of hyperelliptic curves. *Russian J. Numer. Anal. Math. Modelling.* **14**:3, 205–220 (1999)
24. Bogatyrev, A.B.: Fibers of periods map are cells? *J. Comput. Appl. Math.* **153**, 647-548 (2003)
25. Bogatyrev, A.B.: Effective computation of optimal stability polynomials. *Calcolo.* **41**:4, 247-156 (2004)
26. Bogatyrev, A.B.: Chebyshev representation for rational functions. *Sb. Math.* **201** 1579 - 1598 (2010)
27. Bogatyrev, A.B.: Computations in moduli spaces. *Comp. Methods and Function Theory* **7**:1 (2007)
28. Burau, W.: *Über Zopfvarianten*. Abh. Math. Semin. Univ. Hamburg. **4**, 47-72 (1925)
29. Burnside, W.: On a class of authomorphic functions. *Proc. London Math. Soc.* **23**, 49-88 (1892)
30. Buser, P., and Seppala, M.: *Computing on Riemann Surfaces*. Topology and Teichmuller spaces (Katinkulta, 1995), 5-30, World Sci. Publ., River Edge, NJ, 1996
31. Bakhvalov, N. S., Zhidkov, N. P., Kobel'kov, G. M.: *Numerical Methods*. Moscow, Nauka (1987). (in Russian)
32. Beardon, A.F.: *The Geometry of Discrete Groups*. Graduate Texts in Mathematics **91**. Springer-Verlag, New York (1995)
33. Bernstein, S.N.: *Extremal Properties of Polynomials*. Moscow, ONTI (1937).
34. Bers, L.: Holomorphic differentials as functions of moduli. *Bull. Amer. Math. Soc.* **67**, 206–210 (1961).
35. Bobenko, A. I. Schottky uniformization and finite-gap integration. *Dokl. Akad. Nauk SSSR* **295**, 268–272 (1987). English transl. in *Sov. Math., Dokl.* **36**:1, 38-42 (1987) [See also Chap. 5 in: Belokolos, E. D., Bobenko, A.I., Enol'skii, V.Z., Its, A.R., Matveev, V.B.: *Algebro-Geometric Approach to Nonlinear Integrable Equations*. Springer, Berlin (1994)]
36. Bogatyrev, A.B.: A geometric method for solving a series of integral Poincaré-Steklov equations. *Mat. Zametki* **63**:3, 343–353 (1998). English transl. in *Math. Notes* **63**, 302-310 (1998)
37. Bogatyrev, A.B.: Effective computation of Chebyshev polynomials for several intervals. *Mat. Sb.* **190**:11, 15–50 (1999). English transl. in *Sb. Math.* **190**, 1571–1605 (1999).
38. Bogatyrev, A.B.: Manifolds of support sets of Chebyshev polynomials. *Mat. Zametki* **67**, 828–836 (2000). English transl. in *Math. Notes* **67**, 699–706 (2000)
39. Bogatyrev, A.B.: Poincare–Steklov integral equations and the Riemann monodromy problem. *Funktsional. Anal. i Prilozhen.* **34**:2, 9–22 (2000). English transl. in *Funct. Anal. Appl.* **34**, 86-97 (2000)
40. Bogatyrev, A.B.: Effective approach to least deviation problems. *Mat. Sb.* **193**:12, 21–41 (2002). English transl. in *Sb. Math.* **193**, 1749–1769 (2002)
41. Bogatyrev, A.B.: Representation of moduli spaces of curves and the computation of extremal polynomials. *Mat. Sb.* **194**:4, 3–28 (2003). English transl. in *Sb. Math.* **194**, 469–494 (2003)
42. Bogatyrev, A.B.: A combinatorial description of a moduli space of curves and of extremal polynomials. *Mat. Sb.* **194**:10, 27–48 (2003). English transl. in *Sb. Math.* **194**, 1451–1473 (2003).

43. Bogatyrev, A.B.: Effective solution of the problem of the optimal stability polynomial. *Mat. Sb.* **196**:7, 27–50 (2005). English transl. in *Sb. Math.* **196**, 959–981 (2005)
44. Cauer, W.: Ein Interpolationsproblem mit Functionen mit positivem Realteil. *Math. Z.* **38** (1934)
45. Cauer, W.: *Theorie der Linearen Wechselstromschaltungen*. Akademie Verlag, Berlin (1954)
46. Chebotarev, N.G.: *The Theory of Algebraic Functions*. OGIZ, Moscow-Leningrad (1948). (in Russian)
47. Chebyshev, P.L.: Théorie des mécanismes connus sous le nom de parallélogrammes. *Mém. Acad. Sci. Pétersb.* **7**, 539–568 (1854).
48. Chekhov, L.O.: Matrix models: Geometry of moduli spaces and exact solutions. *Teoret. Mat. Fiz.* **127**, 179–252 (2001). English transl. in *Theor. Math. Phys.* **127**, 557–618 (2001)
49. Chen, X., Parks, T.W.: Analytic design of optimal FIR narrow-band filters using Zolotarev polynomials. *IEEE Trans. on Circuits and Systems.* **33**, 1065–1071 (1986)
50. Crowdy, D.G., Marshall, J.S.: Conformal mappings between canonical multiply connected domains. *Computational Methods and Function Theory*, **6** 59–76 (2006)
51. Crowdy, D.G.: Schwarz–Christoffel mappings to unbounded multiply connected polygonal regions. *Math. Proc. Cambridge Philos. Soc.*, **142** 319–339 (2007)
52. Crowdy, D.G., Marshall, J.S.: Green’s functions for Laplace’s equation in multiply connected domains. *IMA. J. Appl. Math.*, **72** 278–301 (2007)
53. Deconinck, B., van Hoeij, M.: Computing Riemann matrices of algebraic curves. *Physica D* **152** 28–46 (2001)
54. Deconinck, B., Heil, M., Bobenko, A., van Hoeij, M., Schmies, M.: Computing Riemann theta functions. *Math. Comp.* **73** 1417–1442 (2004)
55. Deconinck, B., Patterson, M.: Computing the Abel map. *Physica D* **237** 3214–3232 (2008)
56. Dubrovin, B.A.: Theta functions and non-linear equations. *Uspekhi Mat. Nauk* **36**:2, 11–80 (1981). English transl. in *Russian Math. Surveys* **36**:2, 11–92 (1981)
57. Earl, C.J.: On variation of projective structures. In: *Riemann Surfaces and Related Topics*, pp. 87–99. Princeton University Press, Princeton, NJ (1980)
58. *Encyclopaedia of Mathematics*. Sovetskaya Entsiklopediya, Moscow (1984). English transl. Vols. 1–5, Kluwer, Dordrecht (1988–1994)
59. Enol’skii, V.Z., Kostov, N.A.: On the geometry of elliptic solitons. *Acta Appl. Math.* **36**, 57–86 (1994)
60. Farkas, H., Kra, I.: *Riemann Surfaces*. Springer, New York (1992)
61. Fay, J.: *Theta Functions on Riemann Surfaces*. Lecture Notes in Mathematics, Vol. 352. Springer, Berlin-New York (1973)
62. Fock, V.V., Dual Teichmüller spaces. *ArXiv: dg-ga/9702018*, 1998.
63. Fomenko, A.T., Fuchs, D.B.: *A Course of Homotopic Topology*. Nauka, Moscow (1989). (in Russian)
64. Ford, L.R.: *Automorphic Functions*. McGraw-Hill, New York (1929)
65. Franklin, J.N.: Numerical stability in digital and analog computation for diffusion problems. *J. Math. Phys.* **37**, 305–315 (1959)
66. Gardiner, F.P.: *Teichmüller Theory and Quadratic Differentials*. Wiley, New York (1987)
67. Gesztesy, F., Weikard, R.: Picard potentials and Hill’s equation on a torus. *Acta Math.* **176**, 73–107 (1996)
68. Gesztesy, F., Weikard, R.: Elliptic algebro-geometric solutions of the KdV and AKNS hierarchies—an analytic approach. *Bull. Amer. Math. Soc.* **35** 271–317 (1998)
69. Griffiths, Ph., Harris, J.: *Principles of Algebraic Geometry*. Wiley, New York (1994)
70. Gunning, R.C.: *Lectures on Riemann Surfaces*. Princeton University Press, Princeton, NJ (1966)
71. Hairer, E., Wanner, G. *Solving Ordinary Differential Equations. II. Stiff and Differential-Algebraic Problems*. Springer-Verlag, Berlin (1996)
72. Hejhal, D.A.: Sur les paramètres accessoires pour l’uniformisation de Schottky. *C. R. Acad. Sci. Paris Sér. A.* **279**, 713–716 (1974)
73. Hejhal, D.A.: On Schottky and Teichmüller spaces. *Adv. Math.* **15** 133–156 (1975)

74. Hejhal, D.A.: The variational theory of linearly polymorphic functions. *J. Anal. Math.* **30**, 215–264 (1976)
75. van Hoeij, M.: An algorithm for computing the Weierstrass normal form. *ISSAC '95 Proceedings*, 90–95 (1995).
76. van Hoeij, M.: Computing parametrizations of rational algebraic curves. *ISSAC '94 Proceedings*, 187–190 (1994)
77. van der Houwen, P.J., Kok, J.: Numerical solution of a maximal problem. Report 124/71 TW, Mathematical Centre, Amsterdam (1971)
78. Hurwitz, A.: Über Riemannsche Flächen mit gegebenen Verzweigungspunkten. *Math. Ann.* **39**, 1–61 (1891)
79. Hurwitz, A.: Vorlesungen über Allgemeine Funktionentheorie und Elliptische Functione. Herausgegeben und ergänzt durch einen Abschnitt über geometrische Funktionentheorie von R. Courant. Springer-Verlag, Berlin-New York (1964)
80. Hubbard, J.H.: On monodromy of projective structures. In: *Riemann Surfaces and Related Topics*, pp. 257–275. Princeton University Press, Princeton, NJ (1980)
81. Hubbard, J., Masur, H.: Quadratic differentials and foliations. *Acta Math.* **142**:1 (1979), 221–274.
82. Igusa, J.: Problems on Abelian functions at the time of Poincare and some at present. *Bull. Amer. Math. Soc.*, **6** 161–174 (1982)
83. Klein, F.: Vorlesungen über die Entwicklung der Mathematik im 19. Jahrhundert. I. J.Springer, Berlin (1926)
84. Kontsevich, M.L.: Intersection theory on the moduli space of curves. *Funktsional. Anal. i Prilozhen.* **25**:2, 50–57 (1991). English transl. in *Funct. Anal. Appl.* **25**:2, 123–129 (1991)
85. Kra, I.: Automorphic Forms and Kleinian Groups. *Mathematics Lecture Note Series.*, W. A. Benjamin, Inc., Reading, Mass. (1972)
86. Kreĭn, M.G, Levin, B.Ya., Nudel'man, A.A.: On special representations of polynomials that are positive on a system of closed intervals, and some applications. In: *Functional Analysis, Optimization, and Mathematical Economics*, pp. 56–114, Univ. Press, New York, Oxford (1990)
87. Kreĭnes, E.M.: Rational Functions with Few Critical Values. Ph.D. Thesis, Moscow State University (2001). (in Russian).
88. Krichever, I.M.: Integration of nonlinear equations by the methods of algebraic geometry. *Funktsional. Anal. i Prilozhen.* **11**:2, 15–32 (1977). English transl. in *Funct. Anal. Appl.* **11**:2, 12–26 (1977)
89. Krushkal', S.L., Apanasov, B.N., Gusevskii, N.A.: Kleinian Groups and Uniformization in Examples and Problems. Nauka, Novosibirsk (1981). English transl. American Mathematical Society, Providence, RI (1986).
90. Lando, S.K., Ramified coverings of the two-dimensional sphere and intersection theory in spaces of meromorphic functions on algebraic curves. *Uspekhi. Mat. Nauk.* **57**:3, 29–98 (2002). English transl. in *Russian Math. Surveys* **57**, 463–533 (2002)
91. Lando, S.K., Zvonkin, A.K.: Graphs on Surfaces and their Applications. *Encyclopaedia of Mathematical Sciences*, Vol. 141. Berlin: Springer, New York-Berlin (2004)
92. Lavrent'ev, M.A., Shabat, B.V.: Methods of the Theory of Functions of a Complex Variable. Nauka, Moscow (1965). (in Russian)
93. Lebedev, V.I.: How rigid systems of differential equations can be solved by explicit methods. In: Marchuk, G.I. (Ed.) *Vychislitel'nye Protessy i Sistemy*, Vol 8, pp. 237–292. Nauka, Moscow (1991). (in Russian)
94. Lebedev, V.I., Medovikov, A.A.: An explicit method of the second order of accuracy for solving stiff systems of ordinary differential equations. *Izv. Vyssh. Uchebn. Zaved. Mat.* **10**:9, 37–52 (1995). English transl. in *Russ. Math.* **42**:9, 52–60 (1998)
95. Lebedev, V.I.: A new method for determining the roots of polynomials of least deviation on a segment with weight and subject to additional conditions I, II. *Russian J. Numer. Anal. Math. Modelling.* **8**:3, 195–222; **8**:5, 397–426 (1993)

96. Lebedev, V.I.: Zolotarev polynomials and extremum problems Russian J. Numer. Anal. Math. Modelling, **9**:3, 231-263 (1994)
97. Lebedev, V.I.: Extremal polynomials with restrictions and optimal algorithms. In: Advanced Mathematics: Computation and Applications (Eds. Alekseev, A.S., Bakhvalov, N.S.), pp. 491-502. NCC Publishers, Novosibirsk (1995)
98. Lomax, H.: On the construction of highly stable, explicit numerical methods for integrating coupled ordinary differential equations with parasitic eigenvalues. NASA Technical Note, NASATND/4547 (1968)
99. Malyshev, V.A.: The Abel equation. Algebra i Analiz, **13**:6, 1–55 (2001). English transl. in St. Petersburg Math. J. **13**, 893-938 (2002).
100. Markov, A.A.: Lectures on functions deviating least from zero. In: Markov, A.A.: Selected Papers on Continued Fractions and Functions Least Deviating from Zero. Gostekhizdat, Moscow-Leningrad (1948). (in Russian)
101. Markov, A.A.: A question put by D.I.Mendelev. Izv. Pererburg. Akad. Nauk, issue 62, 1-24 (1889). (in Russian)
102. Markov V.A.: Functions Deviating Least from Zero on a Prescribed Interval. St.-Petersburg (1892). (in Russian)
103. Medovikov, A.A.: High order explicit methods for parabolic equations. BIT **38**, 372-390 (1998)
104. Meiman, N.N.: On the theory of polynomials deviating least from zero. Dokl. Akad. Nauk SSSR **130**:2, 257-260 (1960). English transl. in Sov. Math., Dokl. **1**, 41-44 (1960)
105. Metzger, C.: Méthodes de Runge–Kutta de Rang Supérieur à l’Ordre. Thesis, Univ. Grenoble (1967)
106. Mityushev, V.V.: Convergence of the Poincaré series for the classical Schottky groups. Proc. Amer. Math. Soc., **126**, 2399-2406 (1998)
107. Mumford, D.: Curves and Their Jacobians. University of Michigan Press, Ann Arbor (1975)
108. Mumford, D.: Tata Lectures on Theta, I. Birkhäuser, Boston-Basel (1983)
109. Mumford, D., Series, C., Wright, D.: Indra’s Pearls: The Vision of Felix Klein, Cambridge University Press (2002), 416 p.
110. Myrberg, P.J.: Zur Theorie der Convergenz der Poincareschen Reihen. Ann. Acad. Sci. Fenn. (A), **9**:4, 1–75 (1916)
111. Natanzon, S.M.: Moduli of Riemann Surfaces, Real Algebraic Curves, and Their Superanalogs. Moscow Centre for Continued Mathematical Education, Moscow (2003). English transl. American Mathematical Society, Providence, RI (2004)
112. Pakovich, F.B.: Elliptic polynomials. Uspekhi Mat. Nauk **50**:6, 203-204. English transl. in Russian Math. Surveys **50**, 1292-1294 (1995)
113. Pakovitch, F.: Combinatoire des arbres planaires et arithmétique des courbes hyperelliptiques Ann. Inst. Fourier, **48**, 323-351 (1998)
114. Paszkowski, S.: Numerical Applications of Chebyshev Polynomials and Series. Panstwowe Wydawnictwo Naukowe, Warszawa (1983) (in Polish)
115. Peherstorfer, F.: On Bernstein-Szegő orthogonal polynomials on several intervals. II. Orthogonal polynomials with periodic recurrence coefficients. J. Approx. Theory. **64**, 123-161 (1991)
116. Peherstorfer, F.: Orthogonal and extremal polynomials on several intervals. J. Comput. Appl. Math. **48**, 187-205 (1993)
117. Peherstorfer, F.: Deformation of minimal polynomials and approximation of several intervals by an inverse polynomial mapping. J. Approx. Theory. **111**, 180-195 (2001)
118. Peherstorfer, F., Schiefermayr, K.: Description of extremal polynomials on several intervals and their computation I, II. Acta Math. Hungar. **83**, 71-102, 103-128 (1999)
119. Poincaré, H.: Sur la réduction des intégrales Abéliennes. Bull. Soc. Math. France, **12** 124-143 (1884)
120. Poincaré, A.: Théorie des groupes fuchsienues Acta Math. **1**, 1-62 (1882)
121. Poincaré, A.: Sur les fonctions fuchsienues. Acta Math. **1**, 193-294 (1882)

122. Poincaré, A.: Analyse des travaux scientifiques de Henri Poincaré faite par lui-même. *Acta Math.* **38**, 36-135 (1921)
123. Prasolov, V.V., Schwartzman, O.V.: *Alphabeth of Riemann Surfaces*, Phasis: Moscow (1999). (in Russian)
124. Rauch, H.E.: Weierstrass points, branch points, and moduli of Riemann surfaces. *Comm. Pure Appl. Math.* **12** 543-560, (1959)
125. Rauch, H.E.: On the transcendental moduli of algebraic Riemann surfaces. *Proc. Nat. Acad. Sci. USA.* **41**, 42-49 (1955)
126. Remez, Ya.I.: *General Numerical Methods of Chebyshev Approximation*. Publishing House of the Academy of Sciences of Ukr.SSR, Kiev (1957). (in Russian)
127. Riha, W.: Optimal stability polynomials. *Computing.* **9**, 37-43 (1972)
128. Robinson, R.: Conjugate algebraic integers in real point sets. *Math. Z.* **84**, 415-427 (1964)
129. Rockafellar, R.T.: *Convex Analysis*. Princeton University Press, Princeton, NJ (1970)
130. Schiffer, M., Spencer, D.C.: *Functionals of finite Riemann surfaces*. Princeton University Press, Princeton, NJ (1954)
131. Schmies, M.: *Computational Methods for Riemann Surfaces and Helicoids with Handles*. PhD thesis, TU Berlin (2005)
132. Schottky, F.: Über eine specielle Function welche bei einer bestimmten linearen Transformation unverändert bleibt. *J. Reine Angew. Math.* **101**, 227-272 (1887)
133. Seppala, M.: Computational methods in the theory of Riemann surfaces and algebraic curves. *Proceedings of Workshop on Symbolic and Numeric Computation*, (Helsinki, May 30-31, 1991). Computing Centre, University of Helsinki, Research Reports N. **17** 145-150 (1991)
134. Seppala, M.: Computation of period matrices of real algebraic curves. *Discrete Comput. Geom.* **11** 65-81 (1994)
135. Shabat, B.V.: *Introduction to Complex Analysis. Part II*. Nauka, Moscow (1985). English transl. American Mathematical Society, Providence, RI, 1992
136. Shabat, G.B., Zvonkin, A.K.: Plane trees and algebraic numbers. *Contemp. Math.* **178**, 233-275 (1994)
137. Shafarevich, I.R.: *Basic Algebraic Geometry, 1-2*. Nauka, Moscow (1988). English transl. Springer-Verlag, Berlin (1994)
138. Singer, I.: Best Approximation in Normed Vector Spaces by Elements from Subspaces. *Acad. RSR, Bucuresti* (1967). (in Romanian)
139. Sodin, M.L., Yuditskii, P.M.: Functions deviating least from zero on closed subsets of the real axis. *Algebra i Analiz* **4**:2, 1-61 (1992). English transl. in *St. Petersburg Math. J.* **4**, 201-249 (1993)
140. Sodin, M.L., Yuditskii, P.M.: Algebraic solution of a problem of E. I. Zolotarev and N. I. Akhiezer on polynomials with smallest deviation from zero. *Teor. Funkts., Funkts. Anal. Prilozh.* **56**, 56-64 (1991). English transl. in *J. Math. Sci. (New York)* **76**, No.4, 2486-2492 (1995)
141. Springer, G.: *Introduction to Riemann Surfaces*. Addison-Wesley, Reading, Mass. (1957)
142. Stetter, H.J.: *Analysis of Discretization Methods for Ordinary Differential Equations*. Springer-Verlag, New York-Heidelberg (1973)
143. Strebel, K.: *Quadratic Differentials*. Springer, Berlin-New York (1984)
144. Suetin, S.P.: Pade approximants and the effective analytic continuation of a power series. *Uspekhi Mat. Nauk* **57**:1, 45-142 (2002). English transl. in *Russian Math. Surveys* **57**, 43-141 (2002)
145. Sullivan, D.: Entropy, Hausdorff measures old and new, and limit sets of geometrically finite Kleinian groups. *Acta Math.*, **153**, 259-277 (1984)
146. Tikhomirov, V.M.: *Some Problems of Approximation Theory*, Moscow State University Publishing House, Moscow (1976). (in Russian)
147. Todd, J.: A legacy from Zolotarev. *Math Intelligencer.* **10**:2, 50-53 (1988)
148. Totik, V.: Polynomial inverse images and polynomial inequalities. *Acta Math.* **187**, 139-160 (2001)
149. Tsuji, M.: *Potential Theory in Modern Function Theory*. Maruzen, Tokyo (1959)

150. Vassiliev, V.A.: *Ramified Integrals*. Moscow Centre for Continued Mathematical Education, Moscow (2000). English version: Vassiliev, V. A.: *Ramified Integrals, Singularities and Lacunas*. *Mathematics and its Applications*, **315**, Kluwer, Dordrecht (1995)
151. Vassiliev, V.A.: *Introduction to Topology*, Phasis, Moscow (1977). English transl. American Mathematical Society, Providence, RI, (2001)
152. Vekua, I.N.: *Generalized Analytic Functions*. Nauka, Moscow (1988), 2nd edn. English transl. of 1st edn. Pergamon Press, London-Paris-Frankfurt; Addison-Wesley, Reading, Mass. (1962)
153. Verwer, J.W.: Explicit Runge–Kutta methods for parabolic partial differential equations. *Appl. Numer. Math.* **22**, 359–379 (1996)
154. Vlček, M., Unbehauen, R.: Zolotarev Polynomials and optimal FIR filters. *IEEE Trans. on Signal Processing*. **47**, 717–729 (1999)
155. Whittaker, E.T., Watson, G.N.: *A Course of Modern Analysis*. Cambridge University Press, New York (1962)
156. Widom, H.: Extremal polynomials associated with a system of curves in the complex plane. *Adv. Math.* **3** 127–232 (1969)
157. Zakharov, V.E., Zaslavskii, M.M., Kabatchenko, I.M., Matushevskii, G.V., Polnikov, V.G.: Conceptually new wind-wave model. In: *The Wind-Driven Air-Sea Interface* (Ed. Banner, M.L.), pp. 159–164. The University of New South Wales, Sydney, Australia (1999)
158. Zdravkovska, S.: Topological classification of polynomial maps. *Uspekhi Mat. Nauk* **25**:4, 179–180 (1970). (in Russian)
159. Zieschang, H., Vogt, E., Coldewey, H.-D.: *Flachen und Ebene Diskontinuierliche Gruppen*. *Lecture Notes in Mathematics*, Vol. 122, Springer-Verlag, Berlin-New York (1970)
160. Zolotarëv, E.I.: A question on least quantities (1868). In: *Zolotarëv, E.I.: Selected Papers*, Vol. 2, pp. 130–166, USSR Academy of Sciences, Leningrad (1932). (in Russian)
161. Zolotarëv, E.I.: The theory of integral complex numbers with applications to integration (D.Sc. Thesis, 1874). In: *Zolotarëv, E.I.: Selected Papers*, Vol. 1, pp.161–360, USSR Academy of Sciences, Leningrad (1932). (in Russian)
162. Zolotarëv, E.I.: Applications of elliptic functions to questions of functions deviating least and greatest from zero (1877). In: *Zolotarëv, E.I.: Selected Papers*, Vol. 2, pp. 1–59, USSR Academy of Sciences, Leningrad (1932). (in Russian)
163. Zvonkine, D.A., Lando, S.K.: On multiplicities of the Lyashko-Looijenga mapping on discriminant strata. *Funktsional. Anal. i Prilozhen.* **33**:3, 21–34 (1999). English transl. in *Funct. Anal. Appl.* **33**:3, 178–188 (1999)

Further Reading

1. Bogatyrev, A.B.: Extremal polynomials and algebraic curves (a survey). In: *Advances in Constructive Approximations* (Eds. Saff, E., Neamtu, M.), pp. 109–122. Nashboro Press, Brentwood (2004)
2. Chebyshev, P.L.: *Selected Works*. OGIZ, Moscow-Leningrad (1946). (in Russian)
3. Chern, S.S.: *Complex Manifolds*. Instituto de Fisica e Matematica, Universidade do Recife (1959)
4. Dubrovin, B.A., Novikov, S.P., Fomenko, A.T.: *Modern Geometry*. Nauka, Moscow (1986). English transl., Vols. 1–3, Springer-Verlag, New York (1984–1990)
5. Fricke, R., Klein, F.: *Vorlesungen über die Theorie der Automorphen Functionen*. Teubner, Leipzig (1926)
6. Hejhal, D.A.: Monodromy groups and Poincaré series *Bull. Amer. Math. Soc.* **84**, 339–376 (1978)
7. Kowalewski, S.: Über die Reduction einer bestimmten Klasse Abel'schen Integralen 3-ten Ranges auf elliptische integralen. *Acta Math.*, **4**, 393–414 (1884)
8. Laurent, P.-J.: *Approximation et Optimisation*. Hermann, Paris (1972)
9. Lebedev, V.I.: Iterative methods for solving operator equations with a spectrum contained in several intervals. *Zh. Vychisl. Mat. Mat. Fiz.* **9**, 1247–1252 (1969). English transl. in *U.S.S.R. Comput. Math. Math. Phys.* **9**, 17–24 (1972)
10. Magnus, W.: Braids and Riemann surfaces. *Comm. Pure Appl. Math.* **25**, 151–161 (1972)
11. Nuttall, J.: Sets of minimum capacity, Padé approximants and the bubble problem. In: *Bifurcation Phenomena in Mathematical Physics and Related Topics* (Eds. Bardos, C., Bessis, D.), pp. 185–201, D.Reidel Publ. Company (1980)

12. Schiffer, M., Hawley, N.S.: Connections and conformal mappings. *Acta Math.* **107**, 175–274 (1962)
13. Schiffer, M., Hawley, N.S.: Half order differentials on Riemann surfaces. *Acta Math.* **115**, 199–236 (1966)
14. Timan, A.F.: *Theory of Approximation of Functions of a Real Variable*. Fizmatgiz, Moscow (1960). English transl. Macmillan, New York (1963)

Index

A

Abel
 criterion xxii
 equations xxiii–xxv, 29, 73, 80, 89, 99,
 109–111, 118, 127
 Abel–Pell equation xviii, xxii, 15
 Abelian
 differential
 of 1st kind 99
 of 3rd kind 99
 integral 101, 112
 Absolute 94
 Accompanying element 104, 106
 Affine group xi, 29, 30, 51
 Affine transformation 110
 Ahlfors construction 39
 Alphabet 40
 Alternance 5, 8, 9, 116
 Alternation principle xvi, 1
 Annihilator of a subspace 5
 Ansatz xx, xxv
 Automorphism group 38, 47
 Automorphy conditions 98, 110, 127
 Averaging over a group 90, 103

B

Basis
 associated with a labyrinth 75, 84, 89
 of homology lattice 19
 Beltrami
 coefficient 42, 43, 52, 124
 differential xii, 41, 113, 123

 equation 41, 124
 Belyi pair xviii
 Bernstein theorem 9
 Boundary identification 60
 Braid group 73
 Branch
 divisor xi, xxiv, 29, 36, 117, 123
 points 17, 44, 78
 Bundle of homology spaces xxiv
 Bundle trivialization 74
 Bureau representation xxiv, 75, 83, 85, 86

C

Caley graph 92, 95, 96
 Cell 35, 37, 40
 decomposition 37
 neighbourhood relations 68
 Chebyshev
 classical polynomial xv–xvii, 3, 26,
 115
 construction 15, 73
 differential equation xix
 polynomial on E xv
 representation xix
 space 8
 spline 5, 12, 72, 88, 114
 Class 0_{AD} 123
 Comb-like domain 53, 58, 64, 65
 Cone associated with a polynomial 5
 Configuration space xxiv
 Conformal class 29
 Conical hull 5
 Constraints xxv, 112, 119, 128, 129
 Continued fraction xviii

Coset 91, 106, 125
 two-sided 98
 Covering 123
 ramified 32, 36
 two-sheeted xxii, 15
 Critical trajectory xxiv
 Cross ratio 91, 94, 112
 Curve associated with polynomial 15
 Cycle
 canonical basis 110
 even xi, 18, 21, 23, 68
 integral xxiv, 19
 odd xi, 18, 73
 parallel translation xxv
 relative 19
 Schubert 7

D

Deck transformation xxii
 group 31, 43, 85, 123
 Deformation space xii, 29, 31, 35, 44, 50, 90,
 99, 101, 120, 122
 Dehn twist 46, 75, 85
 Dessins d'enfants xviii
 Differential
 abelian xxv, 20, 53
 of 1st kind 80, 91, 126
 of 2nd kind 91
 of 3d kind xxii, 90
 bundle 74, 76
 cyclic period 79
 invariant 49
 jet of 129
 meromorphic 126
 normalization 91, 99, 102, 110, 125
 period xxiv
 polar period 61, 79
 quadratic xxiv, 103, 107
 of finite area 49, 52
 reciprocal 49
 vector bundle xii
 Dilation coefficient 98, 103, 131
 Dirichlet integral 123
 Disc 17
 Distinguished differential 20
 on a curve xxii
 Distinguished divisor 30, 47
 Divisor 8
 of a function xxii, 89, 98
 normalized 30, 78, 82, 100, 117
 space 8

symmetric 29
 Domain of discontinuity xii, xxi, 31, 41, 45,
 92, 113, 122, 123, 126
 Dual cone 6
 DUMKA 3

E

Eisenstein-type series 92–94, 104
 Elementary braid 75, 83
 Elliptic curves xx
 Elliptic elements of a group 52
 Elliptic function 115
 Equivariant map xxii, 15

F

Fixed points 91, 103, 120, 123–125
 Foliation
 critical points 54, 55
 leaf 54, 58
 Formula
 binomial 99
 variational 102, 112, 129
 Fuchsian group 113
 Function
 Akhiezer 21, 73, 110, 118, 126
 automorphic 97, 112
 cutoff 35, 65
 differential of 48
 Green's xx, 54
 Heavyside xiii, 65
 height 58, 59
 jet of 97, 110, 113, 128
 projective jet of 129
 tent xiii, 64
 univalent 123
 width xii, 54, 59
 Fundamental domain xii, 31, 45, 50, 90, 92,
 96, 106, 122
 Fundamental group 33, 37, 38, 40, 43

G

Gauss–Manin connection xxv, 75, 76, 83, 86
 Global height function 86
 Global period map xxv, 53, 76
 Global system of coordinates 35
 Grassmannian 6

Group

- abstract 36
- of braids xi, xxiv, 33, 47, 85
 - action 75, 80, 86
- freely generated 41, 47
- fundamental xxiv, 117
- generators xxv, 32, 36, 37, 42, 43, 101, 104, 122, 131
- Kleinian xii, 29, 31, 90, 113, 120, 126
- Schottky xii, xxv, 31
 - classical 122

H**Hanging**

- edge 69
- vertex 57

Hejhal

- formulae 104, 130
- identity 105, 107
- map 103–105, 132
- matrix xiii, 102

I**Involution**

- anticonformal 17
- fixed points 52
- on a group 125
- hyperelliptic 17, 122

Isometric circle 17, 25, 113**K****Klein's combination theorem** 31, 122, 133**Kleinian group** 52**L****Labyrinth** 32, 36, 40, 50, 51

- space xii, 29, 32, 44, 90

Lattice xxv**Limit cycle** 54**Limit set** xii, 41, 45, 52, 93, 103, 106**Lobachevskii plane** 39, 94**Local coordinate system** 30**M****Map**

- equivariant 21, 45, 49, 123
- gluing 66
- Lyashko–Looijenga xviii

Markov problem xv, 4**Markov's theorem** 12**Matrix**

- intersection 19, 20
- Jacobi 48
- upper triangular 131

Mendelev problem 4**Meromorphic**

- differential 22, 75
- function 22

Method

- convex programming xvi
- iterative 1
- Levedev xvi
- Newton 111
- Peherstorfer–Schiefermayr xvi
- Remez xvi
- Runge–Kutta xvi, 2, 115

Metric associated with quadratic differential 55**Modular group** xii, 30, 32, 38, 47, 51**Modular group action** 38**Moduli** xxiii, 31, 35, 99, 101, 121

- space xi, xxiv, xxv, 29, 30, 33, 73, 83, 90, 111, 117, 120, 122, 135
- total 53, 62, 64

Monodromy 102

- of a connection 75

N**Navigation** 90, 111**Newton method** 132, 135**Nielsen ordering** 106**Norm on a group** 92**Normal subgroup** 37**O****Odd cycle** xxiv**Order star** 11**Oval**

- coreal 17, 18, 29, 78, 85, 116
- real 17, 18, 30, 37, 78, 85

P

Pairing 77
 Pants 31
 Parallel translation of cycles 75
 Parametric representation xvi, 109
 Partial period map 76, 80
 Period map xxiv, 20, 73, 76, 85, 89
 fibre 73, 76, 77, 79, 80
 global xii
 image 74, 84
 partial 83
 Period matrix xiii, xxi, 113
 Picard-Lefschetz formula 85
 Poincaré disc 94, 113
 Poincaré theta series xxv, 126, 130, 135
 linear xxi, 31, 90, 96, 99, 120
 quadratic 48, 103, 107, 113
 relative 91, 104, 106, 131
 Points, extremal 5, 8
 Problem, stiff 2
 Projective plane 17

Q

Quasiconformal
 deformation 41, 42, 44, 46, 100
 map 30, 45

R

Rational fibres 77
 Real curve 17
 Real differential 20, 23, 89, 113
 Reflection xi, xxiii, 17, 31, 74
 Representation, Artin 47
 Representation generated by labyrinth 36, 51, 117
 Riemann relations 20, 25, 73, 99, 100, 127
 Riemann sphere xi, xvi, 17, 25, 31, 37, 42
 Riemann surfaces xx
 Riemann theta function xx
 Riemann-Roch formula 104

S

Schottky criterion 90

Schottky function xiii, xx, 97, 99, 125
 transformation 97, 111, 125, 127
 Schottky group 90, 92, 99, 106, 117
 Schottky model 90, 120, 127, 129
 Schottky problem xx, 136
 Simplex xxv, 74
 Stability 24
 function 3
 region 3, 10, 132
 Stabilizer 47
 Stable graphs 62
 Stratification 77, 82, 135
 Stratum 76, 79
 coordinate system 78
 Subgroup induced by covering 36, 117, 123
 Submersion xxv

T

Tangent vector 49, 80
 Teichmüller class 32, 44
 Teichmüller metric 30, 52
 Teichmüller space xii, 29, 30, 44, 45
 Theorem on cross-cuts 123
 Torus xvi, 25
 Tree 53, 92, 95

U

Uniformization xxiv, 90, 117, 120, 135
 Uniformizing
 variable 110
 Universal covering space xi, xxiv, xxv, 29, 30, 44, 90

V

Vandermonde determinant 77
 Vandermonde matrix 109
 Variational formula xxv

Z

Zhukovskii map 90, 110, 119, 127
 Zolotarëv polynomial xvi, xvii, 3, 115
 Zolotarëv problem xv